

**Post-SAGD Efficiency Improvement**

by

Randy Agra Pratama

A thesis submitted in partial fulfillment of the requirements for the degree of

Doctor of Philosophy

in

Petroleum Engineering

Department of Civil and Environmental Engineering  
University of Alberta

© Randy Agra Pratama, 2023

## Abstract

Steam-assisted gravity drainage (SAGD) has proved to be a technically and commercially successful methodology for recovering heavy-oil in Canada. At present, there are 22 commercial SAGD projects with over 300 pads and 2,700 well pairs, contributing to over 1.5 million bbl/day of production. The steam growth in the steam chamber could recover up to 60% of the oil-in-place by a typical SAGD project. However, some SAGD projects are only able to present less than 20% of the recovery factor, even though they have been producing for almost decades. Currently, the steam-to-oil ratio (SOR) for most SAGD projects ranges between 2 and 4 bbl steam/bbl oil. Nevertheless, some projects are still experiencing SOR of over 4 bbl/bbl due to the aggressive steam injection. Despite the efficacious evidence and enormous contribution to oil production, many questions regarding the current SAGD project performance are still rising. The process and execution are very complex and entail great operational excellence. The thermodynamic processes (heat transfer, wettability alteration), reservoir geology (thickness, vertical conformance, steam channeling), well designs (optimal placement of the pairs, well completions), and environmental concerns (GHG emission) are also limiting factors to be detrimental to SAGD performance. Some other techniques to recuperate heavy-oil and bitumen (e.g., co-injection)—in addition to the principal SAGD—have been insinuated and employed in the projects. The efforts only presented a 5–10% success rate. The steam generation process itself may lead to environmental issues and low economic viability. Many worldwide steam projects, including SAGD projects in Canada, have already reached their maturity with a severe decline in production despite continuous steam injection. Escalating greenhouse gas (GHG) emissions is another crucial downside of steam injection application, contributing to an emission growth rate of about 1.9% worldwide and 0.8%

annually in Canada. This requires us to search for different techniques to deplete the remaining (conditioned) oil efficiently and in an eco-friendly manner. This research focuses on the testing of a new technique to minimize GHG emissions resulting from steam generation while enhancing the ultimate recovery for post-SAGD efficiency improvement.

In obtaining a comprehensive understanding of post-SAGD efficiency improvement process, a new generation steam additive (e.g., switchable-hydrophilicity tertiary amines or SHTA) and a range of condensable and non-condensable solvents as single and multiple components (e.g., methane, propane, heptane), and non-hydrocarbon solvents (e.g., CO<sub>2</sub> gas) were included as potential solvents. We perceived that favorable interfacial tension reduction was achieved, and irreversible wettability could be auspiciously restored after combining SHTA with steam because of the solid-phase surface charge modification to be more negatively charged. Phase distribution or residual oil in the porous media developed after steam injection was able to be auspiciously convalesced, indicating that capillary forces could be reduced. Consequently, over 80% of the residual oil could be recuperated post-SHTA injection presenting favorable oil recovery performance. In addition to this promising evidence, SHTA could be potentially recovered by switching its reversible chemical reaction to be in hydrophobic form; hence, promoting this steam additive to be both reusable and more economically effective. Based on the outputs obtained from different experimental methodologies, the underlying recovery mechanisms induced by the potential steam additives were identified. The results revealed that synergy among the recovery mechanisms presented by steam additives could potentially improve the heavy-oil/bitumen recovery post-SAGD. Furthermore, it was also observed that both hydrocarbon (condensable and non-condensable) and non-hydrocarbon solvents could substantially improve incremental heavy-

oil/bitumen recovery by up to 50%. More essentially, aggressive steam utilization could be terminated entirely, and energy efficiency could be significantly improved by nearly 100% by applying this technique.

A comprehensive analysis of the mechanics of the heavy-oil/bitumen recovery (e.g., interfacial properties, phase distribution in porous media, recovery performance) provides valuable substantiation and understanding, honoring the potential implications of utilizing steam additives as potential steam additives to the post-SAGD recovery process. Moreover, hydrocarbon and non-hydrocarbon solvents with different compositions were introduced as potential solvents to recuperate heavy-oil and bitumen recovery and reduce or even completely cut off the steam injection at late-stage SAGD, diminishing its GHG emission and improving energy efficiency. Valuable findings present beneficial recommendations for low-emission and high-efficiency late-stage heavy-oil recovery as post-SAGD applications, as well as other types of steam injection processes.

## Preface

This thesis is an original work by Randy Agra Pratama. All chapters included in this thesis have been submitted to the peer-reviewed journals and most of them have been officially published. The publications are listed as follow:

1. **Chapter 2:**

Pratama, R. A., and Babadagli, T. 2023. What Did We Learn from SAGD Applications in Three Decades, and What is Next? *Geoen. Sci. Eng.*, vol. 232, Part B, 212449, 2023. <https://doi.org/10.1016/j.geoen.2023.212449>.

Pratama, R. A., and Babadagli, T. 2023. What Did We Learn from SAGD Applications in Three Decades, and What is Next? SPE-212970-MS, 2023 SPE Western Regional Meeting, Anchorage, AK. USA, 22–25 May. <https://doi.org/10.2118/212970-MS>.

2. **Chapter 3:**

Pratama, R. A., and Babadagli, T. 2022. A Review of the Mechanics of Heavy Oil by Steam Injection with Chemical Additives. *J. Pet. Sci. and Eng.*, vol. 208, Part D, 109717, 2022. <https://doi.org/10.1016/j.petrol.2021.109717>.

3. **Chapter 4:**

Pratama, R. A., and Babadagli, T. 2021. New Formulation of Tertiary Amines for Thermally Stable and Cost-Effective Chemical Additive: Synthesis Procedure and Displacement Tests for High-Temperature Tertiary Recovery in Steam

Applications. *SPE J.* **26**(3): 1572–1598. SPE-201769-PA.  
<https://doi.org/10.2118/201769-PA>.

Pratama, R. A., and Babadagli, T. 2020. New Formulation of Tertiary Amines for Thermally Stable and Cost-Effective Chemical Additive: Synthesis Procedure and Testing for High-Temperature Tertiary Recovery in Steam Applications. SPE Annual Technical Conference and Exhibition, Virtual, 26–29 October. SPE-201769-MS. <https://doi.org/10.2118/201769-MS>.

Pratama, R. A., and Babadagli, T. 2020. Reconsideration of Steam Additives to Improve Heavy-Oil Recovery Efficiency: Can New Generation Chemicals be Solution for Steam Induced Unfavorable Wettability Alteration? *Energy & Fuels*. **34**(7): 8283–8300. <https://doi.org/10.1021/acs.energyfuels.0c01406>.

Pratama, R. A., and Babadagli, T. 2020. Tertiary-Recovery Improvement of Steam Injection Using Chemical Additives: Pore-Scale Understanding of Challenges and Solutions Through Visual Experiments. *SPE J.* **26**(03): 1552–1571. SPE-200841-PA. <https://doi.org/10.2118/200841-PA>.

#### 4. **Chapter 5:**

Pratama, R. A., and Babadagli, T. 2023. What is Next for SAGD?: Evaluation of Low GHG and High Efficiency Tertiary Recovery Options. *Submitted to Journal* (Under Review).

Pratama, R. A., and Babadagli, T. 2022. What is Next for SAGD?: Evaluation of Low GHG and High Efficiency Tertiary Recovery Options. SPE-208876-MS, 2022

SPE Canadian Energy Tech. Conf., Calgary, AB. Canada, 16-17 March.  
<https://doi.org/10.2118/208876-MS>.

5. **Chapter 6:**

Pratama, R. A., and Babadagli, T. 2023. Experimental and Visual Investigation on Energy-Efficient and Zero Greenhouse Gas Emission Post-SAGD (Steam Assisted Gravity Drainage) Heavy-Oil Recovery Improvement. *Submitted to Journal (Under Review)*.

I convey my deep appreciation to my cherished wife, Rahmi, whose unwavering support has been a constant presence, days, and nights, throughout my arduous journey in academia. This enduring support has been indispensable, and I am profoundly thankful.

## Acknowledgements

Each stage of my Doctor of Philosophy program has yielded a plethora of invaluable moments and experiences, enriching my in depth understanding of petroleum engineering. These encompass classroom learning, teaching, research publications, as well as laboratory research. Consequently, I wish to extend my foremost gratitude to the divine entity, Almighty Allah *Subhanallahu Wa Ta'ala*, for the myriad blessings and fortitude that have sustained me throughout my pursuit of this advanced academic endeavor.

I wish to express my profound appreciation to my academic supervisor, Prof. Tayfun Babadagli, for his unwavering commitment, remarkable patience, generous mentorship, inspirational guidance, and steadfast encouragement throughout the entirety of my academic journey leading to the attainment of my degree. His tutelage has been instrumental in bridging my knowledge gaps and cultivating the requisite attributes for excellence in academia. It is with sincere acknowledgement that I recognize that, without his invaluable supervision, the realization of my degree and the successful completion of my PhD thesis would not have been attainable.

I would like to extend my gratitude to our lab technicians, Georgeta Istratescu and Lixing Lin, for their unwavering and tremendous support for my research works. Furthermore, I would like to acknowledge the contributions of my research group colleagues, both to the cultivation of a collaborative and cohesive teamwork.

I wish to express my sincere appreciation for the generous sponsorships extended to our research through Professor Babadagli's NSERC Industrial Research Chair in Unconventional Oil Recovery, with contributions from esteemed organizations such as Petroleum Development Oman, Total E&P Recherche Développement, Husky Energy, Saudi Aramco, Suncor, CNRL, and BASF. Furthermore, I am deeply grateful for the support provided by the NSERC Discovery Grant (No: RGPIN-2023-03231). Additionally, I extend my thankfulness to the University of Alberta for their financial support, which has enabled my graduate studies at this university.

# Table of Contents

<b>Chapter 1: Introduction</b> .....	1
<b>1.1 Introduction</b> .....	1
<b>1.2 Statement of the Problem</b> .....	6
<b>1.2.1 SAGD Performance Controlling Factors</b> .....	7
<b>1.2.2 Solvent Types Selection</b> .....	7
<b>1.2.3 Solvent Composition</b> .....	8
<b>1.2.4 Solvent Recovery</b> .....	9
<b>1.2.5 Steam Additives Thermal Stability</b> .....	9
<b>1.2.6 Residual Oil Saturation (ROS) Development Post-SAGD</b> .....	10
<b>1.3 Aims and Objectives</b> .....	11
<b>1.4 Novelty of Research</b> .....	12
<b>1.5 Structure of the Thesis</b> .....	13
<b>Chapter 2: What Did We Learn from Steam Assisted Gravity Drainage (SAGD) Applications in Three Decades, and What is Next?</b> .....	16
<b>2.1 Preface</b> .....	17
<b>2.2 Introduction</b> .....	18
<b>2.3 Approach for Analysis</b> .....	20
<b>2.4 SAGD Projects Performance Analysis</b> .....	21
<b>2.4.1 Overall Canadian SAGD Projects Performance</b> .....	24
<b>2.4.2 Individual SAGD Project Performance</b> .....	26
<b>2.4.3 High-Performing vs. Low-Performing SAGD Projects</b> .....	56
<b>2.5 Controlling Factors in SAGD Performance</b> .....	60
<b>2.5.1 Reservoir Geology</b> .....	60
<b>2.5.2 Water Production and Presence of Bottom Water</b> .....	63
<b>2.5.3 Well Pair Designs</b> .....	64
<b>2.5.4 Steam Injection Pressure</b> .....	66
<b>2.6 What is Next?</b> .....	71
<b>2.6.1 Steam Additives</b> .....	72

2.6.2	Solvent Injection.....	73
2.7	Conclusions.....	76
<b>Chapter 3: Mechanics of Heavy-Oil Recovery by Steam Injection with Steam Additives ..</b>		<b>78</b>
3.1	Preface.....	79
3.2	Introduction.....	80
3.3	Experimental Methodology.....	84
3.4	Residual Oil Saturation (ROS) Development Post-Steam Injection .....	85
3.5	Steam-Based and Steam-Chemical Additives-Based Displacement Mechanisms	88
3.5.1	Micro Displacement Mechanism .....	93
3.5.2	Micro Displacement Mechanism .....	109
3.6	Sensitivity Analysis of Displacement Mechanisms on Heavy Oil Recovery and Estimated Cost of Applications.....	112
3.7	Conclusions.....	114
<b>Chapter 4: New Formulation of Tertiary Amines for Thermally Stable and Cost-Effective Chemical Additive: Synthesis Procedure and Displacement Tests for High-Temperature Tertiary Recovery in Steam Applications.....</b>		<b>116</b>
4.1	Preface.....	117
4.2	Introduction.....	118
4.3	Materials and Experimental Setup.....	122
4.3.1	Oleic Phase.....	122
4.3.2	Steam Additives.....	123
4.3.3	Interfacial Properties.....	124
4.3.4	High-Pressure High-Temperature Capillary Imbibition .....	125
4.3.5	Phase Distribution Visualization in Porous Media .....	126
4.3.6	Steam Core Flooding .....	127
4.4	Materials and Experimental Setup.....	129
4.4.1	Synthesis Process of Low Concentration SHTA .....	129
4.4.2	Interfacial Properties.....	132
4.4.3	HPHT Capillary Imbibition Performance.....	136
4.4.4	Phase Distribution or Residual Oil Behavior in Porous Media .....	139
4.4.5	Core Flooding.....	143

4.5	Conclusions.....	153
<b>Chapter 5: What is Next for SAGD?: Evaluation of Low GHG and High-Efficiency Tertiary Recovery .....</b>		
<b>155</b>		
5.1	Preface.....	156
5.2	Problem Statement and Proposed Solution.....	157
5.3	Material and Experimental Setups.....	159
5.3.1	Oleic Phase.....	159
5.3.2	Studied Solvents .....	159
5.3.3	Solvent(s) Injection Process .....	160
5.3.4	Hele-Shaw Visualization Experiments.....	161
5.3.5	Porous Media Visualization Experiment.....	162
5.3.6	Remaining Oil Saturation (ROS) .....	164
5.4	Experimental Results.....	165
5.4.1	Hele-Shaw Visualization.....	165
5.4.2	Porous Media Visualization .....	174
5.4.3	Oil and Solvent Recoveries.....	183
5.4.4	Viscosity Measurement and SARA Analysis.....	187
5.5	Discussions.....	189
5.5.1	Hele-Shaw Visualization.....	189
5.5.2	Porous Media Visualization .....	192
5.5.3	Future Potential Improvement for Post/Mature SAGD.....	195
5.6	Research Limitations.....	196
5.7	Conclusions.....	197
5.7.1	Hele-Shaw Experiments: .....	197
5.7.2	Porous Media Experiments:.....	198
<b>Chapter 6: An Experimental and Visual Investigation on Energy-Efficient Post-SAGD Recovery Improvement Alternatives .....</b>		
<b>200</b>		
6.1	Preface.....	201
6.2	Introduction.....	202
6.3	Problem Statement and Proposed Solution.....	205
6.3.1	Problem Statement.....	205

6.3.2	Proposed Solution .....	205
6.4	Material and Experimental Setups.....	207
6.4.1	Oleic Phase.....	207
6.4.2	Studied Solvents .....	208
6.4.3	Solvents Injection Procedure .....	209
6.4.4	Hele-Shaw and Porous Media Visualization .....	210
6.4.5	Core Flooding Experiments .....	212
6.5	Experimental Results and Discussions.....	213
6.5.1	CO <sub>2</sub> Injection.....	213
6.5.2	Heptane Injection.....	223
6.5.3	SAGD Pressure and Temperature .....	226
6.5.4	Sample Analysis .....	227
6.5.5	Solvent Recovery Potential.....	233
6.6	Research Limitations .....	235
6.7	Conclusions.....	236
Chapter 7:	Conclusions, Contributions, and Future Work .....	239
7.1	General Conclusions .....	240
7.2	Contributions.....	246
7.3	Future Works .....	247
References	.....	249
Chapter 1	.....	249
Chapter 2	.....	257
Chapter 3	.....	264
Chapter 4	.....	278
Chapter 5	.....	282
Chapter 6	.....	290

## List of Tables

Table 1—List of SAGD Projects in Canada .....	22
Table 2—Overall SAGD Projects Performance in Canada. NCG = non-condensable gas, eMSAGP = enhanced, modified steam and gas push, and SAP = solvent-aided process. ....	23
Table 3—Controlling Factors of SAGD Operations. $h$ = reservoir thickness, $k_v$ = vertical permeability. ....	70
Table 4—Potential GHG emission reduction (adapted from Canadian Energy Research Institute Report 2017). ....	83
Table 5—List of experimental studies. RT = room temperature. ....	84
Table 6—List of the studied potential chemical additives in this research. ....	85
Table 7—Summary of potential displacement mechanisms of each studied chemical additive. .	89
Table 8—Physicochemical of utilized tertiary amines. ....	123
Table 9—Berea sandstone core samples data. ....	126
Table 10—Steam flooding sandpack properties. ....	128
Table 11—Interfacial tension base case measurement of the oleic phase/steam system at the high-pressure–high-temperature steam condition. ....	133
Table 12—Gas chromatography test result.....	147
Table 13—Fluid properties of the utilized heavy-oil. TAN = total acid number. ....	159
Table 14—Gas and liquid GC analysis result of solvent(s) injection post-SAGD.....	184
Table 15—Fluid properties of the utilized heavy-oil.....	208
Table 16—SAGD core flooding properties. ....	212
Table 17—Results of the gas and liquid GC analysis after solvent injection.....	233

## List of Figures

Figure 1—History of operational SAGD projects growth and number of drilled SAGD wells in Canada.....	24
Figure 2—Overall SAGD projects performance over three decades. iSOR = instantaneous steam-to-oil ratio and cSOR = cumulative steam-to-oil ratio. ....	26
Figure 3—Profile of recovered HCPV vs. HCPVI with cSOR. (a) SAGD 1–10, and (b) SAGD 11–22. HCPVI = hydrocarbon pore volume injected. ....	27
Figure 4—Overall SAGD project performance of SAGD 1.....	27
Figure 5—Overall SAGD project performance of SAGD 2.....	28
Figure 6—Overall SAGD project performance of SAGD 3.....	30
Figure 7—Overall SAGD project performance of SAGD 4.....	31
Figure 8—Overall SAGD project performance of SAGD 5.....	32
Figure 9—Overall SAGD project performance of SAGD 6.....	33
Figure 10—Overall SAGD project performance of SAGD 7.....	35
Figure 11—Overall SAGD project performance of SAGD 8.....	36
Figure 12—Overall SAGD project performance of SAGD 9.....	37
Figure 13—Overall SAGD project performance of SAGD 10.....	38
Figure 14—Overall SAGD project performance of SAGD 11.....	39
Figure 15—Overall SAGD project performance of SAGD 12.....	40
Figure 16—Overall SAGD project performance of SAGD 13.....	42
Figure 17—Overall SAGD project performance of SAGD 14.....	44
Figure 18—Overall SAGD project performance of SAGD 15.....	45
Figure 19—Overall SAGD project performance of SAGD 16.....	47
Figure 20—Overall SAGD project performance of SAGD 17.....	48
Figure 21—Overall SAGD project performance of SAGD 18.....	51
Figure 22—Overall SAGD project performance of SAGD 19.....	52
Figure 23—Overall SAGD project performance of SAGD 20.....	53
Figure 24—Overall SAGD project performance of SAGD 21.....	54
Figure 25—Overall SAGD project performance of SAGD 22.....	55

Figure 26—Current state of individual SAGD project performance in Canada. (a) current recovered HCPV vs. HCPVI (adopted and modified after Jimenez 2008), (b) progression of cSOR for SAGD 1–10, (c) progression of cSOR for SAGD 11–22, (d) recovered HCPV vs. HCPVI for SAGD 1–10, and (e) recovered HCPV vs. HCPVI for SAGD 11–22. HCPVI = hydrocarbon pore volume injected..... 57

Figure 27—Average SAGD pay thickness of the entire SAGD projects in Canada: (a) correlation between recovered HCPV and reservoir thickness, and (b) clustered SAGD pay thickness related to the overall SAGD performance. .... 61

Figure 28—Average  $k_v$  of the entire SAGD projects in Canada: (a) correlation between recovered HCPV and vertical permeability, and (b) clustered vertical permeability related to the overall SAGD performance. .... 61

Figure 29—Overall WCT performance of entire SAGD operations in Canada: (a) correlation between recovered HCPV and WCT, (b) clustered WCT related to the overall SAGD performance, and (c) clustered presence of bottom water in each SAGD operation related to the overall SAGD performance. WCT – water cut..... 63

Figure 30—Average well spacing of the entire SAGD projects in Canada. (a) correlation between recovered HCPV and well spacing and (b) clustered well spacing related to the overall SAGD performance. .... 65

Figure 31—Average pad density of the entire SAGD projects in Canada. (a) correlation between recovered HCPV and pad density and (b) clustered pad density related to the overall SAGD performance. .... 66

Figure 32—Average steam injection pressure of the SAGD projects in Canada. (a) correlation between recovered HCPV and average steam injection pressure, (b) clustered steam injection pressure related to the overall SAGD performance, and (c) clustered low and high-pressure SAGD operations determined based on their hydrostatic pressures. .... 69

Figure 33—Potentially applicable methodologies for SAGD/post-SAGD improvements in reducing GHG emissions (adapted from Canadian Energy Research Institute 2020, Lee and Babadagli 2021). .... 71

Figure 34—Description of stages during steam injection process from the recovery and pore-scale points of view: (a) reservoir pore spaces initial condition, (b) steam is injected into the pore spaces, (c) steam fills up and dominates pore spaces, and (d) post-steam injection. G = grain, O = oleic phase, S = steam, and W = water/liquid phase..... 87

Figure 35—Classification of recovery mechanisms under the steam injection..... 93

Figure 36—SARA analysis and viscosity evaluation on steam-solvent-based heavy oil recovery: (a) low-concentration heptane, (b) low-concentration SHTA, and (c) favorable viscosity reduction by SHTA (reproduced after Bruns and Babadagli 2020a; Pratama and Babadagli 2021). .... 95

Figure 37—Viscosity reduction effect on heavy oil recovery performance of each chemical additive/solvent compared to the base case at the HPHT steam condition (reproduced after Bruns and Babadagli 2020a-b; Huang and Babadagli 2020a; Pratama and Babadagli 2020d, 2021). ...	97
Figure 38—Force balance of rock-heavy oil-steam system at HPHT steam condition.....	100
Figure 39—Wettability alteration of sandstones and IFT after co-injecting steam with chemical additives at optimal chemical concentrations performed at HPHT steam application of up to 220°C and 200 psi: (a) quantitative contact angle measurements. The contact angle was measured between the oleic phase and solid phase in steam, and (b) IFT measurements of heavy-oil in steam (reproduced after Pratama and Babadagli 2020a, b). .....	101
Figure 40—Wettability alteration effect on heavy oil recovery performance of each chemical additive compared to the base case at the HPHT steam condition (reproduced after Bruns and Babadagli 2020a; Huang and Babadagli 2020a; Pratama and Babadagli 2020d, 2021). .....	102
Figure 41—Surfactant-heavy oil interaction in rock/heavy oil/steam system: (a) cationic surfactant, (b) anionic surfactant, and (c) nonionic surfactant.....	104
Figure 42—Wettability alteration mechanism dominance presented by anionic surfactant diminishing residual/trapped oil and improving heavy oil recovery in porous media at high-temperature steam conditions. O = oleic phase and W = water phase. (after Pratama and Babadagli 2020d). .....	106
Figure 43—IFT reduction mechanism dominance presented by nonionic surfactant leaving oil traces, diminishing residual/trapped oil, and potentially improving heavy oil recovery in porous media at high-temperature steam conditions. O = oleic phase and W = water phase (after Pratama and Babadagli 2020d). .....	109
Figure 44—Wettability alteration mechanism presented by switchable solvent on sand grain surface post-steam-chemical-based recovery. ....	109
Figure 45—Water-in-oil in-situ emulsion generation induced by a nonionic surfactant (after Pratama and Babadagli 2020c). .....	111
Figure 46—Oil-in-water emulsion generation induced by SHTA (after Pratama and Babadagli 2021). .....	111
Figure 47—Sensitivity analysis of each recovery mechanism against heavy oil recovery. ....	113
Figure 48—Commercial price comparison of tested chemical additives at optimal concentration. ....	113
Figure 49—Unfavorable wettability alteration caused by phase-change during steam injection in porous media. O = oleic phase, W = water/liquid phase, and S = steam/gas phase (after Pratama and Babadagli 2020a, 2020b, 2020c, 2020d). .....	120
Figure 50—Physical properties and SARA test of heavy-oil: (a) type a heavy-oil, (b) type b heavy-oil, and (c) crude oil properties summary. ....	122

Figure 51—TGA measurement of SHTA (N,N-dimethylcyclohexylamine). .....	123
Figure 52—Interfacial properties measurements: (a) complete experimental setup, (b) contact angle, and (c) interfacial tension of oleic phase-steam with pendant drop. ....	125
Figure 53—HPHT capillary imbibition: (a) HPHT cell and (b) complete experimental setup..	126
Figure 54—Phase distribution in porous media study: (a) glass bead micromodel inside a pressurized steel frame and (b) complete micromodel experimental setup for steam injection.	127
Figure 55—Steam core flooding experimental setup. ....	129
Figure 56—Low concentration SHTA synthesis process: (a) complete experimental setup, (b) before CO <sub>2</sub> injection, and (c) after CO <sub>2</sub> injection. ....	130
Figure 57—pH measurement of SHTA chemical solution in each chemical concentration. ....	131
Figure 58—Unfavorable wettability alteration on a quartz surface caused by a phase change occurred during the steam injection process (after Pratama and Babadagli 2020a, 2020b). ....	132
Figure 59—Favorable wettability alteration on a quartz surface presented by SHTA at 200 psi: (a) hot-water condition and (b) steam condition. ....	134
Figure 60—Wettability alteration profile on a quartz surface presented by SHTA at 200 psi: (a) hot-water condition and (b) steam condition. ....	135
Figure 61—HPHT capillary imbibition under the influence of SHTA at 200°C and 250 psi: (a) before the experiment, (b) after the experiment, and (c) heavy-oil recovery performance plot.	138
Figure 62—Tertiary recovery performance in porous media with SHTA at an optimal chemical concentration: (a) lower heavy oil viscosity and (b) higher heavy-oil viscosity. O = oleic phase, W = water/liquid phase, and S = steam phase. ....	140
Figure 63—Recovery performance presented by SHTA obtained from the micromodels: (a) oil recovery performance and (b) residual oil saturation plot. ....	142
Figure 64—Recovery performance presented by SHTA obtained from the core flooding at 220°C and 200 psi: (a) heavy-oil A and (b) heavy-oil B. ....	144
Figure 65—Potential foamy oil recovery mechanisms presented by SHTA at different concentrations collected after core flooding: (a) heavy-oil A and (b) heavy-oil B. ....	147
Figure 66—Observation of emulsions resulted from SHTA post-tertiary recovery at 100X magnification (sample of heavy-oil A): (a) SHTA 1 wt. %, (b) SHTA 3 wt. %, and (c) SHTA 5 wt. %. ....	148
Figure 67—Dispersed gas co-existed in the system at 400X magnification: (a) SHTA 1 wt %, (b) SHTA 3 wt %, and (c) SHTA 5 wt %.....	149
Figure 68—Comparison on properties of produced oleic phase post-tertiary recovery: (a) oil viscosity and (b) SARA analysis. ....	151

Figure 69—Tertiary amines recovery to evaluate the switchability at low chemical concentration: (a) before CO <sub>2</sub> removal, (b) after CO <sub>2</sub> removal, and (c) SHTA pH measurement before and after steam core flooding experiments. ....	152
Figure 70—Chemical additives commercial price comparison at optimal chemical concentration. Tertiary amine commercial price is compared with several chemical additives previously studied by Pratama and Babadagli (2020a, 2020b). ....	153
Figure 71—Comparison of potential GHG emissions reduction by each steam injection/SAGD operation scenario (adopted from CERI 2020). ....	158
Figure 72—Investigation of displacement mechanism in Hele-Shaw cell inside a high-pressure-high-temperature steel frame. ....	162
Figure 73—Investigation of displacement mechanism in porous media inside a high-pressure-high-temperature steel frame. ....	163
Figure 74—(a) Example of heavy-oil displacement by our steam in Hele-Shaw cell, and (b) color intensity of possible areal displacement efficiency. $E_A$ = areal displacement efficiency. ....	164
Figure 75—Summary of Hele-Shaw experimental results with solvent(s). Color representation: black = heavy-oil, orange = condensed steam displacement result, and bright yellow = solvent-oil mixture. ....	168
Figure 76—Average temperature profile observed on Hele-Shaw experiments during SAGD and solvent injection. The dashed line indicates the period when the steam injection was 100% cut-off, and solvent injection was started. ....	169
Figure 77—Summary of porous media experimental results with solvent(s). White-dashed circle = oleic phase, and yellow-dashed circle = water-in-oil emulsion/solvent-oil mixture. ....	177
Figure 78—Average temperature profile observed on porous media experiments during SAGD and solvent injection. The dashed line indicates the period when the steam injection was 100% cut-off, and solvent injection was started. ....	179
Figure 79—Observation of residual oil formation in pore spaces (oil blobs and island of oil) post-SAGD process. ....	179
Figure 80—Oil recovery and solvent recovery profiles during propane and methane–propane mixture injections at designated injection volumes. (a) 100% propane, (b) 30% methane–70% propane, and (c) 50% methane–50% propane. ....	185
Figure 81—Oil recovery and solvent recovery profiles during heptane and methane–heptane mixture injections at designated injection volumes. (a) 100% heptane, (b) 30% methane–70% heptane, and (c) 50% methane–50% heptane. ....	186
Figure 82—Example of viscosity measurements for heptane and methane-heptane injection cases. ....	188

Figure 83—Example of SARA analysis for heptane and methane-heptane injection cases. H = heptane, and M = methane. ....	189
Figure 84—Columns containing solvent(s) gas and residual oil (relative to post-SAGD condition) observed in porous media model at the end of solvent(s) injection. ....	193
Figure 85—Heavy-oil properties: (a) oil viscosity measurement, and (b) SARA analysis. SARA = saturate, aromatic, resin, asphaltene. ....	208
Figure 86—Hele-Shaw cell experimental setup in investigating fluid-to-fluid interaction and displacement mechanism under post-SAGD conditions. A = injection, and B = production. ...	211
Figure 87—Porous media experimental setup in investigating phase distribution behavior and displacement mechanism under post-SAGD conditions. A = injection, and B = production. ...	211
Figure 88—SAGD core flooding experimental setup. ....	213
Figure 89—Hele-Shaw experimental results with solvent(s). Color representation: black = heavy-oil, orange = condensed steam displacement result, bright white = displaced oil by steam/solvent, and bright yellow = solvent-oil mixture. I = injection port and P = production port. ....	216
Figure 90—Average temperature profile observed on Hele-Shaw experiments during SAGD and solvent injection. The dashed line indicates the period when the steam injection was entirely stopped, and solvent injection was started. ....	217
Figure 91—Porous media experimental results with solvent(s). White-dashed circle = oleic phase, and yellow-dashed circle = water-in-oil emulsion/solvent-oil mixture. I = injection port and P = production port. ....	221
Figure 92—Average temperature profile observed on porous media experiments during SAGD and solvent injection. The dashed line indicates the period when the steam injection was entirely stopped, and solvent injection was started. ....	221
Figure 93—Overall performance of SAGD with CO <sub>2</sub> injection: (a) late-stage case and (b) mid-stage case. ....	223
Figure 94—Overall performance of SAGD with late-stage heptane injection. (a) late-stage case, and (b) mid-stage case. ....	225
Figure 95—Performance comparison between late-stage and mid-stage heptane injection cases. ....	226
Figure 96—Average pressure and temperature profiles during SAGD and solvent injection processes: (a) pressure profile and (b) temperature profile. ....	227
Figure 97—Viscosity measurements for each experimental case. ....	228
Figure 98—SARA analysis for the entire solvent injection cases in comparison with the base (steam-only) case. ....	230

Figure 99—Recovered sand and sand particles under the microscope with 100X magnification taken after each experiment: (a) base case, (b) late-stage CO<sub>2</sub> injection, (c) mid-stage CO<sub>2</sub> injection, (d) late-stage heptane injection, and (e) mid-stage heptane injection..... 232

Figure 100—Example of potential asphaltene precipitation in the recovered sands. Dark solid accumulations were perceived after solvent injection. .... 232

Figure 101—Quantification of solvent recovery potential alongside heavy-oil/bitumen recovery post-SAGD: (a) mid-stage CO<sub>2</sub> injection, (b) late-stage CO<sub>2</sub> injection, and (c) late-stage heptane injection..... 235

## Nomenclature

$\mu_o$  = oleic phase viscosity, mPa·s

$\mu_w$  = water viscosity, mPa·s

$P_c$  = capillary pressure, dynes cm<sup>-2</sup>

$r$  = pore radius, cm

$\sigma$  = interfacial or surface tension, dynes cm<sup>-1</sup> or mN m<sup>-1</sup>

$\theta$  = contact angle, degrees

$v$  = linear velocity of displacing fluid, m sec<sup>-1</sup>

cP = centipoise

$S_{wc}$  = connate water saturation, fraction

$S_{wi}$  = initial water saturation, fraction

$S_{or}$  = residual oil saturation, fraction

$N_p$  = cumulative oil production, cc or mL

$PV$  = pore volume, cc or mL

# Chapter 1: Introduction

## 1.1 Introduction

Since heavy-oil and bitumen play an essential role in the world's energy supply, many efforts have been devoted to the research, explorations, and recoveries of heavy-oil and bitumen resources. Steam injection has been extensively applied in various practices to recover heavy-oil and bitumen for decades (Van Dijk 1968; De Haan and Schenk 1969; Hall and Bowman 1970; Butler et al. 1979; Harmsen 1979; Blevins 1990; Fuaadi et al. 1991; Butler 1994; Gael et al. 1994; Jones et al. 1995; Ali 1997). The key concept of utilizing the steam is to enable the thermally-induced viscosity reduction and thermal expansion in mobilizing the heavy-oil in the reservoirs (Ali 1974; Ali and Meldau 1979; Blevins et al. 1984; Haghghi and Yortsos 1997; Al-Bahlani and Babadagli 2009; Gates and Wang 2011; Sheng 2013; Taylor 2018). The application of steam injection—particularly steam-assisted gravity drainage (SAGD)—can be anticipated to deliver the ultimate recovery of up to 60–70% if the steam chamber growth is maintained (Jimenez 2008; Speight 2009).

As a heavy-oil-and-bitumen-rich country, Canada has pioneered the SAGD as a pivotal heavy-oil and bitumen recovery technique from technical and commercial perspectives. The SAGD technique was first conceptualized by Butler (1985) and further tested through the Underground Test Facility (UTF). The UTF was built in the northern part of Fort McMurray and funded by the Alberta Oil Sands Technology and Research Authority (AOSTRA) in 1987. The in-situ test was initiated through the Phase A pilot test involving three horizontal well pairs encompassing 55 m lateral length and 24–25 m well spacing (Edmunds et al. 1994). The injector was assembled parallel to and about 5 m over the producer. The success, lessons learned, and best practices of this pilot test have encouraged the oil and gas industry to invest and establish Phase B, which was the first commercial pilot SAGD performed at the same test facility between 1990 and 1992. Phase B consisted of three horizontal well pairs comprising 500 m lateral completion and 70 m well spacing (Edmunds and Gittins 1994; Collins 1994). Phase B pilot commercial SAGD was forecasted to attain a bitumen recovery of up to 45%. However, the realization of the recovery surpassed the initial plan by over 65%.

Over the last three decades since the pilot SAGD application was studied and successfully tested, more than 20 commercial SAGD projects have been established in Canada, and this recovery technique has been standardized as an ideal technique to recuperate heavy-oil/bitumen. Currently, more than 85% of active SAGD projects are operating in the Athabasca area, and the remaining are in the Cold Lake area—contributing up to 25% of Canadian total oil production. Even though these SAGD fields have been in production for decades, nearly 25% of the active fields are still experiencing less than 20% of heavy-oil/bitumen recovery—even some of them are below 5%. Despite the technical advantage, reliability, and feasibility of SAGD, there are still many aspects needed to comprehend—causing recovery by SAGD remains challenging. More importantly, the aggressive use of steam injection, in fact, presents a significant direct impact on the environment—further intensifying greenhouse gas (GHG) emission with a 1.9% annual emission growth rate contribution globally (Energy Institute 2023; Lee and Babadagli 2021) and projected to escalate by 100% in a decade with current process and base business. This necessitates the exploration of various techniques aimed at the ecologically sustainable depletion of the remaining oil reserves.

The vast development of the oil and gas industry has triggered numerous research studies into the use of chemical additives and solvent-based chemicals for heavy oil and bitumen recovery improvement. These chemicals include conventional chemicals that cover the use and application of:

- alkalis (Wagner and Leach 1959; Chiwetelu et al. 1994; Madhavan and Mamora 2010; Wang et al. 2010; Haas et al. 2013; Cao et al. 2017; Wei and Babadagli 2017a, 2017b; Hashim Noori et al. 2018; Wei and Babadagli 2019; Bruns and Babadagli 2020a),
- ionic liquids (Hanamertani et al. 2015; Wei and Babadagli 2017a, 2017b; Wei and Babadagli 2019; Huang and Babadagli 2020a),
- surfactants (Gupta and Zeidani 2013; Mohammed and Babadagli 2015; Alomair and Alajmi 2016; Wei and Babadagli 2017a, 2017b, 2018; Taylor 2018; Alshaikh et al. 2019; Bruns and Babadagli 2020a, 2020b; Huang and Babadagli 2020a, 2020b; Lee and Babadagli 2021).

These published studies were able to demonstrate a favorable incremental oil recovery of up to 40%. Even though the evidence has presented very positive potential outcomes on heavy-oil thermal recovery, the utilization cost of these chemical additives is still undeniably high.

Most recently, Jessop et al. (2010) performed a synthesis of a recyclable chemical from a group of tertiary amines. This chemical was reported to have switchability and was able to behave as a solvent for the extraction of organic components. The switchability terms fundamentally refer to the functioning principle of this kind of chemical that can be altered from being initially hydrophobic to hydrophilic reversibly. The hydrophilicity of these tertiary amines depends on the existence of carbon dioxide (CO<sub>2</sub>) gas in the water phase. This circumstance was able to control the miscibility of tertiary amines in the chemical solution (Jessop et al. 2011; Wilson and Stewart 2014; Durelle et al. 2015). The miscibility mechanism occurs due to protonation and deprotonation in the reversible chemical reaction. The miscible tertiary amines or switchable-hydrophilicity tertiary amines (SHTA) is initiated by introducing CO<sub>2</sub> gas into the tertiary amines/water system; thus, resulting in a homogeneous chemical solution containing a water-soluble bicarbonate salt—[HCO<sub>3</sub><sup>-</sup>]. Jessop et al. (2011) and Sui et al. (2016) have also reported that the hydrophilicity of this SHTA solution was able to be reversely switched into more hydrophobic (immiscible) chemical solution by elevating the temperature of the system and injecting nitrogen (N<sub>2</sub>) gas at the same time. The separation of tertiary amines from the chemical solution could potentially increase the chemical reusability, leading to more cost-effective and environmentally friendly operations. The development and utilization of a group of amines as switchable solvents were initially implemented for soybean oil extraction and separation (Phan et al. 2009; Jessop et al. 2010), high-density–volume-reduced polystyrene (Jessop et al. 2011), lipid extraction from algae and microalgae (Boyd et al. 2012; Samorì et al. 2013; Du et al. 2015), and phenols extraction from lignin (Fu et al. 2014). Recently, the concept of organic matter removals was then reproduced and adopted in the area of fossil energy. A study in the bitumen extraction was conducted by Holland et al. (2012) and Sui et al. (2016) to evaluate the SHTA performance on bitumen recovery. They reported that the bitumen could be favorably recovered up to 98% from the oil sands by involving SHTA. In addition to the evidence, a synergistic function between SHTA and asphaltenes was successfully instigated. The research perceived that the heavy-oil could be upgraded by also reducing the viscosity (Mozhdehei et al. 2019). Additionally, the oil-water interfacial tension was

able to be lowered throughout the emulsion stabilization mechanism (Li et al. 2018). These studies, however, were performed at much lower than steam temperature.

The forthcoming prospect of SAGD is contingent upon the advancement of novel methodologies geared towards the mitigation of GHG emissions arising from steam generation procedures. Concurrently, there is a need to augment ultimate recovery rates in the post-SAGD phase. The effort includes involving solvents in the SAGD process, which can potentially reduce GHG emissions by 90% (CERI 2017; Lee and Babadagli 2021). In a more classical study centered upon the utilization of a solvent, specifically naphtha, in conjunction with steam injection, the investigation conducted by Ali and Abad (1976) yielded the finding that incremental recovery of bitumen surpassed 20%. This outcome was attributed to the phenomenon of solvent evaporation and the subsequent dissolution mechanism that transpired between the solvent and oleic phase during the steam injection process. The efficacy of solvent-based approaches for the extraction of heavy oil/bitumen was further substantiated in the work of Das and Butler (1998). Their analysis unveiled that upon injecting vapor-phase solvents (e.g., propane, butane) into the systems, two primary mechanisms were observed: first, the diffusion of the solvent into the heavy oil, and second, the dissolution mechanism contributing to the reduction of oil viscosity and thus facilitating the mobilization of the oleic phase.

In more modern SAGD applications, approximately 80% of SAGD operations in Canada have integrated the practice of introducing non-condensable gases (NCGs), primarily methane injection. Nevertheless, these incorporations have failed to yield a substantial enhancement in overall performance, encompassing metrics like production rates and the cumulative steam-to-oil ratio (SOR). The success rate of this approach within SAGD operations is modest, typically ranging from 5% to 10% (Pratama and Babadagli 2023a, b). The discouraging results associated with NCG co-injection have been substantiated by prior research conducted by Butler (1999) and Jiang et al. (2000), which concurred that although NCG co-injection may yield certain advantages, these benefits primarily stem from gas insulation and the "gas push" mechanisms. In essence, methane gas predominantly exerts a "pushing effect" rather than inducing mixing or dissolution, tending to migrate toward the upper stratum of the reservoir. Another potential method to enhance the efficiency of SAGD operations for recovery involves the injection of condensable gases (CGs), with propane being a commonly used option. Propane, at SAGD operating temperatures, exhibits

a notably low K-value (Deng 2005), which implies greater propane solubility in heavy oil/bitumen. This enhances the process of mixing and dissolution between the solvent and heavy oil/bitumen, ultimately resulting in a favorable reduction in viscosity within the reservoir. This reduction in viscosity aids in increasing incremental recovery, facilitated by the force of gravity. In the area of liquid solvent injection, Nasr et al. (2003) initially introduced and developed the concept of Expanding Solvent–SAGD (ES-SAGD), which integrates steam and low-concentration hydrocarbon at steam temperature. The success of this technique hinges on the choice of the hydrocarbon. Hexane was proposed as the most suitable solvent in this context, mainly because it has a vaporization temperature close to that of injected steam. This alignment allows both steam and solvent to move simultaneously towards the steam chamber, effectively mixing with heavy oil/bitumen and reducing viscosity. The first implementation of ES-SAGD took place during the Long Lake Pilot in 2005–2006, resulting in a 6% increase in oil production (Orr 2009). Although the utilization of these types of solvents in SAGD applications has been claimed to present promising results, these techniques have a limited impact on reducing greenhouse gas (GHG) emissions since steam remains the primary component of the injected material.

This research investigates and evaluates a lab-formulated steam additive and solvents as low GHG, and high-efficiency tertiary recovery options applied post-SAGD to further evaluate and investigate their potency and applicability in high-pressure and high-temperature SAGD applications. Despite there being plenty of relevant research publications honoring the steam–solvent co-injection for SAGD applications, we put our focus on these solvent injection post-SAGD with way less or even without any steam injection involvement (no steam–solvent co-injection) that has not previously been studied or researched. The type (and composition) and optimal conditions for using these solvents in post-SAGD reservoirs were determined at a given post-SAGD temperature, as well as the recovery potential of these solvent with oil for an efficient process. Valuable findings of this research will present beneficial recommendations for low-emission and high-efficiency late-stage heavy-oil recovery as post-SAGD applications, as well as other types of steam injection processes, in achieving a more sustainable hydrocarbon production.

## 1.2 Statement of the Problem

Enhanced oil recovery (EOR) is widely regarded as a dependable approach for exploiting untapped oil reserves. Nevertheless, its application, particularly within the context of thermal recovery processes in heavy-oil/bitumen production, presents formidable challenges in oil field operations. Factors such as the utilization of steam, operational costs, and energy efficiency pose persistent difficulties within the thermal recovery methods. In essence, the mature SAGD holds significant importance and demands heightened attention, especially since many SAGD fields have experienced declining production and low recovery during this phase (Pratama and Babadagli 2023a, b). Alongside other challenges faced by SAGD fields, such as reservoir geology, condensate flow, bottom water, well spacing, pad density, steam injection pressure, adverse alterations in wettability due to phase changes at high temperatures have been a major factor affecting heavy-oil recovery and SAGD process efficiency. This leads to an increase in the steam-to-oil ratio (SOR) and directly contributes to a rise in GHG emissions. Moreover, there remain ambiguities surrounding various factors affecting wettability characteristics and the distribution and entrapment of phases, ultimately impacting the recovery of heavy oil. Although chemical additives have demonstrated the potential to enhance oil recovery, the underlying mechanisms are not yet fully elucidated. The scarcity of published research on steam conditions further compounds the complexities inherent in heavy-oil thermal recovery processes. The primary challenge lies in identifying an appropriate formulation for steam additives, one that can maintain component stability under high-pressure and high-temperature conditions.

Technical hurdles and concerns regarding GHG emissions from the steam-based recovery process have generated negative perceptions, both among the public and within the technical community. These perceptions drive the quest for new applications that make the most of existing investments, such as field operations, production facilities, and capital expenditures. A recent trend in SAGD operations is to partially or completely reduce steam usage, aiming to lower operational costs and minimize environmental impacts. Chemical additives and solvents are being considered as potential alternatives to achieve these objectives. However, the current effort still requires steam as a co-injection process. In addition to the physicochemical aspects of the process, the

thermodynamic behavior of hydrocarbon solvents, influenced by pressure and temperature, must also be considered, and understood.

It is imperative to define critical parameters that influence overall to ensure the successful implementation of post-SAGD efficiency improvement in the field. In summary, the challenges associated with recovery methodologies can be delineated as follows:

### **1.2.1 SAGD Performance Controlling Factors**

Thermal Even though SAGD has proven to be the most effective recovery technique for heavy-oil/bitumen, the outcomes and efficiency of such technique vary in every SAGD project. The variety of SAGD project behavior depends on several factors:

- geology or reservoir properties,
- presence of bottom water,
- production–injection optimization and strategy,
- well design (e.g., well placement, well spacing),
- operational excellence.

The quality of a SAGD project is primarily determined by overall SAGD performance (normal SAGD phases/stages), SOR (efficient SAGD operation if  $cSOR < 3$ ), and maturity. Even though there is no exact rule of thumb/guideline honoring maturity, by technical definition, a mature phase is reached when the maximum recovery by steam chamber growth (ultimate recovery) of up to 60% is achieved or at least 40–50% of the recoverable heavy-oil/bitumen, which is categorized as a moderately mature SAGD. In essence, comprehending these potential controlling factors is critical to attain a more conspicuous conception honoring the overall SAGD performance.

### **1.2.2 Solvent Types Selection**

The selection of solvent types plays important role in delivering their potentials to further improve the efficiency of post-SAGD. A wide range of solvent types should be evaluated—to cover the

main objective of this research—according to the phase behavior of each solvent. These solvents include hydrocarbon (condensable and non-condensable) and non-hydrocarbon solvents. A vapor or gaseous type of solvent(s) is advantageous as they can propagate or move upward by gravity. Due to its natural behavior, when injected to the reservoir, this solvent(s) will move toward the upper section of the reservoir. On the other hand, a denser hydrocarbon solvent, such as heptane, may offer improved "cleaning effects." Different types of solvent may lead to a different post-SAGD performance.

### **1.2.3 Solvent Composition**

The composition of a solvent plays a pivotal role in influencing the effectiveness of post-SAGD improvement processes aimed at improving oil recovery efficiency. This is since the selection of specific solvents and their proportion in the mixture represents a fundamental determinant of the success of these recovery operations. By strategically combining various types of solvents, it is possible to potentially enhance the recovery of heavy oil or bitumen. This improvement encompasses not only technical considerations but also economic aspects, making it a multifaceted and crucial aspect of the recovery process.

The reason behind the importance of solvent composition lies in its ability to modify the properties of the reservoir and the oil itself, making the recovery process more effective. Solvents can alter the viscosity of heavy-oil/bitumen, reduce interfacial tension, and improve oil mobility. Additionally, the economic viability of the recovery operation is closely tied to the cost and availability of the selected solvents.

By carefully tailoring the solvent composition, it can be expected to optimize the recovery process, increasing the overall efficiency, and ultimately maximizing the extraction of the oleic phase. This underscores the significance of solvent selection and composition as a crucial factor in the success of post-SAGD recovery efforts, encompassing both technical and economic considerations.

#### **1.2.4 Solvent Recovery**

To strengthen the conclusions drawn from our experimental research, it is crucial to conduct a semi-quantitative analysis. This analysis will allow us to dig more deeply into the performance of different solvents and their mixtures concerning two key aspects: oil recovery and solvent recovery. Oil recovery refers to the efficiency with which we can extract crude oil, and solvent recovery pertains to the effectiveness of recovering and reusing the solvents used in the process.

This scrutiny of solvent recovery is particularly valuable because it can provide us with a deeper understanding of how to optimize the efficiency of SAGD operations, specifically in the context of operating conditions such as pressure and temperature. By analyzing how well solvents are recovered in varying conditions, we can glean valuable insights into the overall effectiveness of the process.

The data generated from this analysis holds the potential to be a critical tool for the post-SAGD efficiency improvement. This means that it can be instrumental in refining and enhancing the processes and outcomes that follow SAGD, ultimately leading to more efficient oil recovery processes.

#### **1.2.5 Steam Additives Thermal Stability**

Thermal stability represents a critical parameter when considering the application of chemicals as steam additives in thermal recovery processes, including SAGD. This parameter can be quantified through the thermal stability test on the studied steam additive. Thermogravimetric analysis (TGA) stands out as the most dependable and commonly employed technique for assessing the thermal stability of chemicals. Essentially, TGA involves the continuous measurement of the substance's mass while incrementally raising the temperature. This measurement provides insights into the extent of chemical decomposition under elevated temperature conditions. It is noteworthy that the thermal stability derived from TGA measurements may be prone to overestimation due to transient stability during abrupt temperature fluctuations (Cao and Mu 2014). The performance of this thermal stability test holds a critical part, allowing for the screening of chemical additives to determine their suitability for use in post-SAGD applications.

### **1.2.6 Residual Oil Saturation (ROS) Development Post-SAGD**

It is undeniable that the heat transfer during the steam injection process (Prats 1982) is substantial for viscosity reduction to mobilize heavy-oil/bitumen in the pore spaces. This becomes a challenging and complex process—impacting the recovery performance—in the latter stages of SAGD. Generally, the SAGD process can be divided into four main phases: (1) initial phase, (2) peak production phase, (3) plateau phase, and (4) decline production/wind-down phase.

In the initial phase of SAGD, steam and oil production began. In this stage, when the rock pores are mostly saturated with heavy oil, the heat transmitted during steam injection produces the oleic phase with two possible mechanisms—viscosity reduction and thermodynamic thermal expansion (Jessup 1930). The viscosity reduction increases the mobility of the oleic phase, whereas the thermal expansion causes swelling oil. Despite high steam injection, oil production is low due to high viscosity. However, as steam propagates and heats the oil phase, viscosity decreases, mobilizing the heavy-oil/bitumen under the gravity force. This requires more heat energy and raises the steam-to-oil ratio (SOR). Subsequently, in the peak production phase, steam creates a chamber for heat transfer to increase oil production. Additional SAGD projects and established ones may also contribute. In the plateau production phase, oil production remains stable despite new wells. The steam chamber has stabilized, steam pressure is constant, and temperature equalizes. These process and mechanisms may continue until plateau phase, resulting a more stable oil production.

In the latter phase of SAGD (decline or wind-down phase), a phase change occurs to subsequently promote the thermodynamic evaporation of the water phase—due to the instability of the wetting water film on the solid phase (Evdokimov et al. 2018). In this circumstance, the strength of surface force changes, van der Waals attractive force dominates the electrostatic repulsive force, and the disjoining pressure becomes negative; thus, allowing direct interaction between the oleic phase and the rock surface to become more or even completely oil-wet state, further rising the capillary pressure, and then creating more resistance force and development of residual oil saturation in the pore spaces and steam condensate flow may also occur. Further evaluation is needed to reduce residual oil and lower the steam-to-oil ratio (SOR).

### 1.3 Aims and Objectives

The primary goal of this research is to develop innovative methods and strategies that can effectively enhance the efficiency of post-Steam-Assisted Gravity Drainage (SAGD) processes. The desired outcomes of these research efforts encompass several crucial aspects:

- **Maximizing oil recovery:** This research aims to devise techniques that can maximize the heavy-oil/bitumen, ensuring that a larger portion of the available resource is efficiently recuperated.
- **Enhancing operational efficiency:** In addition to increasing oil recovery, the research seeks to streamline the overall operational processes associated with SAGD operations, making them more efficient and cost-effective.
- **Reducing steam-to-oil ratio (SOR):** The SOR is a critical performance indicator in the SAGD operations. Lowering the SOR means that less steam is required to extract a unit of oil, which is not only more cost-efficient but also environmentally friendly.
- **Diminishing residual oil saturation (ROS):** By reducing the ROS, it is anticipated that favorable incremental oil recovery could be achieved.
- **Maintaining production performance:** While implementing these improvements, it is essential to ensure that oil production remain consistent or even improve, ensuring that the changes do not compromise the overall SAGD performance.
- **Reducing greenhouse gas (GHG) emissions:** One of the essential objectives of this research is to minimize GHG emissions, specifically by up to 80% or even eliminating them entirely (100%). Achieving this reduction will contribute significantly to environmental sustainability and regulatory compliance.
- **Eliminating steam generation and injection:** One of the main goals of this research is to entirely eliminate the need for steam generation and injection in the SAGD process, which could lead to a paradigm shift in the oil and gas industry.

In pursuit of these efforts, this research endeavors to seek innovative methods and technologies that can revolutionize the post-SAGD stage, making it more efficient, environmentally responsible, and economically viable. Several key objectives of this research include:

- Development of thermally stable new generation steam additive for post-SAGD applications.
- Selection and testing a wide range of solvent types for post-SAGD efficiency improvement by further evaluating their potentials through the interfacial properties, visual, and core flood experimental studies.
- Determining the optimal solvent composition by testing the selected solvents and combining them through the visual and core flood experiments.
- Quantifying the optimal and economical solvent recovery by collecting the produced samples and performing gas chromatography (GC) analysis.
- Proposing the best time to switch to solvent injection by conducting solvent injections at mid-stage and late-stage of SAGD processes.

#### **1.4 Novelty of Research**

This research is merited to address extant challenges and fill the existing gaps in SAGD applications with newly proposed techniques, diverging from conventional applied methodologies and have not been any subject to prior scholarly studies. This research constitutes a contemporary and comprehensive evaluation of existing SAGD fields, surpassing previous analyses carried out by eminent scholars. This comprehensive approach is positioned to yield significant advantages for practitioners, affording them invaluable insights to enhance the prospects of future SAGD field development.

Moreover, this research specifically centered on the assessment of newly formulated steam additives and various solvent types applicable to mature SAGD scenarios. These investigations

encompass a spectrum of scales, ranging from pore- to core-scale visual data to core flooding tests, implemented during the mid- and late-stage of SAGD processes with minimal or even no steam injection is necessitated, further promoting notable enhancement in post-SAGD efficiency, and concurrently resulting in significant GHG emissions reduction. It is believed that this research is invaluable for scientific communities and practitioners.

## **1.5 Structure of the Thesis**

This paper-based thesis encompasses six chapters. Chapter 2 contains two papers which were previously presented at a technical conference in 2023 and submitted to a research journal and currently under review. Chapters 3 and 4 comprise four papers which have been presented at two different technical conferences and published in a two peer-reviewed research journals. Chapter 5 consists of a conference paper which was presented at a research conference in 2023. This paper has been submitted to a research journal and is currently under review for publication. Chapter 6 consists of a research paper which has been submitted to a research journal and is currently under review for publication.

**Chapter 1.** This chapter provides a general overview of this thesis describing the current status of SAGD operations and the implemented technologies, and several challenges regarding the post-SAGD efficiency. Aims and objectives of this research are also stated in this chapter.

**Chapter 2.** SAGD has been implemented successfully in Canada, but concerns remain about recovery efficiency and environmental impact. A key factor determining SAGD performance (e.g., reservoir geology) is still unclear. Some SAGD projects with similar reservoir properties are still experiencing low recovery, and the factors affecting recovery, including thermodynamics, well design, and operational concepts, need more detailed analysis. Co-injection techniques have shown low success rates. This chapter covers a comprehensive analysis of field data from 22 operational SAGD projects in Canada. This chapter also proposes recommendations and insights for more efficient and sustainable SAGD operation for the future of mature and new SAGD projects based on performance indicators and controlling factors, as well as reservoir properties.

**Chapter 3.** Numerous thermally stable steam additives, including surfactants, nanofluids, and water-soluble solvents, have demonstrated the ability to positively change wettability. However, the scientific understanding of the fundamental principles driving this beneficial alteration and other mechanisms remains limited, particularly in the context of novel chemicals operating under specific thermodynamic conditions. This chapter presents the experimental result-based, and comparative analyses of potential chemical additives not only to further evaluate the chemical's performance on the recovery improvement—specifically at the late-stage steam injection—but also to investigate the underlying recovery mechanisms.

**Chapter 4.** This chapter covers evaluation and investigation the potentials of a lab-formulated new generation switchable-solvent as a steam additive, as well as its recovery mechanisms through qualitative and quantitative analyses of fluid properties, interfacial properties (IFT and contact angle), high-pressure–high-temperature spontaneous imbibition, phase distribution in porous media, and steam core flooding. These analyses are essential to obtain both a valuable understanding as well as more solid conclusions regarding the use of this new generation steam additive for SAGD applications since there are no such studies on this potential additive in steam injection applications.

**Chapter 5.** Technical challenges and the perception of GHG emissions associated with steam-based operations have generated unfavorable public and technical opinions. These perceptions have prompted efforts to explore new applications while making the most of existing investments. One proposed solution involves the utilization of chemical additives and solvents to achieve these objectives. However, when employing these methods, attention must be given to various phenomena, including wettability alterations and oil entrapment mechanisms. Among the range of challenges faced in SAGD operations, which include issues like mobility contrast, steam channeling, and steam conformance, one significant problem has been the detrimental alteration of wettability due to phase changes under high-temperature conditions. This factor has notably impacted the efficiency of heavy oil recovery and the SAGD process, ultimately resulting in an increased steam-to-oil ratio (SOR) and a consequent rise in GHG emissions. This chapter aims to provide an extensive exploration of the primary objective of this research, which is to assess and investigate the potential of various types of solvents as highly efficient tertiary recovery options through visual experiments.

**Chapter 6.** This chapter provides a detailed exploration of a current research endeavor that is focused on improving the efficiency of the post-SAGD phase. The research involves an extensive examination of distinct solvents, each formulated with predefined compositions. These solvents are applied at two critical stages within the SAGD process, namely the mid- and late-stages. The primary aim of this research is to offer practical recommendations for optimizing the SAGD operation. These recommendations are the outcome of a rigorous evaluation of how well the chosen solvents perform in terms of recovering oil and their potential for being reclaimed and reused. This evaluation process incorporates a combination of visual experiments, which allow for qualitative observations, and more quantifiable core flood tests, providing a comprehensive understanding of the solvent's effectiveness in the SAGD process.

**Chapter 7.** General conclusions, potential contributions, and future works are covered in this chapter.

## **Chapter 2: What Did We Learn from Steam Assisted Gravity Drainage (SAGD) Applications in Three Decades, and What is Next?**

This chapter of the thesis is a modified version of a published research paper. The conference paper version SPE-212970-MS was presented at the SPE Western Regional Meeting, Anchorage, Alaska, USA on 22–25 May 2023. The journal version of this research paper has been published in *Geoenergy Science and Engineering Journal*.

## 2.1 Preface

Steam-assisted gravity drainage (SAGD) has proved to be a technically and commercially successful methodology for recovering heavy-oil in Canada. At present, there are 22 commercial SAGD projects with over 300 pads and 2,700 well pairs, contributing to nearly 1.4 million bbl/day of production. The steam growth in the steam chamber could recover up to 60% of the oil-in-place by a typical SAGD project. However, some SAGD projects are only able to present less than 20% of the recovery factor, even though they have been producing for almost decades. Currently, the steam-to-oil ratio (SOR) for most SAGD projects ranges between 2 and 4 bbl steam/bbl oil. Nevertheless, some projects are still experiencing SOR of over 4 bbl/bbl due to the aggressive steam injection.

Despite the efficacious evidence and enormous contribution to oil production, many questions regarding the current SAGD project performance are still rising. The process and execution are very complex and entail great operational excellence. The thermodynamic processes (heat transfer, wettability alteration), reservoir geology (thickness, vertical conformance, steam channeling), well designs (optimal placement of the pairs, well completions), and environmental concerns (GHG emission) are also limiting factors to be detrimental to SAGD performance. Some other techniques to recuperate heavy-oil and bitumen (e.g., co-injection)—in addition to the principal SAGD—have been insinuated and employed in the projects. The efforts only presented a 5–10% of success rate.

This paper focuses on extensive evaluation and analysis of the ongoing SAGD projects over the last three decades in Canada and what would be the forthcoming potential of mature SAGD. Lessons learned and limitations from historical and current SAGD applications based on the evaluation of 22 commercial SAGD projects are presented. Success and failure stories were evaluated from geological, technical, environmental, and operational points of view. The reasons behind the successful applications of existing SAGD practices were listed. In the end, suggestions were made as to the proper design of new SAGD projects and future practices in the matured fields.

Some new insights for the future of mature SAGD, including “zero emission” applications using solvents and reduced emission using steam additives, are also discussed. The conclusive analyses

done, and the recommendations made will lead to more efficient SAGD applications (new and matured) in Canada, also providing a useful road map for the other parts of the world.

**Keywords:** History of SAGD, future of SAGD, efficiency improvement, GHG emission, lessons learned

## 2.2 Introduction

Since heavy-oil and bitumen play an essential role in the world's energy supply, many efforts have been devoted to the research, explorations, and recoveries of heavy-oil and bitumen resources. As a heavy-oil-and-bitumen-rich country, Canada has pioneered the SAGD as a pivotal heavy-oil and bitumen recovery technique from technical and commercial perspectives. The SAGD technique was first conceptualized by Butler (1985) and further tested through the Underground Test Facility (UTF). The UTF was built in the northern part of Fort McMurray and funded by the Alberta Oil Sands Technology and Research Authority (AOSTRA) in 1987. The in-situ test was initiated through the Phase A pilot test involving three horizontal well pairs encompassing 55 m lateral length and 24–25 m well spacing (Edmunds et al. 1994). The injector was assembled parallel to and about 5 m over the producer. The success, lessons learned, and best practices of this pilot test have encouraged the oil and gas industry to invest and establish Phase B, which was the first commercial pilot SAGD performed at the same test facility between 1990 and 1992. Phase B consisted of three horizontal well pairs comprising 500 m lateral completion and 70 m well spacing (Edmunds and Gittins 1994; Collins 1994). Phase B pilot commercial SAGD was forecasted to attain a bitumen recovery of up to 45%. However, the realization of the recovery surpassed the initial plan by over 65%.

Over the last three decades since the pilot SAGD application was studied and successfully tested, more than 20 commercial SAGD projects have been established in Canada, and this recovery technique has been standardized as an ideal technique to recuperate heavy-oil/bitumen. Currently, more than 85% of active SAGD projects are operating in the Athabasca area, and the remaining

are in the Cold Lake area—contributing up to 25% of Canadian total oil production. Even though these SAGD fields have been in production for decades, nearly 25% of the active fields are still experiencing less than 20% of heavy-oil/bitumen recovery—even some of them are below 5%. Despite the technical advantage, reliability, and feasibility of SAGD, there are still many aspects needed to comprehend—causing recovery by SAGD remains challenging.

A classical analysis of SAGD project performance was first initiated by Ali (1997), highlighting the complexity of the SAGD process with four major concerns, such as condensate flow, geology, effects of geomechanics, and well spacing. In a more field-data-based SAGD performance analysis, Jimenez (2008) performed the analysis of up to 8 SAGD projects in Canada. The analysis done was based on 32 SAGD pads. Moreover, the analysis also captured that the operational excellence and optimization in SAGD projects appear to be the determining factor of heavy-oil/bitumen recovery in addition to the reservoir geology, well spacing, and well pair lateral length. Another method of performance analysis was conducted by Ito (2014). A well-pair-based analysis and numerical simulation were adopted as a point of view in evaluating the performance of SAGD projects in Canada. According to the analysis, the steam chamber is a critical parameter governing the overall SAGD performance. Hence, controlling the steam chamber height to the optimal level could substantially improve SAGD performance. Two decades after the first SAGD paper was published, Ali (2016) performed another field-data-based analysis, highlighting the performance of 11 SAGD projects, including the evaluation of the co-injection technique. In addition, despite all these critical parameters affecting SAGD performance (e.g., geology, geomechanics, condensate flow, steam chamber height, well completion, operational excellence), reservoir dynamics might also add some contributions to overall SAGD performance (Al-Bahlani and Babadagli 2008).

Although SAGD has been successfully implemented in Canada for decades, questions honoring recovery efficiency and environmental issues are still raised. A predominant determining factor (e.g., reservoir geology) that might influence overall SAGD performance is still unclear since some SAGD projects with relatively similar reservoir properties are still experiencing low heavy-oil/bitumen recovery. Factors controlling the process and recovery efficiency such as reservoir thermodynamics (e.g., wettability, interfacial properties), well designs, and operational concepts require more detailed analysis. Moreover, the SAGD projects implementing the co-injection

technique (mainly non-condensable gases) showed a relatively low success rate. A comprehensive field-data-based analysis is required to further address these challenges. This paper reviews and analyzes field data from a total of 22 operating SAGD projects in Canada as well as provides new insights (aligned with the new era low emission operations) for the future of mature and new SAGD projects. Analysis, lessons learned, and recommendations are proposed not only from the reservoir properties perspective but also from other performance indicators and controlling factors in attaining more efficient and sustainable SAGD operation.

### **2.3 Approach for Analysis**

A total of 22 operating SAGD projects in Canada were included in the field-data-based analysis in further evaluating overall SAGD performance. Analysis, discussions, and proposed recommendations are presented and explained based on the adopted methodology as follows:

- All field data and information utilized for each analysis are publicly available and reported by Alberta Energy Regulator (AER) in the forms of in-situ performance annual presentations and statistical reports (ST53) up to Q4 2022.
- Analysis of SAGD performance indicators includes recovery factor, SOR, oil rate, water rate, steam rate, changes in rates, and normalized numbers of drilled wells.
- Analysis of performance controllers includes reservoir geology (e.g., thickness, permeability,  $k_v/k_h$  ratio, porosity), horizontal well lateral length, well spacing between pairs, injector-to-producer vertical distance, and operational executions (e.g., injection strategy, steam distribution, steam pressure, energy input).
- SAGD project clustering is valuable and beneficial for more detailed lessons learned and recommendations. This analysis includes low and high-performing SAGD projects and some well-based analyses (e.g., ramp-up, plateau, and decline stages).

- Some geological information and reservoir properties (e.g., area, thickness, fluid saturations, porosity, permeability, OOIP) provided by each company and accessible through their yearly performance reports were considered in the analyses.
- The pore volume (PV) term was calculated by incorporating the provided data and is expressed as:

$$PV = \frac{OOIP}{S_o} \dots\dots\dots (1)$$

or

$$PV = A h \varnothing \dots\dots\dots (2)$$

where  $A$  represents the reservoir area,  $h$  represents the reservoir net thickness,  $\varnothing$  represents the porosity, and  $S_o$  represents the oil saturation.

- Overall SAGD projects performance demonstrates all active SAGD projects in Canada grouped and plotted to further investigate the performance profile (e.g., oil production, steam injection, recovered oil).
- Information on operational issues experienced by each SAGD project might not be disclosed in detail (or even unavailable) to the public. Hence, some of the analyses, interpretations, and conclusions speculatively rely on the available data from each company, and most of them are limited.

## 2.4 SAGD Projects Performance Analysis

**Tables 1** and **2** present the list of SAGD projects included in this paper and detailed SAGD projects in Canada. Two types of performance analyses are comprised: (1) overall performance and (2) the performance of individual SAGD projects.

**Table 1—List of SAGD Projects in Canada**

No.	Code	Start Production	Oil Prod. (Mbbl/day)	Pads	Well Pairs	Infills	Months of Prod.
1	SAGD 1	2007	123	29	229	-	176
2	SAGD 2	1997	16	11	43	-	306
3	SAGD 3	2014	45	12	81	-	102
4	SAGD 4	2007	15	8	41	25	178
5	SAGD 5	2008	108	23	312	-	166
6	SAGD 6	2010	22	7	39	13	142
7	SAGD 7	2018	7	2	15	-	54
8	SAGD 8	2020	2	2	11	-	30
9	SAGD 9	2013	49	13	118	16	105
10	SAGD 10	2011	1	1	3	-	132
11	SAGD 11	2016	11	8	42	4	78
12	SAGD 12	2015	9	5	24	-	90
13	SAGD 13	2017	23	6	32	-	66
14	SAGD 14	2012	16	5	33	19	125
15	SAGD 15	2002	251	32	352	-	244
16	SAGD 16	2001	193	47	397	-	252
17	SAGD 17	2002	26	9	137	-	238
18	SAGD 18	1999	4	6	23	-	280
19	SAGD 19	2003	226	31	308	51	234
20	SAGD 20	2007	145	16	186	-	181
21	SAGD 21	2003	57	30	216	-	234
22	SAGD 22	2006	19	6	109	7	193
<b>Canadian SAGD Projects Total</b>			<b>1,398</b>	<b>309</b>	<b>2,751</b>	<b>135</b>	

**Table 2—Overall SAGD Projects Performance in Canada. NCG = non-condensable gas, eMSAGP = enhanced, modified steam and gas push, and SAP = solvent-aided process.**

Code	Start Production	Oil Production (Mbb/day)	Water Production (Mbb/day)	Steam Injection (Mbb/day)	cSOR (bbl/bbl)	Pore Volume (MMbbl)	Developed OOIP (MMbbls)	Project OOIP (MMbbls)	Developed RF	Project RF	Avg. Net Pay (m)	Avg. Porosity	Avg. Perm $K_r$ (mD)	Avg. Perm $K_v$ (mD)	Kv/Kh	Pads	Well Pairs	Infills	Avg. Well Pair Spacing (m)	Avg. Well Lateral Length (m)	P – I Vert. Distance (m)	Initial Reservoir Pressure (psi)	Avg. Inj. Pressure (psi)	Initial Reservoir Temp. (°C)	Started Co-Injection	Implemented Co-Injection
SAGD 1	2007	123	330	295	2.5	1,388	1,064	4,780	35%	7.8%	38	33.9%	4,000	1,100	0.3	29	229	-	100	-	5	-	409	-	2018	NCG - fuel gas, methane
SAGD 2	1997	16	70	69	4.0	161	106	315	44%	14.8%	21	33.0%	4,000	3,400	0.9	11	43	-	90	850	5	464	464	15	-	-
SAGD 3	2014	45	136	136	3.8	442	281	7,059	36%	1.4%	35	32.0%	7,000	6,250	0.9	12	81	-	100	700	5	-	232	-	2019	NCG
SAGD 4	2007	15	55	52	4.2	149	119	888	44%	5.9%	25	33.0%	3,000	2,500	0.8	8	41	25	100	750	5	653	477	13	2020	NCG
SAGD 5	2008	108	277	243	2.4	1,014	780	4,199	36%	6.7%	24	33.0%	5,000	2,500	0.5	23	312	-	100	750	5	305	342	13	2013	eMSAGP
SAGD 6	2010	22	75	63	3.2	196	165	544	42%	12.7%	26	34.0%	5,300	4,100	0.8	7	39	13	100	850	5	363	454	14	2019	NCG
SAGD 7	2018	7	18	22	3.0	71	65	253	15%	3.8%	26	31.0%	4,500	2,600	0.6	2	15	-	100	-	5	-	539	-	-	-
SAGD 8	2020	2	12	14	10.0	56	38	38	2%	1.7%	22	32.0%	2,700	1,970	0.7	2	11	-	100	700	5	94	306	8.5	-	-
SAGD 9	2013	49	186	182	2.8	361	321	1,698	33%	4.9%	23	33.3%	5,000	1,450	0.3	13	118	16	100	750	5	-	-	-	-	-
SAGD 10	2011	1	2	2	3.6	88	5	126	31%	1.3%	25	36.0%	3,450	3,024	0.9	1	3	-	100	-	5	247	301	13	-	-
SAGD 11	2016	11	51	60	4.3	216	170	2,891	10%	0.5%	13	33.0%	3,300	2,400	0.7	8	42	4	125	850	5	45	279	6	2018	NCG
SAGD 12	2015	9	33	32	4.5	119	95	126	20%	15.0%	27	34.6%	4,840	3,380	0.7	5	24	-	100	750	5	87	296	8	2020	NCG
SAGD 13	2017	23	75	70	2.8	124	97	685	36%	5.2%	23	33.0%	5,800	4,050	0.7	6	32	-	100	750	5	-	591	-	2020	NCG
SAGD 14	2012	16	58	55	2.8	102	95	1,147	44%	3.6%	17	35.8%	3,500	3,010	0.9	5	33	19	100	800	5	435	439	20	2019	NCG
SAGD 15	2002	251	550	511	1.9	1,892	1,145	4,881	57%	13.5%	45	31.0%	10,000	7,000	0.7	32	352	-	90	700	5	363	380	12	2013	NCG
SAGD 16	2001	193	469	436	2.5	1,891	1,378	4,554	54%	16.3%	30	34.0%	10,000	8,000	0.8	47	397	-	100	700	5	392	453	12	2013	NCG, SAP (Propane)
SAGD 17	2002	26	69	73	2.7	440	405	1,313	47%	14.4%	21	33.7%	5,000	2,500	0.5	9	137	-	100	1,000	5	58	190	6	2011	NCG
SAGD 18	1999	4	26	25	3.6	109	94	170	42%	22.9%	24	30.0%	5,774	5,132	0.9	6	23	-	100	900	5	348	537	-	2020	NCG
SAGD 19	2003	226	627	615	2.9	3,213	2,377	8,309	33%	2.1%	40	32.2%	3,500	2,500	0.7	31	308	51	150	900	5	116	345	8	2018	NCG
SAGD 20	2007	145	413	385	2.9	1,294	1,035	20,606	32%	1.6%	23	31.8%	4,107	3,415	0.8	16	186	-	135	1,000	5	217	429	-	2017	NCG
SAGD 21	2003	57	157	150	4.3	1,248	824	2,560	21%	6.7%	22	31.0%	4,470	2,270	0.5	30	216	-	100	-	5	-	240	-	2014	NCG
SAGD 22	2006	19	101	91	4.7	394	281	560	25%	12.6%	30	32.0%	3,000	1,800	0.6	6	109	7	100	1,000	5	363	370	16	2020	NCG

### 2.4.1 Overall Canadian SAGD Projects Performance

Since the first successful commercial SAGD in Canada, the development of SAGD projects has been emerging over the last three decades. **Figure 1** displays the historical Canadian SAGD projects growth from 1997. Statistically, about 1–2 SAGD projects were established with over 200 drilled wells per year on average. As of today, Canada has established and achieved 22 active SAGD projects with more than 2,700 wells pairs, 130 infills, and 300 well pads in total.

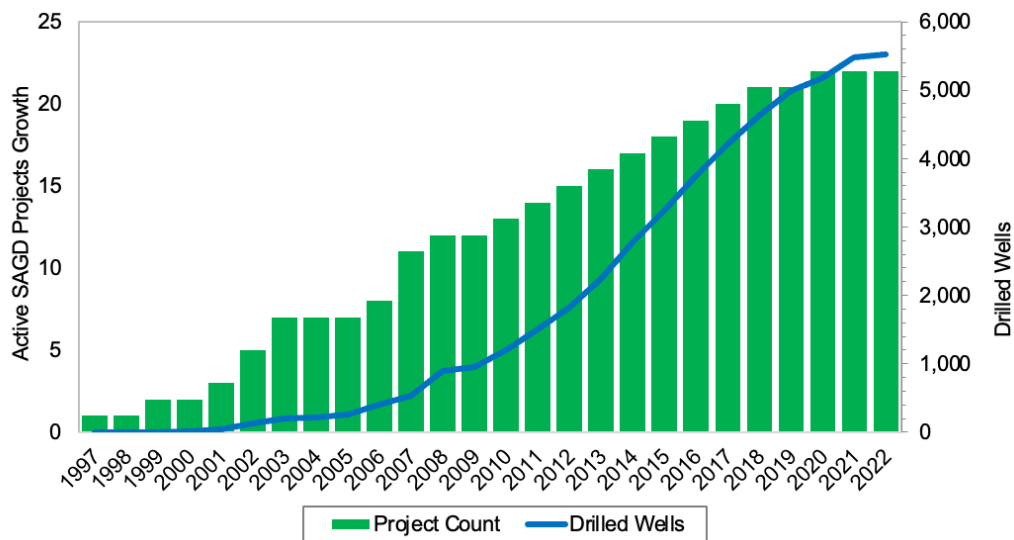


**Figure 1—History of operational SAGD projects growth and number of drilled SAGD wells in Canada.**

These SAGD projects reached a total of nearly 1.4 million bbl/day of production comprising nearly 25% of Canada’s oil production. In a more detailed fashion, **Figure 2** exhibits the overall SAGD projects performance in Canada since 1997. One may observe through the trends in this plot that the establishment of the SAGD projects and the number of drilled and active well pairs hold an essential impact in ramping up the heavy-oil/bitumen production in addition to the successful SAGD technique. A noticeable oil production occurred in the period of 1997–2002. The additional 4 SAGD projects were able to substantially improve the oil production a hundred times the production from one SAGD project in 1997.

Through the production profiles provided in **Figure 2**, one may identify three main phases: (1) initial phase, (2) peak production phase, and (3) plateau production phase. The initial phase represents the beginning of steam injection and oil production. In the first three years of SAGD operation (no additional SAGD projects during this period), a substantial amount of steam was introduced into the reservoirs. During this period, the oil production response was low, which is very common in SAGD operations. At this phase, the steam starts to propagate and initiate the heat transfer to the oleic phase. Due to this mechanism and the involvement of gravity force, oil viscosity reduction and mobilization of some portion of the heavy-oil/bitumen was possible. In other words, a higher amount of heat energy is needed at the initial phase to conductively heat up and initiate the production of cold heavy-oil/bitumen in the reservoir. Hence, a significant rise in the steam-to-oil ratio (SOR) was expected.

The peak production phase embodies the period when oil production starts to ramp up. Technically, at this phase, the steam continues to propagate, expand, and grow a steam chamber upwards and laterally. This mechanism allows the heat transfer between the steam phase and the oleic phase to persist. As a result, more oil production was anticipated—reflected by the significant changes in the production and the SOR profiles. Nevertheless, the rise in oil production might be attributed to the additional SAGD projects and the further response of the previously established SAGD projects.

The plateau production phase is accomplished when the oil production rate persists stably for a certain period, even with additional wells. At this phase, the steam chamber has expanded and stabilized, the steam pressure becomes constant, and the temperature equalizes (close to the steam temperature). In addition, the steam condensate flow might occur, and the residual oil saturation might start to develop during this phase. Up to the present, according to the actual field data, the oil production trend is still at the plateau rate and may or may not continue. However, it is too untimely to make a judgement; thus, more data are still required.

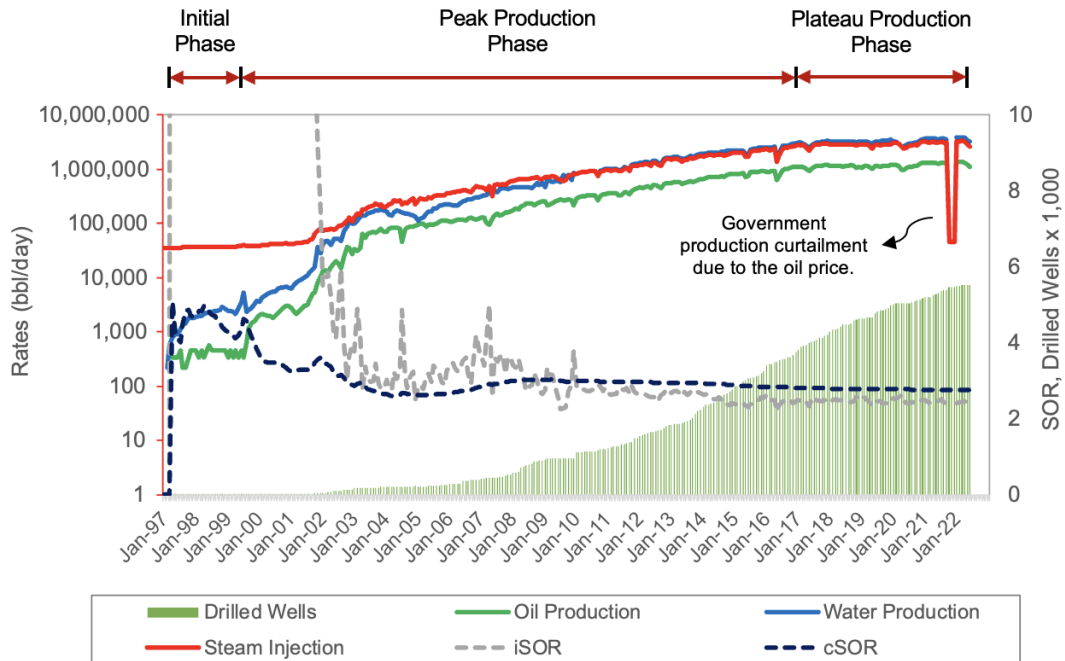


**Figure 2—Overall SAGD projects performance over three decades. iSOR = instantaneous steam-to-oil ratio and cSOR = cumulative steam-to-oil ratio.**

## 2.4.2 Individual SAGD Project Performance

Even though this evidence of overall SAGD project performance gives us some insights into how Canadian commercial SAGD projects have been performing over the last three decades, analyses of individual SAGD project performance are still required to summarize the lessons learned and make decisions for future trends.

### 2.4.2.1 SAGD 1

SAGD 1 is one of the five largest SAGD operations in Canada and has been in production since 2007 and is considered a high-performing SAGD project, comprising 29 pads and 229 well pairs. Non-condensable gas co-injection has been part of this SAGD project since 2018, mainly for steam reallocation and maintaining steam chamber pressure. With technically favorable average oil saturation ( $S_o$  nearly 80%) and stable cSOR at 2.5—considered an efficient SAGD operation—

SAGD 1 contributes over 123,000 bbl/day of oil production, or nearly 3% of Canada’s total oil production. However, the current recovery factor is still less than 40%. This challenge might be caused by the steam propagation/conformance issue—corroborated by the geological data showing that the ratio between the vertical permeability ( $k_v$ ) and horizontal permeability ( $k_h$ ) is only 0.3, i.e., the  $k_v$  is way lower than the  $k_h$ —limiting the steam propagation and expansion upwards, and steam chamber expansion and stabilization. **Figures 3 and 4** exhibit the overall performance of SAGD 1.

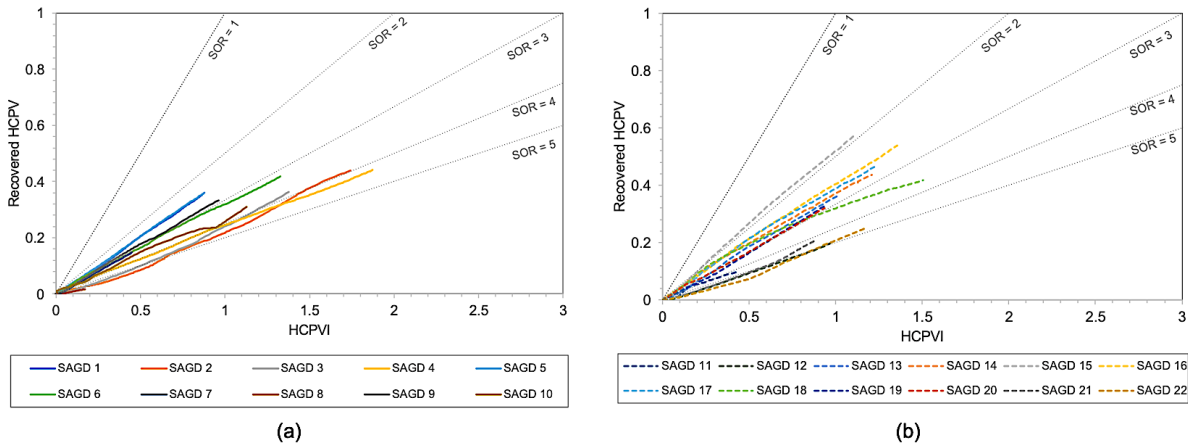


**Figure 3—Profile of recovered HCPV vs. HCPVI with cSOR. (a) SAGD 1–10, and (b) SAGD 11–22. HCPVI = hydrocarbon pore volume injected.**

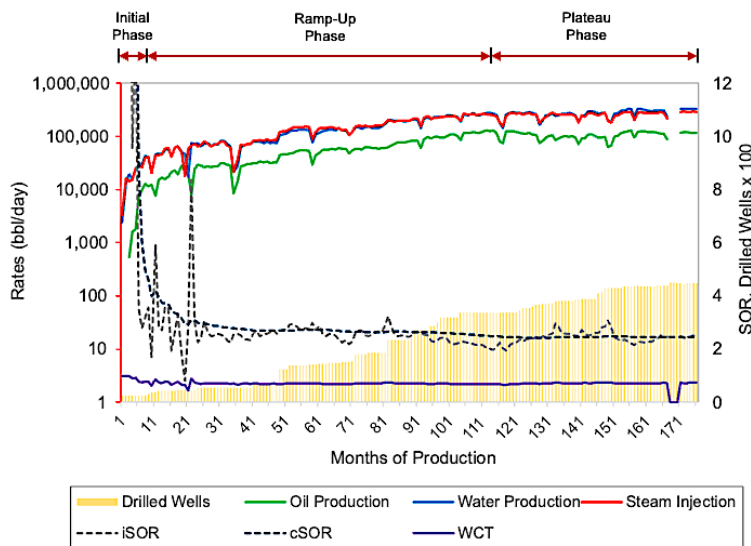


**Figure 4—Overall SAGD project performance of SAGD 1.**

Since the beginning of its operation, SAGD 1 has been able to maintain its production performance. Even when the first steam injection was commenced, SAGD 1 resulted in a very good oil production response at the initial phase. By the time of continuous steam injection, more production response was perceived supported by increasing well counts (peak production period). Based on the performance profile, SAGD 1 is currently at the plateau phase, indicated by the consistency of the oil production profile for over 6 years, regardless of the additional well counts. Moreover, the recovered HCPV vs. PVI plot shows a rising slope with even improving cSOR, meaning that SAGD 1 still encompasses valuable prospects to be unlocked.

### 2.4.2.2 SAGD 2

Located in the Cold Lake area, SAGD 2 is one of the oldest Canadian SAGD projects and is still in operation. From 11 pads and 43 well pairs in total, SAGD 2 is currently producing about 16,000 bbl/day from the Grand Rapids formation with the cSOR over 4, indicating that the project is still marginally efficient. However, the recovery factor is below 50% even though this SAGD project has been functioning for almost three decades and is considered fairly mature. The overall project performance is depicted in **Figures 3 and 5**.

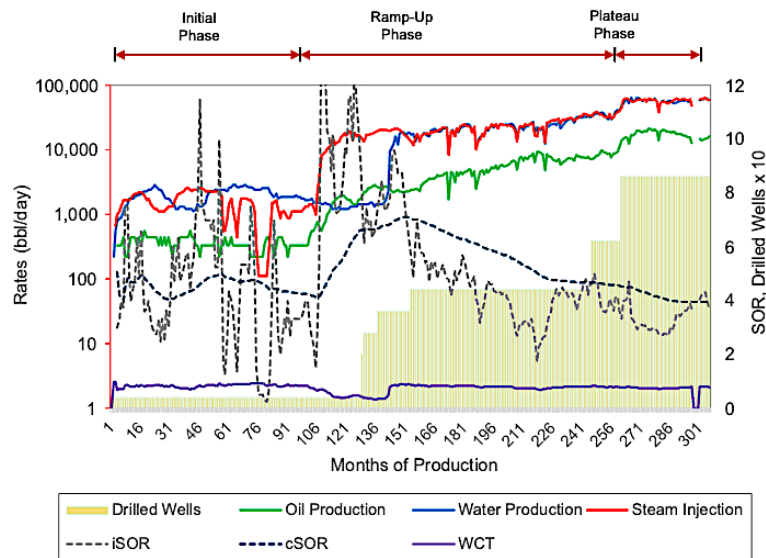


**Figure 5—Overall SAGD project performance of SAGD 2.**

As shown in the performance profile, the initial phase, ramp-up phase, and plateau/decline production phase can be identified. When the project started in 1997 with only 2 well pairs, the oil production was about 350 bbl/day on average and remained persistent for almost 10 years. The delay in the oil production response might be caused by the lack of steam injection (e.g., fewer well pairs, lower steam generation capacity), as more heat energy is needed during the initial phase to initiate the recovery of the heavy-oil/bitumen from the reservoir. The oil production ramped up as SAGD 2 entered the peak production phase circa 2005 and continued for nearly 15 years. This was due to the integration of the increasing amount of steam injection and additional well counts. This phenomenon was also validated by the change of the profile slope in the recovered HCPV vs. cumulative injection/HCPV plot towards improved/lower cSOR, indicating that more oil could be recuperated. The declining oil production profile can be observed not long after the peak production phase. SAGD project optimization efforts should be taken into consideration to prevent further production decline, as the inclining slope in the recovered HCPV vs. PVI profile is still observed—meaning that the improvement for SAGD 2 is still possible.

#### **2.4.2.3 SAGD 3**

Starting its operation in 2014, SAGD 3 is one of the youngest SAGD operations in the Athabasca area, consisting of 12 pads and 81 well pairs in total. As of today, 45,000 bbl/day of oil is being produced from SAGD 3. In terms of the oil production capability, SAGD 3 project can be considered a good performer. However, with such an amount of injected steam (cSOR = 3.8), the recovery factor from the current developed original oil-in-place (OOIP) is still less than 40% (**Figures 3 and 6**).

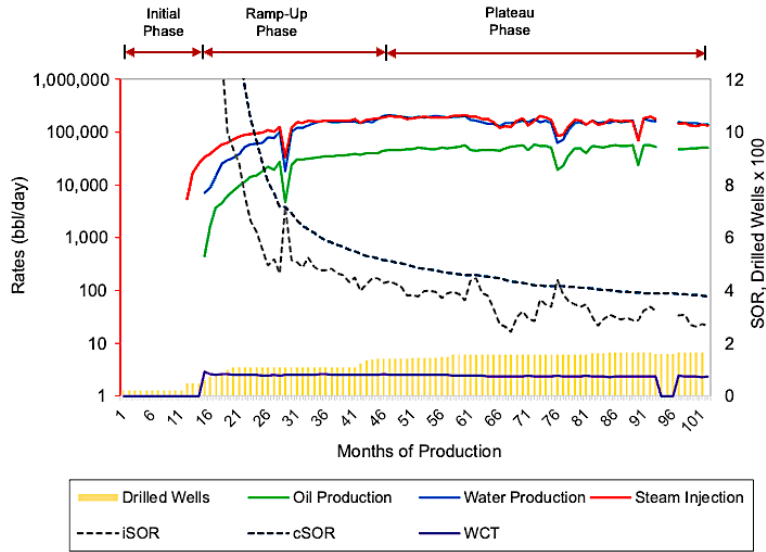


**Figure 6—Overall SAGD project performance of SAGD 3.**

Over the last 9 years of operation, SAGD 3 experienced a delayed oil production response at the beginning of the project life (initial phase). The oil production response was attained several months after the start of steam injection in addition to the additional well counts. At this period, the steam propagated upwards and sideways, initiated the steam chamber, and convectively heated up the cold oil; thus, more oil production was possible (peak production phase). The peak production phase was achieved and continued with a more stable oil production rate (plateau production phase). Furthermore, at this phase, the overall performance improved as the amount of steam injection could be reduced by also maintaining the oil production. This is also implied by the change in recovered HCPV vs. HCPVI slope toward lower cSOR. In other words, the SAGD project performance improvement and optimization are still possible to extend the plateau production phase. In addition to its operation, SAGD 3 has implied the co-injection (NCG) since 2019. However, this effort seems to have no impact on overall oil production.

#### 2.4.2.4 SAGD 4

SAGD 4 encompasses 8 pads, 41 well pairs, and 25 infill wells among the pads. This SAGD project has been operational for almost two decades and is producing more than 15,000 bbl/day of heavy-

oil/bitumen with excessive steam injection; nevertheless, the recovery factor is still 44% even with the cSOR of more than 4. The overall project performance of SAGD 4 is summarized in **Figures 3 and 7**.

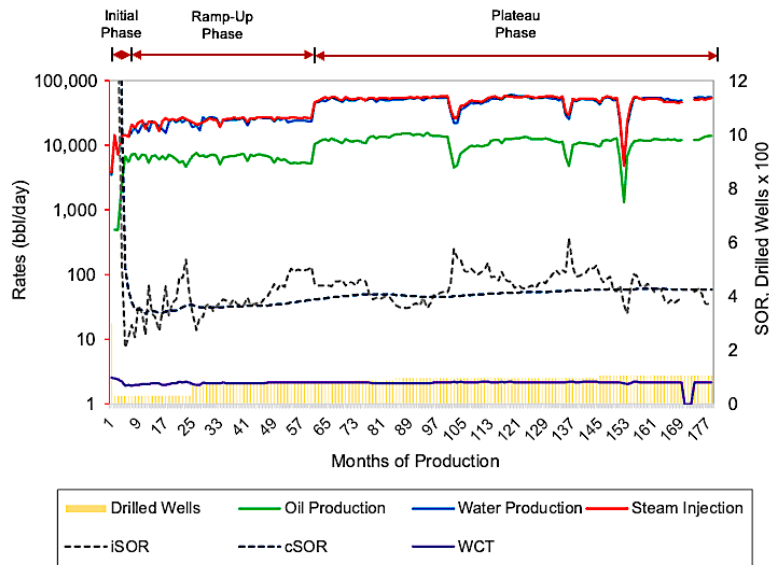


**Figure 7—Overall SAGD project performance of SAGD 4.**

Despite being no delayed production response since the first steam injection and having a longer plateau production phase, the cSOR trend worsened, indicating that escalating amount of steam injection did not present any favorable response to the oil production. The additional well counts did not have any substantial impact on oil production either. The unfavorable outcome might be caused by the steam vertical conformance issue; hence, the steam chamber could not be favorably formed and stabilized—causing ineffective and inefficient heat transfer to the cold oil. In addition, the NCG co-injection effort has been initiated in this SAGD project since 2020 with the main objective of reducing the SOR and improving the production performance, but the improvements in both aspects have not been realized.

### 2.4.2.5 SAGD 5

Since its first operation in 2008, SAGD 5 consistently maintained the overall project performance with a total of 23 pads and 312 well pairs, achieving 108,000 bbl/day of oil production. Moreover, SAGD 5 could auspiciously sustain its cSOR at 2.5 up to the present, shown by the stable cSOR profile and inclining slope in the recovered HCPV vs. HCPVI performance plot. From this perspective, SAGD 5 is considered a good performer (**Figures 3 and 8**).

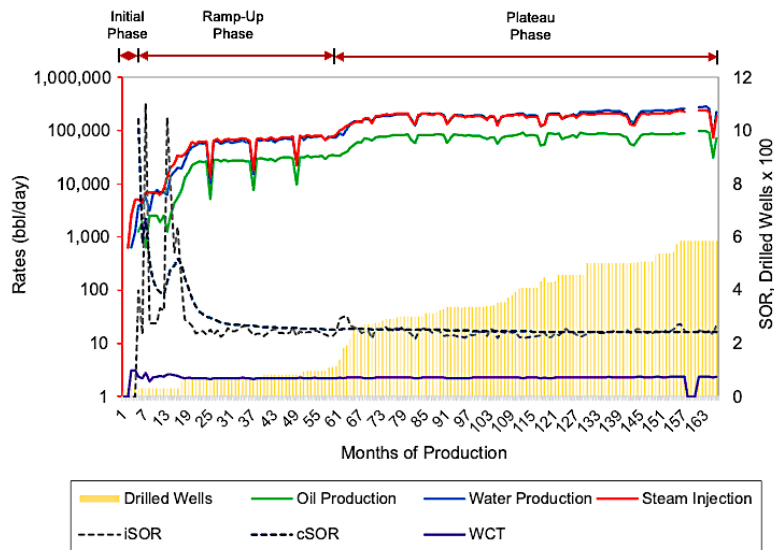


**Figure 8—Overall SAGD project performance of SAGD 5.**

According to the overall SAGD project performance plot, three production phases could be determined. In the initial phase, SAGD 5 experienced a short-term production delay of about 3–4 months, which is very common. Not long after the first commenced operation, SAGD 5 could achieve the peak production phase and ramp up the oil production with the response from the steam injection by also increasing the steam injection rate, in addition to the supplementary well counts. This peak production phase continued for over 6 years and was then followed by the plateau production phase. At this phase, SAGD 5 has been able to sustain its oil production for nearly a decade. Besides, during this phase, a modified steam and gas push was introduced as a co-injection of NCG. However, NCG did not gain any impact neither on the oil production nor the SOR. It is also noticeable that the additional amount of well counts over time did not present any significant

response to the incremental oil production. In other words, the production decline phase might be avoided/postponed due to the response from the additional wells.

### 2.4.2.6 SAGD 6

SAGD 6 has been in operation for over a decade since its first steam injection. With a total of 7 pads, 39 well pairs, and 13 infill wells, SAGD 6 currently contributes 22,000 bbl/day of oil production to overall Canada’s oil production. Considered a moderately mature SAGD operation, SAGD 6 has recovered over 40% of its OOIP and cumulatively injected the steam for more than 1.2 times its pore volume, resulting in the cSOR over 3, which is a marginal value. **Figures 3 and 9** summarize the overall performance of SAGD 6.

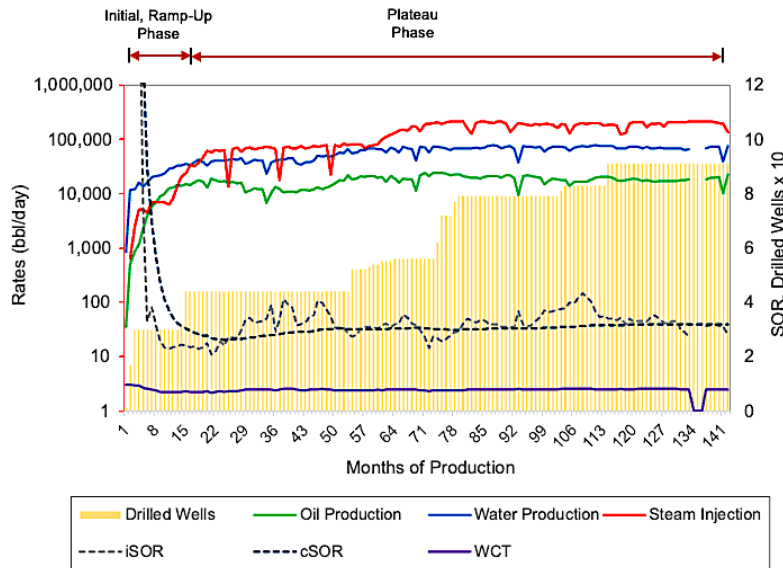


**Figure 9—Overall SAGD project performance of SAGD 6.**

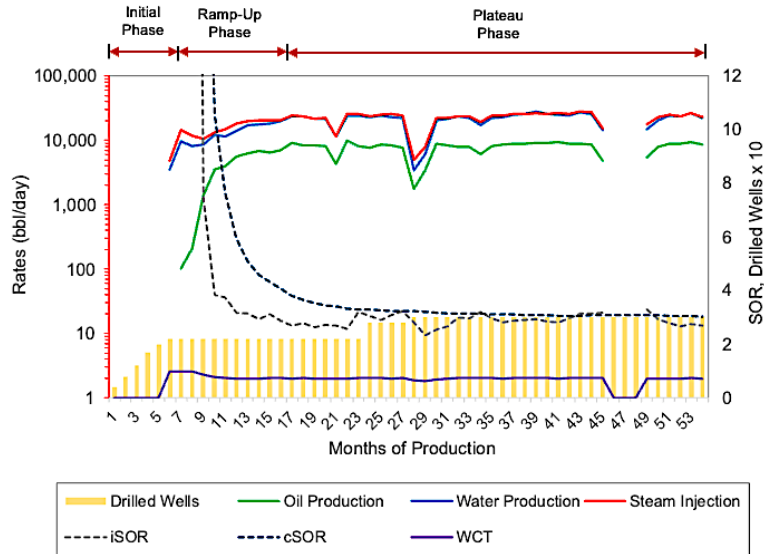
Even though there was no delayed oil production response during the initial phase, SAGD 6 was only able to maintain its peak production for less than 2 years since the beginning of the first steam injection. For the plateau production phase, following observations can be made:

- Additional well counts did not substantially affect the oil production. This could be an indication of the low well productivity of the wells. Hence, no substantial impact on oil production during the plateau production phase was observed. This evidence was substantiated by the geological data (e.g., well logs, cross sections, formation evaluations) provided by the operating company. From these geological data, it can be inferred that the targeted formation comprises shaly/muddy sands—impacting reservoir inflow performance and well deliverability.
- The increasing amount of steam injection (5 years after the first steam injection) did not exhibit any impact on oil production. This case might be instigated by the steam conformance issue. The steam did not propagate and expand effectively. Subsequently, the expansion and stabilization of the steam chamber could not be achieved efficiently; thus, the heat energy distribution could be detrimental, resulting in much less effective oleic phase mobilization in the reservoir. As a result, no significant oil production response, and the cSOR shifted toward a higher value.
- The “do nothing” case (previously established well pairs) could still sustain oil production.

In addition to this SAGD performance insights, SAGD 6 has also implemented the NCG co-injection since 2019 with the foremost objective of optimizing the SOR. However, honoring the overall SAGD project performance, a significant shift in the SOR has not been perceived.

#### 2.4.2.7 SAGD 7

In terms of oil production capability, SAGD 7 is one of the smallest and youngest SAGD operations in Canada, comprising 2 pads and 15 well pairs. With nearly 5 years of project operation, SAGD 7 is able to bring more than 7,000 bbl/day of heavy-oil/bitumen to Canada’s total oil production. Due to the relatively short period of project life, SAGD 7 has only recovered about 15% of its OOIP and injected the steam with nearly half of its pore volume (**Figures 3 and 10**). In other words, SAGD 7 is still immature.



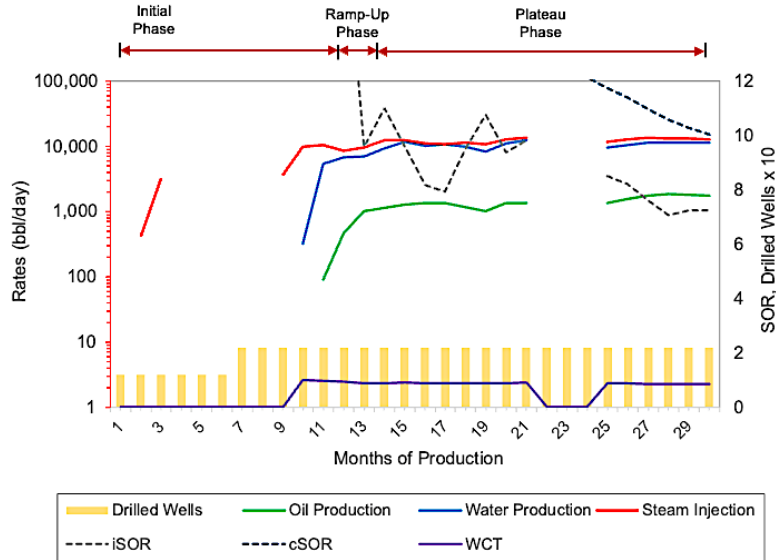
(a)

Figure 10—Overall SAGD project performance of SAGD 7.

The cSOR of over 3 indicates fairly aggressive steam injection. However, for a juvenile SAGD project, it is very common and acceptable to inject more steam to heat up the reservoir as more heat energy is required at this initial phase to initiate the oil production. By evaluating SAGD 7 project performance, one may state that there are still plenty of opportunities to gain its performance by implementing well pairs development program, production-injection strategy, and operational excellence.

#### 2.4.2.8 SAGD 8

Similar to SAGD 7 project, this SAGD 8 project is one of the smallest and youngest SAGD operations in Canada. Starting its operation in 2020, SAGD 8 is currently producing 2,000 bbl/day from 2 pads and 11 well pairs. The overall summary of the SAGD 8 project performance is given in **Figures 3** and **11**. SAGD 8 project was shut-in in 2015 until another operating company took over in 2019.



**Figure 11—Overall SAGD project performance of SAGD 8.**

SAGD 8 has been undergoing with very high cSOR value of over 10 and is currently the highest cSOR among Canadian SAGD operations. At this point, SAGD 8 seems to be underperforming; nonetheless, it is too early to establish any conclusion as this project is still premature with a recovery factor below 2%. Besides, SAGD 8 comprises the lowest  $k_v$  and  $k_h$  values (only the order of 2,000 mD) among the entire SAGD projects in Canada. These reservoir properties might also be the predominant factors affecting the overall SAGD 8 recovery performance. However, more field performance data are still required to further evaluate SAGD 8 project—particularly validating the oil production in response to steam injection, even though the production phases could be speculated from the current performance. The improvement and optimization efforts (e.g., additional well pairs, production–injection strategy, lateral length extension) for this SAGD project could be feasible since this is still a young SAGD project.

#### 2.4.2.9 SAGD 9

With the current oil production of 49,000 bbl/day produced from the McMurray formation, SAGD 9 could constantly maintain its performance for a decade. Since its first operation in 2013 with the 13 developed pads, 118 developed well pairs, and 16 infills, SAGD 9 was able to recuperate less

than 40% of its developed OOIP—meaning that SAGD 9 has not reached its maturity. By maintaining the cSOR between 2–3, SAGD 9 could sustain its performance up to the present. The overall project performance of SAGD 9 is presented in **Figures 3** and **12**.

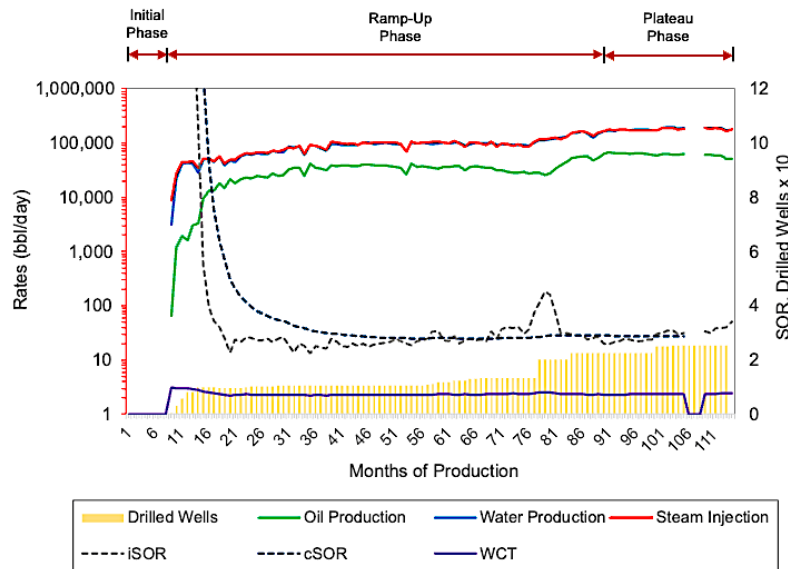


**Figure 12—Overall SAGD project performance of SAGD 9.**

According to the project performance of SAGD 9, the oil production delay after the first steam injection can be observed at the initial phase, which was expected. As the steam was continuously injected, after about 3–4 months, the oil production ramped up. At this peak production stage, oil production kept rising in response to the continuous steam injection. The additional number of well pairs also presents valuable contributions to the production performance. A similar behavior could also be observed after about 7 years since the first SAGD 9 operation. The increasing amount of steam injection, as well as the additional well counts, could present positive impacts on the incremental oil production until achieving the plateau production phase. This evidence indicates that SAGD 9 responds very favorably to the steam injection and well pairs development program (additional well counts)—creating this SAGD project one of the high-performing SAGD projects in Canada. Despite the favorable overall SAGD project performance, a potential oil production decline trend could be noticed in the last several months.

### 2.4.2.10 SAGD 10

SAGD 10 is the smallest SAGD project in Canada in terms of oil production. Encompassing only one pad and 3 well pairs in total, SAGD 10 is currently producing less than 1,000 bbl/day and has only reached 30% of the recovery factor, which is underperforming for a SAGD project with more than a decade of operation. Moreover, the cSOR has reached nearly 4 (Figures 3 and 13), which is a marginal value for an efficient process.

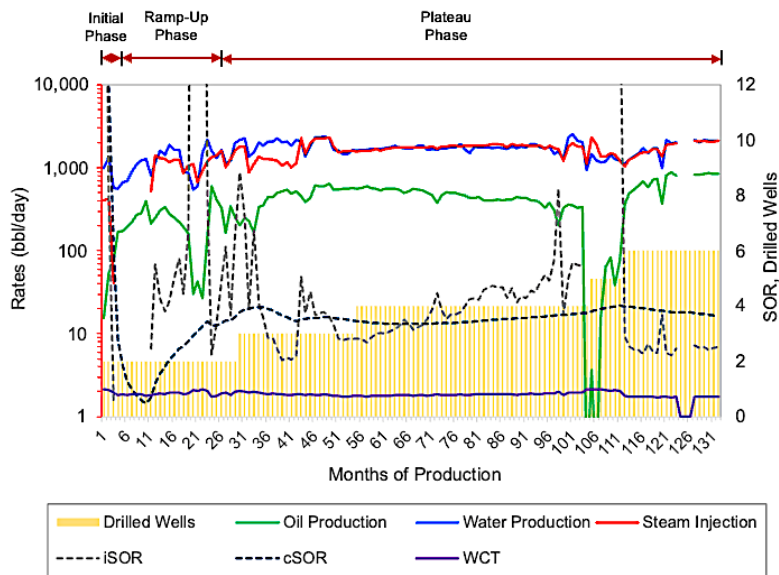


Figure 13—Overall SAGD project performance of SAGD 10.

Even though the performance profile presents no production delay after the first steam injection, SAGD 10 might have experienced individual/well pair issues, indicated by the unstable production profile. This phenomenon is also corroborated by the acid jobs data provided by the managing company—meaning that the wells might have been experiencing severe scale build-up in the wellbores; therefore, blocking the production. In terms of the geological point of view, the well logs present relatively clean sand. The ratio between the vertical permeability ( $k_v$ ) and horizontal permeability ( $k_h$ ) is close to 1, indicating that there should have been no concerns regarding the steam propagation/conformance. In other words, the predominant factor impacting SAGD 10 performance could be due to the scale build-up in the wellbore triggered by several factors, such

as incompatibility of injected steam and formation water (e.g., components, ions), temperature, partial pressure difference, and pH difference between the injected steam and existing formation water.

### 2.4.2.11 SAGD 11

Entailing a total of 8 well pads, 42 well pairs, and 4 infills, SAGD 11 is currently producing heavy-oil/bitumen of around 11,000 bbl/day from the MacMurray formation. After more than 7 years of SAGD operation, SAGD 11 has only achieved 10% of the recovery factor. For a SAGD project which has been in operation for almost a decade, SAGD 11 is considered a low-performing SAGD project in Canada with such a high cSOR over 4. In addition, NCG co-injection has also been implemented in this SAGD project since 2018 to pressurize the top gas zone/gas cap but no significant impact on oil production was observed. **Figures 3 and 14** depict the overall project performance of SAGD 11.

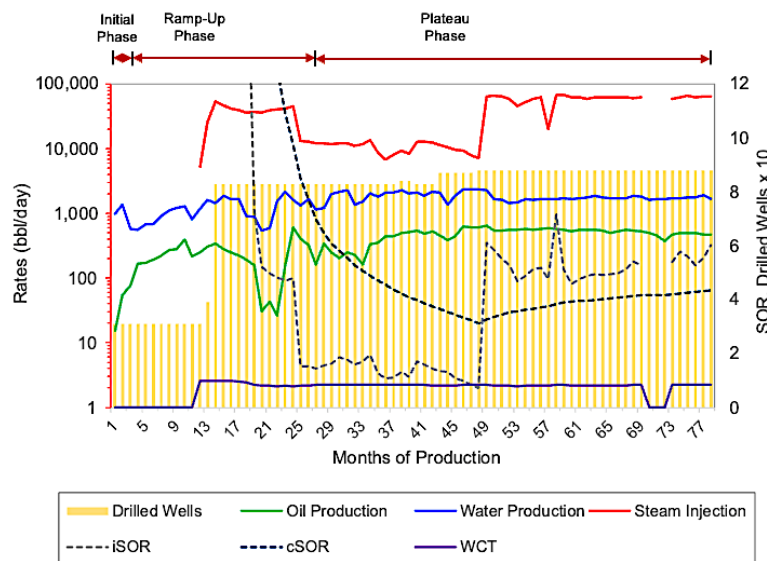


**Figure 14—Overall SAGD project performance of SAGD 11.**

Based on the performance profile, it can be inferred that SAGD 11 has been undergoing challenging production and injection performance, particularly during the peak production phase. The increased steam injection rate was not reflected in the fluid production. The water production

is way lower than the steam injection which is not common. This phenomenon could be triggered by the geological aspect of the reservoir (e.g., heterogeneity, thickness) which could be disadvantageous to the inflow performance as well as steam conformance. This indication is confirmed by the data provided by the managing company, elaborating that the presence of top gas and geological barriers (mud bed) zones—further impacting the steam chamber growth as well as the heat transfer mechanism.

**2.4.2.12 SAGD 12**

SAGD 12 has been part of the active SAGD operations in Canada since 2015. The project has been in production for almost a decade with the current oil production of 9,000 bbl/day from 5 pads and 24 well pairs, and cSOR of almost 5. SAGD 12 recovered nearly 20% of its OOIP prospect, meaning that this project is still underperforming (**Figures 3 and 15**). Similar to the majority of SAGD projects in Canada, it was also reported that SAGD 12 initiated the NCG co-injection, starting in 2015. Nevertheless, the co-injection seems to exhibit no substantial impact on overall SOR or production improvement.

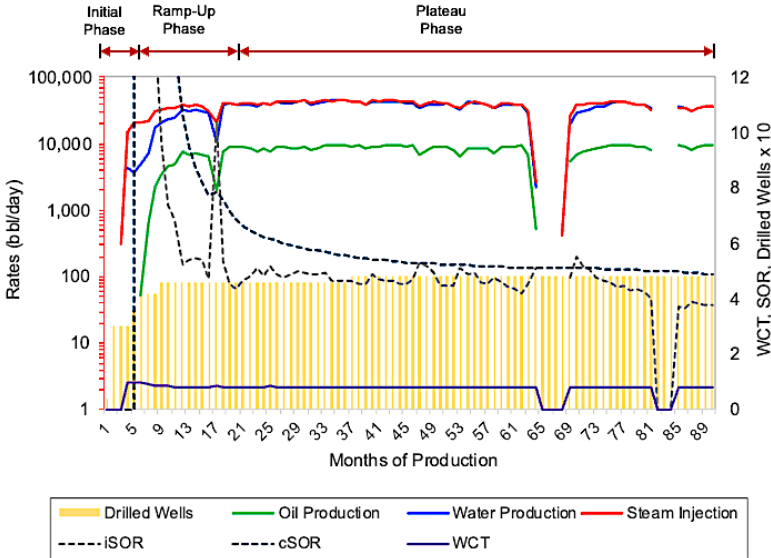


**Figure 15—Overall SAGD project performance of SAGD 12.**

According to the historical SAGD project performance presented in **Figures 3** and **15**, overall performance appears to have no significant issues. However, there is an interesting fact that should be pointed out. The water cut (WCT) profile shows a relatively high magnitude (80–90%), even from the beginning of the project operation. A rise in the water cut in SAGD operation could be instigated by some parameters, such as:

- *Steam quality/steam dryness.* This factor could be a detrimental factor to the overall SAGD performance. Lower steam quality could limit the heat energy transfer to the cold oil and the reservoir and lead to much more water production.
- *Steam condensation.* A relatively quick steam condensation could be triggered by the heat loss during the steam injection process in the reservoir; therefore, limiting the heat transfer and oil production as well as accelerating more water production, even before the steam chamber is stabilized.
- *Reservoir properties (e.g., fluid saturations).* Lower oil saturation ( $S_o$ ) zones could present an essential impact on the overall SAGD performance, particularly oil production performance. According to the provided data, the overall net pay water saturation ( $S_w$ ) is equal to or less than 50%. In other words, some zones comprise even less  $S_o$ ; thus, more water production could be anticipated.

Additionally, the NCG co-injection has been part performed since 2020. Nonetheless, no positive impact on either SOR or oil production could be observed even after almost 3 years of the injection period.

#### **2.4.2.13 SAGD 13**

Starting its first steam injection in 2017, SAGD 13 is currently able to contribute 23,000 bbl/day of heavy-oil/bitumen production from 6 pads and 32 well pairs in total. As of today, the recovery factor of SAGD 13 has achieved almost 40% signifying that this project has reached its maturity. However, plenty of optimization prospects are still available for improving performance. The overall performance of SAGD 13 can be seen in **Figures 3** and **15**.

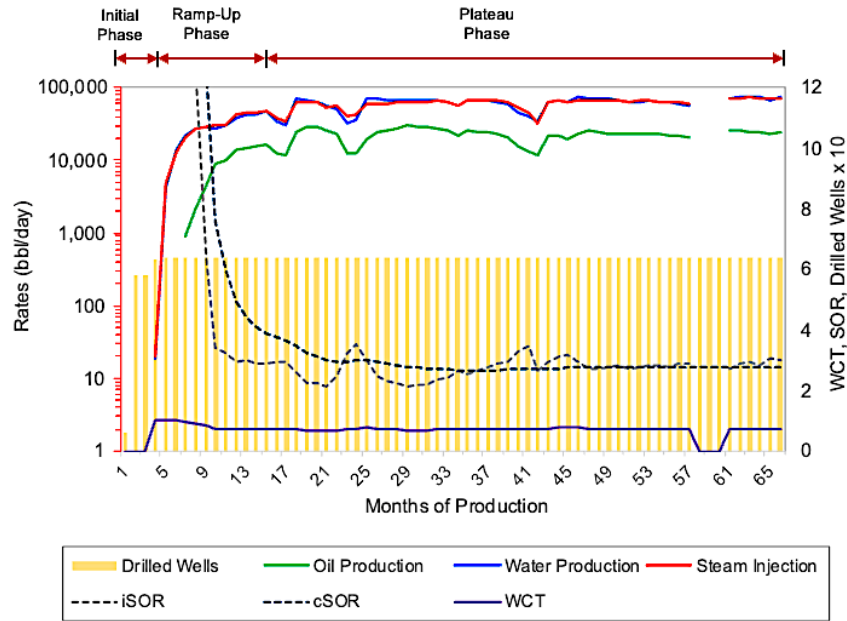


**Figure 16—Overall SAGD project performance of SAGD 13.**

In the initial phase when the steam was first injected, SAGD 13 experienced delayed production response for almost 4 months and the response could be perceived then after. From the beginning of the peak production phase, oil production continued to intensify due to the response from the steam injection in addition to the continuous well pair development. Besides, at this stage, the amount of steam introduced was significantly increased—allowing the steam to heat up the cold oil. As the plateau production was achieved, the oil production of SAGD 13 became more stable. At this stage, the stabilization of the steam chamber and heat distribution could be anticipated. The overall WCT also shows a value below 75% which is a good sign. NCG co-injection has been employed in SAGD 13 operation beginning in 2020 for pressure maintenance. No substantial improvement was evidenced in either overall cSOR or oil production; thus, the NCG co-injection effort might be revisited.

#### 2.4.2.14 SAGD 14

SAGD 14 is one of a few Canadian SAGD projects located in the Cold Lake area comprising Lloydminster formation as a primary producing reservoir. SAGD 14 pilot project was initiated in

2012 with an initial production of over 16,000 bbl/day from only one well pair. As the number of well pairs increased, SAGD 14 was able to ramp up its production capacity to 15,000 bbl/day with an overall cSOR below 3 (**Figures 3 and 17**). In terms of the recovery factor, 36% of its OOIP has been achieved. For a SAGD project which has been in operation for over a decade, SAGD 14 can be categorized as an immature and high-performing project.

From the project performance standpoint, the additional numbers of well pairs and increased amount of steam injection contributed to the overall SAGD performance. A remarkable oil production response was perceived shortly after the amount of steam injection was increased during the peak production phase. To be specific, the integration between the steam injection and additional well pairs provided a very favorable impact and contribution to oil production. As SAGD 14 reached the plateau production phase, the oil production rate is perceived to be fairly constant for almost 7 years. Nonetheless, the additional wells during this period seemed to present no significant impact on oil production. This undesirable condition could be possibly affected by:

- *Lower oil content/ $S_o$  in the producing reservoir.* According to the geological data (e.g., well logs), it is reported that at the lower part of the formation—in which the producers were drilled—zones with lower resistivity zone exist, meaning that the producers are positioned in the intervals encompassing higher  $S_w$ .
- *Penetration of the lateral section of the producer into the oil/water contact (OWC).* The well logs also confirmed the presence of OWC existed just below the lowest known oil (LKO) zone in one sand body without any barriers. There is a possibility of the producer hit the OWC.
- *Bottom water coning.* As confirmed by the geological data, the existence of the OWC in one sand body could be detrimental to the oil production performance. Furthermore, SAGD 14 utilizes an electrical submersible pump (ESP) as its artificial lift method. This type of artificial lift could lead to a relatively significant pressure difference; thus, the bottom water could enter the producer. One may contemplate that bottom water coning is possible in this field (Sugianto and Butler 1990; Shahbaz et al. 2012).

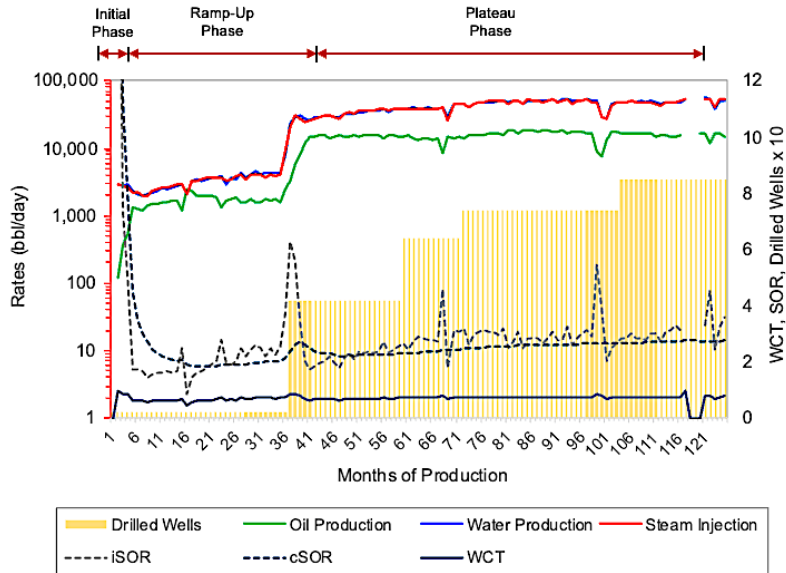


**Figure 17—Overall SAGD project performance of SAGD 14.**

This evidence is also validated by the project performance profile (**Figure 17**). Significant water production was observed during this stage with no incremental oil production reflected by significantly increasing WCT value —resulting in the shift of the recovered HCPV vs HCPVI profile toward a higher SOR value. In addition, SAGD 14 has implemented NCG co-injection since 2019. Regardless of this implementation, no notable improvements in SOR or production performance could be perceived.

#### **2.4.2.15 SAGD 15**

SAGD 15 is currently the major contributor to SAGD operations in Canada, producing 251,000 bbl/day or more than 5% of total Canada’s oil production. SAGD 15 consists of 32 pads and 352 well pairs. Having been in operation for more than two decades, SAGD 15 has accomplished a recovery factor of almost 60%. Based on its recovery factor, it can be said that SAGD 15 has reached its maturity stage. Despite its maturity stage, this high-performing SAGD project has been able to maintain an excellent overall cSOR. The overall SAGD project performance is presented in **Figures 3 and 18**.

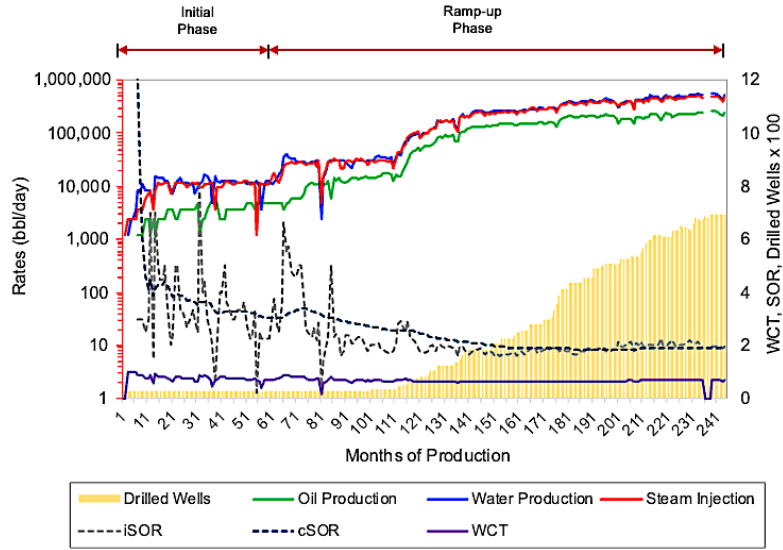


**Figure 18—Overall SAGD project performance of SAGD 15.**

SAGD 15 shows a distinctive behavior compared to other SAGD projects in Canada. It is still in the ramp-up phase even though the project has been active for a very long period (over two decades). This auspicious performance is also signified by its SOR value of 1.9—enabling this to be the best cSOR of the entire SAGD projects in Canada. This remarkable performance can be attributed to the following factors:

- *Better geology/reservoir properties.* Although most SAGD projects in Canada are located in the Athabasca area and producing from the McMurray formation, SAGD 15 encompasses very propitious reservoir quality compared to the other SAGD projects. The permeability of the formation is on the order of 10,000 mD which enables SAGD 15 to have way better oleic phase mobilization and steam chamber propagation/expansion and stabilization in the reservoir.
- *High oil content ( $S_o$ ).* From the reported geological/reservoir data, it is evidenced that the average  $S_o$  in SAGD 15 reached 80% which is very ideal for oil reservoirs. The WCT was maintained below 70% which is the best WCT value among all SAGD projects so far.
- *Project optimization.* With a more established and continuous realization of project optimization (e.g., production–injection strategy, well pair development program), SAGD 15 has been able to sustain its overall performance. The outcome of these efforts is reflected

by the capability of SAGD 15 in maintaining and even continuously improving oil production over the years.

- *Smaller well spacing.* Comprising a smaller well spacing is a good strategy in a SAGD operation. This method does not only allow a SAGD project to have more well pairs in a single pad but also to potentially improve drainage area and promote production acceleration.

Regarding the co-injection effort, SAGD 15 has been implementing the NCG co-injection since 2013. However, since the date of the first gas injection, no noticeable impacts have been carried out. Neither SOR nor production performance has presented any improvements over this period.

#### **2.4.2.16 SAGD 16**

SAGD 16 is the largest SAGD operation in Canada, consisting of 47 pads with nearly 400 well pairs in total. This significantly large operation has positioned SAGD 16 to be the third leading heavy-oil/bitumen producer in Canada with 193,000 bbl/day of oil production originating from the McMurray formation. Furthermore, SAGD 16 has recovered its oil prospect of about 55%. From the overall recovery perspective, it can be considered that SAGD 16 has reached its maturity stage. For a project that has functioned over the last two decades, SAGD 16 has succeeded to sustain its overall performance by also maintaining a good cSOR of 2.5 with a WCT value of below 75%. The project performance of SAGD 16 is summarized in **Figures 3 and 19**.

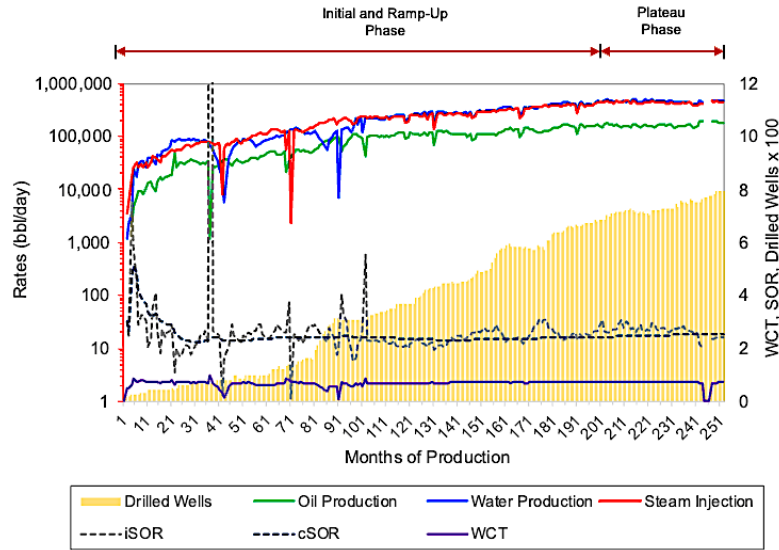


**Figure 19—Overall SAGD project performance of SAGD 16.**

The overall performance profile demonstrates that SAGD 16 project kept up a good performance over the last two decades. The project has been able to prolong the ramp-up phase for more than 10 years which is remarkable. Nonetheless, the plateau phase has been already reached for the SAGD 16 project. Comparable to the SAGD 15 operation, the predominant success factor for the SAGD 16 performance is the reservoir quality of the main producing formation. Based on the geological data provided by the managing company, the average reservoir permeability was reported to be in the order of 10,000 mD with a  $k_v/k_h$  ratio of 0.8. From the fluid saturation standpoint, SAGD 16 comprises an excellent  $S_o$  of up to 85%. Furthermore, all these favorable geologies are strengthened by a good project optimization execution (e.g., production–injection strategy, well pair development program, workovers/routine services) as well as operational excellence. Additionally, the effort of co-injection has also been employed in SAGD 16 project since 2013. There are two types of co-injections implemented in this project: NCG co-injection and solvent-aided process (SAP); however, both techniques resulted in no substantial impact on the overall cSOR and production performance.

### 2.4.2.17 SAGD 17

Similar to overall SAGD projects located in the Athabasca area, SAGD 17 is producing from the McMurray formation with a current oil production of 26,000 bbl/day. To date, SAGD 17 has developed a total of 9 pads and 137 well pairs and has maintained an overall cSOR of 2.7, which is still considered an efficient SAGD operation. Over the last two decades of operation, SAGD 17 has convalesced close to 50% of its prospective OOIP which can be categorized as a moderately mature SAGD operation. **Figures 3 and 20** depict the summary of the SAGD 17 project performance in general.

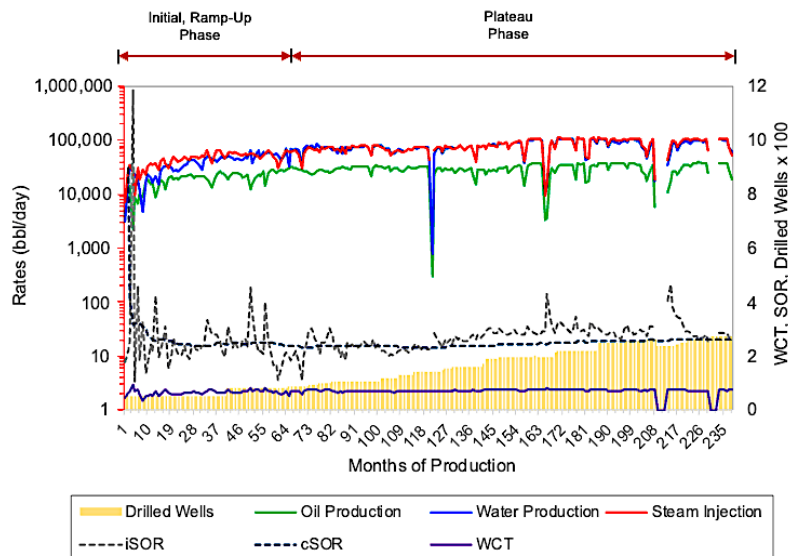


**Figure 20—Overall SAGD project performance of SAGD 17.**

Since the first steam injection, no production delay was observed during the initial phase. In other words, steam propagation and expansion as well as the heat transfer mechanism could effectively occur; therefore, the mobilization of the heavy-oil/bitumen was possible. As SAGD 17 reached the ramp-up phase, the oil production continuously increased as a response to the incremental amount of steam injection and additional well pairs. As the plateau phase was reached, there are a few interesting points to be specified:

- The recovered HCPV vs. HCPVI profile shifted toward higher cSOR (cSOR = 3), indicating that the SAGD operation became less efficient. This condition might be triggered by declining individual well performances.
- The continuous establishment of additional well pairs did not present a significant impact on the overall SAGD performance. Even though the amount of steam injection was increased, no noticeable incremental oil production was perceived. Besides, more water production could be observed during this phase—corroborated by the escalating WCT value. One possible reason causing this phenomenon is the presence of OWC/bottom water in one sand body at some well patterns which has been validated by the available geological data (e.g., well logs, cross-sections). In this case, the additional well pairs could only prolong the plateau phase which is good to a great extent. However, without proper project optimization—with the heterogeneity across the reservoir—the decline phase could be expected soon.

Similar to most SAGD operations in Canada, the implementation of NCG co-injection has been conducted since 2011 with the primary purpose to improve overall SOR and production performance; nevertheless, the realization of the improvements has not been attained.

#### **2.4.2.18 SAGD 18**

SAGD 18 is one of the oldest SAGD projects in Canada and has been in operation since 1999, consisting of 6 pads and 23 well pairs. From these pads and well pairs, SAGD 18 is able to produce 4,000 bbl/day of heavy-oil/bitumen. Over the last two decades, SAGD 18 has recovered up to 40% of OOIP and is still considered an immature SAGD operation. From the overall performance (**Figures 3 and 21**), a few points can be made:

- The plot in the recovered HCPV vs. HCPVI profile has substantially changed toward a much higher overall cSOR value of nearly 4, which is a marginal number for an efficient SAGD application. It is also noticeable from the production profiles that SAGD 18 had been undergoing a circumstance in which the increasing amount of steam injection could not exhibit significant improvement/gain in production performance.

- It can also be observed that SAGD 18 is currently in the decline phase. No plateau phase was perceived after about 6 years of the ramp-up phase which is distinctive compared to the other SAGD projects. Furthermore, additional well counts did not present any improvement in the production performance at all. Besides, the WCT profile shows an increasing trend toward 90%, meaning that more water is produced. This early decline phase might usually occur due to the strong influence of OWC/bottom water just below the lowest known oil (LKO) in one sand body; however, no sufficient geological data (e.g., individual well logs, formation evaluation) were available to validate this speculation.
- SAGD 18 well patterns have reached their maturity stage. The steam chamber has grown/well-developed or even coalesced. More steam condensate flow might have occurred in the steam chamber and be produced; thus, the heat transfer became less efficient because the heat energy generated by the steam was consumed to heat up the steam condensate first and subsequently the adjacent cold oil convectively. If this mechanism occurs, much more amount of steam injection is required to produce more oil or maintain the production performance.

This SAGD operation has also instigated the NCG co-injection effort in 2020. According to available data provided by the operating company, the key objective of this co-injection effort was pressure maintenance and SOR improvement. Nonetheless, the overall SAGD performance profile shows no noticeable improvements in both SOR and production performance.

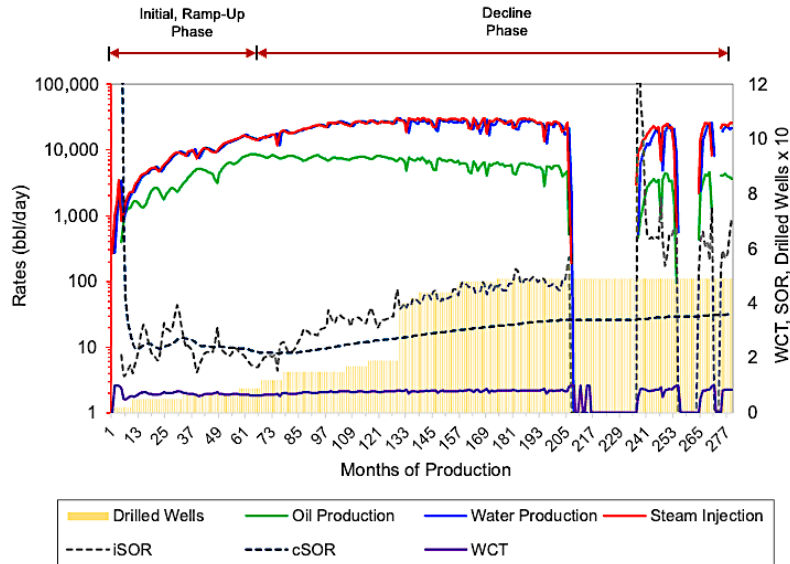


**Figure 21—Overall SAGD project performance of SAGD 18.**

#### 2.4.2.19 SAGD 19

SAGD 19 is currently the second leading SAGD operation after SAGD 15. The project is currently producing 226,000 bbl/day of heavy-oil/bitumen from the McMurray formation in the Athabasca area. SAGD 19 project has developed 31 pads, 308 well pairs, and 51 infills since the beginning of its operation in 2003. Having been on stream over the past two decades, SAGD 19 project has convalesced more than 30% of its recoverable heavy-oil/bitumen. The overall project performance of SAGD 19 can be seen in **Figs. A-1b** and **A-11a**. Based on the production performance, several key messages can be elaborated:

- It is clearly noticeable that SAGD 19 is currently at the plateau production phase—showing a steady production performance for more than 8 years.
- Recovered HCPV vs. HCPVI profile shifted toward a lower cSOR value of less than 3 (cSOR = 2.9), signifying that SAGD 19 turns out to be a more efficient SAGD operation due to the reduced amount of steam injection.
- Well pair development efforts seemed to present less impact on oil production than expected. This occurrence might be potentially caused by the lean zones (mobile water

zones) as the geological data showed lean zones in several parts of the development areas which could hinder the overall production performance.

An NCG co-injection has been implemented in the mature pads. The improvement in overall SOR was noticeable after employing this co-injection effort; however, no substantial gain in production performance was perceived.

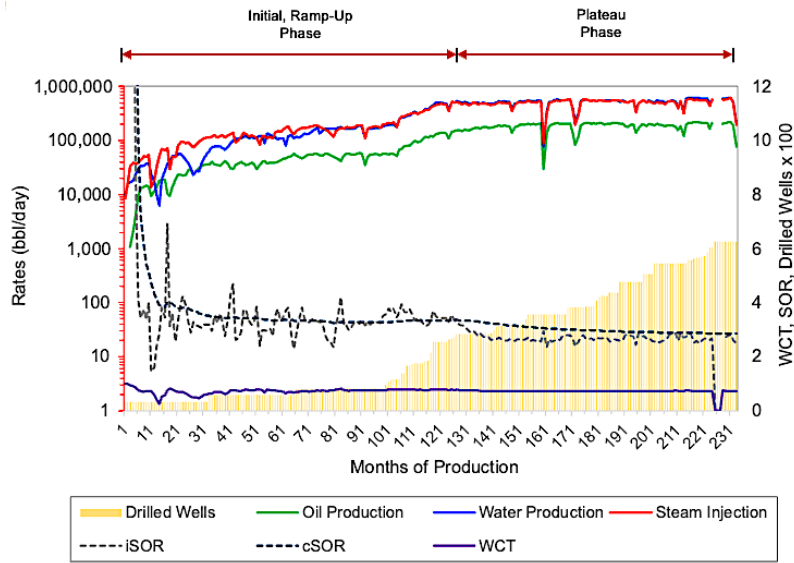


Figure 22—Overall SAGD project performance of SAGD 19.

#### 2.4.2.20 SAGD 20

Operating in the Athabasca area, SAGD 20 is one of the five largest SAGD production contributors in Canada. From a total of 16 pads and 186 well pairs, SAGD 20 is currently delivering more than 130,000 bbl/day of heavy-oil/bitumen production (from the McMurray formation). In the last 16 years of production, SAGD 20 has attained a recovery factor of over 30%. By referring to the recovery factor, SAGD 20 has not reached its maturity—meaning that plenty of prospects are still available. Moreover, NCG co-injection has also been implemented in this SAGD project since 2017. **Figures 3 and 23** exhibit the overall performance of SAGD 20 over almost two decades of SAGD operation. Through the performance indicators given in this plot, it can be inferred that:

- The overall SAGD performance has improved. This improvement is specified by the profile plot of recovered HCPV vs. HCPVI (**Figure 3b**). The slope has shifted to the lower SOR (cSOR = 2.9) which is considered to be an efficient SAGD operation.
- Additional well pairs presented a good response to the incremental oil production. Integration of steam injection management and well pair development effort resulted in a significant improvement in SAGD 20 overall performance.
- The plateau phase could still be prolonged by implementing good production optimization, production–injection strategy, and operational excellence. Therefore, SAGD 20 could still unlock the remaining potential, substantially improve its recovery, and reach its maturity.

Despite the desirable performance of SAGD 20, close monitoring and regular surveillance are essential since the presence of the potential top and bottom water zones were reported in the geological data, which could be the limiting factors to the production performance. These factors must also be considered when proposing additional well pairs.

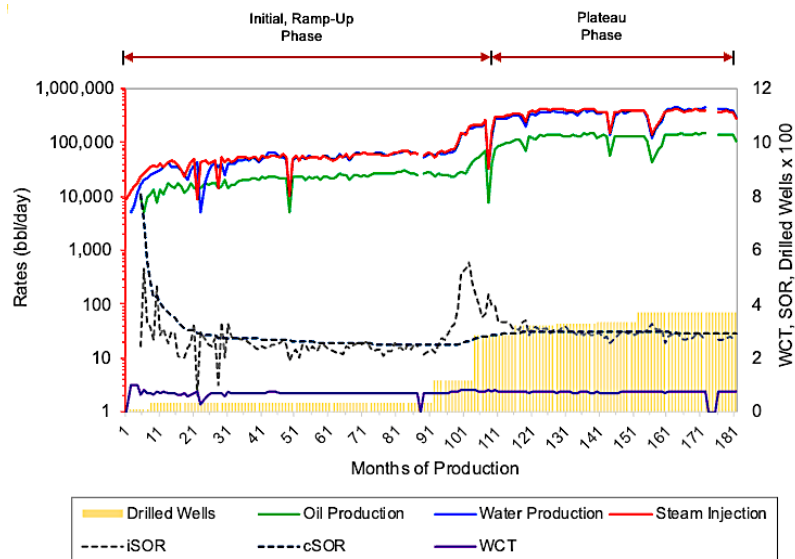


**Figure 23—Overall SAGD project performance of SAGD 20.**

### 2.4.2.21 SAGD 21

SAGD 21 had its first steam injection in 2003. With the current production of 43,000 bbl/day, this project was able to produce more than 20% of its recoverable asset over the past two decades from a total of 30 pads and 216 well pairs. Despite a long period of operation, SAGD 21 still has a long way to reach maturity (even though nearly 20% of its existing pads have reached maturity). Similar to most of the SAGD projects in Canada, SAGD 21 has also employed the co-injection effort utilizing NCG since 2014, but this co-injection effort was suspended in 2015 due to the facility turnaround. The summary of SAGD 21 overall project performance is depicted in **Figures 3 and 24**.

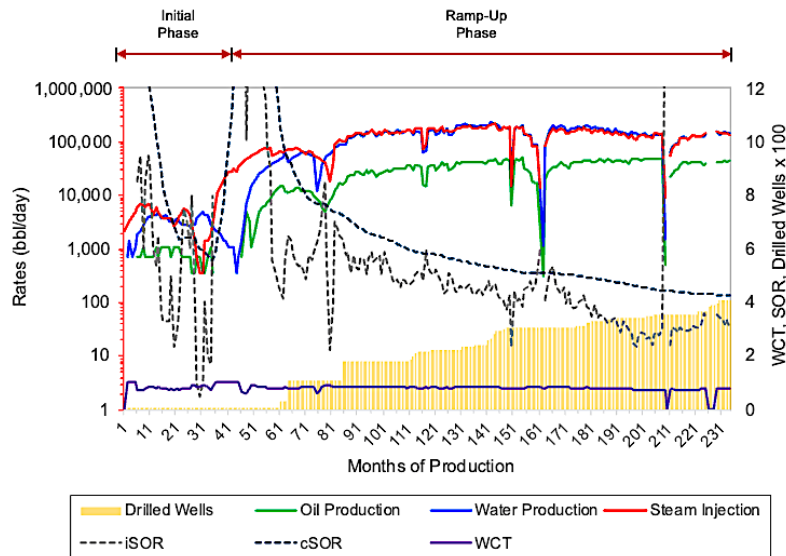


**Figure 24—Overall SAGD project performance of SAGD 21.**

From the overall performance perspective, it can be observed that the establishment of additional well pairs could favorably ramp up the production performance of SAGD 21. This, however, resulted in an increase in water production—validated by the WCT value of nearly 80%. This unfavorable behavior might be triggered by geological/reservoir challenges. According to the available geological data, it was described that SAGD 21 comprises the top and bottom water zones across the reservoir. Subsequently, high  $S_w$  zones ( $S_w$  close to 50%) were also found in the targeted reservoir/intervals. These conditions could be disadvantageous for the SAGD

performance with such high reservoir permeability (in the order of 4,000–5,000 mD)—leading to a slow heavy-oil/bitumen recovery process. Additionally, this ramp-up phase is indicated by the change in the recovered HCPV vs. HCPVI profile slope from a higher cSOR value to a lower cSOR value (**Figure 3**) even though the current cSOR value of 4.3 is still marginal.

#### 2.4.2.22 SAGD 22

SAGD 22 is one of the three SAGD projects operating in the Cold Lake area, encompassing 6 well pads, 109 well pairs, and 7 infills. The first steam injection was started in 2006. SAGD 22 is unique compared to other SAGD projects in Canada since this SAGD project encompasses three producing reservoirs. It is reported that 89% of the well pairs are dominantly producing from the Clearwater formation and the remaining well pairs and infills are producing from the Grand Rapids and Colony formations. From these three producing formations, SAGD 22 has been able to deliver 20,000 bbl/day of oil production with a current recovery factor of 25% (**Figures 3 and 25**).

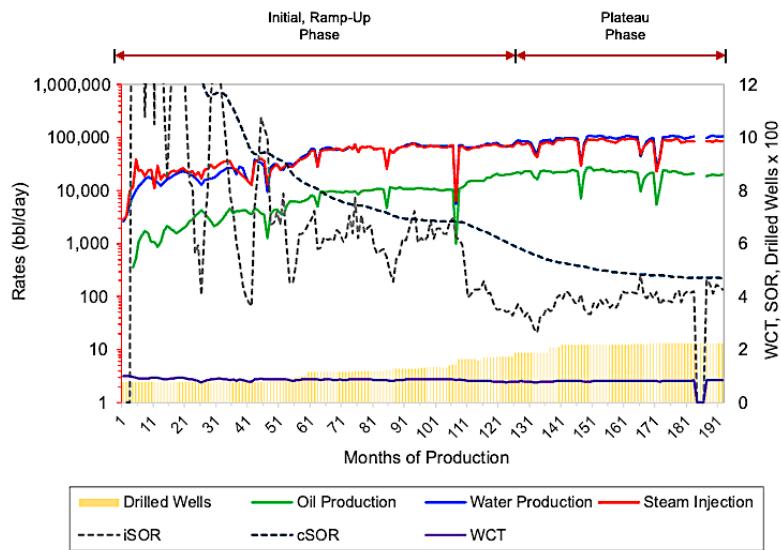


**Figure 25—Overall SAGD project performance of SAGD 22.**

The NCG co-injection has also been part of this SAGD project initiated in 2020. However, since this co-injection effort is new, no available data provided by the company.

A few points can be highlighted from the overall performance:

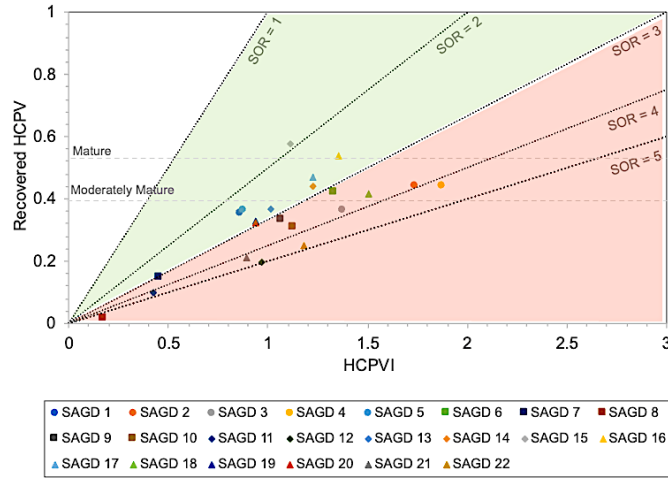
- It is perceived that the slope of the recovered HCPV vs. HCPVI plot has shifted toward lower cSOR, meaning that, technically, SAGD 22 experienced performance improvement. However, the cSOR value still shows a magnitude of 4.9, which is relatively a high value.
- Long-winded recovery might be potentially caused by the geological issues in this SAGD operation, such as the existence of OWC/bottom water in one formation body. The geological data of this SAGD 22 has corroborated this reservoir condition. The bottom water was discovered across all producing formations. Besides, some producers were also found to be drilled in the transition zone. Therefore, more water production could be anticipated. This unfavorable condition is also verified by the WCT value, which is currently close to 90%.

In addition, it is also reported that the producing formations—particularly the Grand Rapids formation—comprise way lower reservoir permeability than other SAGD projects (in the order of 1,000–2,000 mD). This reservoir quality could also be detrimental to the sustainability of the overall project performance.

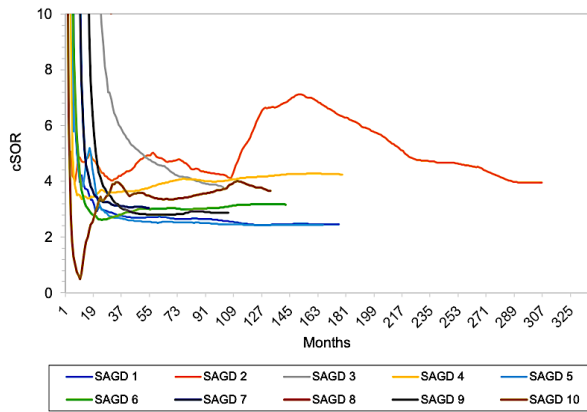
### **2.4.3 High-Performing vs. Low-Performing SAGD Projects**

The quality of a SAGD project is primarily determined by overall SAGD performance (normal SAGD phases/stages), SOR (efficient SAGD operation if cSOR <3), and maturity. Even though there is no exact rule of thumb/guideline honoring maturity, by technical definition, a mature phase is reached when the maximum recovery by steam chamber growth (ultimate recovery) of up to 60% is achieved or at least 40–50% of the recoverable heavy-oil/bitumen, which is categorized as a moderately mature SAGD.

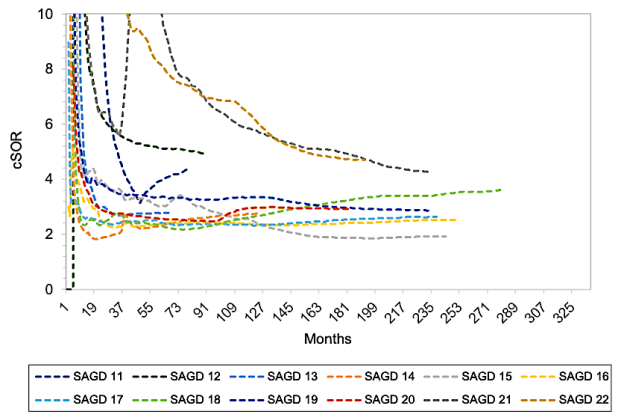
**Figure 26** presents the individual SAGD project performance from the beginning of the project life, showing the cumulative steam-to-oil ratio (cSOR) over time, and recovered HCPV vs. HCPVI plots.



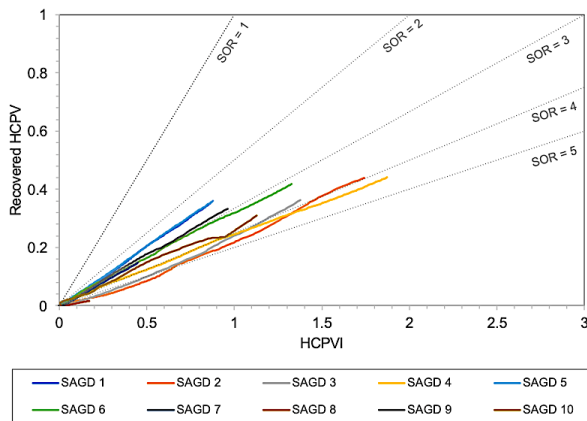
(a)



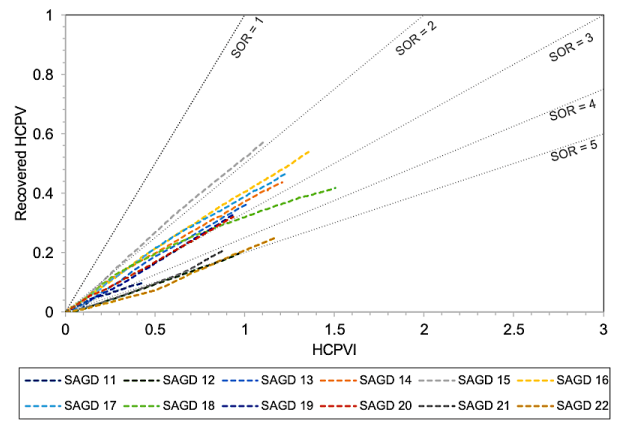
(b)



(c)



(d)



(e)

Figure 26—Current state of individual SAGD project performance in Canada. (a) current recovered HCPV vs. HCPVI (adopted and modified after Jimenez 2008), (b) progression of cSOR for SAGD 1–10, (c)

progression of cSOR for SAGD 11–22, (d) recovered HCPV vs. HCPVI for SAGD 1–10, and (e) recovered HCPV vs. HCPVI for SAGD 11–22. HCPVI = hydrocarbon pore volume injected.

Several key messages can be taken out from these diagnostic plots:

- Based on this performance profile, SOR tends to show incredibly high magnitudes at the beginning of the project life (initial phase), which is very common in SAGD operations. At this phase, more heat energy was required to initiate the mobilization of the oil in the reservoir. By the time steam was continuously injected into the reservoir, more heavy-oil/bitumen could be produced as the steam chamber expanded and stabilized and the reservoir temperature raised (ramp-up phase or plateau phase). The SORs would drop and tend to relatively stabilize. In other words, these SOR values could vary depending on the production and injection strategies.
- Only about 9% of SAGD projects in Canada were able to favorably achieve ~ 60% recovery factor (mature SAGD). Up to 30% of SAGD projects achieved 40–50% (moderately mature SAGD), and the remaining only reached a recovery factor of less than 40% (premature SAGD) even though they have been producing for decades.
- In most SAGD projects, the SOR varies between 2 and 4. However, some SAGD projects have been undergoing SORs greater than 4 or even 5, which is considered not efficient due to the aggressive steam injection.
- In terms of the SAGD operation efficiency, only around 40% of all SAGD projects have been able to operate efficiently in terms of SOR (cSOR <3). On the other hand, the remaining 60% of SAGD projects are experiencing operational problems. Operations are mostly impacted by unfavorable geological conditions (e.g., lower reservoir permeability), the presence of top or bottom water zones/OWC close to LKO, lean (mobile water) zones, and high  $S_w$  zones in the targeted SAGD intervals.
- Historically, the cSOR slope in the recovered HCPV vs. HCPVI plot (**Figure 26c**) changed over the period of SAGD operation. A good example of the SAGD project transitioning toward a more efficient SAGD operation is SAGD 19 (from cSOR = 3.5 to cSOR = 2.9). This SAGD project was able to reduce the steam injection amount while maintaining

overall production performance. However, some of the SAGD projects have experienced shifted cSOR slope toward a higher magnitude of more than 3 or 4 such as SAGD 6, SAGD 11, and SAGD 18. This inauspicious slope shifting was predominantly instigated by adverse geological conditions (e.g., shale/mud barriers, low-quality sand) and steam chamber expansion issues (e.g., steam conformance, earlier steam chamber coalescence).

- Two most mature SAGD operations in Canada—SAGD 15 and SAGD 16—showed certain characteristic similarities. In terms of reservoir geology, they both comprise excellent permeability in the order of 10,000 mD and have produced from the same targeted formation (McMurray) with high oil content ( $S_o > 80\%$ ). Furthermore, both SAGD 15 and SAGD 16 utilized large pads—consisting of more than 8 wells per pad on average. Despite the similarities, SAGD 15 still has a better overall project performance than SAGD 16. SAGD 15 is still in the ramp-up phase whereas SAGD 16 has entered its plateau phase. The possible reason why SAGD 15 has been able to prolong its ramp-up phase is due to the smaller well spacing (90 m). A smaller well spacing could potentially accelerate the oil production, improve the drainage area, and eventually improve the oil recovery. This is also the reason why SAGD 15 encompasses a higher recovery factor than SAGD 16.
- SAGD 15 has been able to maintain its overall cSOR of less than 2 (cSOR = 1.9) which is the best cSOR of the entire SAGD operations in Canada. The integration of a high permeability reservoir (both  $k_v$  and  $k_h$ ), high  $S_o$  formation ( $S_o > 80\%$ ), smaller well spacing (90 m), and good project execution allow SAGD 15 to maintain or even continuously improve its overall SAGD performance.
- Two SAGD projects (SAGD 21 and SAGD 22) are currently experiencing a relatively low-efficiency (cSOR close to 5) and lower recovery factor (RF <25%) even though they have been in operation for two decades. These SAGD fields have a lower permeability (on the order of 1,000–4,500 mD) compared to other SAGD projects, and this could be a limiting factor to the overall production performance. Another limiting factor impacting these SAGD project performances is the presence of bottom water in one sand body found in the producing formation intervals; thus, more water production is anticipated.

- A very high overall cSOR value (cSOR >10)—currently the highest cSOR of all SAGD operations—and very low recovery factor (RF <2%) comprised by SAGD 8 is due to the maturity of the project (the youngest SAGD project in Canada and has just started its operation 3 years ago). It is very common to have such a cSOR as this SAGD project is still in the initial phase. In this phase, a high-pressure and vast amount of steam injection is required to initiate steam propagation/expansion and steam chamber growth. This process/mechanism is essential for heavy-oil/bitumen mobilization in the reservoir.

A very high cSOR value (cSOR >10)—currently the highest cSOR of all SAGD operations—and very low recovery factor (RF <2%) comprised by SAGD 8 is due to the maturity of the project (the youngest SAGD project in Canada and has just started its operation 3 years ago). It is very common to have such a cSOR as this SAGD project is still in the initial phase. In this phase, a high-pressure and vast amount of steam injection is required to initiate steam chamber growth. This mechanism is essential for heavy-oil/bitumen mobilization in the reservoir.

## 2.5 Controlling Factors in SAGD Performance

### 2.5.1 Reservoir Geology

Many have said that the geology comprised by the SAGD project holds the most essential role in controlling the overall performance, which is valid to a great extent. **Figures 27** and **28** show the effect of vertical permeability ( $k_v$ ) and pay thickness on SAGD performance and efficiency. SAGD 15 and SAGD 16 are excellent examples of SAGD operations with very auspicious reservoir properties. By encompassing the SAGD pay thickness ( $h$ ) of over 40 m and  $k_v$  in the order of 8,000 mD, both SAGD projects have been able to deliver and maintain their exceptional performance for more than two decades—leading to the most high-performing mature SAGD operations in Canada. According to these correlation plots, both pay thickness and vertical permeability present a good trend/relationship with the recovery performance, i.e., the higher the  $h$  and  $k_v$ , the higher the oil recovery. In a more technical fashion, a thicker reservoir—typically with higher oil content ( $S_o > 80\%$ ) and cleaner sand—would contain much more heavy-oil/bitumen volume, thus, increasing reservoir productivity and deliverability. A higher  $k_v$  indicates better

vertical conformance, allowing the injected steam to have more favorable steam propagation, expansion, and chamber growth for better heavy-oil/bitumen mobilization.

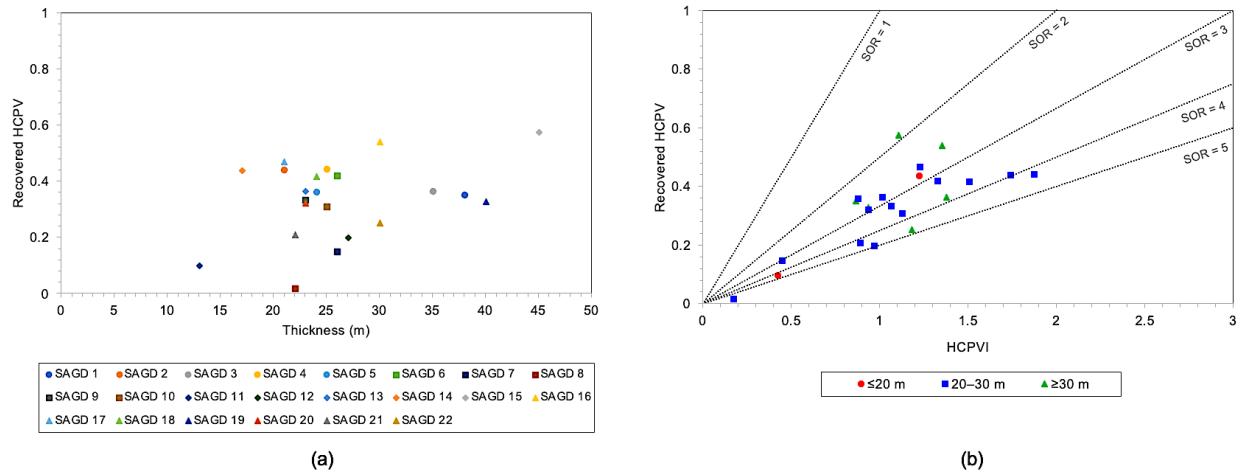


**Figure 27—Average SAGD pay thickness of the entire SAGD projects in Canada: (a) correlation between recovered HCPV and reservoir thickness, and (b) clustered SAGD pay thickness related to the overall SAGD performance.**

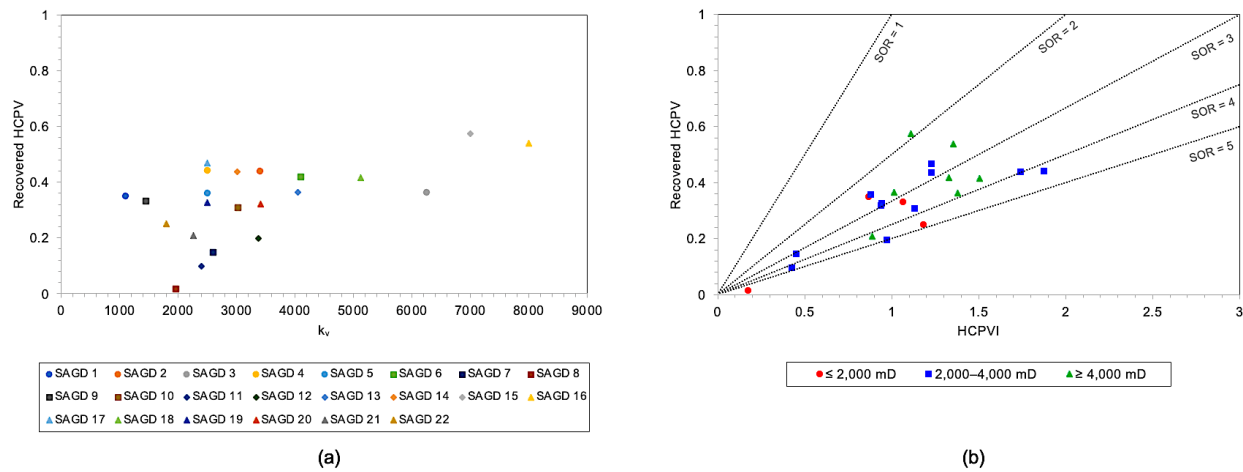


**Figure 28—Average  $k_v$  of the entire SAGD projects in Canada: (a) correlation between recovered HCPV and vertical permeability, and (b) clustered vertical permeability related to the overall SAGD performance.**

In a more extreme case, SAGD 11 is a good representative of low-performing SAGD operation, comprising a thinner reservoir ( $h < 15$  m) and lower vertical permeability ( $k_v < 2,500$  mD), with a recovery factor of up to 10%. The integration of reservoir properties could potentially influence the overall SAGD performance. This evidence, however, does not guarantee that having a good reservoir thickness and/or permeability just simply means a better SAGD. This case applies to, for instance, SAGD 3 and SAGD 18, which are still immature ( $RF \leq 40\%$ ) with a  $SOR > 3$  despite good reservoir thickness and permeability. Other factors (e.g., mud barriers, bottom water, operational problems) seemed to take over its overall performance. Based on this evidence, a few key points should be highlighted:

- Pay thickness could be the most critical parameter to consider in determining the overall SAGD performance. Reservoirs with a good thickness, clean sand, and oil-rich are preferable as thin and/or shaly sand could be detrimental to the success of the steam chamber growth and heavy-oil/bitumen mobilization in the reservoir.
- The steam chamber growth relies on vertical permeability. A reservoir with good vertical permeability would be more favorable for SAGD operations. A low vertical permeability could potentially delay the steam chamber growth, hindering the overall production performance.
- Reservoirs with high  $k_v$  would be good and preferable for steam vertical conformance. However, the overall performance could potentially be perturbed if bottom water exists.
- Additionally, oil viscosity could present potential impact to the overall SAGD performance as the viscosity value may vary between SAGD projects. The variation in the oil viscosity could also lead to the disparity in transmissibility since reservoir permeability and thickness hold essential role in SAGD project performance. High transmissibility in the reservoir is preferable to achieve more favorable oil production.

Reservoir geology could be the predominant parameter controlling the overall SAGD performance; nevertheless, the performance of SAGD operations should not be appraised solely based on their geology. Other factors could be crucial in controlling the overall SAGD performance.

## 2.5.2 Water Production and Presence of Bottom Water

Uncontrolled water production might inauspiciously influence the SAGD performance even if the reservoir exhibits exceptional geology. The water production in SAGD operations could be affected by: (1) high water saturation zones of the targeted formation, (2) steam condensation, and (3) the presence of bottom water/OWC, especially in one sand body. The impact of water production on the overall performance is depicted in **Figure 29**.

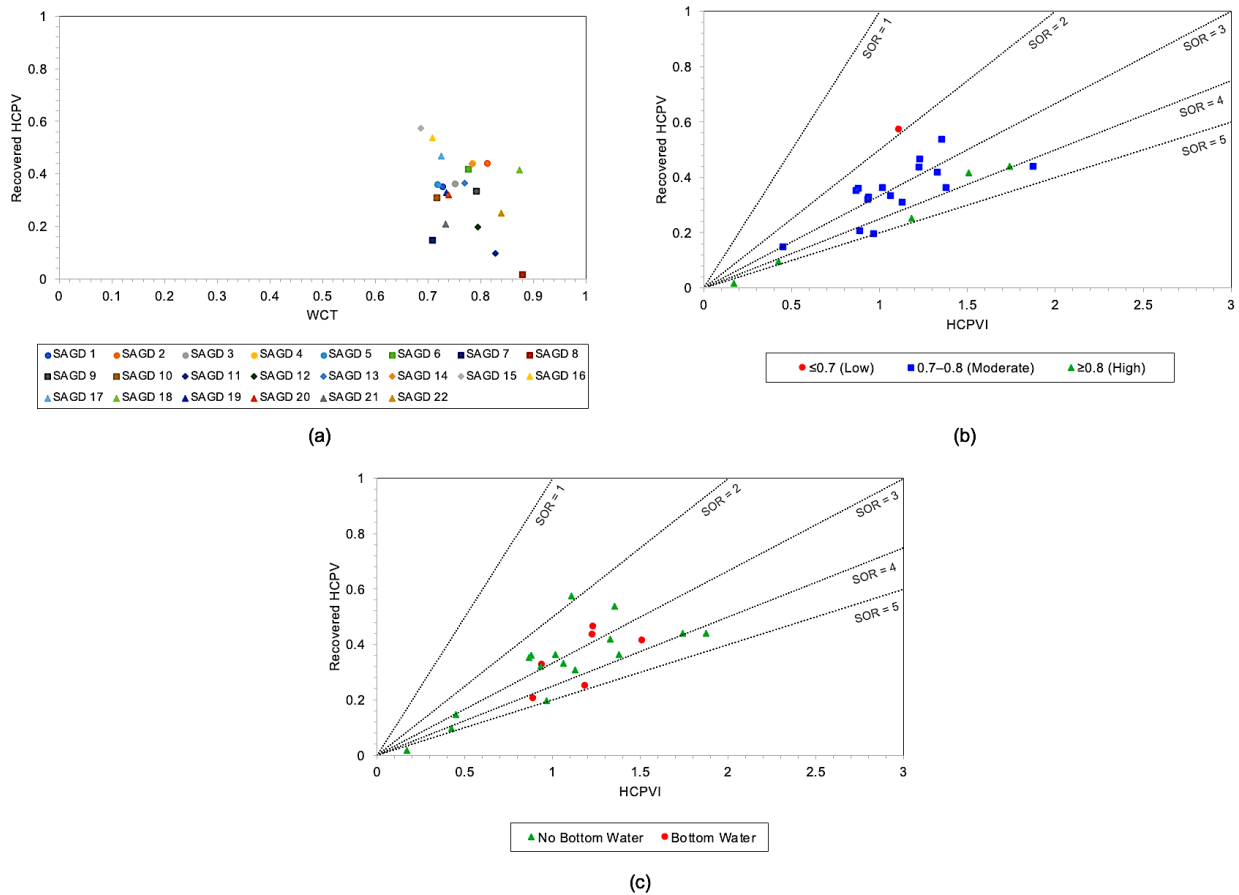


**Figure 29—Overall WCT performance of entire SAGD operations in Canada: (a) correlation between recovered HCPV and WCT, (b) clustered WCT related to the overall SAGD performance, and (c) clustered presence of bottom water in each SAGD operation related to the overall SAGD performance. WCT – water cut.**

One may infer the following from these trends:

- SAGD operations encompassing higher WCT values tend to experience lower recovery performance. This evidence validates that water production could also be the indicator of the SAGD performance—hindering the overall recovery performance.
- This relationship has also been corroborated by the recovered HCPV vs. HCPVI performance plot presenting that SAGD projects comprising high WCT magnitude (WCT >80%) tend to have a much higher cSOR value (cSOR >3.5).
- More than 25% of SAGD operations in Canada have been undergoing bottom water at the targeted SAGD reservoirs. From performance plots, it could also be validated that the presence of the bottom water promotes a moderate-to-high WCT as well as high cSOR values—limiting the overall SAGD performance. In a more extreme case, for the SAGD operations utilizing ESP, this artificial lift could lead to a high-pressure difference; thus, more water production could be anticipated.

## 2.5.3 Well Pair Designs

### 2.5.3.1 Well Spacing

It is very common for SAGD projects in Canada to establish a typical well spacing of 100 m. Hence, in general, there is no clear correlation between the well spacing and overall recovery performance. **Figure 30** summarizes the influence of well spacing on the overall SAGD project performance in Canada.

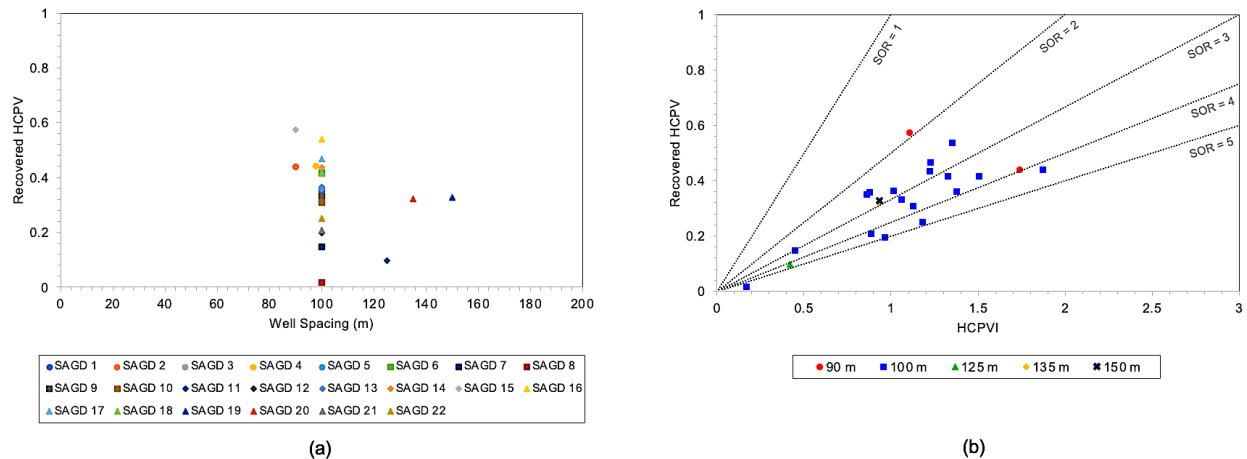


**Figure 30—Average well spacing of the entire SAGD projects in Canada. (a) correlation between recovered HCPV and well spacing and (b) clustered well spacing related to the overall SAGD performance.**

The smallest well spacing (e.g., SAGD 15) delivered the highest recovery factor (**Figure 30a**). Expectedly, implementing a smaller well spacing could potentially lead to better production acceleration, drainage area, and oil recovery. Some SAGD projects adopting a larger well spacing (e.g., SAGD 11, SAGD 19, SAGD 20) presented relatively lower recovery performance, particularly SAGD 11. The well spacing might present an influence on the overall SAGD project performance to some extent. Several SAGD projects have proved to attain favorable results after reducing the well spacing from the original well spacing by implementing infill wells. Nevertheless, reservoir geology and other factors could offset the well spacing effect. Well spacing of 100 m is still a good option and could be standardized for typical SAGD operations in Canada. A smaller well spacing might also be another alternative for a SAGD project comprising a more heterogeneous reservoir and expecting a more favorable production acceleration and better oil recovery.

### 2.5.3.2 Pad Density and Lateral Length

The relationship between pad density and overall SAGD performance is presented in **Figure 31**. Technically, the pad density may potentially affect the production performance. The more well pairs in a pad, the better production acceleration and recovery. However, in general, there is no

clear trend between the pad density and the recovery performance. Some SAGD projects with denser pads could deliver better performance, but some are still experiencing low-performance and low-efficiency SAGD operations. In other words, there are other parameters to be considered with the pad density in the performance analysis of SAGD operations. To some extent, pad density might be able to involve in the overall performance, but not a main controlling factor in SAGD operations.

A similar condition applies to the lateral length implemented in the SAGD projects in Canada. Any relationship between lateral length and overall recovery performance is still unclear. Theoretically, a well with a longer lateral section could potentially improve a reservoir with lower vertical permeability. This application is reflected in some SAGD operations in Canada comprising lower vertical permeability like SAGD 17, SAGD 20, and SAGD 22 with a lateral length of 1,000 m. However, these implementations do not reflect in their overall SAGD performance since these SAGD projects are still low performers.

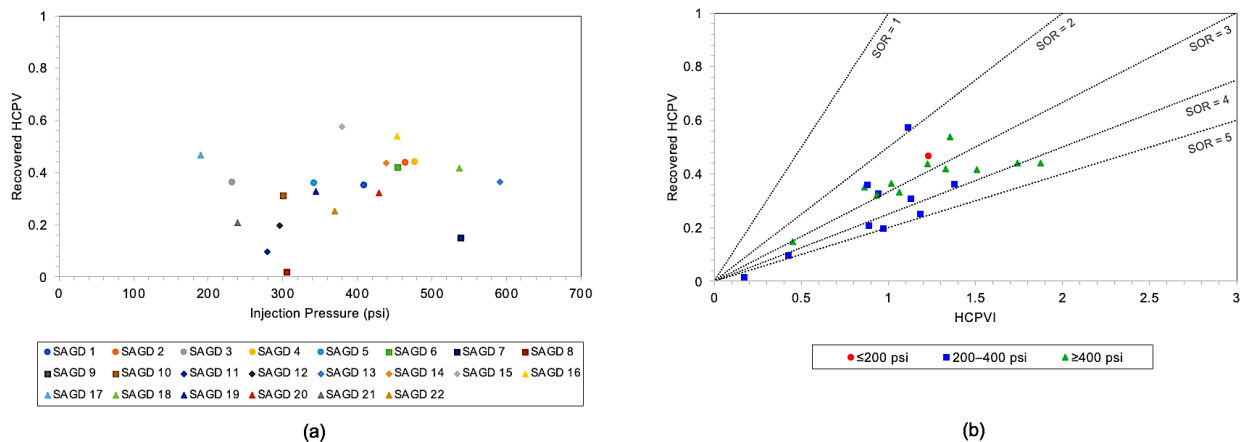


**Figure 31—Average pad density of the entire SAGD projects in Canada. (a) correlation between recovered HCPV and pad density and (b) clustered pad density related to the overall SAGD performance.**

## 2.5.4 Steam Injection Pressure

The steam injection pressure is one of the critically functioning elements in SAGD operations, but its effect on the overall performance is still questioned. The terms of low or high pressure SAGD

is relative. In this study, the hydrostatic pressure is utilized as a basis to determine low-pressure (LP) and high-pressure SAGD. LP SAGD is when the steam injection pressure is below its hydrostatic pressure ( $P_{inj} < P_{hydrostatic}$ ), whereas an HP SAGD occurs when the steam injection pressure is above its hydrostatic pressure ( $P_{inj} > P_{hydrostatic}$ ). Both techniques have adequate steam injection pressure for steam injectivity.

The impact of steam injection pressure on the SAGD performance is summarized in **Figure 32**. From these presented data, several important aspects can be highlighted:

- Generally, SAGD operations with higher steam injection pressure tend to exhibit more favorable recovery. This could be validated by the correlation between the recovered HCPV and the steam injection pressure showing an inclining trend (**Figure 32 a**). In other words, the higher the steam injection pressure, the greater the recovery could potentially be achieved.
- Although SAGD 7 operates with a steam injection pressure  $>500$  psi, this SAGD operation is still categorized as an LP SAGD because its hydrostatic pressure is still beyond the operating steam injection pressure. However, it is too early to establish a judgement related to the effect of steam injection pressure on the overall performance since this SAGD operation is still young and has only been in operation since 2018.
- Over 75% of HP SAGDs present better overall SAGD performance (e.g., higher efficiency, better recovery) compared to LP SAGDs (**Figure 32c**). The HP SAGD technique could promote a higher steam chamber expansion rate; therefore, more oil mobilization, higher oil recovery, and lower cSOR could be expected. However, about 25% of HP SAGDs are still underperforming, mainly due to younger SAGD operation (e.g., SAGD 8) and other predominant limiting factors, such as bottom water or zones with higher  $S_w$  (e.g., SAGD 12).
- LP SAGD provides higher latent heat of vaporization with lower operating temperature in the reservoir that may lead to an improved (lower) SOR and better heat energy efficiency. This has also been supported by previous study performed by Edmunds and Chhina (2001) showing the correlation between LP-SAGD and low SOR throughout analytical and

simulations studies. However, this mechanism could inhibit the viscosity reduction process—leading to a slower oil production.

- In contrast with LP SAGD, HP SAGD presents lower latent heat of vaporization with higher operating temperature in the reservoir which could potentially present very favorable viscosity reduction and higher oil production rate, which is also in agreement with the previous study conducted by Collins (2007) concluding that HP SAGD could present more favorable SAGD operation and performance than LP SAGD, showing less effective performance. Nevertheless, energy efficiency and SOR remain challenging for this HP SAGD technique.
- Better steam injection strategy should apply to achieve a more optimal SAGD performance.
- From the operational strategy and economic perspectives, an HP SAGD operation requires more energy than an LP SAGD. Hence, to achieve a more favorable and economical SAGD operation, a combined steam injection strategy should be implemented. In the early stage of SAGD operation, an HP SAGD technique is preferable to accelerate oil production. As the steam chamber grows, expands, and even coalesces, the steam injection strategy can be switched to and continued with an LP SAGD since the heat energy has already been accumulated in the reservoir.

Based on the above qualitative and quantitative analyses, the influencing factors in SAGD operations are listed in **Table A-3**.

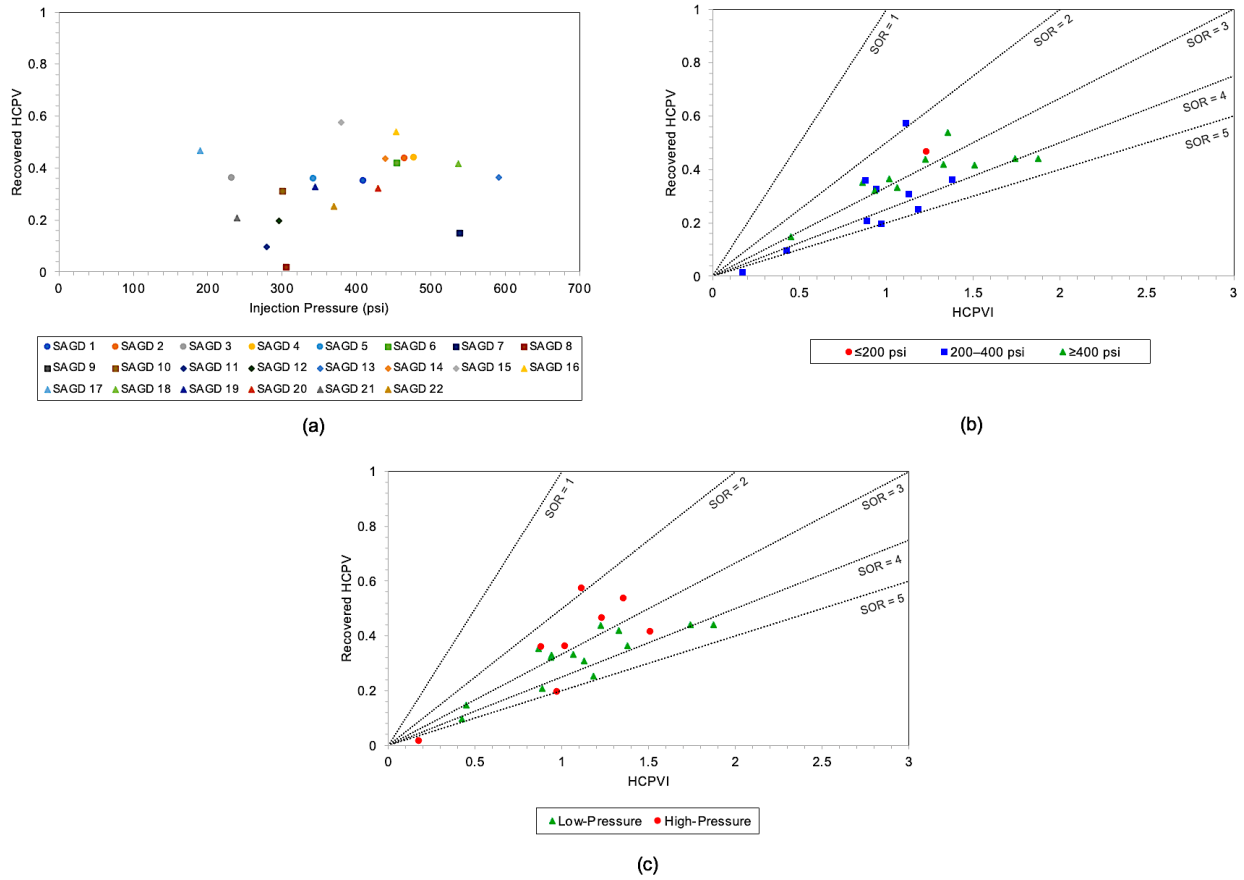


**Figure 32—Average steam injection pressure of the SAGD projects in Canada. (a) correlation between recovered HCPV and average steam injection pressure, (b) clustered steam injection pressure related to the overall SAGD performance, and (c) clustered low and high-pressure SAGD operations determined based on their hydrostatic pressures.**

**Table 3—Controlling Factors of SAGD Operations. h = reservoir thickness, k<sub>v</sub> = vertical permeability.**

Code	Limiting Factors						Performance	Maturity
	h	k <sub>v</sub>	Bottom Water	Pads/Well Pairs Size	Well Spacing	Operational Problems		
SAGD 1							High-Performing	Not Mature
SAGD 2				X		X	Low-Performing	Moderately Mature
SAGD 3						X	Low-Performing	Not Mature
SAGD 4		X					Low-Performing	Moderately Mature
SAGD 5							High-Performing	Not Mature
SAGD 6		X				X	Low-Performing	Moderately Mature
SAGD 7				X		X	Low-Performing	Not Mature
SAGD 8		X				X	Low-Performing	Not Mature
SAGD 9							High-Performing	Not Mature
SAGD 10		X		X		X	Low-Performing	Not Mature
SAGD 11	X	X				X	Low-Performing	Not Mature
SAGD 12		X				X	Low-Performing	Not Mature
SAGD 13							High-Performing	Not Mature
SAGD 14	X	X	X				Low-Performing	Not Mature
SAGD 15							High-Performing	Mature
SAGD 16							High-Performing	Mature
SAGD 17		X	X			X	Low-Performing	Moderately Mature
SAGD 18			X			X	High-Performing	Not Mature
SAGD 19			X				High-Performing	Not Mature
SAGD 20							High-Performing	Not Mature
SAGD 21		X	X			X	Low-Performing	Not Mature
SAGD 22		X	X			X	Low-Performing	Not Mature

## 2.6 What is Next?

It is obvious that the SAGD technique has been able to successfully recover heavy-oil/bitumen to a great extent. The success parameters of this recovery technique would be mainly maturity, recovery capability, and operational efficiency (cSOR). The SAGD operations that are not mature yet (or about to reach maturity) should keep functioning as are, as long as the overall performance could be well-maintained or even prolonged. The critical question is the time to switch to other techniques for the SAGD operations, which have reached their maturity and are in the decline phase—particularly when the steam chamber has coalesced or even reached the wind-down stage.

Technically, when a SAGD operation has reached its decline phase, steam coalescence, or even wind-down stage (post-SAGD), the operation is close to its end-of-life phase—with a “do nothing” case. Options for attempts may still be available for any SAGD projects to improve or even revive SAGD performance. In other words, the future of SAGD is still here to fulfill the energy demands. Reducing the amount of steam injection while improving production would be the preferred methodologies in aligning with greenhouse gas (GHG) emissions reduction for a more sustainable SAGD operation. **Figure 33** exhibits the potential of some applicable SAGD/post-SAGD improvement techniques in diminishing GHG emissions.

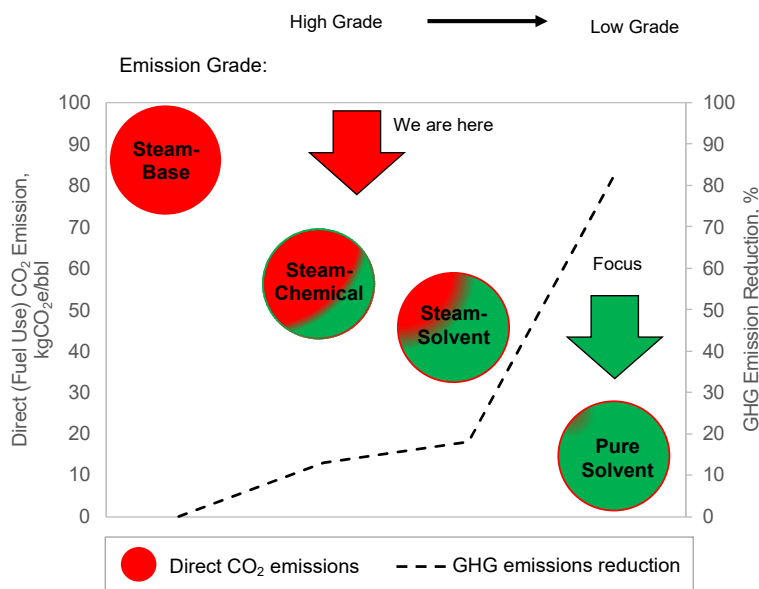


**Figure 33—Potentially applicable methodologies for SAGD/post-SAGD improvements in reducing GHG emissions (adapted from Canadian Energy Research Institute 2020, Lee and Babadagli 2021).**

Current steam-based SAGD presents no GHG emission reduction as the steam still needs to be continuously generated to support the steam chamber expansion as well as maintain production. On the other hand, co-injecting chemical additives and/or solvents could potentially diminish GHG emissions while improving oil recovery. However, this technique could only lessen the GHG emission by up to 20%. Among these techniques, pure solvent injection would be the most desirable recovery technique, which could potentially deliver the most oil recovery and diminish the GHG emissions by up to 80% and even 100% by also cutting off 100% of steam injection. To summarize, the future of SAGD comprises several key objectives:

- improve operational efficiency,
- substantially reduce cSOR,
- diminish residual oil saturation (ROS) post-SAGD,
- improve recovery and maintain production performance,
- attain sustainable operation,
- eventually, switch to minimized (if not “no-steam/zero GHG emission”) type methods.

### **2.6.1 Steam Additives**

Involving chemical additives for potential steam injection/SAGD applications have been extensively studied and experimented with for decades to improve recovery by providing improvements in interfacial properties (e.g., IFT reduction and wettability alteration). These potential chemicals include:

- Alkalis (Wagner and Leach 1959; Chiwetelu et al. 1994; Madhavan and Mamora 2010; Wang et al. 2010; Haas et al. 2013; Cao et al. 2017; Wei and Babadagli 2017a, 2017b; Hashim Noori et al. 2018; Wei and Babadagli 2019; Bruns and Babadagli 2020a),
- Surfactants (Gupta and Zeidani 2013; Mohammed and Babadagli 2015; Alomair and Alajmi 2016; Wei and Babadagli 2017a, 2017b; Taylor 2018; Alshaikh et al. 2019; Bruns and Babadagli 2020a, 2020b; Huang and Babadagli 2020a, 2020b; Lee and Babadagli 2021),

- Ionic liquids (Hanamertani et al. 2015; Wei and Babadagli 2017a, 2017b; Wei and Babadagli 2019; Huang and Babadagli 2020a),
- Solvent-based chemicals (e.g., dimethyl ether, diethyl ether) (Alkindi et al. 2016; Haddadnia et al. 2018a, 2018b; Sheng et al. 2018; Baek et al. 2019; Bruns and Babadagli 2020a; Huang and Babadagli 2020a),
- New generation additives (e.g., nanoparticles, chelating agents, deep eutectic solvents, biodiesel, switchable-hydrophilicity solvent) (Babadagli et al. 2010; Babadagli and Ozum 2010; Argüelles-Vivas et al. 2012; Maghzi et al. 2012; Mahmoud and Abdelgawad 2015; Mohammed and Babadagli 2016; Almubarak et al. 2017; Cao et al. 2017; Wei and Babadagli 2017a, 2017b, 2019; Lee et al. 2018; Taylor 2018; Medina et al. 2019; Mozhdhehi 2019; Rezk and Allam 2019; Bruns and Babadagli 2020a, 2020b; Fehr et al. 2020; Huang and Babadagli 2020a; Pratama and Babadagli 2020; Pratama and Babadagli 2021).

Studies and reviews have proven and summarized that these steam additives could demonstrate incremental recovery of up to 30-40% (Pratama and Babadagli 2022). However, integrating chemical additives into SAGD operations still requires the amount of steam injection to carry out these chemicals as a vapor phase to reach the steam chamber. Besides, the chemical stability at steam temperature should be considered as a concern.

## 2.6.2 Solvent Injection

The solvent injection has been studied for years to enhance recovery and efficiency in SAGD operations. The technique has been evaluated at lab or pilot scales and can be categorized as follows:

- *Non-condensable gas (NCG) solvent injection.* Nearly 80% of SAGD operations in Canada have implemented NCG (e.g., methane) injection. But no significant improvement in overall performance (e.g., production, cSOR) has been observed in general, with only about a 5-10% of success rate in SAGD operation. This inauspicious outcome presented by NCG co-injection was also corroborated by previous studies performed by Butler et al. (1999)

and Jiang et al. (2000)—concluding that, even though the NCG co-injection might provide an advantageous result to some extent, the result was mainly due to the gas-insulation and “gas push” mechanisms. In other words, the methane gas could only provide a “pushing effect” instead of a mixing/dissolution effect and tend to move to the top of the reservoir. Furthermore, a recent laboratory scale study performed by Pratama and Babadagli (2023) showed that the utilization of methane gas for SAGD applications did not present favorable results on SAGD recovery improvement if applied after the SAGD case as a sole injection material. A methane gas comprises a high K-value, indicating that the solubility of this gas is low in the oleic phase, limiting the mixing/dissolution process of solvent and heavy-oil/bitumen. Therefore, mobilization of oil is limited, and recovery improvement was not critically effective even in the post-SAGD conditions.

- *Condensable gas (CG) solvent injection.* Another potential recovery technique for SAGD operation improvement is CG injection. Most CG injection utilizes propane. This recovery technique has also been implemented by SAGD 16 since 2013. At SAGD temperature, the K-value of propane is considerably low (Deng 2005), meaning more solubility of propane in heavy-oil/bitumen, promoting the mixing/dissolution process between solvent and heavy-oil/bitumen. This mechanism allows favorable viscosity reduction to occur in the reservoir, advancing incremental recovery under the influence of gravity force. A similar mechanism was recently observed by Pratama and Babadagli (2023) through Hele-Shaw and porous media visualization experimental study, concluding that propane injection (pure composition) delivered a good recovery performance when applied after SAGD in the form of “gas injection only.” An alternative to condensable gases such as propane-butane is CO<sub>2</sub>. Injection of this gas into SAGD wells as a replacement to steam (with or without other gases such as methane or so) requires further laboratory-scale investigations.
- *Liquid solvent injection.* This was first introduced and developed by Nasr et al. (2003) as expanding solvent SAGD (ES-SAGD) comprising the concept of integrating the steam and low-concentration hydrocarbon at a steam temperature. The success factor of the technique is determined by the selection of the hydrocarbon. In this case, hexane was suggested to be the most suitable hydrocarbon solvent as it encompasses the vaporization temperature close to the injected steam. This allows the movement/propagation of steam and solvent

simultaneously toward the steam chamber to mix with heavy-oil/bitumen and reduce the viscosity more effectively. The Long Lake Pilot was the first SAGD operation implementing the ES-SAGD in 2005–2006. During this pilot test, the oil production rate increased by 6% (Orr 2009). This technique has a limited effect on reducing GHG emissions as the steam is still the main component of the injected material. An alternative is to switch to pure liquid solvent injection. Recently, Pratama and Babadagli (2023) performed experiments utilizing heptane (comprising a vaporization temperature of 98.4°C), recommending it to be applied after SAGD. This experimental study resulted in the highest recovery compared to the NCG (methane) and CG (propane) injections. The K-value of the heavier solvents (e.g., hexane, heptane) is much lower than the NCG and CG, meaning that the solubility of these solvents would be much higher in heavy-oil/bitumen. The study concluded that solvent injection could be feasible without involving steam injection once a SAGD project reached its maturity.

Some other successful SAGD field implementations using solvents (e.g., Surmont, Long Lake, Firebag, Leismer, DOVAP, Christina Lake, Algar, Mahihkan North) have also been well-reviewed by Bayestehparvin et al. (2019) summarizing the potential incremental oil recovery of nearly 40% and solvent recovery of up to 90%. Despite the potential and practicality of solvent injection, several essential parameters should be considered when implementing this technique in SAGD fields after steam injection:

- given the existing pressure and temperature at the late stages of SAGD,
- selection of the solvent types,
- optimal solvent composition and phase behavior,
- optimal and economical solvent recovery,
- time to switch to solvent injection (existing condensed steam may hinder the propagation of the hydrocarbon solvent and its interaction with the oil).

## 2.7 Conclusions

1. Twenty-two SAGD cases were analyzed and the phases (initial, ramp-up, plateau, and decline) were identified. The majority (more than 85%) of the projects are currently in the plateau production phase. Only nearly 10% of the projects are still undergoing the ramp-up phase, even though they have been in operation for decades. The remaining has already experienced the decline phase.
2. In general, most SAGD projects are not mature yet (only ~35% of the projects are currently in their maturity phase). Only 45% of the SAGD operations are considered high-performing operations, while the rest operate inefficiently. To improve and maintain SAGD performance, optimizing production, production–injection strategy, well pair development, operational excellence, and even tertiary recovery options are crucial.
3. For most SAGD operations in Canada, the SOR varies between 2 and 4. However, some SAGD projects have been undergoing a cSOR greater than 4 or even 5, which are relatively low-efficiency operations due to the aggressive steam injection.
4. The best performing and the largest SAGD operations are SAGD 15 and SAGD 16, with overall cSOR of 1.9 and 2.5, respectively. These SAGD projects have reached a recovery of close to 60%, indicating that these projects have attained their maturity. Despite the maturity, both SAGD projects have been able to maintain an efficient SAGD performance, especially SAGD 15, yielding a prolonged ramp-up phase.
5. Reservoir geology is crucial for SAGD performance. A highly-performing project (high efficiency and high recovery) requires a formation with good  $k_v$ , no lean/thief zones, and a thickness over 15 m to allow for efficient steam propagation, conformance, and chamber growth. However, operational issues such as steam shortage and facility turnaround can substantially impact the overall SAGD performance.
6. Bottom water can be disadvantageous to the overall SAGD performance, particularly if most of the utilized artificial lifts are ESPs. A high-pressure difference could potentially

trigger this bottom water to move toward the producer. Therefore, much water production is anticipated.

7. The size of pads and well pairs are also critical factors impacting the overall SAGD performance. The SAGD operations that encompass a larger number of pads and well pairs tend to have higher oil production, higher recovery factor, and higher operational efficiency (cSOR <3).
8. A SAGD operation comprising smaller well spacing tends to have higher production, recovery, and operational efficiency. Technically, the small well spacing could potentially accelerate production, improve the drainage area, improve the oil recovery, and improve operational efficiency.
9. Steam injection pressure is a supplementary contributor to the SAGD performance. A combined steam injection strategy (HP SAGD continued with LP SAGD) is recommended for a more desirable and efficient SAGD operation.
10. A limited number of projects (around 5–10% of all SAGD operations in Canada) were successful in implementing NCG co-injection. Nevertheless, for solvent injection applications, liquid types of condensable solvents could have more potential to improve recovery and reduce GHG emissions.
11. Reducing GHG emissions and increasing recovery by replacing steam with condensable (preferentially liquid hydrocarbon) gas injection is an option for matured SAGD applications. Optimizing solvent recovery, phase behavior, and solvent composition at post-SAGD conditions are crucial for efficiency.
12. Finally, one might note after this comprehensive data analysis and review that the operational issues in SAGD projects might not be fully disclosed to the public, leading to a limited and speculative analysis based on the available data from each company. Limitations of the analysis should apply since the data and information provided by AER and involved companies are limited and might not be available publicly.

## **Chapter 3: Mechanics of Heavy-Oil Recovery by Steam Injection with Steam Additives**

This chapter of thesis is a modified version of a paper published in the Journal of Petroleum Science and Engineering.

### 3.1 Preface

The efficiency improvement of steam injection (more oil, less steam) is a critical challenge in heavy oil recovery. Using chemical additives is one option to achieve this efficiency improvement, but many different mechanisms are involved in this process, and different considerations need to be taken depending on the existing conditions and chemical type. For example, many tested thermally stable chemicals—surfactants, nanofluids, and water-soluble solvents—were able to favorably alter the wettability. The underlying physics behind this favorable alteration and other mechanisms are not well comprehended yet, especially for new generation chemicals under thermodynamic conditions. The discussions presented in this research paper mainly focus on the improvements on heavy-oil and bitumen thermal recovery, particularly on the late-stage steam injection as well as the fundamentals of the residual oil development mechanism post-steam injection, affecting the heavy-oil and bitumen recovery performance. More importantly, this paper presents the experimental result-based, and comparative analyses of potential chemical additives (alkali, ionic liquid, surfactants, hydrocarbon solvents, water-soluble solvents, and new generation chemicals) applied to improve heavy oil recovery. This analysis is necessary not only to further evaluate the chemical's performance on the recovery improvement—specifically at the late-stage steam injection—but also to investigate the underlying recovery mechanisms, such as viscosity reduction, wettability alteration, interfacial tension (IFT) reduction, foaming effect, and emulsification presented by the chemical additives.

Based on the outputs obtained from different experimental methodologies, the underlying recovery mechanisms induced by the potential chemical additives were identified. The results revealed that synergy among the recovery mechanisms presented by chemical additives could potentially improve the heavy oil recovery by more than 80% during steam injection.

A comprehensive analysis of the mechanics of the heavy oil recovery provides valuable substantiation and understanding, honoring the potential implications of utilizing chemical additives as potential steam additives to the heavy oil recovery process. The results present beneficial information and recommendations for oil fields operating under steam injection applications.

**Keywords:** Steam injection mechanics, SAGD efficiency, alteration of interfacial properties, chemical additives, Hele-Shaw, micromodel, spontaneous imbibition, core flooding.

## 3.2 Introduction

Despite the constant world oil production decline rate in general, oil is anticipated to be the predominant energy source over the next two decades. Heavy oils signify more than 60% of total oil reserves. It is estimated that a total of more than  $5.9 \times 10^{12}$  bbl are available as heavy-oil-in-place, and only about 17% are technically recoverable (Bata et al. 2019).

The extraction of heavy-oil from the reservoirs remains challenging compared to the conventional/light oil due to its characteristics in having higher viscosity and specific gravity, lower hydrogen-to-carbon ratios, as well as higher asphaltene, sulphur, and heavy metals content at the reservoir conditions (Speight 2009). In order to recover potential heavy oil reserves, there are two possible recovery methods which are non-thermal recovery and thermal recovery. Non-thermal recovery is the heavy-oil recovery method that does not involve the source of the heat in the recovery process, primarily including waterflooding, gas injection, and cold production (Speight 2009). The thermal recovery (mainly steam injection) is the most practical and reliable method applied, as the thermodynamic heat transfer created during this process enables substantial viscosity reduction and thermal expansion, yielding a more favorable heavy oil mobilization in the rock pores (Ali 1974; Ali and Meldau 1979; Blevins et al. 1984; Haghghi and Yortsos 1997; Al-Bahlani and Babadagli 2009; Gates and Wang 2011; Sheng 2013; Taylor 2018). However, the increase in reservoir temperature due to heat transfer could create a thermal momentum dynamic, eventually influencing the entire system in the reservoir.

The steam injection can be applied as a secondary recovery and evidently delivers successful applications, as reflected by thermal recovery projects such as the Duri field steam flooding in Indonesia (Fuaadi et al. 1991; Gael et al. 1994; Silalahi et al. 2019; Winderasta et al. 2018), the Schoonebeek steam drive project in the Netherlands (Van Dijk 1968; Harmsen 1979; Shepherd et al. 2012), the Tia Juana steam flood project in Western Venezuela (De Haan and Schenk 1969), and some historical steam injection projects in Texas (Hall and Bowman 1970) and California

(Blevins 1990; Jones et al. 1995; Hanzlik and Mims 2003). In more practical applications, most steam injection techniques are applied as a primary stage of field production, particularly for oils with extremely high viscosity (extra-heavy oil and bitumen) like what is found in most SAGD projects in Canada (Jimenez 2008; Al-Bahlani and Babadagli 2009; Ito 2014). The foremost intention of this effort is to attain more favorable heavy oil mobilization, recovery, and project economic viability (Fair 2008; Jimenez 2008; Al-Bahlani and Babadagli 2009; Babadagli 2020).

It is undeniable that the heat generated during the steam injection process is very effective and beneficial in mobilizing the heavy oil—thus leading to the desirable oil recovery—at the early stage of steam injection; nevertheless, when the steam injection reaches its mature/late stage, the reservoir thermodynamic condition changes. Our earlier research identified and proved that when steam is continuously injected into the rock-oil-water system, a phase change (from a liquid phase to a steam phase) occurs, eventually leading to unfavorable wettability alteration (Pratama and Babadagli 2020a, 2020b), affecting heavy oil recovery performance. This finding is also supported through the results from several experimental studies on heavy oil, performed through micromodel and sandpack flooding at extremely high steam temperatures (up to 220°C), presenting that heavy oil production depleted and the recovery plot remained constant after reaching the late stages of steam injection (Zhao et al. 2003; Yuan et al. 2006; Pratama and Babadagli 2020c, 2020d; Zhao 2020). In the case of producing steam injection fields, rapid production decline has been evidenced in the Duri steam flood field in Indonesia (Winderasta et al. 2018) and some steam injection fields in the United States and SAGD fields in Canada (Blevins et al. 1984; Blevins 1990; Jones et al. 1995; Punase et al. 2014) after reaching the mature stage. This evidence undoubtedly indicates that steam injection presents an auspicious performance at the early stage but remains challenging at the mature stage, as a manifestation of the unfavorable wettability alteration post-steam injection (Blevins et al. 1984; Hoffman and Kovsky 2004).

The vast development of the oil and gas industry has triggered numerous research studies into the use of chemical additives and solvent-based chemicals for heavy oil and bitumen recovery improvement as well as the in-situ upgrading mechanisms to make the heavy-oil and bitumen even more saleable by the addition of hydrogen and the reduction/removal of the asphaltene composition from the crude oil (Speight 2009). However, the main challenge of utilizing the chemical additives in steam application is the thermal stability; therefore, a thermal stability test

for chemical additives is necessary before field implementation (Handy et al. 1982). In a more field-based evaluation, the use of chemicals as steam additives seemed to present very promising results in terms of heavy-oil and bitumen recovery (Castanier and Brigham 1991). According to the necessity of implementing chemical additives for steam applications, this paper covers the experimental studies and review of potential chemical additives. These chemicals include conventional chemicals that cover the use and application of:

- alkalis (Wagner and Leach 1959; Chiwetelu et al. 1994; Madhavan and Mamora 2010; Wang et al. 2010; Haas et al. 2013; Cao et al. 2017; Wei and Babadagli 2017a, 2017b; Hashim Noori et al. 2018; Wei and Babadagli 2019; Bruns and Babadagli 2020a),
- ionic liquids (Hanamertani et al. 2015; Wei and Babadagli 2017a, 2017b; Wei and Babadagli 2019; Huang and Babadagli 2020a),
- surfactants (Gupta and Zeidani 2013; Mohammed and Babadagli 2015; Alomair and Alajmi 2016; Wei and Babadagli 2017a, 2017b, 2018; Taylor 2018; Alshaikh et al. 2019; Bruns and Babadagli 2020a, 2020b; Huang and Babadagli 2020a, 2020b; Lee and Babadagli 2021),
- solvent-based chemicals (Alkindi et al. 2016; Haddadnia et al. 2018a, 2018b; Sheng et al. 2018; Baek et al. 2019; Bruns and Babadagli 2020a; Huang and Babadagli 2020a),
- CO<sub>2</sub> injection (Khatib et al. 1981; Issever et al. 1993; Sahin et al. 2008; Babadagli et al. 2009; Seyyedsar et al. 2016; Shilov et al. 2019; Mohammedalmojtaba et al. 2020; Xu et al. 2020).

and new generation chemicals that include:

- nanofluids (Maghzi et al. 2012; Mohammed and Babadagli 2016; Cao et al. 2017; Wei and Babadagli 2017a, 2017b, 2019; Taylor 2018; Medina et al. 2019; Rezk and Allam 2019; Bruns and Babadagli 2020a, 2020b; Fehr et al. 2020; Huang and Babadagli 2020a, 2020b),
- chelating agents (Mahmoud and Abdelgawad 2015; Almubarak et al. 2017; Pratama and Babadagli 2020b),

- biodiesel (Babadagli et al. 2010; Babadagli and Ozum 2010; Argüelles-Vivas et al. 2012; Lee et al. 2018; Bruns and Babadagli 2020a, 2020b; Huang and Babadagli 2020a),
- deep eutectic solvent (Mohsenzadeh et al. 2015, 2016; Huang and Babadagli 2020b),
- switchable-hydrophilicity solvent (Mozhdehei 2019; Pratama and Babadagli 2020b; Pratama and Babadagli 2021).

Even though these published studies were able to demonstrate a favorable incremental oil recovery of up to 40%, the mechanics of steam additives remains unclear, particularly in the scope of high-temperature steam injection applications, particularly for late-stage steam injection/SAGD.

This research aims to further investigate the mechanics of heavy oil recovery by potential chemical additives as high-efficiency tertiary recovery options—particularly for late-stage steam injection/SAGD applications—since the research and studies in this area remain limited and have never been studied. More essentially, the use of chemical additives (including solvents) can potentially reduce steam usage and greenhouse gas (GHG) emissions (**Table 4**) as well as improve energy efficiency and cost-effectiveness. The experimental results and analysis presented in this study are invaluable to reveal a better understanding of the rock-fluids interaction mechanisms as well as residual oil development post-steam injection/SAGD, affecting heavy oil recovery performance under extremely high-temperature conditions in steam injection applications. More importantly, the findings of this research will present beneficial recommendations for low-emission and high-efficiency late-stage heavy-oil recovery as a post-steam injection or SAGD applications in achieving a more sustainable hydrocarbon production.

**Table 4—Potential GHG emission reduction (adapted from Canadian Energy Research Institute Report 2017).**

<b>Implemented Technique</b>	<b>Direct GHG Emission</b>
Steam injection/SAGD base	60.4 kgCO <sub>2</sub> eq/bbl
Pure solvent	75–80% reduction
Steam-solvent	15–20% reduction
Steam-chemical	10–15% reduction

### 3.3 Experimental Methodology

The results and analyses presented in this study were acquired from different experimental studies published earlier by our research group honoring the steam-chemical-based heavy oil recovery mechanisms. Different models and experimental measurements, including fluid properties, interfacial properties, high-pressure-high-temperature (HPHT) imbibition, Hele-Shaw model, micromodel, HPHT sandpack flooding, and produced sample analysis were used in these studies. All experiments were performed at high-pressure and high-temperature steam injection/SAGD up to 220°C, 200 psi pressure, and 500 psi overburden pressure (sandpack flooding). The list of studies used in this analysis is given in **Table 5**.

All experiments utilized crude heavy oil samples obtained from heavy oil fields in Western Alberta, Canada. The oil viscosity ranges from 5,000 cP to 50,000 cP, and the average heavy oil density ranges from 0.98 g/cm<sup>3</sup> to 0.99 g/cm<sup>3</sup>, measured at 25°C. **Table 6** presents the studied potential chemical additive applications in this research.

**Table 5—List of experimental studies. RT = room temperature.**

Experimental Study	Operating Temperature (°C)	Operating Pressure (psi)	Reference
Fluid analysis	RT to 90	Ambient	Bruns and Babadagli (2020a); Pratama and Babadagli (2021)
Contact angle	200–220	200	Pratama and Babadagli (2020a); Pratama and Babadagli (2020b)
Interfacial tension	200–220	200	Pratama and Babadagli (2020a); Pratama and Babadagli (2020b)
Capillary imbibition	180–220	200–250	Wei and Babadagli (2017b); Wei and Babadagli (2019); Pratama and Babadagli (2021)
Micromodel	200–220	10–20	Pratama and Babadagli (2020c); Pratama and Babadagli (2020d)
Hele-Shaw model	200	3–10	Bruns and Babadagli (2020b); Huang and Babadagli (2020a)
Sandpack flooding	200–220	200	Bruns and Babadagli (2020a); Pratama and Babadagli (2021)

**Table 6—List of the studied potential chemical additives in this research.**

<b>Chemical Type</b>	<b>Components</b>
Hydrocarbon solvent	Heptane (C <sub>7</sub> H <sub>16</sub> )
High pH solution	Sodium metaborate
Ionic liquid	1-butyl-2,3-methylimidazolium tetrafluoroborate
Cationic surfactant	Dodecyl trimethylammonium bromide
Anionic surfactant	Linear-alkyl toluene sulfonate
Nonionic surfactant	Sorbitan monooleate
Nanofluids	Silicon oxide
Water-soluble solvents	Dimethyl ether
Chelating agents	Diethylenetriaminepenta acetic acid
Biodiesel	Fatty acids methyl ester
Switchable-hydrophilicity solvent (SHTA)	N,N-dimethylcyclohexylamine
Deep eutectic solvent (DES11)	Sodium carbonate and 1-butyl-3-methylimidazolium tetrafluoroborate

### **3.4 Residual Oil Saturation (ROS) Development Post-Steam Injection**

It is undeniable that the heat transfer during the steam injection process (Prats 1982) is substantial for viscosity reduction to mobilize heavy oil in the pore spaces. This becomes a challenging and complex process—impacting heavy oil recovery performance—in the latter stages of steam injection. Generally, the steam injection process can be divided into two main stages, namely the early (initial production and heating) and the late (mature) stage. **Figure 34** explains the mechanisms occurring in pore spaces during the steam injection. In the early stage, when the rock

pores are mostly saturated with heavy oil, the heat transmitted during steam injection produces the oleic phase with two possible mechanisms—viscosity reduction and thermodynamic thermal expansion (Jessup 1930). The viscosity reduction increases the mobility of the oleic phase, whereas the thermal expansion causes swelling oil. At this stage, a phase change occurs to subsequently promote the thermodynamic evaporation of the water phase—due to the instability of the wetting water film on the solid phase (Evdokimov et al. 2018). In this circumstance, the strength of surface force changes, van der Waals attractive force dominates the electrostatic repulsive force, and the disjoining pressure becomes negative (Hirasaki 1991); thus allowing direct interaction between the oleic phase and the rock surface to become more or even completely oil-wet state, further rising the capillary pressure, and then creating more resistance force and development of residual oil saturation in the pore spaces (Pratama and Babadagli 2020a, 2020d). This evidence clearly indicates that the wettability of the rock had been altered and further impacts the relative permeability and eventually the heavy oil recovery. Scientifically, the major reason for the residual oil development is the capillary pressure, which can be physically described by the following equation:

$$P_c = \frac{2\sigma \cos \theta}{r} \dots\dots\dots (1)$$

where  $P_c$  defines the capillary pressure in the rock pores,  $\sigma$  defines the IFT,  $\theta$  defines the wettability (contact angle), and  $r$  defines the pore radius. This capillary pressure consequently influences the interplay between viscous force and capillary force represented by the capillary number ( $N_c$ ) introduced by Moore and Slobod (1955):

$$N_c = \frac{v\mu_w}{\sigma \cos \theta} \dots\dots\dots (2)$$

where  $N_c$  is the capillary number,  $v$  is the linear velocity of the displacing fluid,  $\mu_w$  is the viscosity of the displacing fluid,  $\sigma$  is the IFT of two immiscible fluids, and  $\theta$  is the wettability (contact angle) of the rock surface.

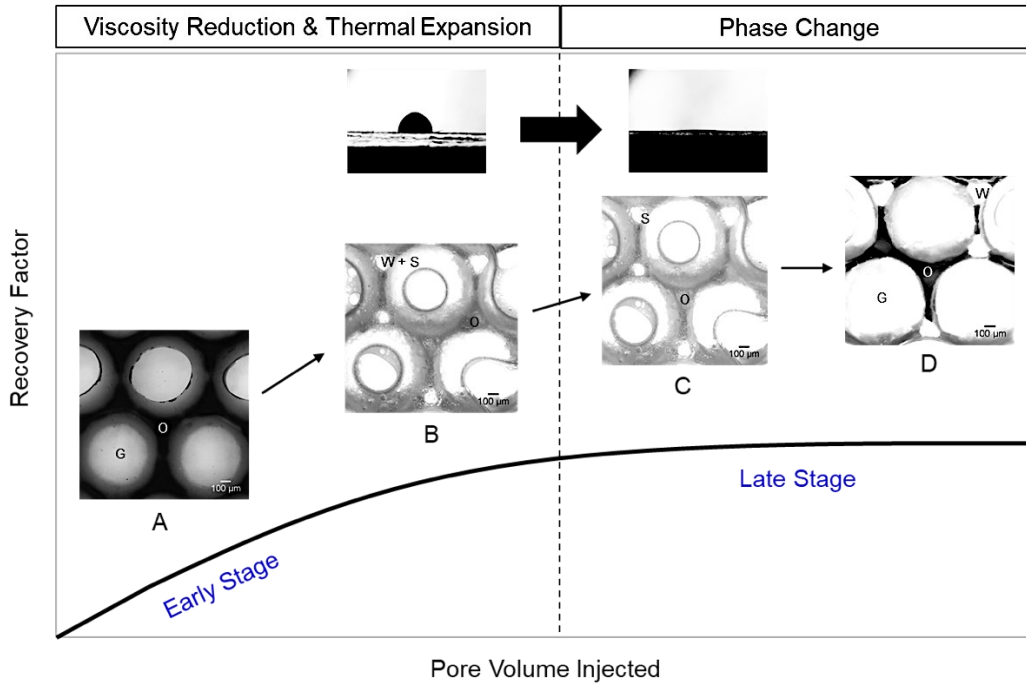


**Figure 34—Description of stages during steam injection process from the recovery and pore-scale points of view: (a) reservoir pore spaces initial condition, (b) steam is injected into the pore spaces, (c) steam fills up and dominates pore spaces, and (d) post-steam injection. G = grain, O = oleic phase, S = steam, and W = water/liquid phase.**

In summary, the mature stage of steam injection is essential to the application and requires further attention in terms of the heavy oil recovery performance—since numerous steam injection fields have evidenced rapid production decline at this stage. Despite some other field problems in steam injection applications (e.g., steam conformance, steam channeling, steam-oil mobility contrast), phase change has been corroborated to be the predominant factor causing the unfavorable wettability alteration of the rock, eventually affecting the heavy oil recovery performance and efficiency of the process causing an increase in steam-oil-ratio (SOR).

### 3.5 Steam-Based and Steam-Chemical Additives-Based Displacement Mechanisms

In steam-based heavy oil recovery, the recovery is predominantly due to two mechanisms—viscosity reduction and thermal expansion. In this case, heavy oil viscosity reduction is achieved by thermally-induced viscosity reduction and water dissolution—becoming even more significant at temperatures greater than 150°C (Glandt and Chapman 1995).

In the case of steam-chemical-based heavy oil recovery, the mechanics of heavy oil recovery can be identified by two displacement mechanisms—micro displacement and macro displacement (Table 7). Figure 35 exhibits the classification of the displacement mechanics on heavy oil recovery presented by the potential chemicals as steam additives. Both displacement mechanisms play an essential role in heavy oil recovery performance/efficiency. We revealed that each chemical additive presented its unique displacement mechanism (even a combined displacement mechanism) that can potentially reduce steam usage and improve heavy-oil recovery, thus improving the SOR.

**Table 7—Summary of potential displacement mechanisms of each studied chemical additive.**

Steam Additive	Thermally Stable?	Potential Displacement Mechanisms				Chemical Principal Mechanisms	References
		Viscosity Reduction	Detergency Effect	Foaming Effect	Emulsion Generation		
Hydrocarbon solvents	YES	X				Diffusion into oleic phase, further altering the solubility of asphaltene components and triggering disruption of the equilibrium between resins and asphaltenes and desorption of resins from heavier components to reinstate new thermodynamic equilibrium.	<ul style="list-style-type: none"> <li>• Nasr et al. (2003)</li> <li>• Pathak et al. (2012)</li> <li>• Naderi et al. (2013)</li> <li>• Roberts and Ghanem (2013)</li> <li>• Keshavarz et al. (2015)</li> <li>• Naderi and Babadagli (2015)</li> <li>• Levya-Gomez and Babadagli (2017)</li> <li>• Bruns and Babadagli (2020a)</li> <li>• Huang and Babadagli (2020a)</li> </ul>
High pH solution	YES		X			Increase pH value of the system to establish surface hydrolysis and surface forces modifications.	<ul style="list-style-type: none"> <li>• Wagner and Leach (1959)</li> <li>• Chiwetelu et al. (1994)</li> <li>• Madhavan and Mamora (2010)</li> <li>• Wang et al. (2010)</li> <li>• Haas et al. (2013)</li> <li>• Cao et al. (2017)</li> <li>• Wei and Babadagli (2017a)</li> <li>• Wei and Babadagli (2017b)</li> <li>• Hashim Noori et al. (2018)</li> <li>• Wei and Babadagli (2019)</li> <li>• Bruns and Babadagli (2020a)</li> </ul>
Ionic liquid	YES		X			Comprises organic cationic group (1-butyl-3-methylimidazolium) and anionic group (tetrafluoroborate) acting as a hydrophilic and hydrophobic functional group in promoting surface activity and surface forces modification.	<ul style="list-style-type: none"> <li>• Hanamertani et al. (2015)</li> <li>• Wei and Babadagli (2017a)</li> <li>• Wei and Babadagli (2017b)</li> <li>• Wei and Babadagli (2019)</li> <li>• Huang and Babadagli (2020a)</li> </ul>

Cationic surfactant	YES			X		<p>The surface activity is presented by the hydrophilic polar head and hydrophobic tail.</p> <ul style="list-style-type: none"> <li>• Gupta and Zeidani (2013)</li> <li>• Mohammed and Babadagli (2015)</li> <li>• Alomair and Alajmi (2016)</li> <li>• Wei and Babadagli (2017a)</li> <li>• Wei and Babadagli (2017b)</li> <li>• Wei and Babadagli (2018)</li> <li>• Taylor (2018)</li> <li>• Alshaikh et al. (2019)</li> <li>• Bruns and Babadagli (2020a)</li> <li>• Bruns and Babadagli (2020b)</li> <li>• Huang and Babadagli (2020a)</li> <li>• Huang and Babadagli (2020b)</li> <li>• Lee and Babadagli (2021)</li> </ul>
Anionic surfactant	YES		X	X		<p>The surface activity is presented by the hydrophilic polar head and hydrophobic tail. A negatively charged polar head can potentially modify surface forces and initiate electrostatic repulsive forces between heavy oil and solid surface (sandstone).</p> <ul style="list-style-type: none"> <li>• Huang et al. (1985)</li> <li>• Mujis et al (1988)</li> <li>• Shallcross et al. (1990)</li> <li>• Osterloh and Jante (1994)</li> <li>• Gupta and Zeidani (2013)</li> <li>• Cuenca et al. (2014)</li> <li>• Mohammed and Babadagli (2015)</li> <li>• Alomair and Alajmi (2016)</li> <li>• Wei and Babadagli (2017a)</li> <li>• Wei and Babadagli (2017b)</li> <li>• Mukherjee et al. (2018)</li> <li>• Wei and Babadagli (2018)</li> <li>• Taylor (2018)</li> <li>• Alshaikh et al. (2019)</li> <li>• Li et al. (2019)</li> <li>• Nguyen et al. (2019)</li> <li>• Bruns and Babadagli (2020a)</li> <li>• Bruns and Babadagli (2020b)</li> <li>• Huang and Babadagli (2020a)</li> <li>• Huang and Babadagli (2020b)</li> <li>• Lee and Babadagli (2021)</li> </ul>

Nonionic surfactant	YES		X	X	X	The surface activity is presented by the hydrophilic polar head and hydrophobic tail. Low HLB value presents hydrophobic functional group dominance—further promoting water-in-oil emulsion generation.	<ul style="list-style-type: none"> <li>• Gupta and Zeidani (2013)</li> <li>• Mohammed and Babadagli (2015)</li> <li>• Alomair and Alajmi (2016)</li> <li>• Wei and Babadagli (2017a)</li> <li>• Wei and Babadagli (2017b)</li> <li>• Wei and Babadagli (2018)</li> <li>• Taylor (2018)</li> <li>• Alshaikh et al. (2019)</li> <li>• Bruns and Babadagli (2020a)</li> <li>• Bruns and Babadagli (2020b)</li> <li>• Huang and Babadagli (2020a)</li> <li>• Huang and Babadagli (2020b)</li> <li>• Lee and Babadagli (2021)</li> </ul>
Water-soluble solvent	YES	X	X			Polarity characteristic enables partition of the chemical into oleic phase—resulting in oleic phase swelling and viscosity reduction.	<ul style="list-style-type: none"> <li>• Alkindi et al. (2016)</li> <li>• Haddadnia et al. (2018a)</li> <li>• Haddadnia et al. (2018b)</li> <li>• Sheng et al. (2018)</li> <li>• Baek et al. (2019)</li> </ul>
Silica nanofluid	YES		X			Carries negative surface charges at neutral pH value. Adsorption of nanoparticles on the rock surface can benefit in favorable surface forces modification, electrostatic repulsive forces initiation, and positive disjoining pressure.	<ul style="list-style-type: none"> <li>• Maghzi et al. (2012)</li> <li>• Mohammed and Babadagli (2016)</li> <li>• Cao et al. (2017)</li> <li>• Wei and Babadagli (2017a)</li> <li>• Wei and Babadagli (2017b)</li> <li>• Wei and Babadagli (2019)</li> <li>• Taylor (2018)</li> <li>• Medina et al. (2019)</li> <li>• Rezk and Allam (2019)</li> <li>• Bruns and Babadagli (2020a)</li> <li>• Bruns and Babadagli (2020b)</li> <li>• Fehr et al. (2020)</li> <li>• Huang and Babadagli (2020a)</li> <li>• Huang and Babadagli (2020b)</li> </ul>
Chelating agent	YES		X			Functional groups (carboxyl, hydroxy, ether, and amines) act like a solvent-based agent and high pH solution at the same time—further favorably modifying solid surface charge.	<ul style="list-style-type: none"> <li>• Mahmoud and Abdelgawad (2015)</li> <li>• Almubarak et al. (2017)</li> <li>• Pratama and Babadagli (2020b)</li> </ul>

Biodiesel	YES	X	X			Replacement of hydrogen bonds triggers dissociation of asphaltene aggregates in heavy oil—further diminishing asphaltene fractions and reducing heavy oil viscosity. Hydrophilic group (COOCH <sub>3</sub> ) and hydrophobic group (hydrocarbon chains) potentially improve surface wettability and interfacial properties.	<ul style="list-style-type: none"> <li>• Babadagli et al. (2010)</li> <li>• Babadagli and Ozum (2010)</li> <li>• Argüelles-Vivas et al. (2012)</li> <li>• Lee et al. (2018)</li> <li>• Bruns and Babadagli (2020a)</li> <li>• Bruns and Babadagli 2020b</li> <li>• Huang and Babadagli (2020a)</li> </ul>
Switchable solvent (SHTA)	YES	X	X		X	Hydrophilic and hydrophobic functional groups enable this chemical to wet both heavy oil and water simultaneously. Ion transfer enables the formation of ion pairs. Cations (C <sub>8</sub> H <sub>17</sub> NH <sup>+</sup> ) are absorbed on heavy oil surfaces, and anions (HCO <sub>3</sub> <sup>-</sup> ) reduces interaction between heavy oil and sandstones by reducing surface forces and initiating electrostatic repulsive forces.	<ul style="list-style-type: none"> <li>• Mozhdehei (2019)</li> <li>• Pratama and Babadagli (2020b)</li> <li>• Pratama and Babadagli (2021)</li> </ul>
Deep eutectic solvent	YES	X	X			Interaction of sodium carbonate (acting as a base) with carboxylic acid functional group contained in heavy oil to form and activate in-situ surfactant. The ionic liquid part acts as hydrophilic and hydrophobic functional groups in modifying surface forces.	<ul style="list-style-type: none"> <li>• Mohsenzadeh et al. (2015)</li> <li>• Mohsenzadeh et al. (2016)</li> <li>• Huang and Babadagli (2020b)</li> </ul>
CO <sub>2</sub> injection	YES	X				Acts like a solvent. CO <sub>2</sub> dissolves into heavy-oil and bitumen to swell the oil, reduce the viscosity, and diminish the interfacial tension.	<ul style="list-style-type: none"> <li>• Khatib et al. (1981)</li> <li>• Issever et al. (1993)</li> <li>• Sahin et al. (2008)</li> <li>• Babadagli et al. (2009)</li> <li>• Naderi and Babadagli (2012)</li> <li>• Seyyedsar et al. (2016)</li> <li>• Shilov et al. (2019)</li> <li>• Mohammedalmojtaba et al. (2020)</li> <li>• Xu et al. (2020)</li> </ul>

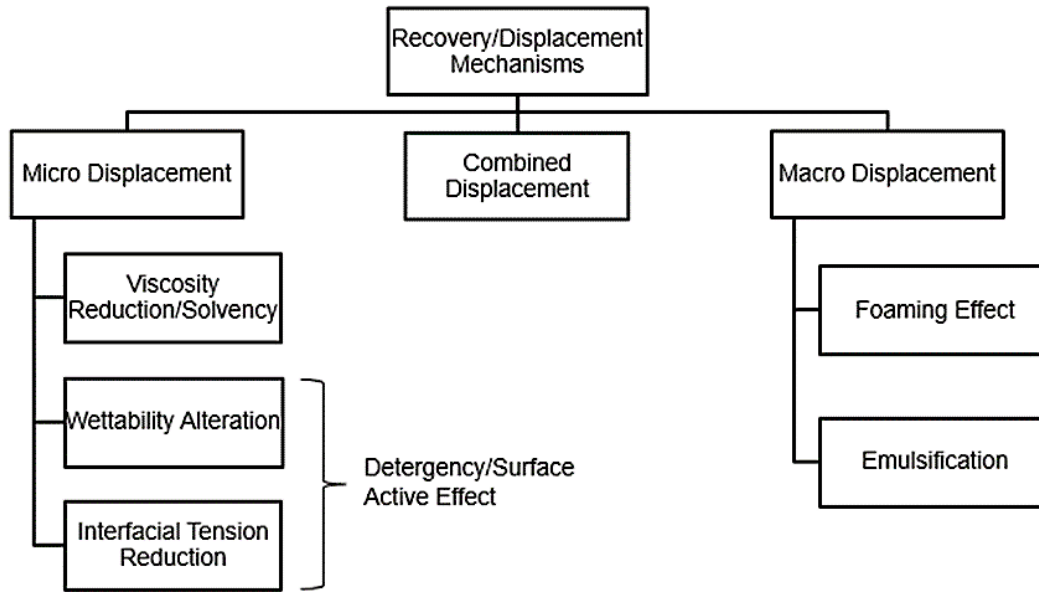


Figure 35—Classification of recovery mechanisms under the steam injection.

### 3.5.1 Micro Displacement Mechanism

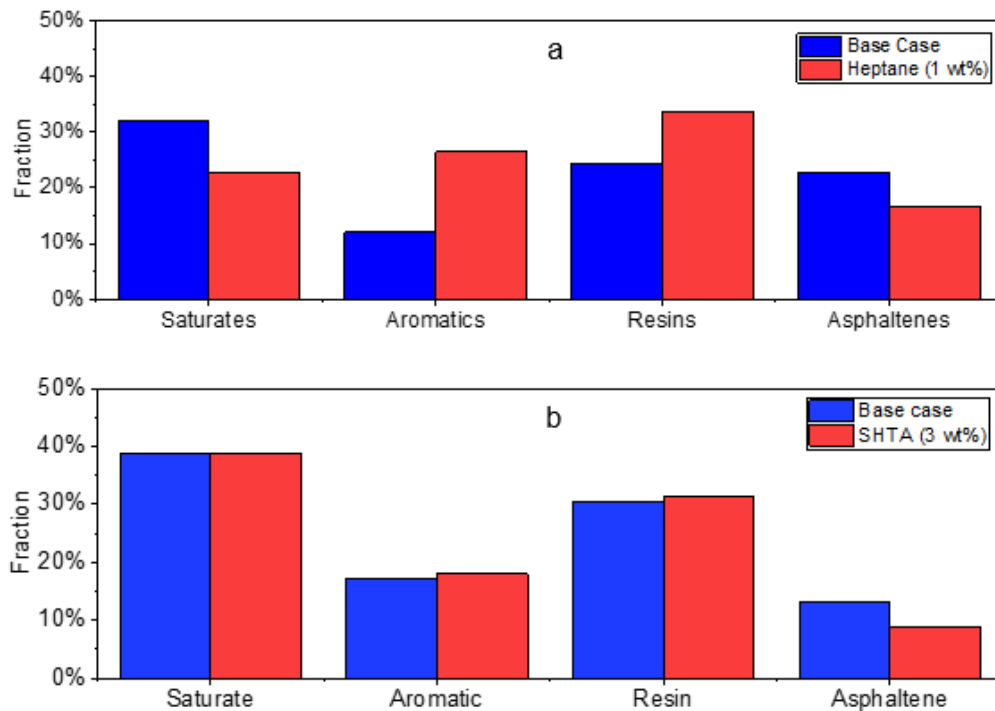
The micro displacement mechanism reflects the ability of chemical additives to mobilize the heavy oil in pore spaces by modifying the reservoir rock-fluid interaction that includes interfacial properties and intermolecular interactions, such as surface force and disjoining pressure—further impacting the capillary pressure and relative permeability. The micro displacement mechanisms include viscosity reduction/solvency and detergency/surface-active effect (wettability alteration and IFT reduction).

#### 3.5.1.1 Viscosity Reduction or Solvency

Heavy oil viscosity reduction can be attained when the favorable interaction between the oleic phase and chemical additives (or solvents) is formed—either further dissolving into the oleic phase or reducing oil-water IFT (potential oil-in-water emulsion). More importantly, the use of solvents in heavy-oil and bitumen recoveries has been extensively studied and implemented; proving that hydrocarbon solvents contribute to favorable oil recovery by providing essential viscosity reduction through the diffusion mechanism of solvent into the heavy-oil and bitumen (Ali and

Abad 1976; Das and Butler 1998; Nasr et al. 2003; Al-Bahlani and Babadagli 2008, 2009; Naderi and Babadagli 2012, 2015; Pathak et al. 2012; Naderi et al. 2013; Roberts and Ghanem 2013); thus, further creating a more auspicious recovery by better sweep (steam flooding) and steam chamber growth (SAGD). In this particular research, some of the studied chemical additives, such as hydrocarbon solvent (heptane), water-soluble solvent dimethyl ether (DME), biodiesel, switchable-hydrophilicity tertiary amines (SHTA), and deep eutectic solvent (DES), have proven to potentially exhibit favorable viscosity reduction at steam conditions, even at a lower chemical concentration.

The addition of solvent-type chemicals as steam additives could diminish the heavy oil viscosity by favorably altering the crude oil properties because of the dissolution effect and lowered interface free energy. Some representative results gained from this research are depicted in **Figure 36**, in the case of heptane (**Figure 36a**) and SHTA (**Figure 36b**), showing the co-injection with steam during the heavy oil recovery process.



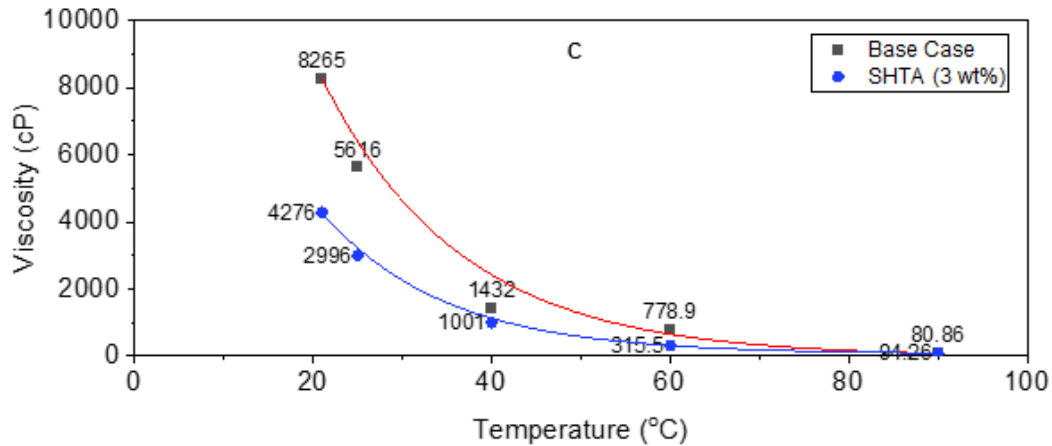


**Figure 36—SARA analysis and viscosity evaluation on steam-solvent-based heavy oil recovery: (a) low-concentration heptane, (b) low-concentration SHTA, and (c) favorable viscosity reduction by SHTA (reproduced after Bruns and Babadagli 2020a; Pratama and Babadagli 2021).**

Through the saturates, aromatics, resins, and asphaltenes (SARA) analysis, it was perceived that the heavy oil properties could be upgraded (in-situ upgrading). The dynamic interaction between the solvent and heavy oil at high-temperature steam conditions resulted in the improvement of the lighter components and the reduction of the heavier components; therefore, improving the mobility of the heavy oil.

Scientifically, the hydrocarbon solvents act to reduce the heavy oil viscosity by diffusing it into the oleic phase and present the in-situ upgrading mechanism by diminishing the heavier constituents like asphaltene. It is observed that this mechanism is able to reduce the asphaltene fraction significantly to 16%, whereas the resins fraction is substantially enhanced to 34% due to the suspension and stabilization of the asphaltene particles by the resins in the oleic phase (Hammami et al. 2000; Ahmadi et al. 2014). Furthermore, the addition of this alkane solvent could alter the solubility of the asphaltenes, further triggering disruption of the thermodynamic equilibrium between resins and asphaltenes and the desorption of resins from the heavier components (asphaltenes). This circumstance is able to initiate the potential energy reduction and solid phase formation due to the particle accumulation—resulting in the produced heavy oil with a lower asphaltene fraction and a higher fraction of resins (**Figure 36a**). In addition, a hydrocarbon solvent like heptane can also potentially trigger the asphaltene precipitation that further promotes

a better mobilization of the heavy oil in reservoirs. A solvency effect presented by heptane was also evidenced through the Hele-Shaw visualization. Promising steam chamber growth was achieved without leaving any oil traces—indicating that there was a possibility to establish miscibility between heptane and the lighter components of heavy oil. This growth triggers miscible flooding—hence reducing the heavy oil viscosity, improving the oleic phase mobility, and eventually improving the heavy oil recovery and sweep efficiency (Bruns and Babadagli 2020b; Huang and Babadagli 2020a).

In the case of steam co-injected with SHTA, favorable viscosity reduction and heavy oil composition alteration—as a result of the in-situ upgrading (Figs. 3b and 3c)—were possible due to the unique feature of this switchable-hydrophilicity solvent comprising functional hydrophilic and hydrophobic groups—enabling this additive to establish an auspicious surface activity, wetting both the water phase and oleic phase and reducing the IFT, in turn further reducing the heavy oil viscosity by triggering an oil-in-water emulsion (Pratama and Babadagli 2021). Furthermore, the reversible chemical reaction—involving CO<sub>2</sub> gas in establishing a stable and homogeneous chemical solution—comprised by SHTA was able to present a stable foamy oil mechanism (observed after the steam flooding process). This foamy oil mechanism was caused by the dissolution of the CO<sub>2</sub> gas phase in heavy oil at high-pressure-high-temperature steam-chemical-based recovery that was validated by gas chromatography—leading to a significant viscosity reduction (Pratama and Babadagli 2021). Additionally, the switchable-hydrophilicity solvent is able to establish an intermolecular interaction with the larger molecules (like asphaltenes) to destabilize the self-association of asphaltenes and diminish the aggregates into smaller sizes. This circumstance enables the diffusion mechanism of this SHTA into the oleic phase; therefore, further diminishing the asphaltenes (**Figure 36b**), upgrading the crude oil quality, and reducing the heavy oil viscosity (**Figure 36c**). Similar behavior was also observed by Holland et al. (2012) and Mozhdzhehi et al. (2019), concluding that heavy oil/bitumen upgrading was possible using a switchable solvent.

In general, the potency of each chemical additive/solvent in diminishing heavy oil viscosity is represented and validated in the heavy-oil recovery performance summarized in **Figure 37**. At least up to 20% of average incremental oil could be recuperated by applying steam-chemical/solvent co-injections. The uppermost incremental heavy oil recovery was attained by

SHTA up to 40%, followed by heptane up to 20%. DME, biodiesel, and DES presented a similar behavior regarding an incremental heavy oil recovery of 10% on average.

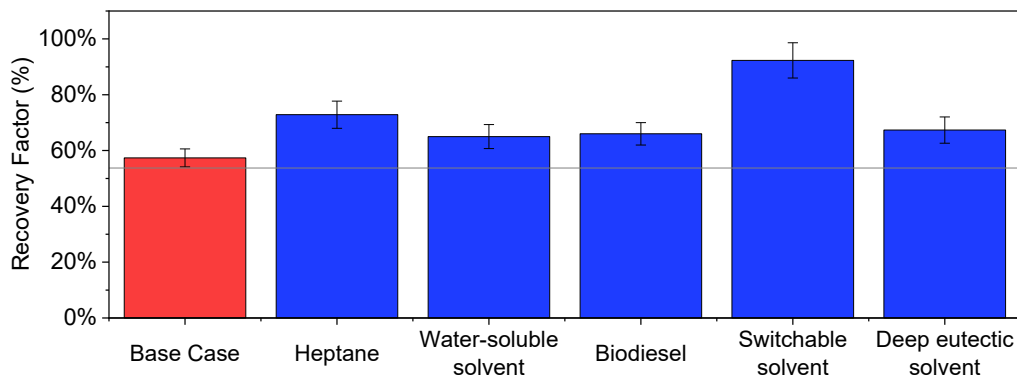


**Figure 37—Viscosity reduction effect on heavy oil recovery performance of each chemical additive/solvent compared to the base case at the HPHT steam condition (reproduced after Bruns and Babadagli 2020a-b; Huang and Babadagli 2020a; Pratama and Babadagli 2020d, 2021).**

A water-soluble solvent like DME encompasses a polarity characteristic as its unique feature—enabling further solubility in water and miscibility in hydrocarbon at the first contact (Ratnakar et al. 2016; Haddadnia et al. 2018b). It is also proven experimentally that DME presents a higher solubility/miscibility in heavy oil at steam conditions than other gas types of hydrocarbon solvents like propane or butane (Haddadnia et al. 2018b). This unique feature enables DME to partition into the oleic phase resulting in the oleic phase swelling and viscosity reduction, thus increasing the mobility of heavy oil, diminishing the residual oil, and ultimately increasing heavy oil recovery. Moreover, Haddadnia et al. (2018b) have reported that the application of DME as a steam additive was able to exhibit in-situ heavy-oil upgrading. Additionally, from a Hele-Shaw visualization perspective, DME was able to generate bubbles in the heavy oil—further leading to a favorable viscosity reduction and areal sweep efficiency (Huang and Babadagli 2020a).

Biodiesel has its mechanism in exhibiting solvency effect. The ability of biodiesel to be dissolved into heavy oil might be the solid cause in triggering heavy oil viscosity reduction when co-injected with steam (Babadagli and Ozum 2010). Furthermore, a replacement of hydrogen bonds by biodiesel instigates the dissociation of asphaltene aggregates in the heavy oil. This mechanism

further diminishes the fraction of asphaltenes, reduces the viscosity of the heavy oil, and eventually improves the steam chamber growth and heavy oil ultimate recovery. A bright white steam chamber growth with minimum residual oil was also evidenced through a Hele-Shaw experiment (Huang and Babadagli 2020a)—indicating that the solvency effect is possible by combining the steam injection with biodiesel.

The experimental studies (Mohsenzadeh et al. 2015, 2016; Huang and Babadagli 2020a, 2020b) also revealed that a lab-synthesized deep eutectic solvent (DES) could potentially improve the heavy oil recovery performance by providing a favorable viscosity reduction of the oleic phase due to the special characteristic comprised by DES. Furthermore, the experimental study performed by Mohsenzadeh et al. (2016) evidenced that the use of the DES in steam injection applications could promote the in-situ heavy-oil upgrading by diminishing the asphaltene content, improving the saturate hydrocarbons, and promoting desulphurization. Fundamentally, a eutectic solvent is formulated by involving two or more components—allowing them to establish the eutectic mixture (Mohsenzadeh et al. 2015, 2016; Huang et al. 2020). In this particular study, DES was lab-synthesized by mixing sodium carbonate and ionic liquid (1-butyl-3-methylimidazolium tetrafluoroborate) in a 5:1 molar ratio. A favorable viscosity reduction was achievable predominantly due to the interaction between the sodium carbonate—acting as a base—and carboxylic acid functional group contained in heavy oil to form and activate in-situ surfactant; therefore, triggering the IFT reduction and potential oil-in-water emulsion. The other possible reason for viscosity reduction is the solvency effect of the other gradient, which is the ionic liquid. This combined mechanism enables the heavy oil to achieve favorable viscosity reduction—resulting in steam chamber and heavy oil recovery improvements. This mechanism is also validated by the Hele-Shaw visualization, confirming that a favorable steam chamber was developed with no residual oil at the top of the cell, and more heavy oil was mobilized as a result of auspicious heavy oil viscosity reduction (Huang and Babadagli 2020a).

The CO<sub>2</sub> application is renowned to be an effective EOR method for light oil reservoirs. However, CO<sub>2</sub> injection has been tested and proven to dissolve in heavy-oil and bitumen; thus, swelling the oil and lowering its viscosity (Khatib et al. 1981). The recent study honoring the CO<sub>2</sub> injection in steam applications has evidenced that the use of CO<sub>2</sub> not only could auspiciously lower the heavy-oil viscosity but also reduce the interfacial tension (Mohammedalmojtaba et al. 2020). The other

lab-based studies performed by Seyyedsar et al. (2016) and Shilov et al. (2019) concluded that the improvement on the heavy-oil properties due to the use of CO<sub>2</sub> in steam injection was able to improve the incremental heavy-oil recovery of up to 20%. In a more field case, the CO<sub>2</sub> injection contributed at least 10% of the heavy-oil incremental recovery (Issever et al. 1993; Sahin et al. 2008; Babadagli et al. 2009). This evidence has proven that the CO<sub>2</sub> injection can potentially be applied in late-stage steam injection. More importantly, this method can reduce the steam usage; therefore, promoting GHG emissions reduction and more sustainable heavy-oil and bitumen production (Xu et al. 2020).

### 3.5.1.2 Detergency Effect (Wettability Alteration and IFT Reduction)

The surface wettability of the reservoir rocks has been a prevalent factor affecting oil recovery, particularly in heavy oil steam injection applications. It is also responsible for the remaining/residual oil saturation and the capillary pressure. In the surface sciences, rock wettability is generally termed as the capability of the specific phase to spread on the rock surface in the existence of the other phases due to the intermolecular forces. These intermolecular forces occur in the reservoir system thermodynamically (Hirasaki 1991) and can be approximated through the Derjaguin, Landau, Velwey, and Overbeek (DLVO) theory, consisting of van der Waals and electrostatic/electrical double layer (EDL) interactions in a molecular scale. In addition to this DLVO approach, the energy change per unit area or disjoining pressure—the force separating or disjoining two interfaces—is also a parameter describing the thermodynamics of reservoir rock wettability.

A relationship between reservoir rock wettability and IFT (**Figure 38**) can be determined through the quantitative contact angle measurement that satisfies Young’s force balance as follows:

$$\cos \theta = \frac{\gamma_{steam/solid} - \gamma_{oil/solid}}{\gamma_{oil/steam}} \dots \dots \dots (3)$$

where  $\theta$  indicates the contact angle between the oleic phase and the solid phase,  $\gamma_{steam/solid}$  indicates the IFT between the solid phase and the steam phase,  $\gamma_{oil/steam}$  indicates the IFT between the oleic phase and the steam phase, and  $\gamma_{oil/solid}$  indicates the IFT between the oleic phase and the solid phase.

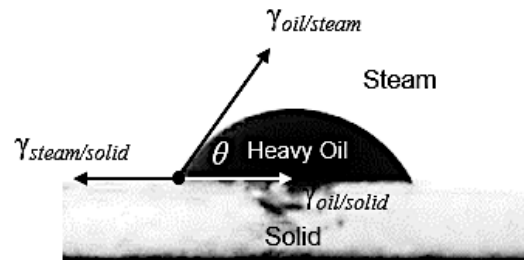


**Figure 38—Force balance of rock-heavy oil-steam system at HPHT steam condition.**

Favorable wettability alteration and IFT reduction could be achieved predominantly due to the rock-fluid-chemical interactions in the reservoir, affecting surface force and/or disjoining pressure and thus improving the capillary force and relative permeability. Chemicals considered in this study were able to predominantly present wettability alteration, whereas some of them were evidenced to exhibit IFT reduction as their principal displacement mechanism (**Figure 39**), therefore favorably improving heavy oil recovery at steam conditions (**Figure 40**). The analysis given in these figures indicate that remarkable chemical-induced wettability alteration and IFT reduction were achievable even at HPHT steam conditions.

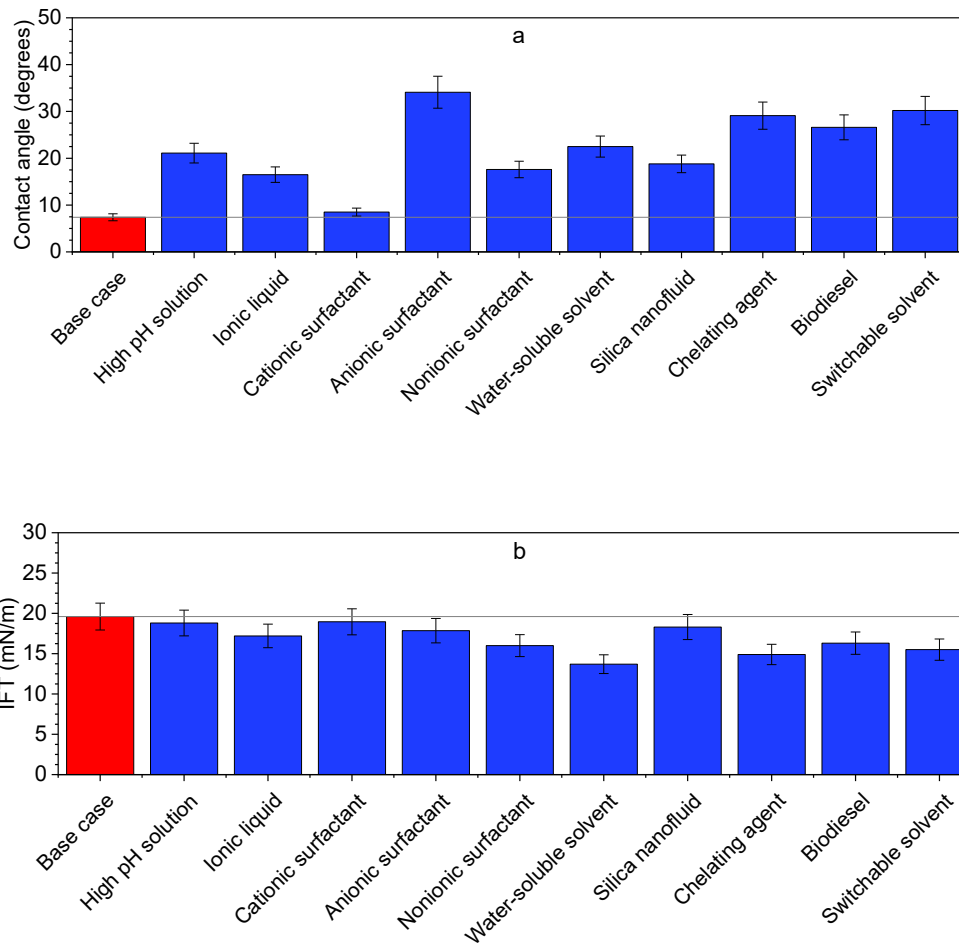


**Figure 39—Wettability alteration of sandstones and IFT after co-injecting steam with chemical additives at optimal chemical concentrations performed at HPHT steam application of up to 220°C and 200 psi: (a) quantitative contact angle measurements. The contact angle was measured between the oleic phase and solid phase in steam, and (b) IFT measurements of heavy-oil in steam (reproduced after Pratama and Babadagli 2020a, b).**

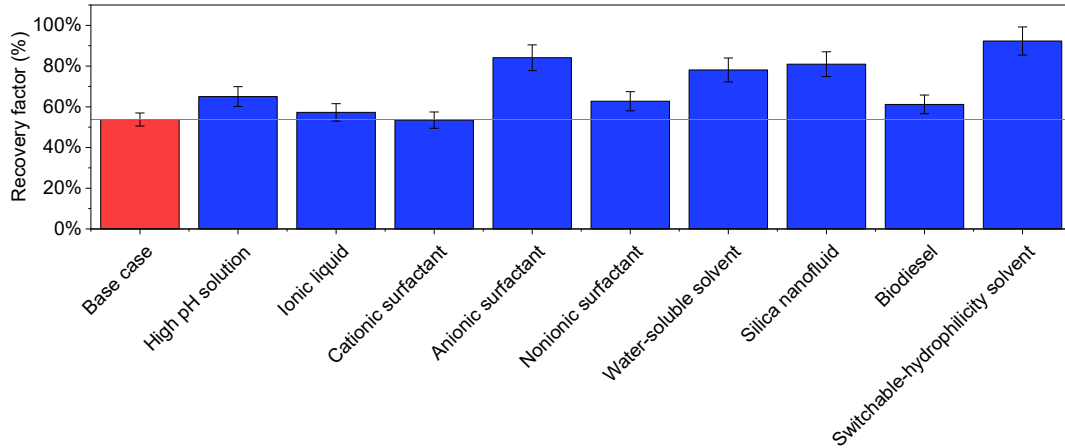
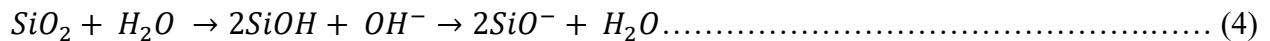


**Figure 40—Wettability alteration effect on heavy oil recovery performance of each chemical additive compared to the base case at the HPHT steam condition (reproduced after Bruns and Babadagli 2020a; Huang and Babadagli 2020a; Pratama and Babadagli 2020d, 2021).**

The use of alkaline agents could potentially improve the heavy oil recovery performance in steam injection applications by favorably altering the rock wettability. **Figure 39a** presents the change in wettability observed in sandstone after adding sodium metaborate (NaBO<sub>2</sub>) as a steam additive. Adding a high-pH solution during the steam injection will increase the pH value of the system. The rise in pH increases the chance of surface hydrolysis of the reservoir rocks (Flury et al. 2014), satisfying the following chemical reaction:



This surface hydrolysis potentially increases/restores the hydrophilicity of the rock surface that ultimately leads to the improvement of rock surface wettability. Raising the pH value of the system could also lead to the rock surface charge modification to a more negatively charged surface (Masliyah et al. 2011). This condition increases the strength of the electrostatic repulsive force between the rock surface and the heavy oil. Moreover, the contribution of this repulsive force leads to a more positive disjoining pressure that tends to the separation of heavy oil from the reservoir rock surface. In other words, the change in the surface force presents the auspicious wettability

alteration that leads to the improvement of heavy oil recovery (Chiwetelu et al. 1994; Flury et al. 2017).

In addition to the potential surface hydrolysis and surface charge modification, increasing the pH value of the rock-heavy oil-steam system by involving high pH solution could also potentially trigger the activation of natural surfactant (carboxylic acid functional group) contained in the heavy oil—further reducing heavy-oil-water/steam IFT. However, the IFT reduction was evidenced to not be significant. In other words, the wettability displacement mechanism plays an essential role in contributing to the heavy-oil recovery performance in the case of a high pH solution.

The ionic liquid comprises the organic cationic group (1-butyl-3-methylimidazolium) acting as a hydrophobic group and the anionic group (tetrafluoroborate) acting as a hydrophilic group. These ionic groups are potentially able to alter the rock surface wettability as well as reduce heavy oil-water/steam IFT (Hogshead et al. 2011; Dahbag et al. 2015; Hanamertani et al. 2015; Huang and Babadagli 2020a; Pratama and Babadagli 2020a), as presented in **Figure 39**. The ability of this chemical to establish the detergency effect is due to the surface activity of the ionic liquid. The IFT reduction can be initiated when the interaction between the ionic liquid molecules and the water/steam occurs by establishing an attractive force between counterpart ions. The positively charged ions contained in the ionic liquid are neutralized by the negatively charged ions in the water/steam. This interaction speeds up the accumulation of ionic liquid molecules at the heavy oil-water/steam interface; hence, further decreasing the heavy oil-water/steam IFT.

On the other hand, the chemical-induced wettability alteration potentially occurs with a different mechanism by modifying the surface charge of the reservoir rock in addition to the surface adhesion forces (Hogshead et al. 2011). The anionic group of the ionic liquid could be adsorbed onto the reservoir rocks (e.g., sandstones)—naturally comprising a negative charge—thus modifying the solid phase surface charge to be even more negatively charged. This phenomenon leads to electrostatic repulsive forces between the heavy oil—containing negatively charged carboxylic acid group—and the rock surface. Moreover, the ionic liquid has been validated to diminish the heavy oil-rock surface adhesion forces and reduce the separation (Hogshead et al. 2011). This circumstance further promotes heavy oil-solid surface separation, positive disjoining pressure and eventually triggers wettability alteration. However, these potential mechanisms were

not reflected in the heavy oil recovery performance (**Figure 40**). Substantial heavy oil incremental recovery was not perceived during the steam injection co-injected with ionic liquid compared to the other studied chemical additives. Even though the ionic liquid has proven to exhibit potential displacement mechanisms, the recovery performance presented by this chemical additive has to be taken into account when it comes to field applications.

The surface activity of a chemical additive plays a vital role in the detergency effect—modifying interfacial properties (e.g., IFT/surface tension, wettability). The surface activity mechanism is possible when the adsorption of the surfactant is initiated to form micelles. Furthermore, at the interface, the hydrophobic functional group (tail) interacts with the heavy oil, whereas the hydrophilic functional group (polar head) tends to interact with water/steam. This mechanism leads to the accumulation of the surfactant molecules at the interface, consequently reducing heavy oil-water/steam IFT. In addition to the IFT reduction mechanism, surfactants are able to potentially alter the reservoir rock surface wettability, depending on the adsorption of the surfactant molecules on the rock surface, the natural charge of the reservoir rock surface, and the charge of the hydrophilic functional groups—further modifying the total solid surface charge, the surface forces (e.g., adhesion forces), and disjoining pressure (**Figure 41**).

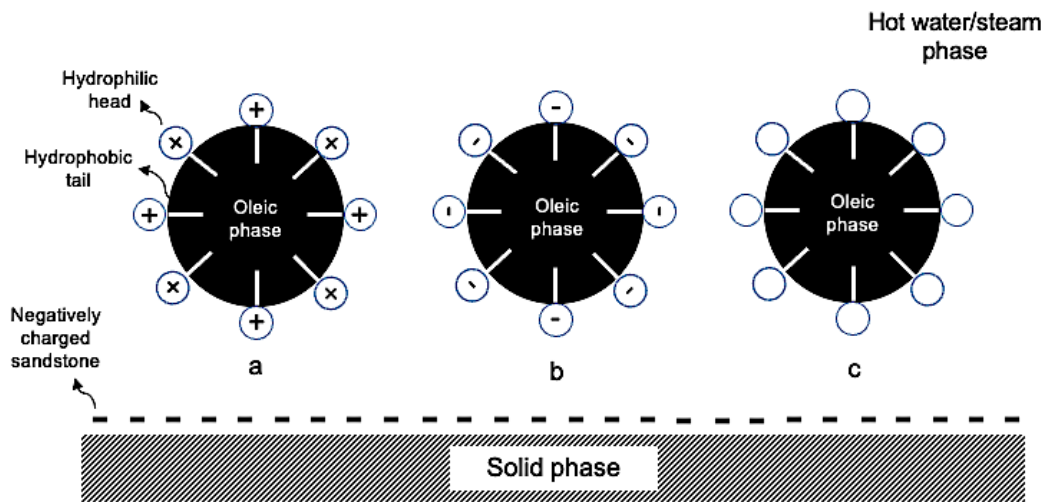


**Figure 41—Surfactant-heavy oil interaction in rock/heavy oil/steam system: (a) cationic surfactant, (b) anionic surfactant, and (c) nonionic surfactant.**

The experimental results gained from the use of surfactants as steam additives are also influenced by reservoir rock types in addition to the physical characteristics of the surfactants themselves. Most of the experiments presented in the study utilized sandstones as a solid phase to represent most of the heavy oil reservoirs (particularly Canadian reservoirs), meaning the reservoir rocks were expected to have a more negatively charged surface (Masliyah et al. 2011). In the case of cationic surfactant, the detergency effect was not achievable (**Figure 39**). Even though the heavy oil-steam IFT was perceived to slightly decrease due to the surface activity, the favorable wettability alteration was unattainable primarily due to the contribution from the interaction between positively charged hydrophilic polar heads comprised by the cationic surfactant and the negatively charged solid surface. The adsorption of the surfactant molecules on the rock surface could modify the total solid surface charge towards a more positive charge due to the adsorption mechanism on the sandstones, thus further triggering attractive forces between the reservoir rock surface and the heavy oil molecules. In this circumstance, an improvement to the surface forces and the wettability was not possible—affecting capillary pressure and eventually resulting in poor heavy oil recovery performance at steam conditions (**Figure 40**). Similar heavy oil recovery behavior was also evidenced in the use of cationic surfactant on the sandstone reservoir rocks system at HPHT steam conditions. Steam-chemical-based recovery was not able to improve ultimate heavy oil recovery compared to steam-based recovery (Wei and Babadagli 2017b; Seng and Hascakir 2021).

Conversely, favorable improvement of heavy oil recovery was presented by the anionic surfactant when co-injected with steam in the sandstones/heavy oil/steam system—resulting in significant incremental heavy oil recovery of up to 30% (**Figure 40**). Furthermore, the anionic surfactant could favorably present the detergency effect displacement mechanism as observed through the experimental studies outlined in **Figure 39**. The surface activity of the anionic surfactant could be established even at HPHT steam applications—yielding the heavy oil-steam IFT reduction. Nevertheless, the recovery mechanism is still dominated by the wettability alteration mechanism represented by a substantial rock surface wettability improvement (**Figure 39a**). The dominance of the wettability alteration mechanism could also be observed through the phase distribution in porous media presented in **Figure 42**. The residual oil developed post-steam injection was diminishable without any oil traces left after co-injecting anionic surfactant with steam, indicating that the wettability of the solid surface was favorably altered. Fundamentally, anionic surfactant

encompasses a negatively charged hydrophilic functional group (head) that can affect the total surface charge of the rock surface when adsorption of the surfactant molecules occurs on the rock surface. The total solid surface charge can potentially be modified to be more negatively charged in the case of sandstone reservoirs. This mechanism promotes repulsive forces between the solid phase and the heavy oil (negatively charged naturally), further resulting in lower surface forces (adhesion), positive disjoining pressure, and eventual wettability alteration to be less oil-wet.

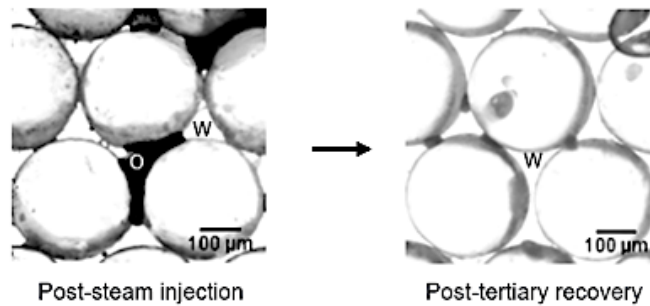


**Figure 42—Wettability alteration mechanism dominance presented by anionic surfactant diminishing residual/trapped oil and improving heavy oil recovery in porous media at high-temperature steam conditions. O = oleic phase and W = water phase. (after Pratama and Babadagli 2020d).**

A total solid surface charge is not influenced by the adsorption of the neutrally charged hydrophobic head of nonionic surfactant on the solid surface during the steam-chemical-based heavy oil recovery. Even though the quantitative wettability measurement still exhibited contact angle shifting during the steam-chemical-based injection, the recovery mechanism was dominated by IFT reduction evidenced through the interfacial tension measurement at HPHT steam conditions (**Figure 39**). This evidence is also corroborated by the interesting finding of phase distribution behavior in porous media (**Figure 43**). The experimental study performed by Pratama and Babadagli (2020d) shows that the trapped oil in pore spaces was able to be mobilized predominantly due to the IFT reduction mechanism occurring during the steam-chemical-based recovery process. The oil films observed post-tertiary recovery are a solid indication that the wettability of the solid surface still could not be favorably altered; therefore, the IFT reduction mechanism presented a substantial contribution in the heavy oil recovery. The surface activity of nonionic surfactants can be characterized by the hydrophilic-lipophilic balance (HLB) number. A

high HLB value comprised by the nonionic surfactant indicates that the hydrophilic functional group (head) prevails, whereas a low HLB number indicates the dominance of the hydrophobic functional group (tail). In other words, a nonionic surfactant encompassing a high HLB number is more water-soluble than a nonionic surfactant with a low HLB number. A sorbitan monooleate used as a nonionic surfactant has a low HLB value of  $\sim 4.5$ , which promotes a water-in-oil emulsion generation—hence further reducing the heavy oil-water/steam IFT at HPHT steam conditions.

The application of nanofluids—in steam injection/SAGD applications—have obtained more attention in the past few years. Study and research have also been conducted to investigate and evaluate the potency of nanofluids in improving heavy-oil and bitumen recovery. Our recent research honoring the use of nanofluids—specifically at late-stage steam injection applications—perceived that the rock wettability post-steam injection could be favorably improved to be less oil-wet and the interfacial tension was able to be reduced (Pratama and Babadagli 2020b, 2020d). Similar interfacial properties behavior was also evidenced by some other published experimental studies. The addition of nanoparticles as chemical additives could successfully improve the interfacial properties, even at high-temperature steam conditions; thus, further adding incremental heavy-oil and bitumen recovery of up to 25% on average (Maghzi et al. 2012; Mohammed and Babadagli 2016; Cao et al. 2017; Wei and Babadagli 2017a, 2017b, 2019; Taylor 2018; Medina et al. 2019; Rezk and Allam 2019; Bruns and Babadagli 2020a, 2020b; Fehr et al. 2020; Huang and Babadagli 2020a, 2020b). Scientifically, nanofluids (containing nanoparticles)—particularly silicon oxide ( $\text{SiO}_2$ ), are able to favorably modify the interfacial properties of the reservoir rocks due to the negative surface charge carried by the nanoparticles naturally at a moderately neutral pH, naturally (Maghzi et al. 2012; Keramati et al. 2016; Agista et al. 2018). The negatively charged nanoparticles can be adsorbed onto the reservoir rock surface. This mechanism modified the total surface charge of the reservoir rock to a more negatively charged and hydrophilic surface. At this circumstance, the dynamics of surface force occurs—promoting electrostatic repulsion between the reservoir rock surface and the heavy-oil; thus, leading to a favorable wettability alteration (Masliyah et al. 2011; Maghzi et al. 2012).

The use of chelating agents as steam additives could potentially improve the heavy-oil and bitumen recovery. Recently, Pratama and Babadagli (2020b), through the lab-based experimental study, evidenced that the thermal stability and the detergency effect (wettability alteration and

interfacial tension reduction) at high-pressure-high-temperature steam conditions were possible after involving the chelating agents at the late-stage steam injection that could potentially improve the incremental heavy-oil and bitumen recovery. This evidence was also supported by other published lab-scale experimental studies performed by Mahmoud and Abdelgawad (2015) and Almubarak et al. (2017), concluding that the improvement of detergency effect (rock wettability improvement and lower IFT value) and recovery improvement were attained. Over 80% of ultimate recovery was attainable after involving chelating agents. The detergency effect is possible with chelating agents due to the characteristics of the chemicals. Chelating agents are fundamentally the chemicals that can instigate metal ion bonds. These chemicals contain various functional groups, such as hydroxy, carboxyl, ether, and amines, that are able to establish stable complexes by encapsulating cations in the reservoir system (Mahmoud and Abdelgawad 2015). These functional groups can act like solvent and high-pH solution at the same time due to the presence of amines and ether. A solvent-like characteristic presented by chelating agents can potentially establish the in-situ upgrading, whereas the high-pH condition can modify the rock surface charge to a more negatively charged; thus, promoting electrostatic repulsive force between heavy-oil and the rock surface (Masliyah et al. 2011)—resulting in favorable detergency effect.

The detergency effect—improving heavy oil recovery—induced by the switchable solvent like SHTA was due to the distinctive characteristic of this switchable solvent. Fundamentally, a switchable solvent (SHTA)—synthesized from tertiary amines—encompasses two functional groups, including hydrophobic and hydrophilic, enabling this chemical to wet heavy oil and water at the same time, an action that further diminishes the IFT between heavy oil and steam (**Figure 39**). In addition to the IFT reduction recovery mechanism, the wettability alteration mechanism was also observed post-steam-chemical-based heavy oil recovery. This recovery mechanism is possible due to the ion transfer from the chemical to the rock/heavy oil system, forming the ion pairs. The cations ( $C_8H_{17}NH^+$ ) are absorbed on the heavy oil surface, whereas the anions ( $HCO_3^-$ ) reduce the interaction between the heavy oil and sandstone by reducing the surface forces and initiating electrostatic repulsive force, and then altering the sandstone surface wettability to a less oil-wet state. A favorable wettability alteration was perceived through the sand grain surface observation performed post-tertiary recovery (**Figure 44**). It is clearly observed that the surface of the sand grain shifted from a darker color to a much lighter color, indicating that the wettability of the sand grain surface has been favorably altered post-steam-chemical-based recovery. More

importantly, a synergistic recovery mechanism exhibited by this chemical additive was able to significantly improve the ultimate heavy oil recovery by 40% (Pratama and Babadagli 2021).

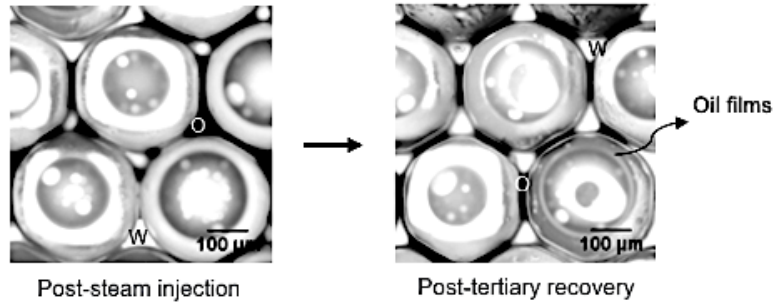


**Figure 43—IFT reduction mechanism dominance presented by nonionic surfactant leaving oil traces, diminishing residual/trapped oil, and potentially improving heavy oil recovery in porous media at high-temperature steam conditions. O = oleic phase and W = water phase (after Pratama and Babadagli 2020d).**



**Figure 44—Wettability alteration mechanism presented by switchable solvent on sand grain surface post-steam-chemical-based recovery.**

### 3.5.2 Micro Displacement Mechanism

#### 3.5.2.1 Foaming Effect

Surfactants can potentially generate foam in the reservoir if they are injected together with steam and non-condensable gases, such as CO<sub>2</sub> or N<sub>2</sub> (Friedmann et al. 1994). Their lab-based experimental study and field trial have concluded that in-situ foam generation was able to improve

the steam conformance and suspend the steam breakthrough phenomenon in the reservoir. Moreover, the foam generation presented by surfactants could substantially improve both areal and vertical sweep efficiency (Friedmann et al. 1994).

This evidence is also corroborated by other published lab-based experiments and field tests. Lau and Borchardt (1991) performed a field trial with steam-surfactants injection in Kern River. They evidenced that the foam could be generated and sweep efficiency could be improved; thus, diminishing the residual oil saturation and improving incremental heavy-oil recovery of up to 14%. Similar evidence was also perceived by some other published experimental studies. The steam-foam generation could be successfully established even at high-temperature steam conditions (Huang et al. 1985; Mujis et al. 1988; Shallcross et al. 1990; Osterloh and Jante 1994; El-Abbas and Shedid 2001; Cuenca et al. 2014; Mukherjee et al. 2018; Li et al. 2019; Nguyen et al. 2018; Nguyen et al. 2019). In other words, the late-stage steam injection can be potentially improved by a synergy between steam and surfactants.

### **3.5.2.2 Emulsion Generation**

Steam-chemical-based recovery could potentially improve steam conformance, vertical and areal sweep efficiency, and mobility control when co-injected at high-temperature conditions. Moreover, this recovery technique can potentially generate in-situ foam in the reservoir, for instance, in the case of non-condensable gas and surfactants combined injection—further promoting steam conformance improvement as well as suspending steam breakthrough (Du et al. 2021). According to our experimental studies, we were able to evidence emulsion generation at HPHT steam conditions with nonionic surfactant (sorbitan monooleate) and switchable solvent (SHTA). **Figures 45** and **46** exhibit the in-situ emulsion generation induced by a nonionic surfactant.

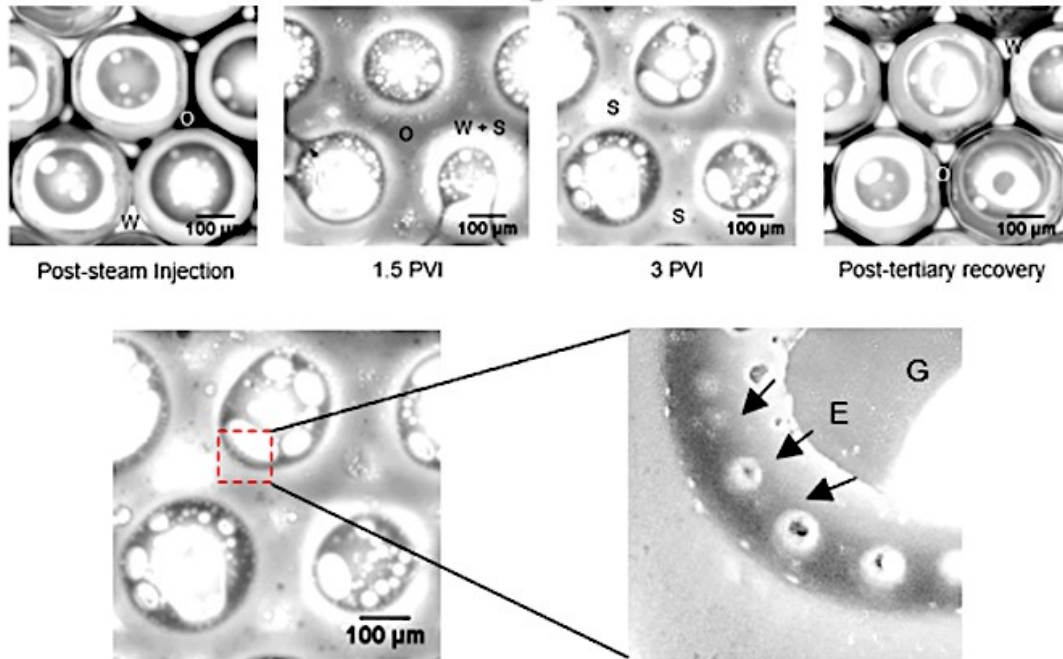


Figure 45—Water-in-oil in-situ emulsion generation induced by a nonionic surfactant (after Pratama and Babadagli 2020c).

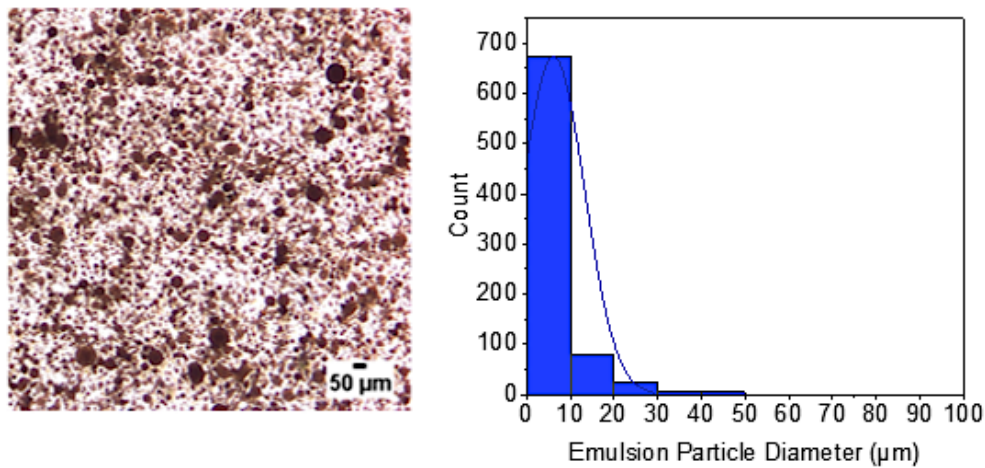


Figure 46—Oil-in-water emulsion generation induced by SHTA (after Pratama and Babadagli 2021).

Emulsification by the nonionic surfactant was possible due to the hydrophilic and lipophilic functional group of the surfactant, explainable through the hydrophilic-lipophilic balance (HLB) number. A Low HLB number usually promotes water-in-oil emulsification, whereas a higher HLB number promotes oil-in-water emulsification. This mechanism validates the experimental result

presented in **Figure 41**. A different emulsification mechanism was presented by the switchable solvent post-steam-chemical-based recovery. The oil-in-water emulsion was observed in the produced sample obtained from sandpack flooding. A possible explanation of this oil-in-water emulsion generation is due to the unique feature of this switchable solvent. A switchable-solvent like SHTA contains functional hydrophilic and hydrophobic groups, which can establish surface activity and intermediate wetting to further diminish the IFT and generate oil-in-water emulsion (**Figure 42**).

### **3.6 Sensitivity Analysis of Displacement Mechanisms on Heavy Oil Recovery and Estimated Cost of Applications.**

The analyses done in the previous sections indicate that potential chemical additives (including solvents) could favorably improve the heavy oil recovery performance, and researchers discussed relevant displacement mechanisms to achieve steam-chemical-based recovery improvement. **Table 3** summarizes the potential displacement mechanisms presented by each studied chemical additive.

The sensitivity analysis of each displacement mechanism to the incremental heavy oil recovery is also performed to acquire more understanding regarding the degree of displacement mechanism influence on the ultimate oil recovery. Fundamentally, heavy-oil ultimate recovery was established from each steam additive, presenting a specific displacement mechanism evidenced in our experimental studies, represented by a tornado chart (**Figure 47**). It is perceived that wettability alteration is the most predominant parameter affecting heavy oil recovery, presenting the largest influence on the heavy oil recovery performance.

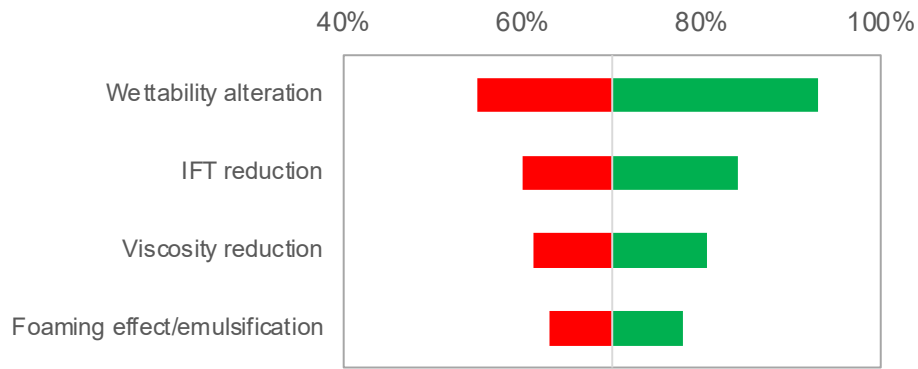


**Figure 47—Sensitivity analysis of each recovery mechanism against heavy oil recovery.**

Additionally, **Figure 48** presents the commercial price for all studied chemical additives. This chemical price comparison is valuable to make a more objective evaluation of the field application potential. Most of the chemical additives, such as are still considerable and economical for field implementations—particularly alkali, water-soluble solvent, biodiesel, switchable-solvent, and CO<sub>2</sub> injection; nevertheless, a few of them—like ionic liquids—still need further economic evaluation as they can present substantially high cost and may limit their applications in heavy-oil fields.

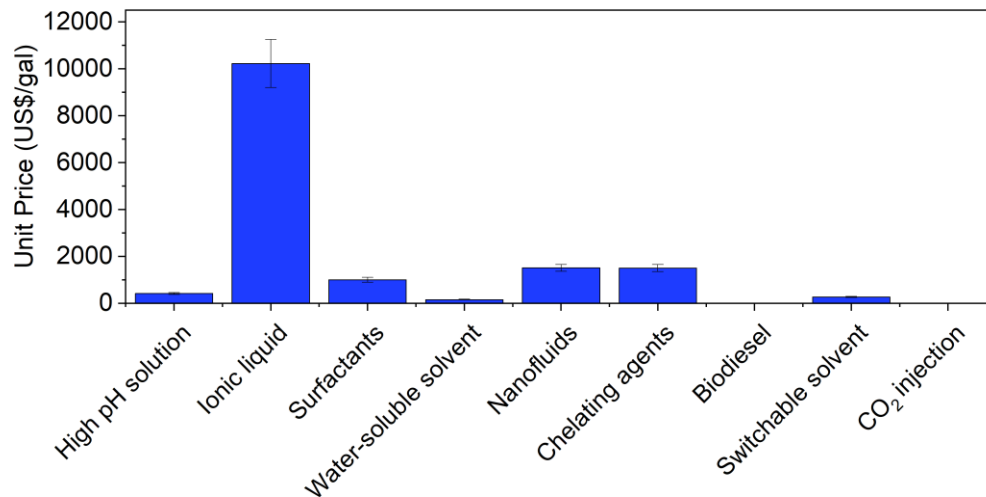


**Figure 48—Commercial price comparison of tested chemical additives at optimal concentration.**

### 3.7 Conclusions

1. Detergency effect—wettability alteration and steam-heavy oil IFT reduction—in addition to other recovery mechanisms, plays an essential role in heavy oil recovery, particularly under steam applications.
2. Certain chemical additives (e.g., ionic liquid, surfactants, DME, chelating agents, biodiesel, SHTA) were validated to present a combined displacement mechanism.
3. Ionic liquid could present a combined displacement mechanism and promising thermal stability; however, potential displacement mechanisms gained from the interfacial properties' evaluation were not reflected in the heavy oil recovery performance. This evidence has to be taken into consideration when it comes to field applications.
4. The surface activity of surfactants was still maintainable even at HPHT steam conditions. However, only anionic, and nonionic types of surfactants presented favorable detergency effects (IFT reduction, wettability alteration) and heavy oil recovery improvement. A cationic surfactant exhibited neither auspicious displacement mechanisms nor heavy oil recovery improvement. Therefore, the use of cationic surfactant as a steam additive is not recommended for steam injection applications.
5. A switchable solvent (SHTA) was proved to exhibit its solvency effect and deliver the most favorable heavy oil recovery by providing four combined recovery mechanisms—viscosity reduction, wettability alteration, IFT reduction, and oil-in-water in-situ emulsification.
6. Nonionic types of surfactants and switchable solvent are considered to be effective steam additives in generating emulsions.
7. Non-condensable gas like CO<sub>2</sub> can act as a solvent. This chemical additive can potentially reduce the viscosity of heavy-oil and improve the recovery. Therefore, this chemical additive is recommended for late-stage steam/SAGD applications.
8. The use of nanoparticles can be considered as a potential heavy-oil and bitumen recovery method since this chemical additive is proven to present favorable detergency effects, even

at high-temperature steam conditions; however, the application cost of this chemical additive should be considered for further field applications.

9. According to the sensitivity analysis of each displacement mechanism, wettability alteration is the most predominant factor affecting heavy oil recovery performance at steam conditions; thus, it is recommended to co-inject steam with chemical additives encompassing potential wettability alteration displacement mechanism as well as the combined mechanisms for steam injection field applications.
10. Most of the chemical additives—including solvents—have presented promising displacement mechanisms potentially recommended for steam applications; however, additional research/studies on some other aspects, such as chemical adsorption, cost of applications, large-scale sweep efficiency impact, and effect on oil-water separation, must be taken into account when it comes to the field applications.

## **Chapter 4: New Formulation of Tertiary Amines for Thermally Stable and Cost-Effective Chemical Additive: Synthesis Procedure and Displacement Tests for High-Temperature Tertiary Recovery in Steam Applications**

This chapter of thesis is a modified version of a paper (SPE 201769) presented at the SPE Annual Technical Conference and Exhibition held through virtual meeting, 26–29 October 2020. The journal version of this research paper has been published in SPE Journal.

## 4.1 Preface

A newly formulated chemical additive from a group of amines has been tested and applied to in-situ heavy-oil thermal recovery. Switchable-hydrophilicity chemical additives were successfully synthesized from N,N-dimethylcyclohexylamine in the form of homogeneous and hydrophilic solution. Fundamentally, tertiary amines comprise functional groups of hydrophilic and hydrophobic components. These unique features enable this chemical additive to wet both water and heavy-oil, yielding potential interfacial tension improvement. Furthermore, the reversible chemical reaction of this chemical additive yields both positive and negative ions. An ion pair formed due to the adsorption of cations— $[C_8H_{17}NH^+]$ —on the surface of heavy-oil, whereas the anions— $[HCO_3^-]$ —promoted solid phase surface charge modification; therefore, resulting in the repulsive forces between heavy-oil and the rock surface—substantially improving water-wetness and restoring an irreversible wettability alteration due to the phase change phenomenon during steam injection. We have substantiated that the application of these switchable-hydrophilicity tertiary amines (SHTA) could lead to auspicious recovery mechanisms—wettability alteration and interfacial tension reduction—even in extremely high-temperature steam flooding, thus promoting phase distribution improvement in porous media by diminishing the capillary forces and the eventual favorable heavy-oil recovery performance.

In this research, two types of heavy-oil acquired from a field in western Alberta encompassing the viscosity of 5,000 cP–47,000 cP at 25°C was utilized in each experiment. All experiments were performed and measured at high-pressure-high-temperature steam conditions up to 200 psi and 200°C. To study the interfacial properties, quantitative contact angle and interfacial tension measurements were performed on rock/heavy-oil/hot-water and steam systems using a high-pressure high-temperature IFT cell under different chemical concentrations. On the other hand, dynamic experimental studies in investigating the residual oil behavior in porous media and oil recovery performance were conducted through micromodel visualization and core flood experiments. These micromodels and sandstone cores were initially saturated with synthetic brine water and then displaced by heavy-oil to mimic reservoir saturation history. Subsequently, steam was continuously injected (3 pore volumes) and followed with the injection of SHTA as tertiary recovery.

We perceived that favorable interfacial tension reduction was achieved, and irreversible wettability could be auspiciously restored after combining SHTA with steam as a result of the solid-phase surface charge modification to be more negatively charged. Phase distribution/residual oil in the porous media developed after steam injection was able to be auspiciously convalesced, indicating that capillary forces could be reduced. Consequently, over 80% of the residual oil could be recuperated post-SHTA injection presenting favorable oil recovery performance. In addition to this promising evidence, SHTA could be potentially recovered by switching its reversible chemical reaction to be in hydrophobic form; hence, promoting this chemical additive to be both reusable and more economically effective.

Comprehensive studies and analyses on interfacial properties, phase distribution in porous media, and recovery performance exhibit essential points of view in further evaluating the potential of SHTA for tertiary recovery improvement. Valuable substantiations and findings provided by our research present useful information and recommendations for fields with steam injection applications.

**Keywords:** Steam injection, tertiary amines, switchable-hydrophilicity solvent, wettability alteration, interfacial properties, micromodel, phase distribution, residual oil.

## 4.2 Introduction

Our global crude oil production is dominated by heavy-oils, contributing more than 60% in the forms of conventional heavy-oil, extra heavy-oil, and bitumen. Recent data regarding the world's potential heavy-oil reported by Meyer et al. (2007) presented that only around 8% of the estimated 7,800 billion barrels of potential heavy-oil-in-place is technically recoverable—including natural bitumen. In unlocking these potential reserves, steam injection is the most generic and practical technique applied to the heavy-oil fields. A steam injection technique comprises steam flooding, cyclic steam stimulation (CSS), and steam-assisted gravity drainage (SAGD)—all methods that have been practiced for decades. Thermodynamically, injecting steam into the heavy-oil reservoirs

is aimed to reduce the oil viscosity, therefore increasing the chance of an oleic phase to be more mobile in the rock pores (Blevins et al. 1984; Sheng 2013).

At the same time, concern regarding steam injection operations has been rising and becomes even more problematic. Typical steam injection operations require designated temperatures up to 250°C (Butler 1994; Shen 2013) to recover heavy-oil from reservoirs, presenting in high energy usage, operating cost, and particularly environmental issues, such as greenhouse gas emissions. To alleviate the steam-to-oil ratio and increase steam use efficiency, any valuable actions and alternatives are essential. This exigence has triggered more studies and implementations in diminishing energy consumption due to steam generation, including the utilization of solvents (viscosity reduction) and chemical additives (interfacial properties alteration). The applications of these alternatives, however, are still limited in terms of field-scale implementations. Besides, the thermal stability and expenditure presented by these steam additives persists as a challenge.

Research advancements and innovations in thermal enhanced oil recovery have promoted the use of chemicals as steam additives. In recent times, researchers have put attention to further study and evaluate the thermal stability of the potential chemicals at steam temperatures to encounter the unfavorable wettability alteration in the steam injection process. Pratama and Babadagli (2020a, 2020b)—through their quantitative study in the interfacial properties—have come into a solid conclusion regarding the irreversible wettability alteration triggered by a phase-change (**Figure 49**). In a natural state, reservoirs—particularly sandstones—typically still have their water-wetness; thus, allowing the water phase to encapsulate the oleic phase inside the rock pores. An irreversible wettability alteration occurs when the steam injection is initiated to the rock/oleic phase/steam system and reaches late-stage. During this stage, the layer of the water phase formed on the rock surface vaporized thermodynamically, leading to a direct interaction between the rock surface and oleic phase. The wettability state of the rock surface remains constant even when the steam/gas phase is reversely changed to liquid phase post-steam injection.

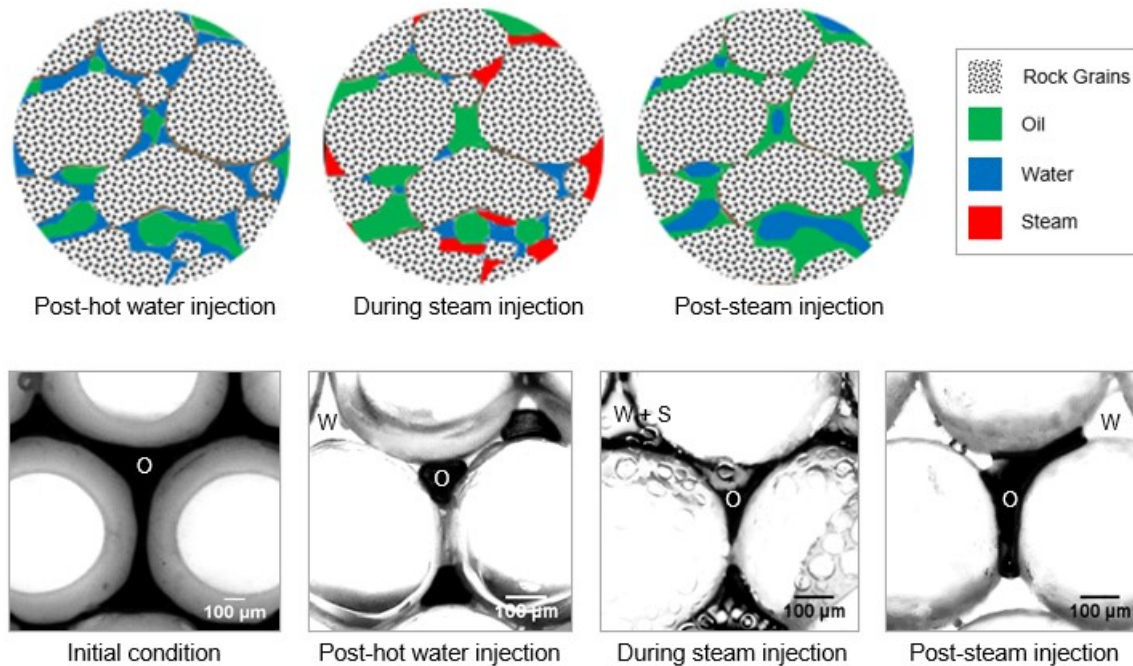


**Figure 49—Unfavorable wettability alteration caused by phase-change during steam injection in porous media. O = oleic phase, W = water/liquid phase, and S = steam/gas phase (after Pratama and Babadagli 2020a, 2020b, 2020c, 2020d).**

This substantial and valuable finding urged researchers to perform a sequence of experiments to assess the performance of conventional additives—surfactants, alkalis, and ionic liquids—and new generation additives—nanoparticles, water-soluble solvents, chelating agents, and biodiesel—at steam temperature and pressure. According to their study, most of the potential additives have exhibited excellent thermal stability at steam conditions. Furthermore, these chemicals presented potent results as steam additives in favorably reducing interfacial tension and improving the wettability impairment due to the phase-change phenomenon that occurred during steam injection. The evidence was also validated by the promising results from spontaneous imbibition experiments (Wei and Babadagli 2018), steam core flooding (Bruns and Babadagli 2020a), and auspicious sweep efficiency of heavy-oil perceived throughout Hele-Shaw cell experiments at steam temperature (Bruns and Babadagli 2020b; Huang and Babadagli 2020). In addition to these validations, Pratama and Babadagli (2020c, 2020d) conducted research honoring the phase distribution behavior in porous media using micromodels. It was perceived that a combination of steam injection and said chemical additives could diminish the residual oil saturation to less than

12% and add to oil recovery more than 24% accordingly. Even though the evidence has presented very positive potential outcomes on heavy-oil thermal recovery, the utilization cost of these chemical additives is still undeniably high.

Most recently, Jessop et al. (2010) performed a synthesis of a recyclable chemical from a group of tertiary amines. This chemical was reported to have switchability and was able to behave as a solvent for the extraction of organic components. The switchability terms fundamentally refer to the functioning principle of this kind of chemical that can be altered from being initially hydrophobic to hydrophilic reversibly. The hydrophilicity of these tertiary amines depends on the existence of carbon dioxide (CO<sub>2</sub>) gas in the water phase. This circumstance was able to control the miscibility of tertiary amines in the chemical solution (Jessop et al. 2011; Wilson and Stewart 2014; Durelle et al. 2015). The miscibility mechanism occurs due to protonation and deprotonation in the reversible chemical reaction. The miscible tertiary amines or switchable-hydrophilicity tertiary amines (SHTA) is initiated by introducing CO<sub>2</sub> gas into the tertiary amines/water system; thus, resulting in a homogeneous chemical solution containing a water-soluble bicarbonate salt—[HCO<sub>3</sub><sup>-</sup>]. Jessop et al. (2011) and Sui et al. (2016) have also reported that the hydrophilicity of this SHTA solution was able to be reversely switched into more hydrophobic (immiscible) chemical solution by elevating the temperature of the system and injecting nitrogen (N<sub>2</sub>) gas at the same time. The separation of tertiary amines from the chemical solution could potentially increase the chemical reusability, leading to more cost-effective and environmentally friendly operations.

The development and utilization of a group of amines as switchable solvents were initially implemented for soybean oil extraction and separation (Phan et al. 2009; Jessop et al. 2010), high-density–volume-reduced polystyrene (Jessop et al. 2011), lipid extraction from algae and microalgae (Boyd et al. 2012; Samori et al. 2013; Du et al. 2015), and phenols extraction from lignin (Fu et al. 2014). Recently, the concept of organic matter removals was then reproduced and adopted in the area of fossil energy. A study in the bitumen extraction was conducted by Holland et al. (2012) and Sui et al. (2016) to evaluate the SHTA performance on bitumen recovery. They reported that the bitumen could be favorably recovered up to 98% from the oil sands by involving SHTA. In addition to the evidence, a synergistic function between SHTA and asphaltenes was successfully instigated. The research perceived that the heavy-oil could be upgraded by also reducing the viscosity (Mozhdehei et al. 2019). Additionally, the oil-water interfacial tension was

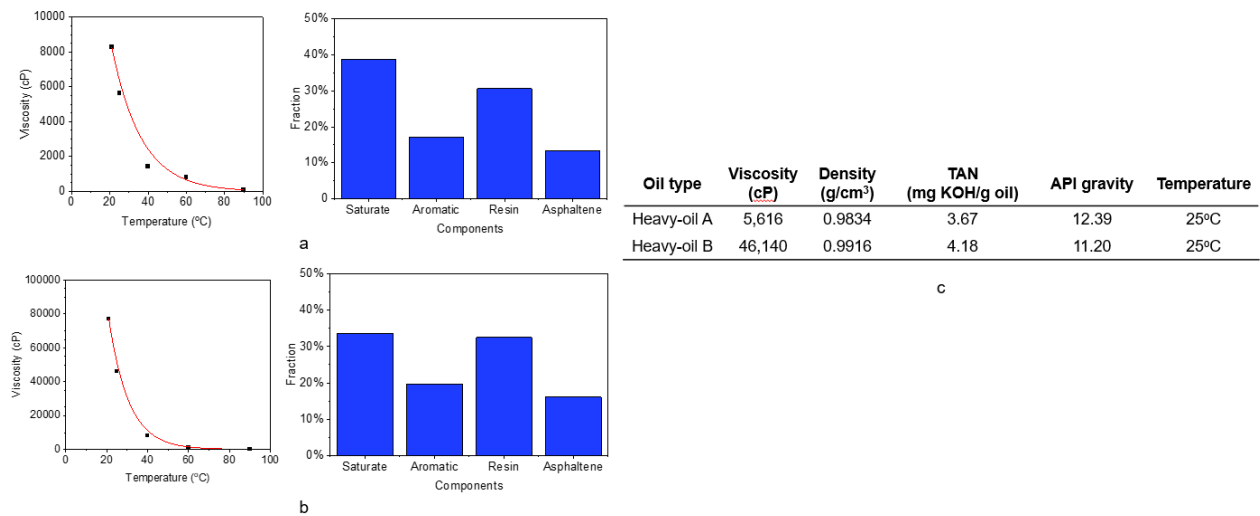
able to be lowered throughout the emulsion stabilization mechanism (Li et al. 2018). These studies, however, were performed at much lower than steam temperature.

In summary, this research aims to further evaluate and investigate the potency and applicability of SHTA as a steam additive in high-pressure and high-temperature steam injection applications. We were also able to identify the recovery mechanisms through qualitative and quantitative analyses of fluid properties, interfacial properties (IFT and contact angle), high-pressure–high-temperature spontaneous imbibition, phase distribution in porous media, and steam core flooding. These analyses are essential to obtain both a valuable understanding as well as more solid conclusions regarding the use of this SHTA for thermal enhanced oil recovery since there are no such studies on this potential steam additive in steam injection applications.

### 4.3 Materials and Experimental Setup

#### 4.3.1 Oleic Phase

This research utilized two types of heavy-oil acquired from western Alberta, Canada. **Figure 50** shows the physical properties of heavy-oil.

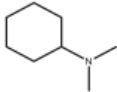


**Figure 50—Physical properties and SARA test of heavy-oil: (a) type a heavy-oil, (b) type b heavy-oil, and (c) crude oil properties summary.**

### 4.3.2 Steam Additives

A list of chemical additives used in this study is presented in **Table 8**. Moreover, thermogravimetric analysis (TGA) of this chemical was conducted and is reported in **Figure 51**. A range of chemical additive concentrations was also part of this study to evaluate the correlation among interfacial properties, phase distribution in porous media, and oil recovery performance.

**Table 8—Physicochemical of utilized tertiary amines.**

Chemical Name	Structure	$\rho$ (g/cm <sup>3</sup> )	pKa	CAS Reg. No.	Concentration
N, N- dimethylcyclohexylamine		14.5	10.48	98-94-2	1–5 wt %

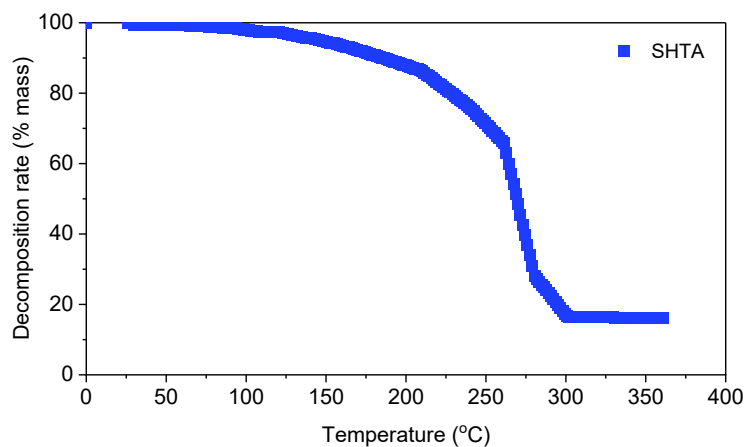


**Figure 51—TGA measurement of SHTA (N,N-dimethylcyclohexylamine).**

### 4.3.3 Interfacial Properties

A quantitative study of contact angle and interfacial tension (IFT) measurements were performed to advance the surface wettability science and interfacial interaction between SHTA and the rock/heavy-oil/steam system. The measurements were conducted for both types of heavy-oil. Each measurement was implemented at the hot-water (up to 200 psi and 90°C) condition and steam (up to 200 psi and 200°C) condition. For the contact angle experiment, quartz was utilized as a substrate, representing most sandstone reservoirs. The substrate was immersed in the oleic phase at 70°C for one week to mimic the natural wettability of the rock surface and allow the adsorption of polar components on the quartz surface. Also, the additional oil yielded from this process was treated with toluene thoroughly.

A Ramé–Hart goniometer/tensiometer—completed with a high-pressure–high-temperature IFT cell—was applied to quantify the interfacial properties. For the contact angle observation, a drop of oleic phase was positioned on a quartz substrate from the needle. In this particular research, oleic phase droplet was put as a reference in measuring the contact angle; therefore, any contact angle  $<90^\circ$  indicates more oil-wet whereas a contact angle of  $>90^\circ$  indicates more water or steam-wet. The data gathered from each experiment was then processed and interpreted through DROPimage Advanced computer software (Ramé–Hart 2019). Each experiment was conducted for 180 minutes to obtain the equilibrium state—indicated by the constant values of measurement. A complete experimental setup is exhibited in **Figure 52**.

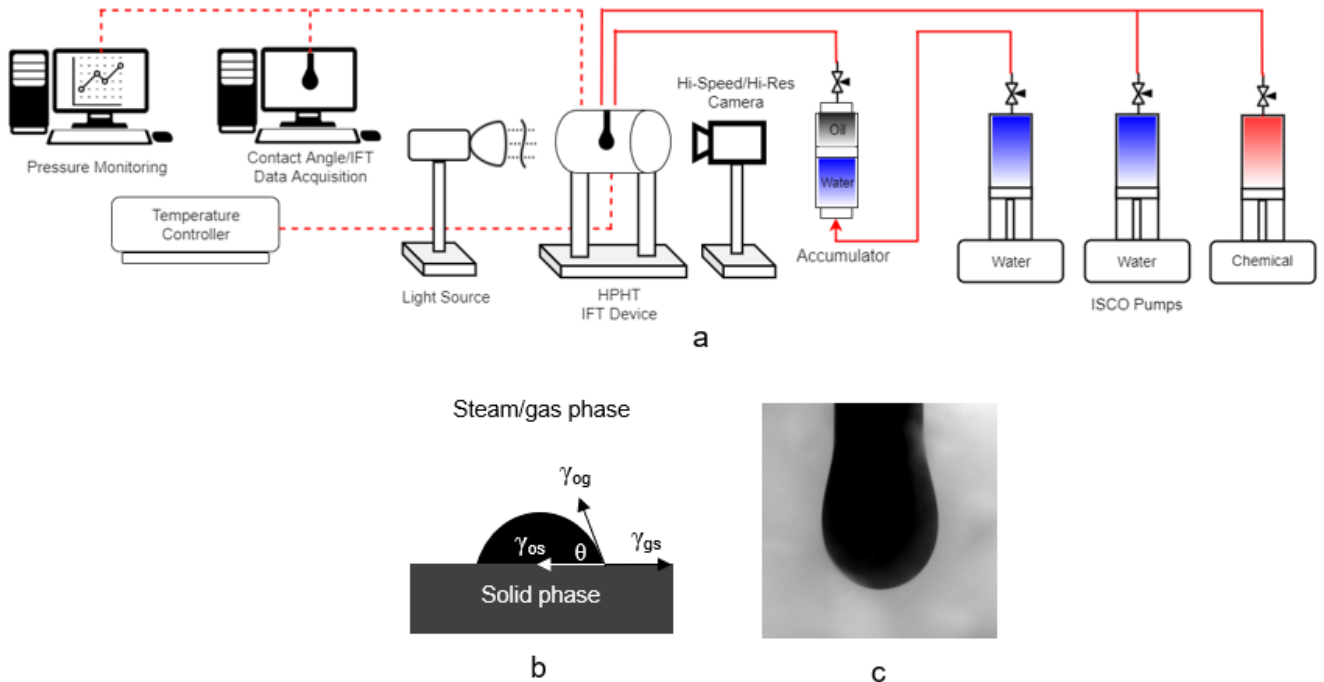


**Figure 52—Interfacial properties measurements: (a) complete experimental setup, (b) contact angle, and (c) interfacial tension of oleic phase-steam with pendant drop.**

#### 4.3.4 High-Pressure High-Temperature Capillary Imbibition

Berea sandstone core samples were utilized in the high-pressure–high-temperature (HPHT) imbibition study. **Table 9** presents the complete core properties for each experiment. Initially, the cores were saturated with heavy-oils for two weeks at 40–50°C for heavy-oil A, and 70°C for heavy-oil B to ensure they were all well-saturated and establish the original wettability state of the core samples. The prepared core samples were put inside the imbibition cells containing deionized water (base case) and SHTA (chemical additive case). Subsequently, the imbibition cell was placed in our specially-designed HPHT cell—positioned inside the oven. Each capillary imbibition experiment was performed at steam temperature up to 200°C and 250 psi for 24 hours. Besides, the system was pressurized by using nitrogen gas. The oil production data was also recorded to obtain an oil recovery versus time plot. To achieve more solid justification, the results obtained from this HPHT capillary imbibition experiment were then compared with the interfacial properties experimental results. **Figure 53** depicts the complete HPHP capillary imbibition experimental setup conducted in this research.

**Table 9—Berea sandstone core samples data.**

Sample	Core diameter (cm)	Core height (cm)	Pore volume (cc)	Porosity (%)	Chemical	Oil viscosity (cP)	Concentration (wt %)
S1	3.81	8.10	16.14	17.47	DI water	5,616	–
S2	3.81	8.10	16.30	17.65	DI water	46,140	–
S3	3.81	8.10	16.76	18.16	SHTA	5,616	3.00
S4	3.81	8.10	16.62	18.00	SHTA	46,140	3.00

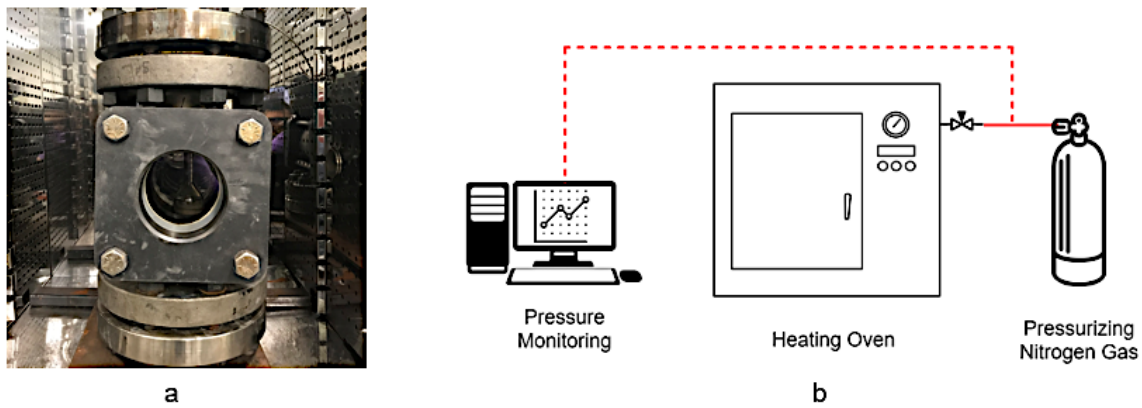


**Figure 53—HPHT capillary imbibition: (a) HPHT cell and (b) complete experimental setup.**

#### **4.3.5 Phase Distribution Visualization in Porous Media**

In this research, the study of fluid phase distribution was performed through a micromodel. In the beginning, the micromodel was prepared and packed with 3-mm silica glass beads and placed in between the 9-mm acrylic plates. A rhombohedral packing structure was adopted in this micromodel to represent the porous media. With a rhombohedral packing structure, the porosity was estimated to be approximately 25–28% (Amyx et al. 1960). The micromodel was then placed and pressurized inside the steel frame and positioned inside a sealed and closed chamber to minimize the heat transfer occurring during the steam injection process.

In establishing the fluid saturation history, the micromodel was initially injected with synthesized formation water (NaCl = 30,000 ppm, CaCl<sub>2</sub> = 1,000 ppm, and MgCl<sub>2</sub> = 100 ppm) and followed by the injection of oleic phase. Oil recovery and fluid saturation were quantitatively measured

from the produced fluid post-tertiary recovery. Data and analysis of oil recovery and fluid saturation were utilized as supporting analysis in addition to the qualitative phase distribution analysis in porous media. According to our micromodel saturation process, the initial water saturation ( $S_{wc}$ ) was measured to be 27.1%. The value was consistent with the reported literature confirming that water-wet rocks comprise  $S_{wc}>20\%$ , whereas more oil-wet rocks contain  $S_{wc}<15\%$  (Baker et al. 2015).

Respectively, the steam (200°C) was continuously injected into the micromodel at 0.5 cc/min until a maximum of 3 pore volumes (PVI) was reached to establish a base case. The injection process was then followed by the SHTA injection (combined with the steam injection) until 3 PVI to represent the tertiary recovery process. The dynamics of phase distribution during the steam injection was captured by our high-resolution and high-speed camera equipped with an optical macro lens. A complete micromodel experimental setup can be referred to as **Figure 54**.

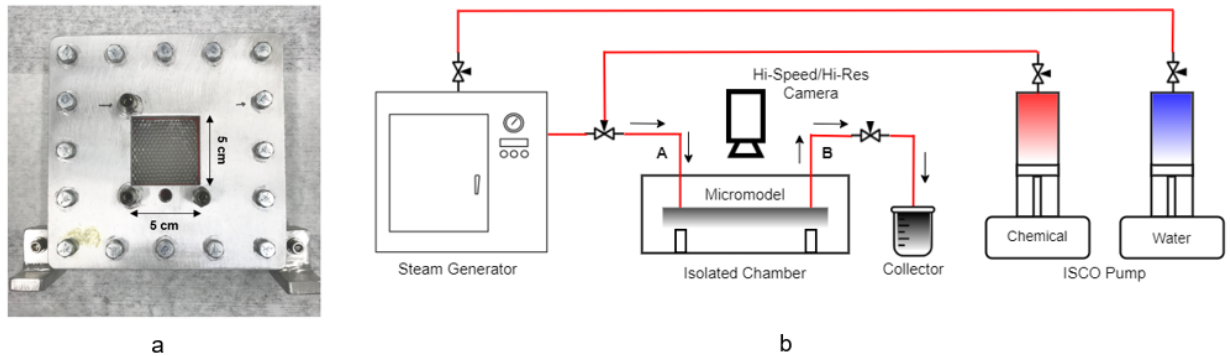


**Figure 54—Phase distribution in porous media study: (a) glass bead micromodel inside a pressurized steel frame and (b) complete micromodel experimental setup for steam injection.**

#### 4.3.6 Steam Core Flooding

The study of dynamic steam flooding was conducted to obtain a comprehensive evaluation and analysis of the oil recovery performance and mechanisms presented by SHTA. In this research, a sandpack was utilized to embody the reservoirs containing heavy-oil and bitumen. At first, the sandpack was prepared by using the sand, sieved with sand screens to obtain a sand particle size of 250–500  $\mu\text{m}$ . The sandpack was then saturated by mixing with the previously synthesized

formation brine and heavy-oil to mimic the saturation history of the sandstone reservoirs. The process was continued by loading the prepared oil sands into the core holder, consequently and manually applying compressions. A similar procedure was implemented for each sandpack sample to ensure that all core samples were identical. **Table 10** shows the details of sandpack properties utilized in our steam flooding experiment.

**Table 10—Steam flooding sandpack properties.**

<b>Parameter</b>	<b>Value</b>
Sandpack diameter, in	1.5
Sandpack length, in	5.0
Pore volume, cc	45
Porosity, %	30.0
Initial water saturation, %	27.0
Steam injection pressure, psi	200
Steam temperature, °C	220
Overburden pressure, psi	500
Steam injection rate, cc/min	0.25 and 1.0

The steam flooding process was initiated by injecting the steam into the core with up to 220°C of steam temperature, 200 psi of injection pressure, and 500 psi of overburden pressure for the maximum of 3 PVI. Furthermore, the process was resumed by combining SHTA at a low chemical concentration (1–5 wt. %) with steam injection as tertiary recovery. The results obtained from the tertiary recovery process were then analyzed to get a more robust conclusion honoring the performance of this chemical additive in thermal recovery—particularly for steam injection applications. Additionally, a complete steam flooding experimental setup is depicted in **Figure 55**.

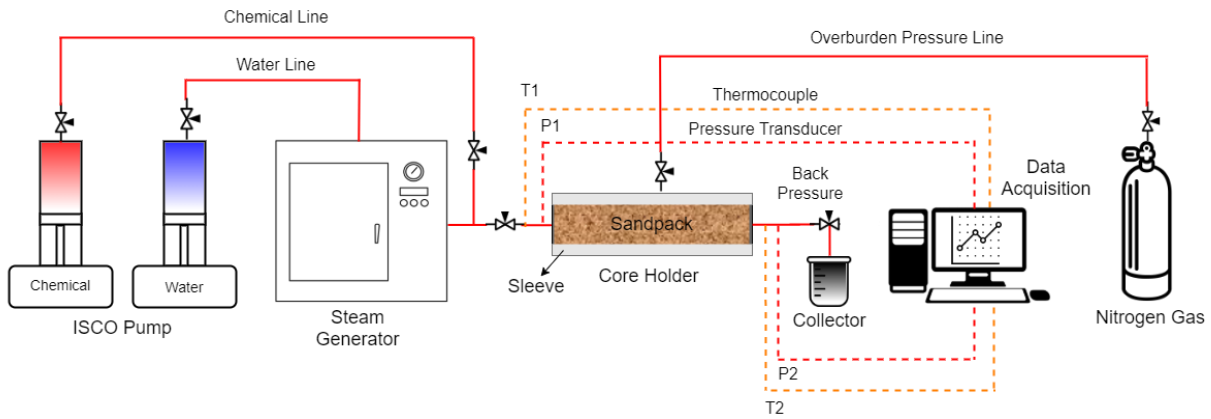


**Figure 55—Steam core flooding experimental setup.**

## 4.4 Materials and Experimental Setup

### 4.4.1 Synthesis Process of Low Concentration SHTA

A kind of tertiary amine—N,N-dimethylcyclohexylamine (purity = 99%)—was used to synthesize the SHTA. A thermal stability test—obtained from TGA—also confirmed its applicability in extremely high-temperature steam injection applications. In this research, a low concentration of a tertiary amine was applied to generate a homogeneous switchable chemical solution for steam injection applications— compared to the other published research reporting about 50 wt. % tertiary amine concentration was used to generate the chemical solution (Sui et al. 2016; Li et al. 2018; Mozhdehei et al. 2019). In creating a hydrophilic SHTA solution, CO<sub>2</sub> gas was involved in a reversible chemical reaction. Due to this reversible chemical reaction, the tertiary amine can potentially be recovered by switching the chemical reaction to the left-hand side, satisfying a reversible chemical reaction as follows:



**Figure 56** shows the complete process of low concentration (1–5 wt. %) SHTA synthesis. A hydrophilic and switchable SHTA was prepared by mixing the tertiary amine with water and CO<sub>2</sub> gas. In the beginning, it was perceived that both tertiary amine and water was immiscible due to

the natural characteristics of tertiary amines. The interface between the tertiary amine and water was observed (**Figure 56b**). Subsequently, the CO<sub>2</sub> gas was injected into the mixture at 10 mL/min until both substances became miscible to each other. As a result, the homogeneous chemical solution was created, and its hydrophilicity shifted from initially hydrophobic to the more hydrophilic chemical solution (**Figure 56b**). A comparable synthesis process was also applied to each chemical concentration. When the homogeneous chemical solution was heated at the temperature around 60–70°C and bubbled with N<sub>2</sub> gas, the tertiary amine was able to be recovered—indicating that the reversible chemical reaction had been shifted. At this circumstance, the interface between the water and tertiary amine was perceived (**Figure 56b**). Fundamentally, the presence of CO<sub>2</sub> in the reversible chemical reaction generates the water-soluble cations—[C<sub>8</sub>H<sub>17</sub>NH<sup>+</sup>]<sup>+</sup>—and bicarbonate salt—[HCO<sub>3</sub><sup>-</sup>]<sup>-</sup>—causing a more hydrophilic circumstance in the chemical solution. Furthermore, these ions (cations and anions) are a functional group of hydrophilic and hydrophobic components that can distinctively wet both the oleic phase and water phase—thus diminishing the interfacial tension. This feature can also potentially promote the surface charge modification of the rock surface, resulting in the repulsive forces between the oleic phase and rock surface, and substantially improving the water-wetness.

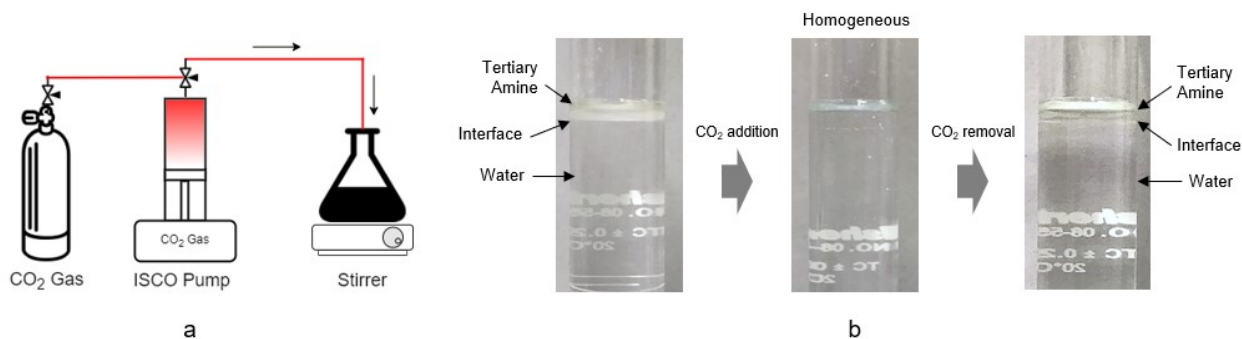


**Figure 56—Low concentration SHTA synthesis process: (a) complete experimental setup, (b) before CO<sub>2</sub> injection, and (c) after CO<sub>2</sub> injection.**

In addition to the potential surface charge modification, we also measured the pH of this switchable chemical solution for each chemical concentration to validate its potency—since there is a

correlation between pH and solid phase surface charge (Masliyah et al. 2011). The result from the pH measurement is presented in **Figure 57**.

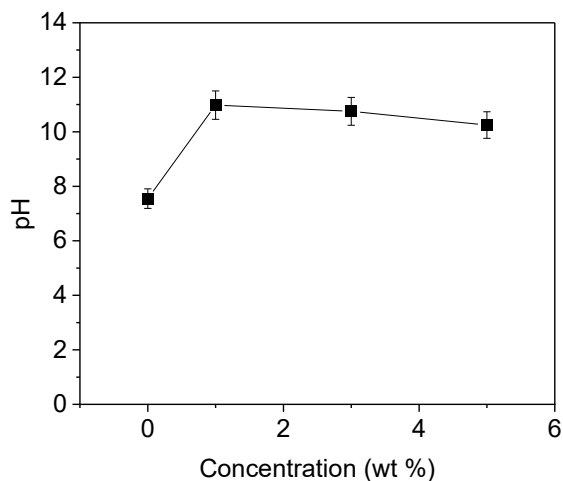


**Figure 57—pH measurement of SHTA chemical solution in each chemical concentration.**

It was observed that there was a significant increase in the pH of the SHTA chemical solution compared to the base case (synthesized formation brine). The pH increased from originally 7.55 to on average 10.66. This phenomenon occurred predominantly because of the formation of  $[\text{HCO}_3^-]$  in the chemical reaction. In natural behavior,  $[\text{HCO}_3^-]$  has been reported to have a  $\text{pK}_a$  value at least 10.30, depending on its concentration. It is also noticeable that there was a slight decrease in pH value when the SHTA concentration was elevated. The excess of  $\text{CO}_2$  gas in the chemical solution might cause this phenomenon to occur since more  $\text{CO}_2$  was needed to succeed in the reversible chemical reaction at a higher tertiary amine concentration. Dissolved  $\text{CO}_2$  gas in water could also potentially create a slightly acidic solution; therefore, influencing the total pH value of the chemical solution.

According to the results, it has been validated that this switchable chemical solution could potentially lead to a solid phase surface charge modification, yielding to even more negatively charged rock surface. Therefore, a favorable wettability alteration mechanism could potentially be attained.

## 4.4.2 Interfacial Properties

### 4.4.2.1 Phase Change Investigation

Our previous research (Pratama and Babadagli 2020a, b, c, d) has confirmed that the wettability is a predominant factor affecting the heavy-oil recovery performance. Necessarily, the steam injection can exhibit favorable oil recovery at the early stage due to the two potential mechanisms—thermal expansion and viscosity reduction. When steam starts to fill up the rock pores at the late stage of steam injection, a phase change occurs, resulting in unfavorable oil recovery performance. To further gain more understanding in surface sciences, a study of the phase change mechanism was performed on the quartz surface. **Figure 58** presents the irreversible wettability alteration during the steam injection process under the influence of brine chemistry.

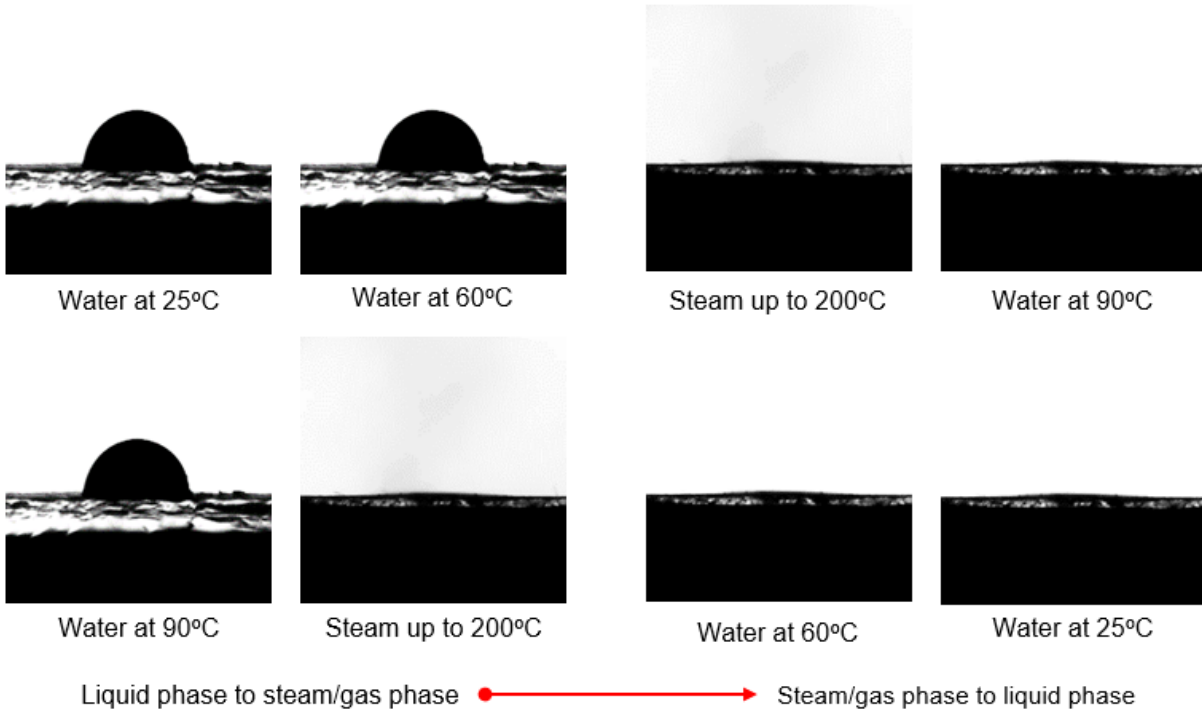


**Figure 58—Unfavorable wettability alteration on a quartz surface caused by a phase change occurred during the steam injection process (after Pratama and Babadagli 2020a, 2020b).**

It was noticed that the wettability of the quartz surface was altered to fully oil-wet after phase change occurred during the steam injection. The contact angle of the quartz surface significantly

plummeted from initially on average 60° to on average 7°. Furthermore, the contact angle was not restored even when the temperature of the rock/oleic phase/steam system was reduced to achieve a liquid phase region. This evidence has confirmed that the wettability alteration during the steam injection process behaves irreversibly.

#### 4.4.2.2 Interfacial Properties Improvement

In this study, SHTA was evaluated for its effectiveness in improving the interfacial properties at hot-water condition (up to 90°C and 200 psi) and steam condition (up to 200°C and 200 psi) of two types of heavy-oils. Before performing the experiments using chemical additive, a base case measurement of interfacial tension and contact angle were initiated. Moreover, the interfacial tension base case measurement on the oleic phase/steam system was compared with other published literature regarding a similar interfacial tension measurement at the steam condition as presented in **Table 11**. According to this research, it is noticeable that the interfacial tension measurement is in line with some previous studies.

**Table 11—Interfacial tension base case measurement of the oleic phase/steam system at the high-pressure–high-temperature steam condition.**

Interfacial tension (mN/m)		
This study	Huygens et al. (1995)	Naser et al. (2015)
18.8–19.6	18.0	19.0–21.0

**Figures 59** and **60** present the favorable wettability alteration on the quartz surface resulted after adding the SHTA into the rock/oleic phase/water and steam system. At a hot-water condition, a favorable improvement of the wettability was achieved on the quartz surface for both types of heavy-oil. For heavy-oil A, the contact angle of the quartz surface substantially increased from originally on average 60° to 126.4° at the optimal SHTA concentration around 3 wt. %. For heavy-oil B, the contact angle reached its maximum 115° from initially on average 76.3° at the same



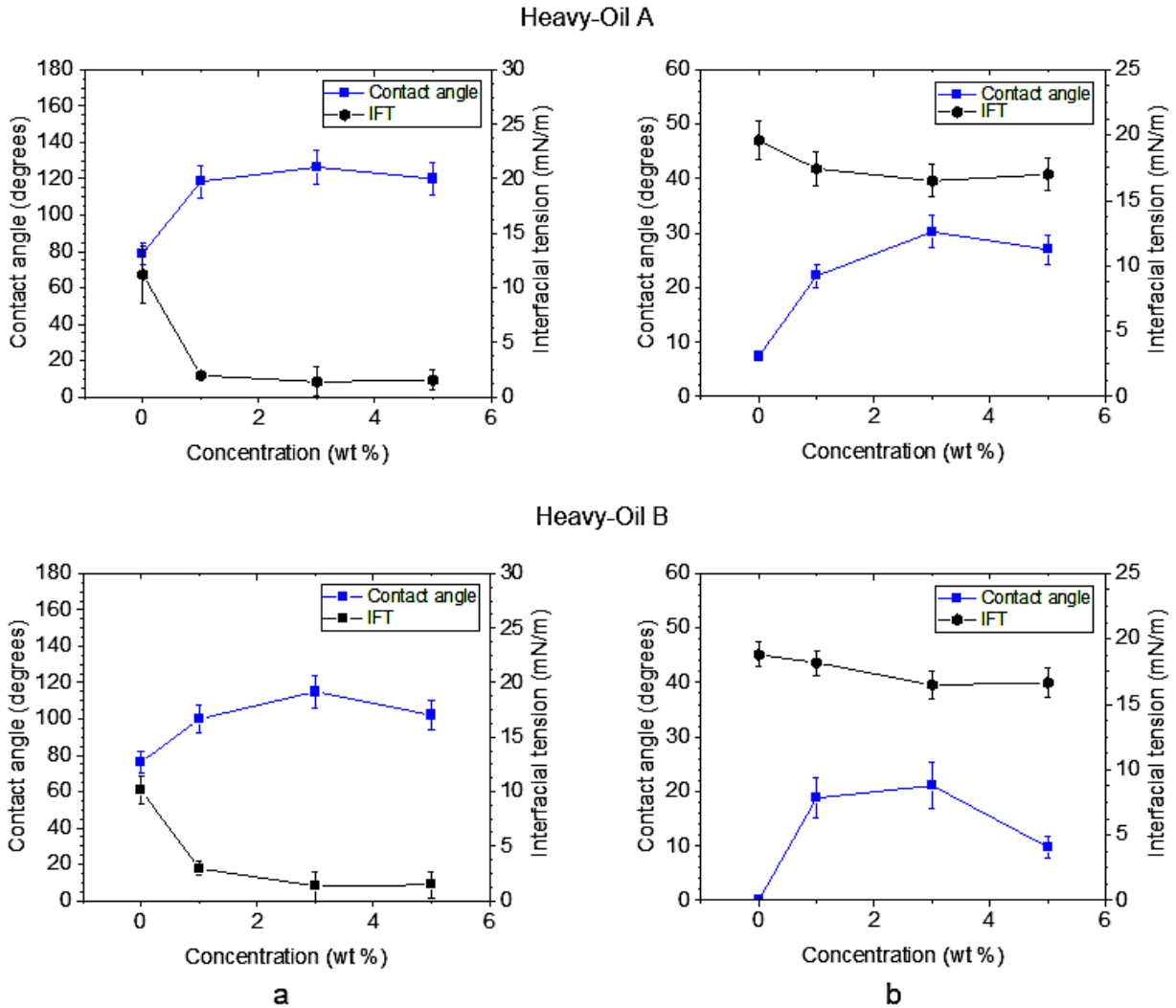


**Figure 60—Wettability alteration profile on a quartz surface presented by SHTA at 200 psi: (a) hot-water condition and (b) steam condition.**

Similarly, an auspicious wettability improvement was also observed on the quartz surface at the steam condition. The contact angle of the quartz surface was improved from on average  $7^\circ$  to on average  $30.2^\circ$  at 3 wt. % SHTA concentration, indicating that the wettability of the solid surface was less oil-wet (**Figures 59 and 60**). Similar behavior was also perceived on the rock/oleic phase/steam system with heavy-oil B. The contact angle was evidenced to improve from  $0^\circ$  to on average  $21.1^\circ$  at a high-pressure-high-temperature steam condition. Moreover, the SHTA also presented a favorable reduction in oleic phase-steam/gas phase interfacial tension at the steam

condition. For heavy-oil A, the interfacial tension was observed to decrease from initially 19.6 mN/m to 16.5 mN/m at the optimal SHTA concentration of 3 wt. % while the interfacial tension diminished from 18.8 mN/m to on average 16.5 mN/m for heavy-oil B. In summary, according to this research, the synthesized SHTA—even at much lower concentration—presented very promising improvement in interfacial properties at extremely high-temperature steam injection applications.

Scientifically, tertiary amines comprise two functional groups that have both hydrophobic and hydrophilic components, enabling wetting of both the oleic phase and water phase. Furthermore, the formation of an ion pair occurred due to the adsorption of cations ( $[C_8H_{17}N^+]$ ) on the surface of negatively charged heavy-oil (validated by a high acid number), resulting in an interfacial tension reduction. The anions ( $[HCO_3^-]$ ) promote the rock surface charge modification, thus leading to repulsive forces between the oleic phase and the rock surface, significantly improving the wettability of the rock surface, and eventually adding more heavy-oil recovery.

Also, according to the experimental result, it is evidenced that an SHTA exhibited an interesting relationship between the interfacial tension and wettability—satisfying the force balance (Young’s) equation of rock/oleic phase/water phase and steam phase as follows:

$$\gamma_{ow} = \frac{1}{\cos \theta} (\gamma_{ws} - \gamma_{os}) \dots\dots\dots (6)$$

where  $\gamma_{os}$  explains oleic-phase/solid-phase interfacial tension (mN/m),  $\gamma_{ow}$  explains oleic-phase/water-phase or steam-phase interfacial tension (mN/m),  $\gamma_{ws}$  explains water-phase or steam-phase/solid-phase interfacial tension (mN/m), and  $\theta$  explains contact angle.

#### 4.4.3 HPHT Capillary Imbibition Performance

In supporting and validating the results of interfacial properties under the influence of SHTA, the capillary imbibition experiments were performed at the high-pressure and high-temperature steam

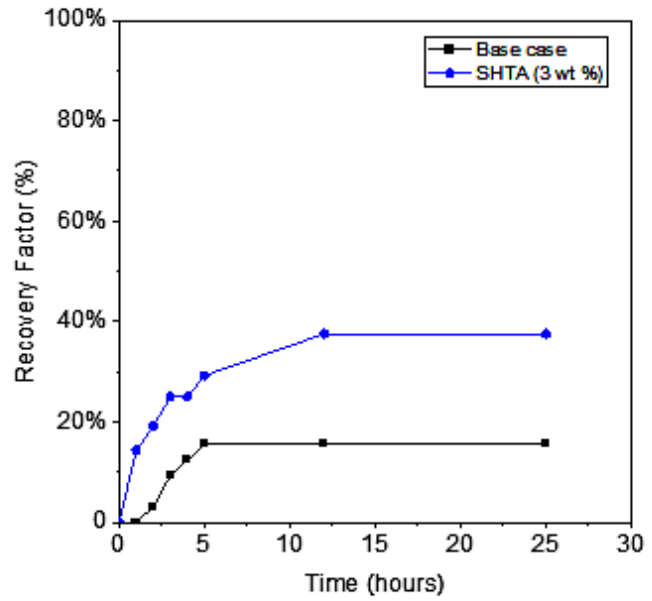
condition (up to 250 psi and 200°C). This experiment utilized two types of heavy-oils, and SHTA concentration of 3 wt. % since the study of interfacial properties showed that 3 wt. % was the optimal SHTA concentration, according to the interfacial properties' measurements and analysis. Moreover, the oil production data were recorded for 25 hours for each case. The diagnostic plot of heavy-oil recovery versus time is depicted in **Figure 61**.

According to our research, it was perceived that a significant heavy-oil recovery improvement was achieved after adding the SHTA chemical solution at its optimal chemical concentration. In the case of core sample containing heavy-oil A, the heavy-oil recovery performance was observed to improve from 15.5% ultimate recovery (base case) to 37.5% ultimate recovery (chemical additive case). In other words, the ultimate heavy-oil recovery could be substantially increased by more than 240% with SHTA compared to the base case. On the other hand, the HPHT capillary imbibition study presented that at a low SHTA concentration, for an extremely high oil viscosity, oil recovery could still be improved. The ultimate recovery of a core sample containing heavy-oil B was evidenced to convalesce from originally 7.7% (base case) to 21% with SHTA as a chemical additive. This study is able to show that up to 270% incremental ultimate heavy-oil recovery was possible, even for extremely high oil viscosity; however, the ultimate oil recovery was not as high as the core sample containing heavy-oil A. The addition of SHTA was confirmed to improve both wettability and interfacial tension; thus, potentially reducing the capillary pressure in the rock pores that satisfies the capillary pressure equation:

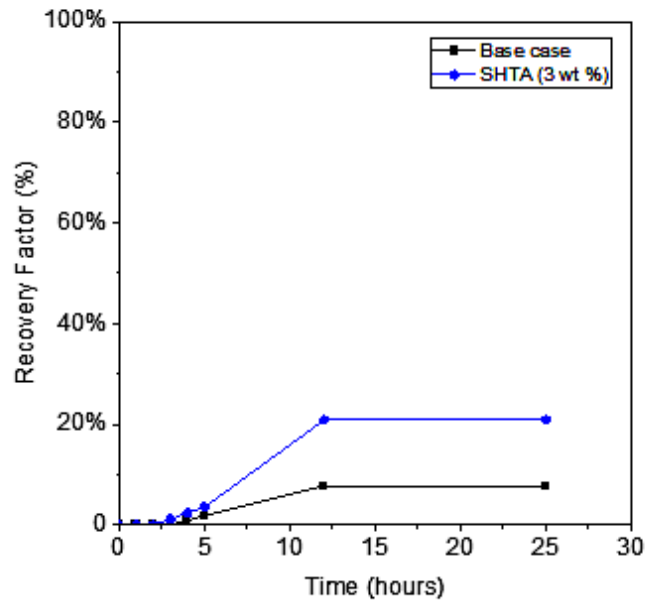
$$P_c = \frac{2\sigma \text{Cos } \theta}{r} \dots\dots\dots (7)$$

Where  $\sigma$  indicates the oleic phase-water phase interfacial tension,  $\theta$  indicates the oleic phase-solid phase contact angle, and  $r$  indicates the radius of pore space.

### Heavy-Oil A



### Heavy-Oil B



a

b

c

Figure 61—HPHT capillary imbibition under the influence of SHTA at 200°C and 250 psi: (a) before the experiment, (b) after the experiment, and (c) heavy-oil recovery performance plot.

#### 4.4.4 Phase Distribution or Residual Oil Behavior in Porous Media

Understanding the phase distribution/residual oil behavior in porous media is necessary to further explain the reservoir condition—particularly for steam injection applications—in addition to the oil recovery performance. A micromodel was selected to be utilized in this research because of its capability to foresee the wettability state of a solid surface through the shape of residual/trapped oil. This ability has made the micromodel an exceptional technique to characterize porous media. In this phase distribution study, SHTA chemical solution at its optimal concentration of 3 wt. % was applied as a steam additive for the tertiary recovery process at steam temperature (up to 240°C). The effectiveness of this chemical additive was compared with the base case—steam injection only.

**Figure 62** shows the tertiary recovery process applied to the micromodel. Initially, the steam was injected into the micromodel at a constant injection rate (0.5 cc/min) for a maximum of 3 PVI. During the steam injection process, phase change was clearly observed through the micromodel for both cases. As a result, the residual oil developed post-steam injection. The oleic phase was perceived to be the continuous phase inside the pores, indicating that the wettability of the solid surface had been altered to a complete oil wet-state (**Figures 62a and 62b**).

In the case of micromodel saturated with lower heavy-oil viscosity, when SHTA was added along with steam injection, favorable phase distribution improvement was attained. No residual oil was observed in the porous media post-tertiary recovery, indicating that the capillary force was diminished and residual oil mobilization in porous media was possible even at extremely high-temperature steam applications (**Figure 62a**). In contrast, a desirable diminution in residual oil was not evidenced in the case of micromodel saturated with higher heavy-oil viscosity (**Figure 62b**). According to this study, extensive residual oil was still perceived in the pores post-tertiary recovery. This evidence indicates that the capillary force did not improve. In other words, the same viscous force (at the same chemical concentration) was not able to sufficiently mobilize the higher heavy-oil viscosity in addition to the capillary number. This evidence also confirms that there is a relationship between oil viscosity and residual oil saturation in porous media. In addition to the porous media visualization, quantitative measurements of oil recovery and residual oil saturation were conducted to support the investigation of SHTA.

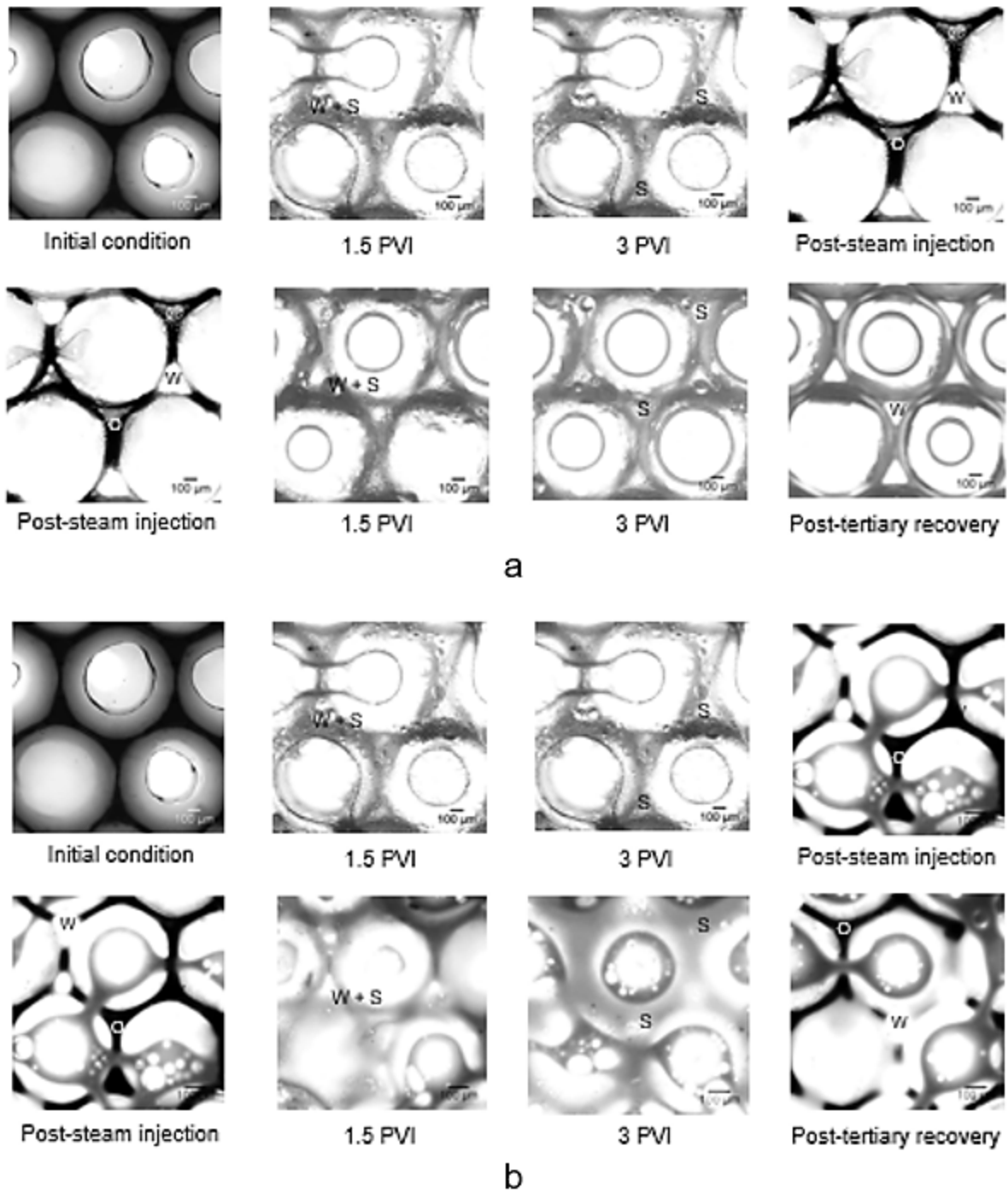


Figure 62—Tertiary recovery performance in porous media with SHTA at an optimal chemical concentration: (a) lower heavy oil viscosity and (b) higher heavy-oil viscosity. O = oleic phase, W = water/liquid phase, and S = steam phase.

**Figure 63** exhibits the oil recovery and residual oil performance after tertiary recovery with SHTA at 3 wt. %. In the early-stage of steam injection, the porous media system presented noticeable oil recovery. This anticipated performance was instigated by two potential recovery mechanisms—viscosity reduction and thermal expansion. Therefore, the oleic phase could be auspiciously mobilized from the pores. When the system achieved the late-stage of steam injection, the oil recovery performance initiated to flatten-off, indicating that the oil production has declined. In this stage, the maximum oil recovery was 56% for micromodel containing lower heavy-oil viscosity and maximum 46% of the heavy-oil recovery obtained from a micromodel containing higher heavy-oil viscosity. This poor recovery performance was triggered by the phase change and steam domination inside the porous media; thus, unfavorably altering the wettability of the solid phase to be even more oil-wet. Furthermore, when SHTA was combined with the steam injection, the incremental oil recovery was achieved as 20% post-tertiary recovery for a micromodel with lower heavy-oil viscosity. On the other hand, the addition of SHTA as a steam additive only presented a total of 12% incremental oil post-tertiary recovery in the case of a micromodel saturated with higher heavy-oil viscosity.

Similar to the heavy-oil recovery performance, the residual oil saturation from the micromodel experiments were quantitatively analyzed to support the heavy-oil recovery performance presented by this SHTA. In obtaining the residual oil saturation value ( $S_{or}$ ) at each PVI, the initial oil saturation was subtracted by the produced oleic phase obtained from each experiment as expressed in the following equation:

$$S_{or} = (1 - S_{wi}) - \frac{N_p}{PV} \dots\dots\dots (8)$$

where  $S_{or}$  describes the residual oil saturation,  $S_{wi}$  describes the initial water saturation,  $N_p$  describes the produced oleic phase after the steam injection and tertiary recovery, and  $PV$  describes the pore volume. In the case of a micromodel containing lower heavy-oil viscosity, the residual oil saturation in the porous media could be diminished from initially 25% to a minimum of 11%. In contrast, the residual oil saturation could only be diminished to a minimum of 36% by SHTA in a

micromodel comprising higher heavy-oil viscosity. In general, the study of phase distribution and residual oil behavior in porous media shows that as a steam additive, SHTA is more effective and favorable for steam injection applications in the reservoirs containing lower heavy-oil viscosity.

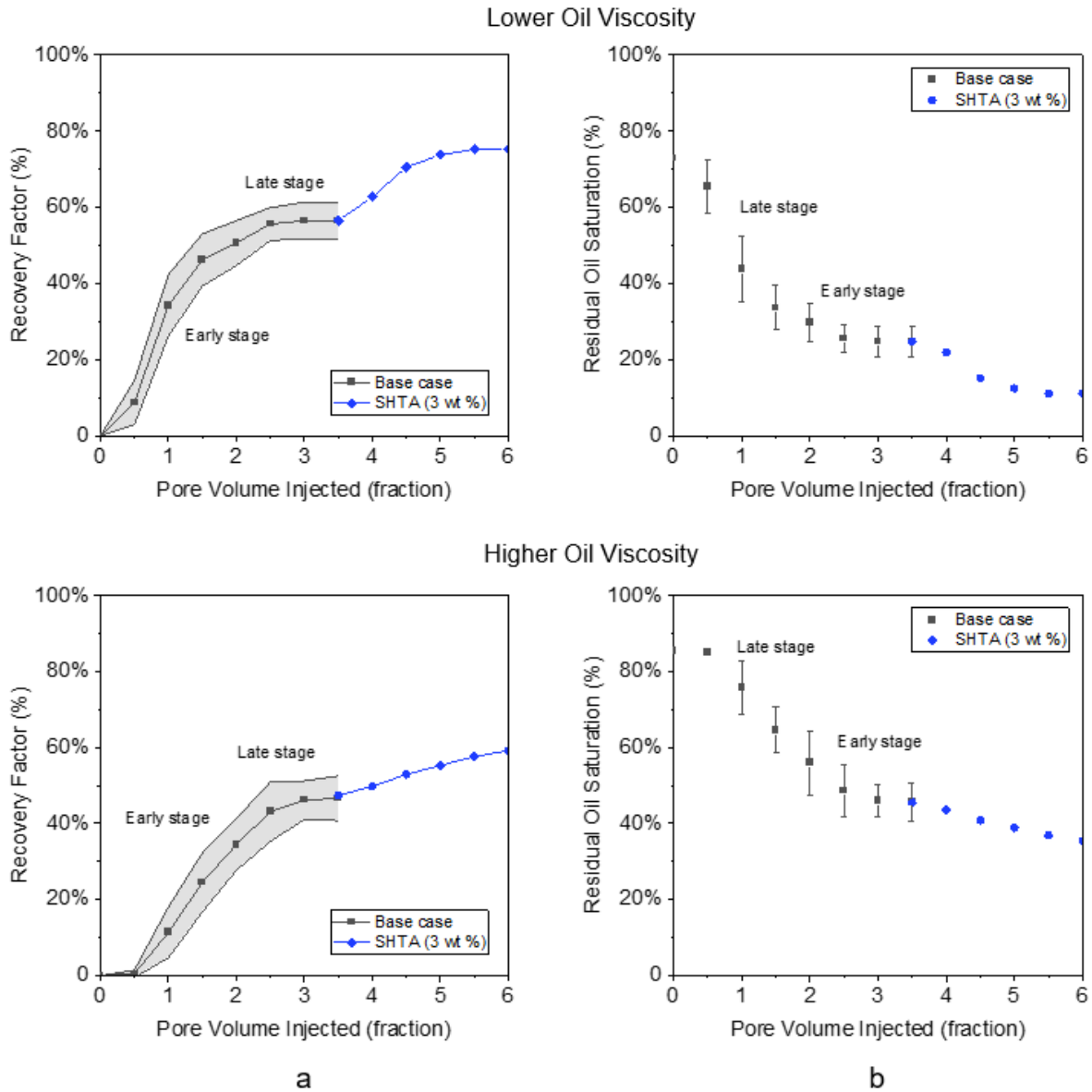


**Figure 63—Recovery performance presented by SHTA obtained from the micromodels: (a) oil recovery performance and (b) residual oil saturation plot.**

This evidence validates the mobilization of oleic phase by SHTA as a steam additive; thus, consequently affecting the interaction between viscous force and capillary force as stipulated in the capillary number (Moore and Slobod 1955) as follows:

$$N_c = \frac{v\mu_w}{\sigma \text{Cos } \theta} \dots\dots\dots (9)$$

Where  $v$  represents displacing linear fluid velocity,  $\mu_w$  represents water viscosity,  $\sigma$  represents interfacial tension of two immiscible phases, and  $\theta$  represents the solid phase-oleic phase contact angle. Also, these diagnostic plots provide valuable data in analyzing phase distribution/residual behavior in porous media—particularly under the influence of SHTA. However, the results gained from this study must be compared further with the results obtained from the steam core flooding experiment also part of this research.

#### 4.4.5 Core Flooding

##### 4.4.5.1 Oil Recovery and Residual Oil

Core flooding is essential to further investigate and analyze the heavy-oil recovery performance and underlying oil recovery mechanisms presented by this chemical additive at different chemical concentrations under the steam condition. The experiments were conducted for both types of heavy-oils. Each experiment was performed at high-pressure and high-temperature steam condition (200 psi and 240°C) with applied overburden pressure of 500 psi for the maximum of 3 PVI. The results acquired from the steam core flooding experiments are summarized in **Figure 64**.

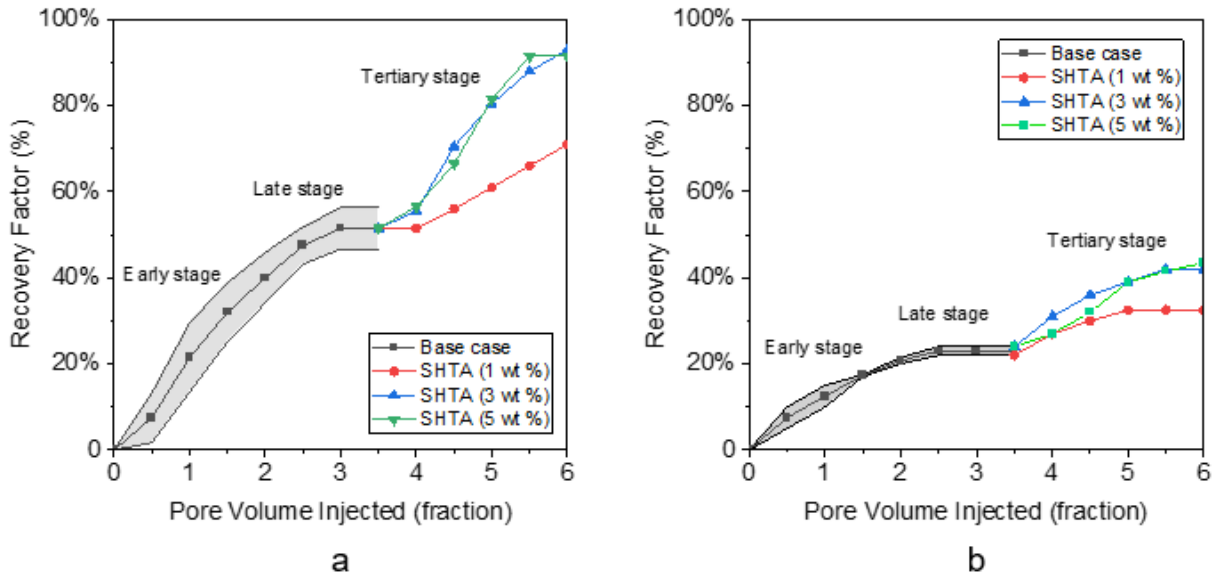


**Figure 64—Recovery performance presented by SHTA obtained from the core flooding at 220°C and 200 psi: (a) heavy-oil A and (b) heavy-oil B.**

Similar to the results obtained from micromodel experiments, early-stage and late-stage were perceived through steam core flooding experiments, validating that the experimental results acquired from both micromodel and steam core flooding experiments are consistent; thus, yielding to a more solid conclusion regarding the steam injection stages that occurred in the reservoirs. Furthermore, it was noticed that the base case could only deliver the maximum oil recovery of 22–41% for both types of heavy-oils. In general, the addition of SHTA as a steam additive could favorably improve the heavy-oil recovery. According to this study, SHTA with the chemical concentration of 1 wt. % was only able to deliver a maximum of 19% incremental heavy-oil recovery for heavy-oil A and 10% incremental heavy-oil recovery post-tertiary recovery for a maximum of 3 PVI. A significant additional heavy-oil recovery was observed when the chemical additive concentration was increased to 3 wt. % and 5 wt. %. These SHTA concentrations presented a similar performance at the steam condition observed on both cases. The heavy-oil recovery could be auspiciously risen from 41% post-steam injection to, on average, 87% post-tertiary recovery for a maximum of 3 PVI. In other words, the incremental oil recovery presented by these chemical concentrations was about 46% post-tertiary stage in the case of sandpack containing heavy-oil A (**Figure 64a**). Furthermore, for a sandpack comprising heavy-oil B, the

maximum heavy-oil recovery was perceived to be lower than heavy-oil A. The addition of SHTA as a steam additive was able to only improve the heavy-oil recovery from 22% to a maximum of 42% recovery post-tertiary recovery, meaning that only 22% incremental oil recovery was attainable, according to this research.

This evidence validates that low SHTA concentration is sufficient to promisingly improve heavy-oil recovery performance in steam injection applications. We revealed that the SHTA concentration of 3 wt. % was the optimal chemical concentration for steam injection applications, according to this research. The results are also consistent with the analysis of interfacial properties, reporting that the chemical concentration of 3 wt. % was optimal.

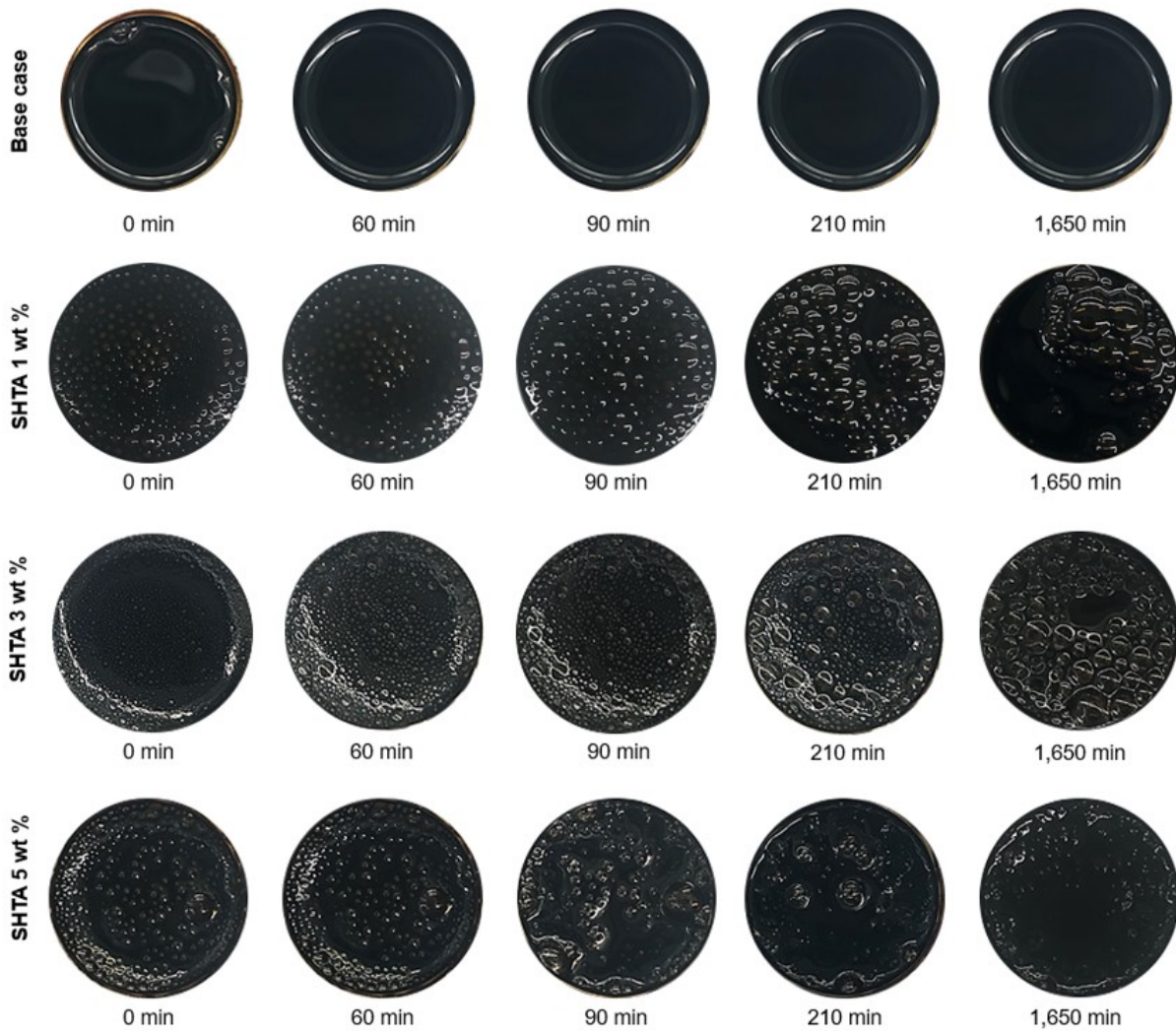
#### **4.4.5.2 Foamy Oil Recovery Mechanism**

In this study, we revealed that SHTA presented not only the favorable wettability alteration and interfacial tension reduction but also the potential foamy oil recovery mechanism. **Figure 65** exhibits the foamy oil (collected after core flooding experiments) stability after 28 hours of observation for both types of heavy-oils.

It was evidenced that SHTA presented the most stable foamy oil at 3 wt. % chemical concentration. The presence of gas-in-heavy-oil (as foamy oil) could reduce the heavy-oil viscosity; thus, increasing the mobilization of heavy-oil in the rock pores. This phenomenon might be triggered by the reversible chemical reaction, involving CO<sub>2</sub>. During the injection of the SHTA chemical solution along with steam, the thermodynamic heat transfer might cause the reversible chemical reaction to move to the left-hand side; thus, releasing CO<sub>2</sub> in the form of the gas phase. With such high-pressure steam injection, the dispersion process of a gas phase in heavy-oil was possible, leading to the formation of foamy oil. In corroborating the presence of CO<sub>2</sub> gas in the heavy-oil—triggering the foamy oil recovery mechanism, the gas chromatography (GC) test was performed. At the end of the tertiary stage, the foamy oil was collected in the Erlenmeyer flask attached to the vessel/accumulator—initially vacuumed—to receive any liberated gas. Subsequently, the accumulator was connected to the GC test device to analyze the gas composition. **Table 12** presents the result attained from the gas chromatography test.

The GC test result shows that the CO<sub>2</sub> gas was present in the system. This result also confirms that the CO<sub>2</sub> gas was generated during the steam and SHTA injections—indicating that the reversible chemical reaction had shifted. It is also noticed that some other gases existed in the system. This phenomenon might occur since the Erlenmeyer flask was not vacuumed at the beginning of the experiment; therefore, causing the other gases to co-exist together. However, the CO<sub>2</sub> gas was still dominant in the system—triggering the foamy oil recovery mechanism.

According to this research, SHTA was able to present auspicious foamy oil recovery mechanism post-tertiary recovery regardless of the oil viscosity. This evidence shows that the mobilization of heavy-oil by foamy oil mechanism was possible, even for an extremely high oil viscosity.



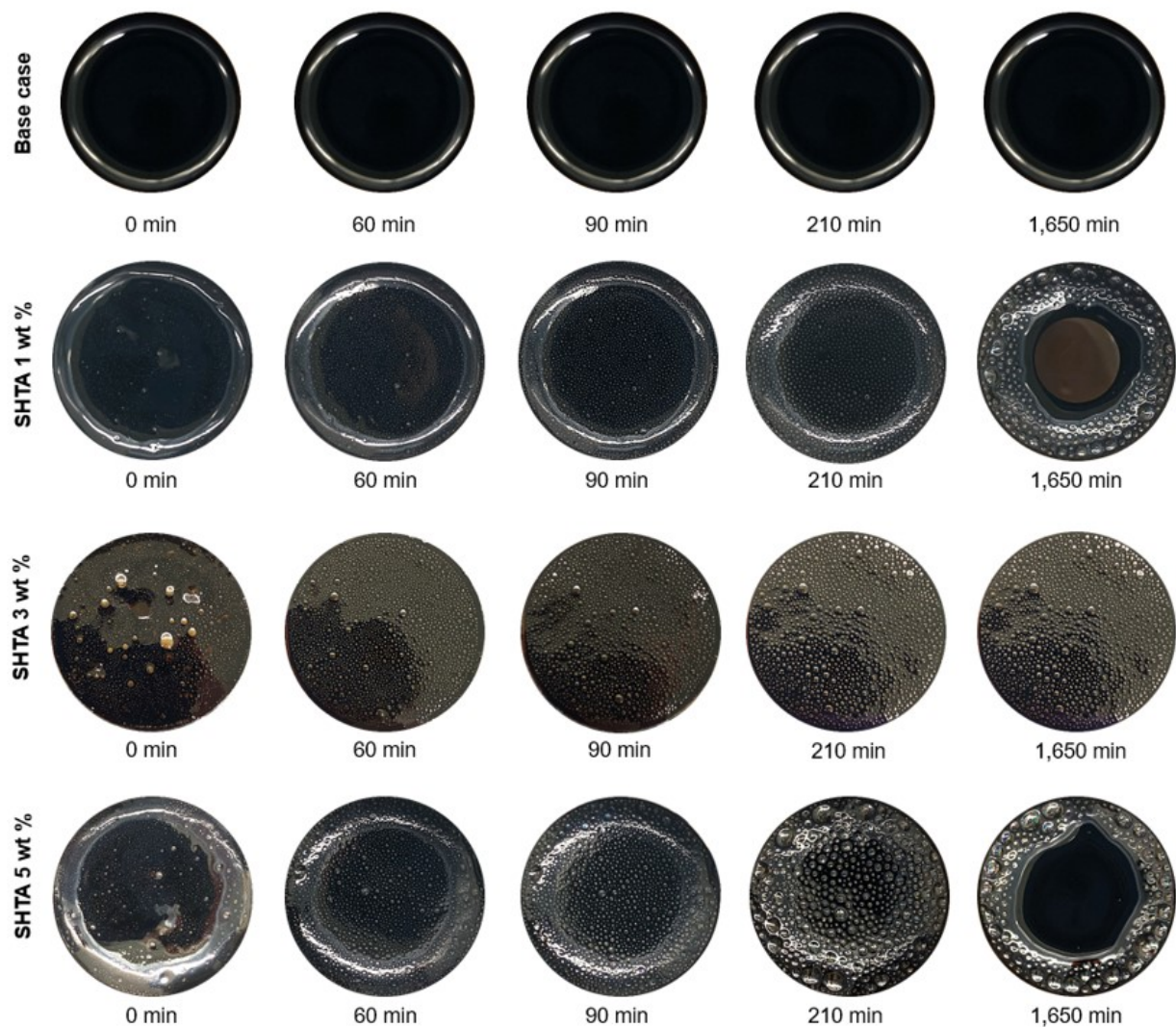


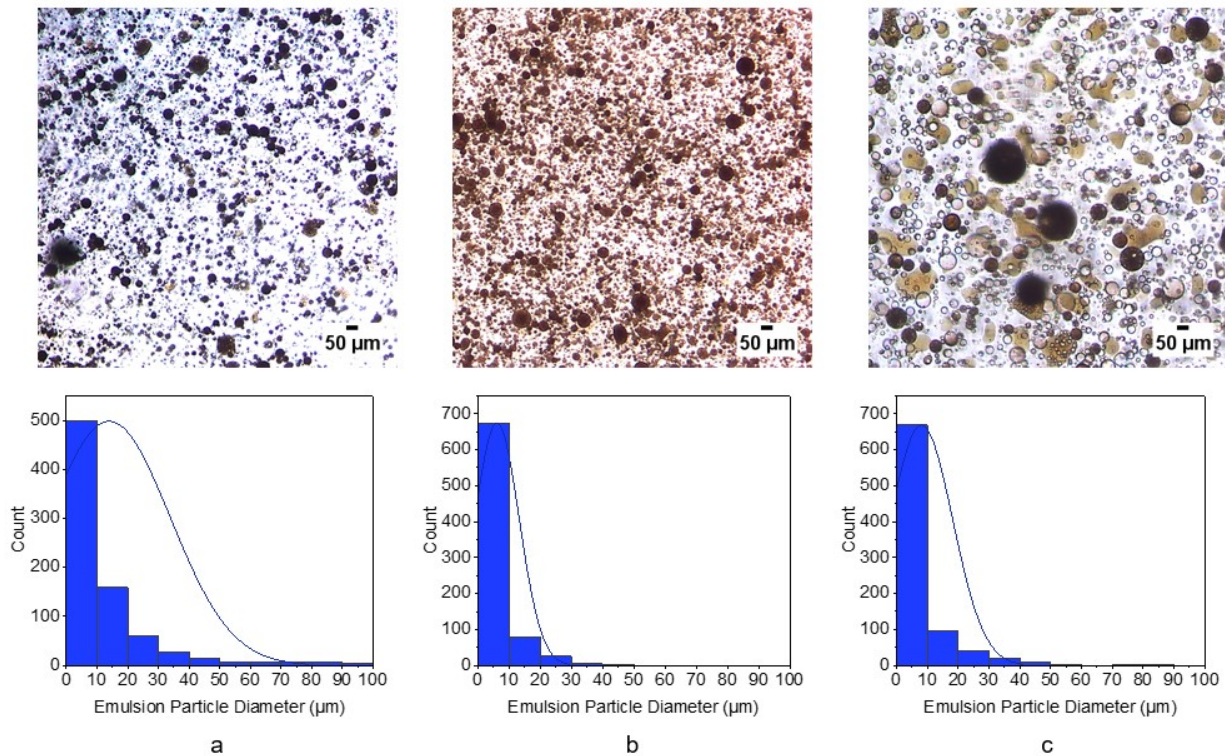
Figure 65—Potential foamy oil recovery mechanisms presented by SHTA at different concentrations collected after core flooding: (a) heavy-oil A and (b) heavy-oil B.

Table 12—Gas chromatography test result.

Component	Retention time (min)	Height (mm)	Area (mm <sup>2</sup> )	Amount (%)
Oxygen	2.333	1.947	0.333	0.944
Nitrogen	3.266	7.357	0.805	3.778
Carbon dioxide	9.700	23.191	0.945	8.935

### 4.4.5.3 Emulsification Recovery Mechanism

In addition to the interesting evidence of foamy oil post-tertiary recovery, another potential recovery mechanism—oil-in-water emulsification—delivered by this switchable chemical additive was also discovered. The observation of this emulsion was performed after the produced oil was collected and placed under the microscope. The results obtained from the observation are summarized in **Figure 66**. Additionally, the emulsion particle size distribution was also evaluated using ImageJ software. According to this research, it was perceived that SHTA with the chemical concentration of 3 wt. % resulted in the most favorable emulsification among other chemical concentrations. The evidence was also supported by the emulsion particle size distribution, showing that the emulsion particle size distribution was dominated by the much smaller emulsion particle size of 0–30  $\mu\text{m}$  (**Figure 66b**).



**Figure 66—Observation of emulsions resulted from SHTA post-tertiary recovery at 100X magnification (sample of heavy-oil A): (a) SHTA 1 wt. %, (b) SHTA 3 wt. %, and (c) SHTA 5 wt. %.**

The least favorable emulsification was delivered by an SHTA concentration of 1 wt. % since much larger emulsion particles existed in the system. This emulsion observation also confirms the optimal SHTA concentration of 3 wt. % for a steam additive. In the case of a system containing heavy-oil B, the emulsion was not observed, even at the optimal chemical concentration. The evidence confirms that the emulsification was less-likely occur in the system containing extremely high oil viscosity. This evidence is able to further validate that the SHTA could substantially reduce the interfacial tension of oleic/water system—substantiated by the interfacial properties measurement (**Figure 60**). Another interesting phenomenon was also perceived through the microscope observation at higher magnification (400X). The dispersed gas phase was present and co-existed in the emulsion system (**Figure 67**); thus, substantiating the foamy oil phenomenon that occurred after tertiary recovery.

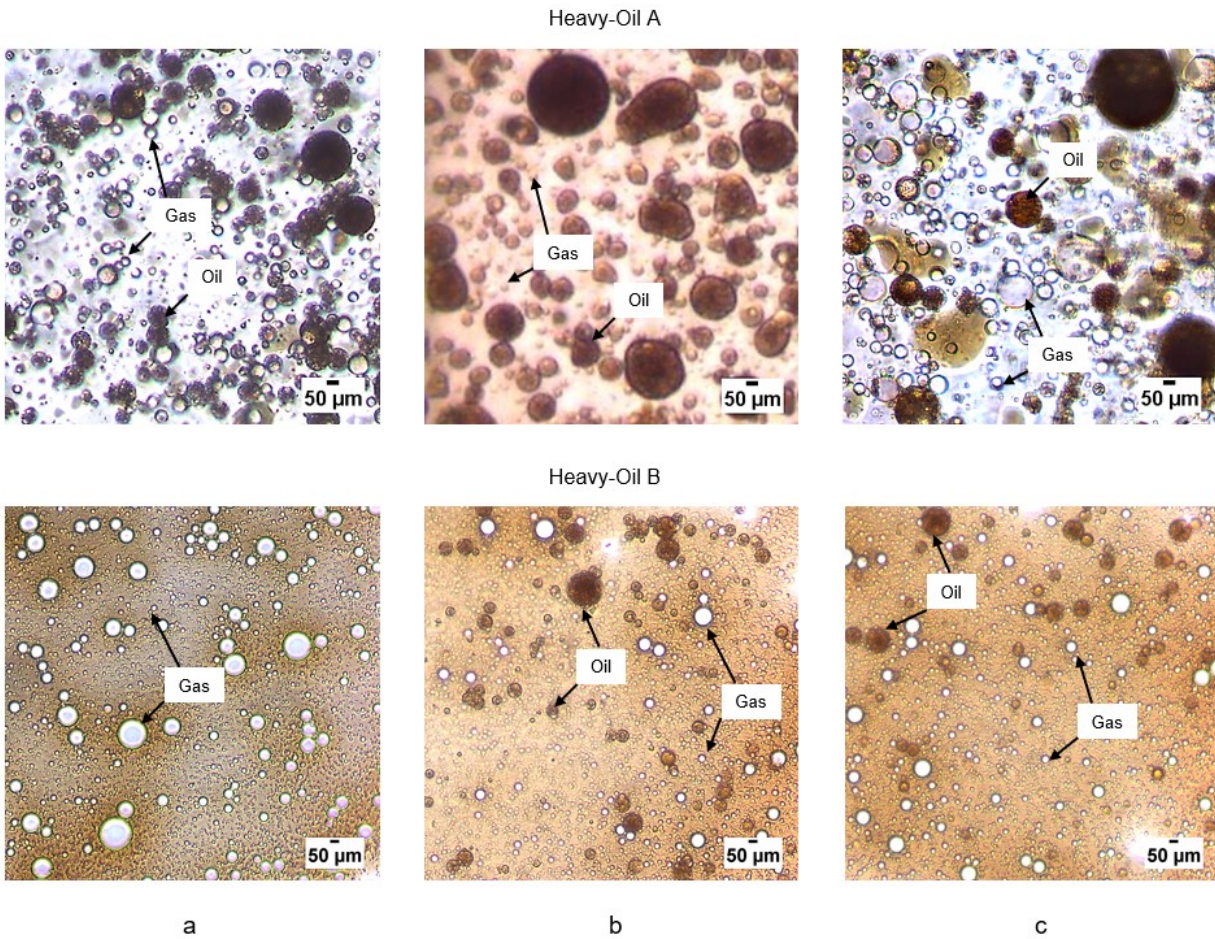


**Figure 67—Dispersed gas co-existed in the system at 400X magnification: (a) SHTA 1 wt %, (b) SHTA 3 wt %, and (c) SHTA 5 wt %.**

#### 4.4.5.4 Heavy-Oil Properties Post-Tertiary Recovery

In addition to the potential foamy oil and emulsification recovery mechanisms, heavy-oil viscosity and SARA analyses were performed to further investigate the heavy-oil characteristics after the tertiary stage. The result obtained from each test was compared with the properties of heavy-oil at the initial condition. **Figure 68** summarizes the heavy-oil viscosity and SARA measurement results in the initial state and after the tertiary recovery. It is noticeable that the heavy-oil viscosity was reduced by over 50% (at 25°C) after implementing tertiary recovery in the case of heavy-oil A (**Figure 68a**); however, the change in heavy-oil viscosity was not noticeable in the case of heavy-oil B. There was only a slight reduction in heavy-oil viscosity by 7%.

Further on, according to the SARA test—performed post-tertiary recovery—the improvement on heavy-oil components was observed. A favorable improvement was evidenced in the fraction of asphaltene. The asphaltene content could be reduced from initially on average 13% to 8–9% for heavy-oil A, whereas for heavy-oil B, the asphaltene fraction was diminished from originally 16% to 13%. At the same time, the aromatic fraction increased. In the case of heavy-oil A, the aromatic fraction was improved from on average 17% to 18% whereas the resin fraction was escalated from on average 30% to 32%. For heavy-oil B, the aromatic fraction improved from on average 20% to 22%. These results confirm that the SHTA was able to modify the heavy-oil properties, according to this study.

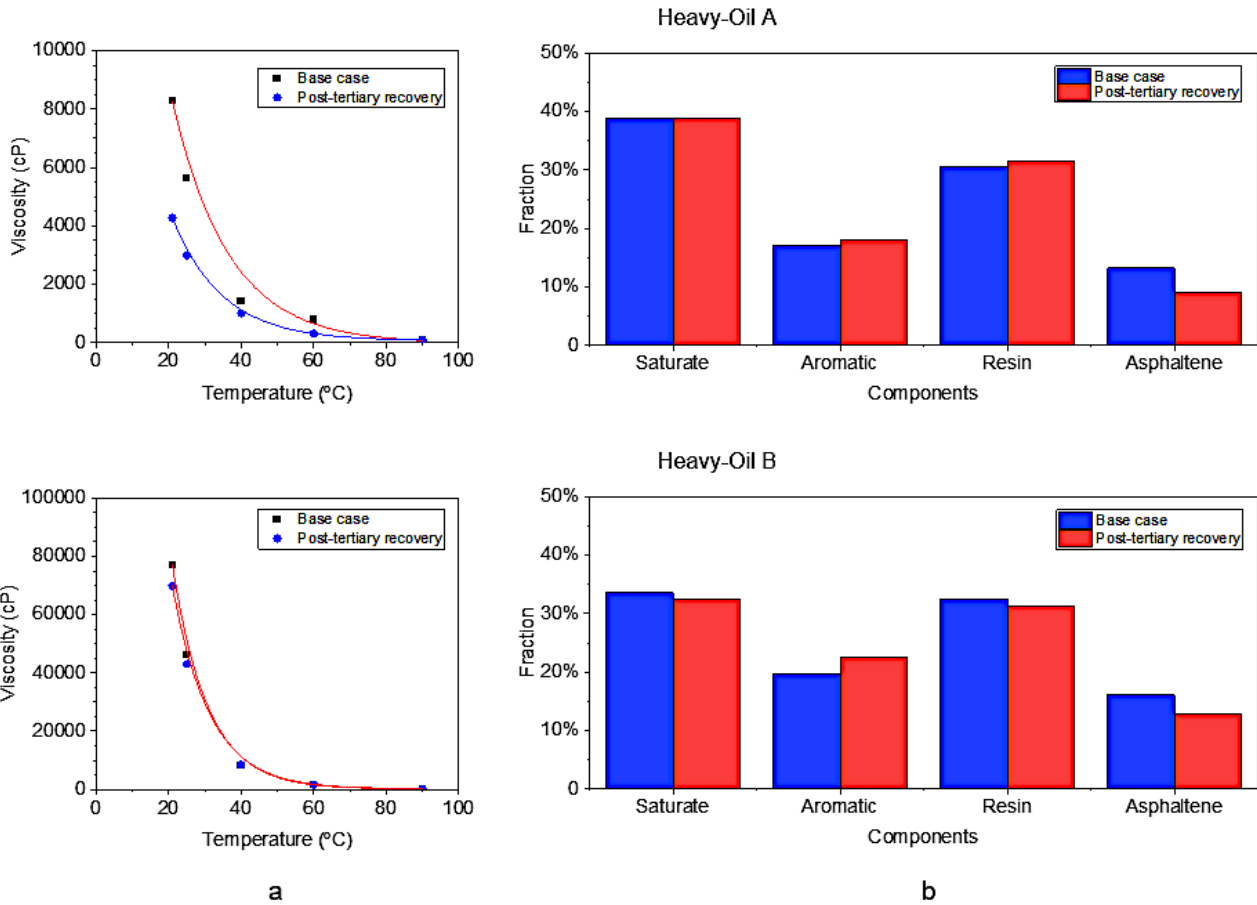
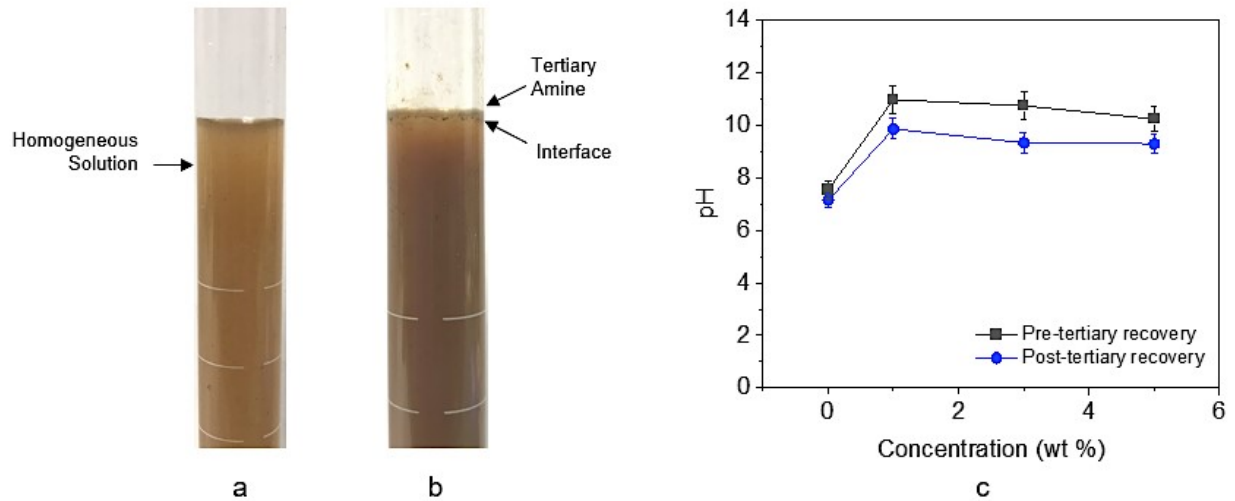


Figure 68—Comparison on properties of produced oleic phase post-tertiary recovery: (a) oil viscosity and (b) SARA analysis.

#### 4.4.5.5 Solvent Recovery Potential and Cost Effectiveness Analysis

In evaluating the switchability of this SHTA at a very low concentration, the effluent chemical solution produced after steam core flooding was collected for CO<sub>2</sub> removal; thus, switching back the chemical reaction to the left-hand side to retrieve the tertiary amines. The removal of CO<sub>2</sub> was conducted by heating the collected solution at 60–70°C and bubbling it with N<sub>2</sub> gas for 2 hours. According to this research, only a few amounts of tertiary amine and thin interface were perceived. **Figure 69** presents the results after the CO<sub>2</sub> removal process and pH measurement of the solution before and after the steam core flooding experiments.



**Figure 69—Tertiary amines recovery to evaluate the switchability at low chemical concentration: (a) before CO<sub>2</sub> removal, (b) after CO<sub>2</sub> removal, and (c) SHTA pH measurement before and after steam core flooding experiments.**

The adsorption of the chemical additive during the steam injection process might cause a small portion tertiary amine recovery. This finding was also consistent with the pH measurement of the solution post-tertiary recovery. The pH was perceived to present a lower value compared to the original pH value of the SHTA solution. This evidence also indicates that the recovery of tertiary amine was less favorable at a low SHTA concentration. To further evaluate the cost-effectiveness of this SHTA, the commercial price of this potential chemical additive is compared with other chemical additives that were previously tested in the lab. The chemical additive commercial prices were calculated and normalized at the optimal chemical concentration as depicted in **Figure 70**. Despite the limitation on tertiary amine recovery post-tertiary stage due to the potential adsorption on the rock surface, the use of SHTA for steam injection applications is very cost-effective as depicted in **Figure 70**. It only needed around US\$ 13–14 per gallon tertiary amine to generate the low-concentration SHTA for steam injection applications.

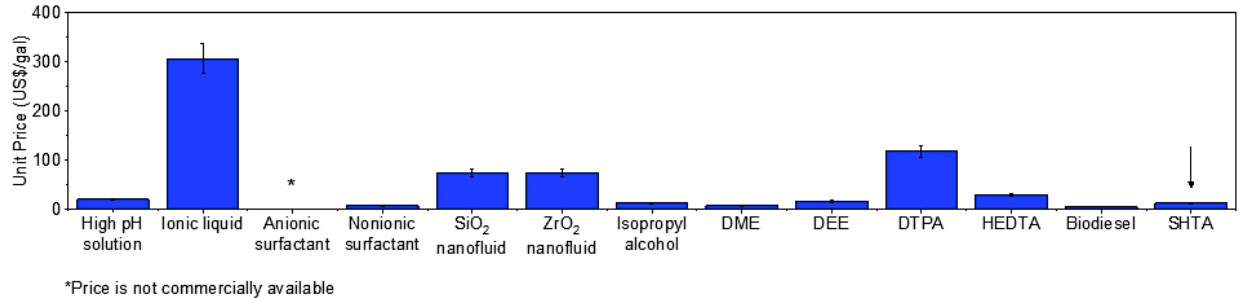


**Figure 70—Chemical additives commercial price comparison at optimal chemical concentration. Tertiary amine commercial price is compared with several chemical additives previously studied by Pratama and Babadagli (2020a, 2020b).**

## 4.5 Conclusions

1. This study is able to validate the suitability of switchable-hydrophilicity tertiary amines (SHTA) at the high-pressure and high-temperature steam condition even at a low chemical concentration. Therefore, the use of this potential chemical additive is considerable for steam injection applications.
2. Newly formulated SHTA was able to present improvements on the interfacial properties; thus, leading to a favorable heavy-oil recovery efficiency and diminishing residual oil saturation at a low SHTA concentration.
3. SHTA could potentially present other recovery mechanisms: foamy oil and oil-in-water emulsification.
4. Foamy oil mechanism could be potentially triggered by combining SHTA and steam injection, regardless of the type of oil and oil viscosity.
5. Emulsification is less-likely occur in the extremely high heavy-oil viscosity.
6. This study has revealed that low-concentration SHTA was able to deliver favorable improvement on heavy-oil displacement at high-pressure and high-temperature steam injection applications. SHTA concentration was perceived to be 3 wt. % as an optimal

chemical concentration, resulting in the maximum wettability alteration degree, minimum interfacial tension reduction, maximum heavy-oil recovery, most stable foamy oil, and most favorable oil-in-water emulsion, according to this research.

7. Potential foamy oil recovery mechanism was triggered by the CO<sub>2</sub> gas generation during the tertiary recovery process—indicating that the reversible chemical reaction had been shifted during this process. The presence of CO<sub>2</sub> in the system was also substantiated by the gas chromatography test.
8. SHTA has the ability to modify the properties of heavy-oil. This interesting finding was validated by the oil viscosity and SARA measurements showing that the heavy-oil viscosity could be favorably reduced, and the heavy-oil composition could be improved.
9. Tertiary amine recovery—performed by switching back the reversible chemical reaction—was less favorable at a low SHTA concentration. The chemical adsorption on the solid surface during the steam core flooding might instigate the occurrence of this phenomenon. However, the utilization of SHTA is still cost-effective for thermal recovery, particularly for steam injection applications.
10. In general, SHTA is more effective with the rock/oleic phase/steam system containing lower heavy-oil viscosity for steam injection applications. This evidence confirms that SHTA still has limitation to oil viscosity.

## **Chapter 5: What is Next for SAGD?: Evaluation of Low GHG and High-Efficiency Tertiary Recovery**

This chapter of thesis is a modified version of SPE-208876-MS that was presented at the SPE Canadian Energy Technology held in Calgary, Alberta, Canada, 16–17 March 2022. The journal version of this research paper has been submitted to the scientific journal for peer-review and publication.

## 5.1 Preface

Steam injection has been widely applied in different forms to recover heavy-oil and bitumen for decades. Even though this method is a proven and effective technology, the steam generation process itself may lead to environmental issues and low economic viability. Also, many worldwide steam projects, including SAGD projects in Canada, have already reached their maturity with a severe decline in production despite continuous steam injection. Escalating greenhouse gas (GHG) emissions is another crucial downside of steam injection application, contributing to an emission growth rate of about 1.1% worldwide and 0.8% annually in Canada. This requires us to search for different techniques to deplete the remaining (conditioned) oil efficiently and in an eco-friendly manner. This paper focuses on the testing of a new technique to minimize GHG emissions resulting from steam generation while enhancing the ultimate recovery post-SAGD.

~50,000 cP heavy crude and processed oil (for visual models) samples were used as an oleic phase in this experimental research. Condensable gases as single and multiple (mixed with methane) components were included as potential solvents to be applied to the already steamed models. Visual Hele-Shaw and glass-bead-pack models were employed to investigate the displacement mechanism, displacement efficiency, and phase distribution in porous media. All experiments were performed at currently existing temperatures in matured SAGD reservoirs to further evaluate the sensitivity of phase behavior of condensable solvents in a heavy-oil/steam system, as well as existing condensed water which is not compatible with hydrocarbon solvents.

We observed that condensable solvents could improve the displacement efficiency/incremental heavy-oil recovery by over 30% by mobilizing residual oil and providing favorable conformance to the steam chamber. More importantly, the steam usage was able to be entirely cut off, and the energy efficiency could be ramped up to almost 100%. Additionally, the type (and composition) for applying condensable solvents were determined at a given post-SAGD temperature. Also, the recovery potential of the condensable solvent with oil was investigated for an efficient process.

Condensable gases with different compositions were introduced as potential solvents to recuperate heavy-oil and bitumen recovery and reduce or even completely cut off the steam injection at late-stage SAGD, diminishing its GHG emission and improving energy efficiency. Valuable findings

present beneficial recommendations for low-emission and high-efficiency late-stage heavy-oil recovery as post-SAGD applications, as well as other types of steam injection processes.

**Keywords:** Steam injection, post-SAGD, condensable gas, low GHG emission, high efficiency.

## **5.2 Problem Statement and Proposed Solution**

### **5.2.1 Problem Statement**

In the meantime, technical challenges and perceptions of GHG on steam operations appear to instigate negative opinions in public as well as in the technical sense. These perceptions entail the efforts in searching for new applications utilizing existing investments (e.g., field operation, production facilities, capital expenditures).

The recent tendency in the steam injection/SAGD operations is to partially or even fully reduce the steam usage in further lessening the operating costs as well as the environmental impacts. The utilization of chemical additives and solvents could be the alternative as a proposed solution in achieving these objectives. However, when these methods are applied, several phenomena, such as wettability alteration and oil entrapment mechanisms, should be looked after. More essentially, pore level phase distribution mechanism should also be comprehended in the application of hydrocarbon solvents as four phases (oil, water, steam, solvent) exist in the reservoir system. In addition to these physicochemical characteristics of the process, the thermodynamic aspect of the phase behavior of hydrocarbon solvents should—affected by the pressure and temperature—also be considered.

In summary, post-SAGD is a very important stage and requires further awareness—since numerous SAGD fields have shown declining production at this stage. Despite other SAGD field problems (e.g., mobility contrast, steam channeling, steam conformance), unfavorable wettability alteration due to phase change at high-temperature conditions has been a major factor influencing heavy-oil recovery and SAGD process efficiency—further increasing in steam-to-oil-ratio (SOR) and leading to a direct impact of increasing GHG emissions (CERI 2020).

### 5.2.2 Proposed Solution

The main objective of this research is to further evaluate and investigate the potency of types of solvents as high-efficiency tertiary recovery options in diminishing residual oil, improving recovery mechanisms, and reducing SOR. Furthermore, with the projected trend of escalating energy-intensive in-situ heavy-oil and bitumen recoveries and increasing GHG emission reduction demands globally to achieve a more sustainable fossil fuel production and address the environmental concerns, this research attempts to search for a feasible solution to gratify these urgencies. Besides, incorporating solvent in the steam injection/SAGD process can potentially diminish GHG emissions by up to 80%, as depicted in **Figure 71** (CERI 2020).

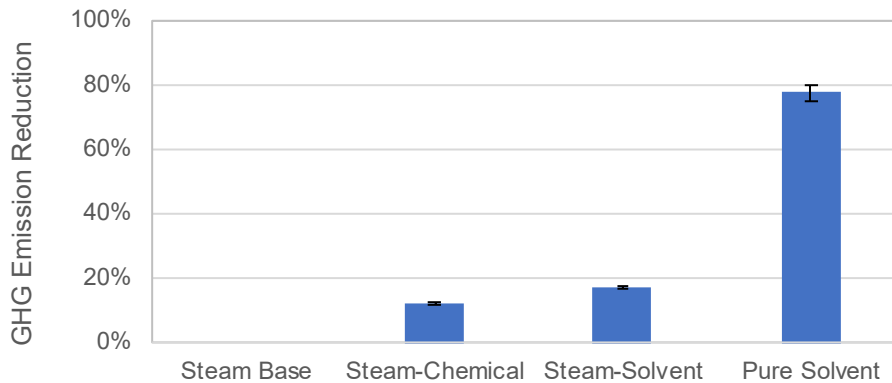


**Figure 71—Comparison of potential GHG emissions reduction by each steam injection/SAGD operation scenario (adopted from CERI 2020).**

In further obtaining even more robust conclusions and recommendations, experimentations of solvents applied post-SAGD were performed as a lab-based experimental study through visualization, including Hele-Shaw cells and 2-D porous media (before core flooding experiments) to qualitatively investigate the performance of the potential solvents through the steam-oleic phase and solvent-oleic phase interactions, particularly in a pore-scale investigation. To further investigate and evaluate the potency of solvents for post-SAGD applications, several injection materials were tested, involving condensable solvents (e.g., propane) and enriched gas/solvent (e.g., methane-propane, methane-heptane) at a given post-SAGD temperature. In addition to this,

the optimal solvent composition was also evaluated for the given pressure and temperature to obtain a more conclusive recommendation for post-SAGD applications. By applying solvents in the post-SAGD stage, we are confident of achieving post-SAGD target improvements, including ROS reduction, recovery mechanisms improvement, SOR reduction, energy efficiency improvement, and a more sustainable heavy-oil and bitumen production.

### 5.3 Material and Experimental Setups

#### 5.3.1 Oleic Phase

Heavy-oil from Western Alberta, Canada (46,000 cP at 25°C), was used for Hele-Shaw visualization whereas a mineral oil (111,600 cP at 25°C) was utilized for porous media experiments. Some other fluid properties for the utilized oleic phase are presented in **Table 1**. Mineral oil was used in the porous media experiment because of its translucent characteristics—making phase distribution investigation at the pore scale possible. Additionally, the saturates, aromatics, resins, and asphaltenes (SARA) test was also conducted for the heavy-oil to obtain the oil composition—resulting in 37.3% saturates, 11.9% aromatics, 36.2% resins, and 13.7% asphaltenes.

**Table 13—Fluid properties of the utilized heavy-oil. TAN = total acid number.**

Oil Type	Viscosity (cP)	Density (g/cm <sup>3</sup> )	TAN (mg KOH/g oil)	API gravity	Temperature
Heavy-Oil	46,140	0.9916	4.18	11.20	25°C
Mineral Oil	111,600	0.9963	-	10.53	25°C

#### 5.3.2 Studied Solvents

We tested condensable gas and enriched gaseous solvents to further evaluate their potential in improving post-SAGD fields. A wide range of solvent types was selected according to the phase

behavior of each solvent and commonly studied hydrocarbon solvents in the area of SAGD applications:

- pure propane with 100% composition,
- a mixture of methane and propane with 50% and 50% compositions,
- a mixture of methane and propane with 30% and 70% compositions,
- pure heptane with 100% composition,
- a mixture of methane and heptane with 50% and 50% compositions,
- a mixture of methane and heptane with 30% and 70% compositions.

A vapor/gaseous type of solvent(s) is advantageous as they are able to propagate/move upward by gravity. Due to its natural behavior, when injected to the reservoir, this solvent(s) will move toward the upper section of the reservoir—further potentially reducing ROS at the area close to the steam chamber zone. Furthermore, a heavier hydrocarbon solvent (e.g., heptane) could potentially present a better “cleaning effect”. Due to the vaporization temperature of 98.4°C, heptane vaporizes at the injected steam temperature and could be produced alongside the heavy-oil under the influence of the gravity force. Combining both types of solvents (with a certain solvent composition) could potentially lead to a more optimal recovery.

### **5.3.3 Solvent(s) Injection Process**

In this research, the selected solvent(s) was placed inside the pump for post-SAGD injection application (without steam). The solvent(s) injection rate was controlled using Teledyne® ISCO (syringe) piston-driven pump equipped with digital flow controller, which can accommodate very low injection rate (since this study utilized 0.2–0.3 cc/min injection rate). Moreover, this pump is commonly used for research purposes/lab experiments (for both liquids and gases)—particularly for smaller scale experimental studies (Zhao et al. (2004); Mazumder et al. (2008); Sun et al (2018); Min et al. (2020); Mohammed et al. (2020); Liang et al. (2023)). Therefore, this methodology (used in this study) is sufficiently representative in accommodating the main objective this study and reflecting the solvent(s) injection for SAGD applications. Furthermore,

the solvent(s) compositions were reflected by the combined injection rates from the studied solvent(s). For instance, in this case, the total injection was set to 0.2 cc/min. A solvent(s) composition of 30% methane–70% propane was represented by the methane injection rate of 0.06 cc/min and propane injection rate of 0.14 cc/min.

#### **5.3.4 Hele-Shaw Visualization Experiments**

Although Hele-Shaw is a much simpler model compared to porous media ones, it acts as a practical methodology for visualizing steam-to-oil and solvents-to-oil interaction at steam conditions in two-dimension. The Hele-Shaw cell can be utilized to further investigate the large-scale dynamics of recovery/displacement mechanisms and phase behavior—particularly viscous fingering phenomenon due to steam condensation—by also honoring pressure and temperature. Furthermore, the Hele-Shaw cell could also be used to identify the steam propagation and the interface between steam/condensate and heavy-oil.

In the beginning, the model was fully saturated with heavy-oil to represent initial oil saturation. The superheated steam (up to 240°C with ~100% steam quality) was generated by flowing the water through the high-temperature oven/steam generator, controlled by Teledyne® ISCO (syringe) piston-driven pump (constant flow rate) and installed metering valve. The steam was injected into the Hele-Shaw cell by applying a low-pressure injection to establish the base/reference case. To mimic the tertiary recovery process as well as the improvement of energy efficiency, the steam injection was completely cut-off, and continuous injection of the gaseous solvent(s) was started. The areal sweep efficiency and instantaneous oil production were monitored to further analyze the steam propagation and condensation, the aspects of the viscous fingering phenomenon, and the contribution of various types of solvents to recovery. A complete setup of the Hele-Shaw experiment is shown in **Figure 72**.

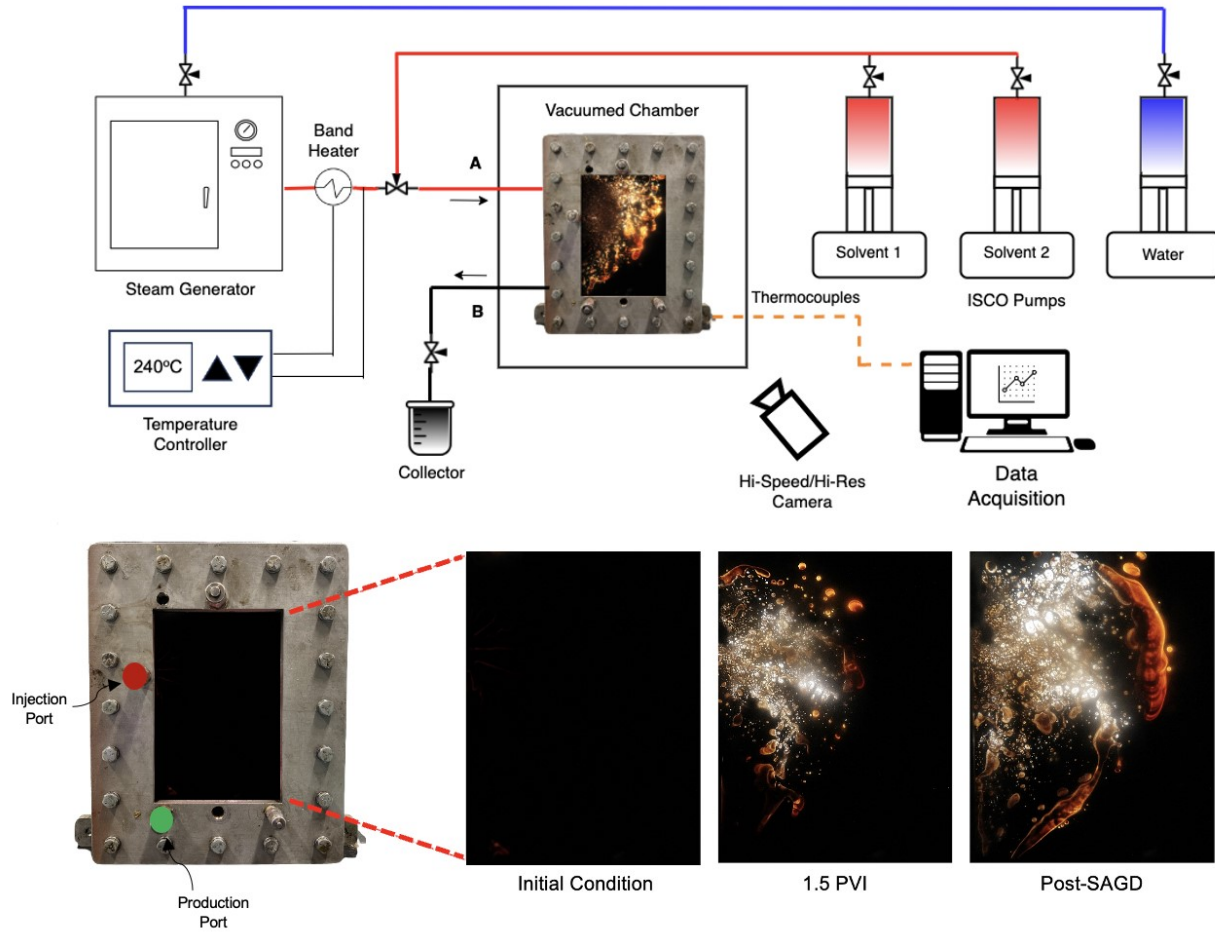


**Figure 72—Investigation of displacement mechanism in Hele-Shaw cell inside a high-pressure-high-temperature steel frame.**

### 5.3.5 Porous Media Visualization Experiment

The study of phase distribution for post-SAGD efficiency improvement was performed through a porous media model. A porous media model is a very beneficial and effective methodology to identify the phase distribution behavior in pore spaces under the presence of capillary interactions.

The porous media model was prepared and packed with 3-mm silica glass beads and placed in between the 9-mm acrylic plates. A rhombohedral packing structure is implemented to represent the porosity of the porous media, which is approximated to be 25–28%. The porous media was mounted and pressurized inside the steel frame and placed inside a sealed and vacuumed chamber

to minimize further heat losses during the experiments. The porous media was initially saturated with the oleic phase to mimic the initial saturation of the reservoir.

Like the Hele-Shaw visualization, the superheated steam (up to 240°C) was constantly injected into the porous media at 0.2–0.3 cc/min until a maximum of 3 pore volumes (PVI) was reached to establish a base case. The steam injection process was stopped and then followed by the solvent injection until 3 PVI to investigate the tertiary recovery process post-SAGD. The dynamics of phase distribution during the SAGD process were captured by our high-resolution and high-speed camera equipped with an optical macro lens. A complete setup of porous media visualization is presented in **Figure 73**.

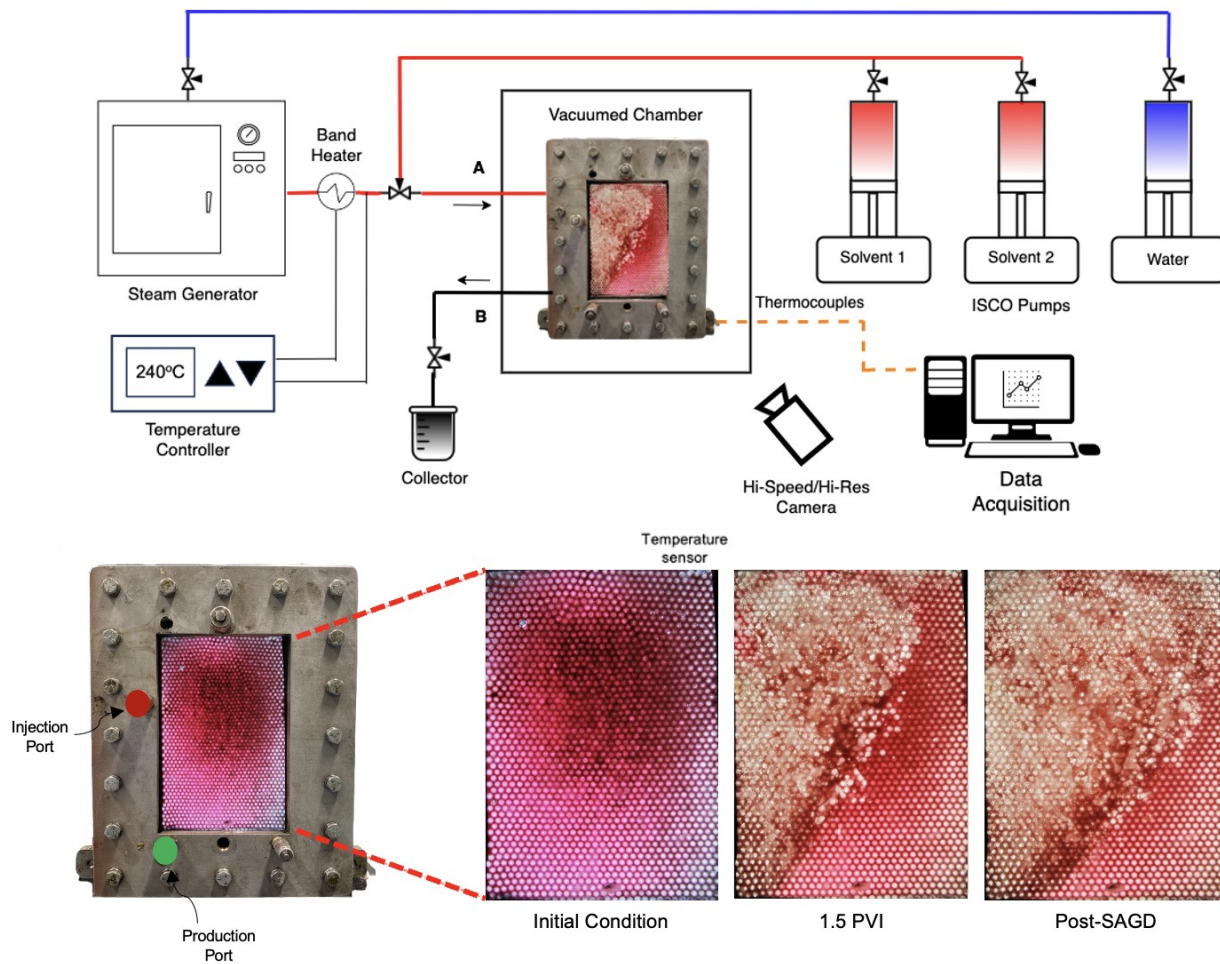


**Figure 73—Investigation of displacement mechanism in porous media inside a high-pressure-high-temperature steel frame.**

### 5.3.6 Remaining Oil Saturation (ROS)

For the Hele-Shaw experiments, ROS is the percentage of oil volume at any time and location inside the cell. The ROS is qualitatively analyzed through the color intensity inside the saturated Hele-Shaw cell. In the beginning, a Hele-Shaw cell was saturated by the heavy-oil, creating a thin oil film inside the cell approximately 0.1 mm thick. Due to the natural behavior of the heavy-oil, the light source placed right behind the Hele-Shaw cell will not be able to infiltrate the thin oil film; therefore, the thin film image captured by the high-speed-high-resolution camera will be completely dark, indicating that the initial oil saturation ( $S_{oi}$ ) was 100%.

During the SAGD and solvent injection processes, the steam or gaseous solvent was injected into the Hele-Shaw cell displacing and/or dissolving the heavy-oil inside the cell. Subsequently, the color intensity of the thin oil film progressively changed from a fully dark color to a brighter color inside the Hele-Shaw cell. This mechanism indicates a gradual change in the heavy-oil saturation in the cell. Additionally, a gradual color change (from a darker to brighter color) also indicates the mixing/dissolution process and interaction between the injected solvent(s) and the oleic phase. A complete displacement of the heavy-oil at a certain position in the Hele-Shaw cell is represented by a bright white image captured by the camera—indicating a very low or 0% ROS. **Figure 74** depicts the ROS of the heavy-oil represented by the color intensity. The range of the color intensity is also divided into five categories presenting the possible areal displacement efficiency.

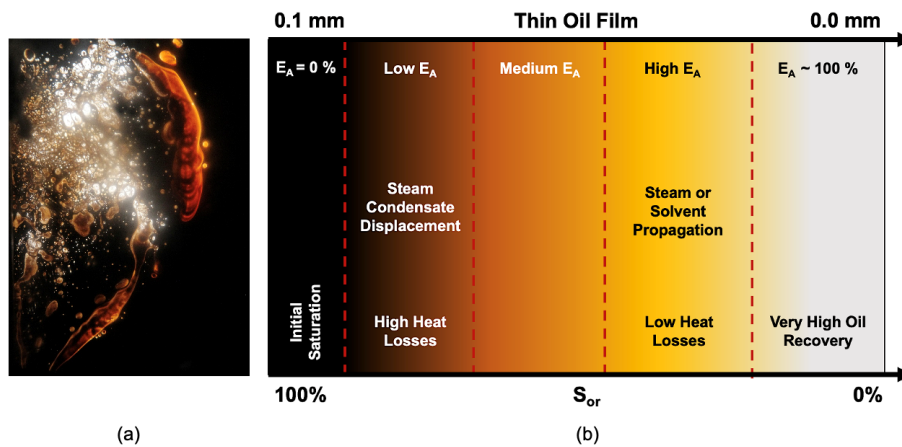


Figure 74—(a) Example of heavy-oil displacement by our steam in Hele-Shaw cell, and (b) color intensity of possible areal displacement efficiency.  $E_A$  = areal displacement efficiency.

## 5.4 Experimental Results

### 5.4.1 Hele-Shaw Visualization

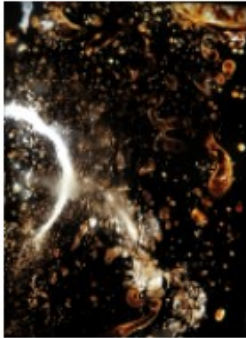
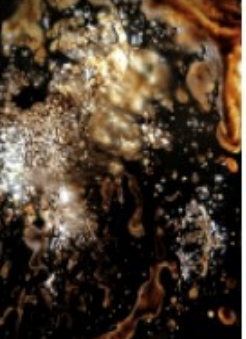
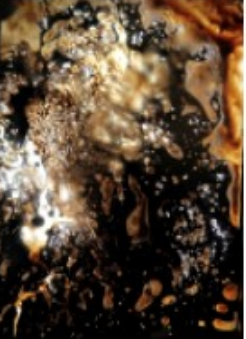
In this study, the Hele-Shaw cell was assembled from two plexiglasses with rubber sleeve in between, encompassing the dimension of 10 cm width x 15 cm length with the clearance between the two plexiglasses of 0.5 mm, placed in between the two steel frames. The band heater and the temperature sensor were installed on the metal tubes and connected to the temperature controller to minimize the potential heat losses during the experiments. Moreover, in minimizing the heat losses in the models (Hele-Shaw cell and porous media), both models were mounted inside the vacuum chamber (**Figure 72**).

In the beginning, the Hele-Shaw cell was fully saturated with the heavy-oil. Subsequently, 0.2–0.3 cc/min pure steam was continuously injected into the cell to mimic the SAGD process until 3 PVI had been completed. Then, the steam injection was cut off, and the selected gaseous solvents or enriched gases with different compositions were injected into the Hele-Shaw cell (3 PVI) for post-SAGD tertiary recovery.

#### 5.4.1.1 Base Case

The base case is defined as the reference SAGD experiment with pure steam/steam-only-based injection. **Figure 75a** presents the flow behavior and steam chamber growth during the heavy-oil displacement process by SAGD at initial conditions, early-stage (0.5 PVI), middle-stage (1.5 PVI), and late-stage (3 PVI/post-SAGD), respectively. It was observed that, at the early stage of steam injection, heat transfer (from the steam phase to the oleic phase) was initiated. Despite the heat transfer, the displacement instability (viscous fingering) was noticeable in the Hele-Shaw cell. Additionally, the gravity effect can also be observed during the early stage of SAGD as some of the fingers move toward the production port of the Hele-Shaw cell.

Case	Results			
Base/reference case				
(a)				
100% Propane				
(b)				
30% Methane–70% propane				
(c)				

<p>50% Methane– 50% propane</p>				
(d)				
<p>100% Heptane</p>				
(e)				
<p>30% Methane– 70% heptane</p>				
(f)				

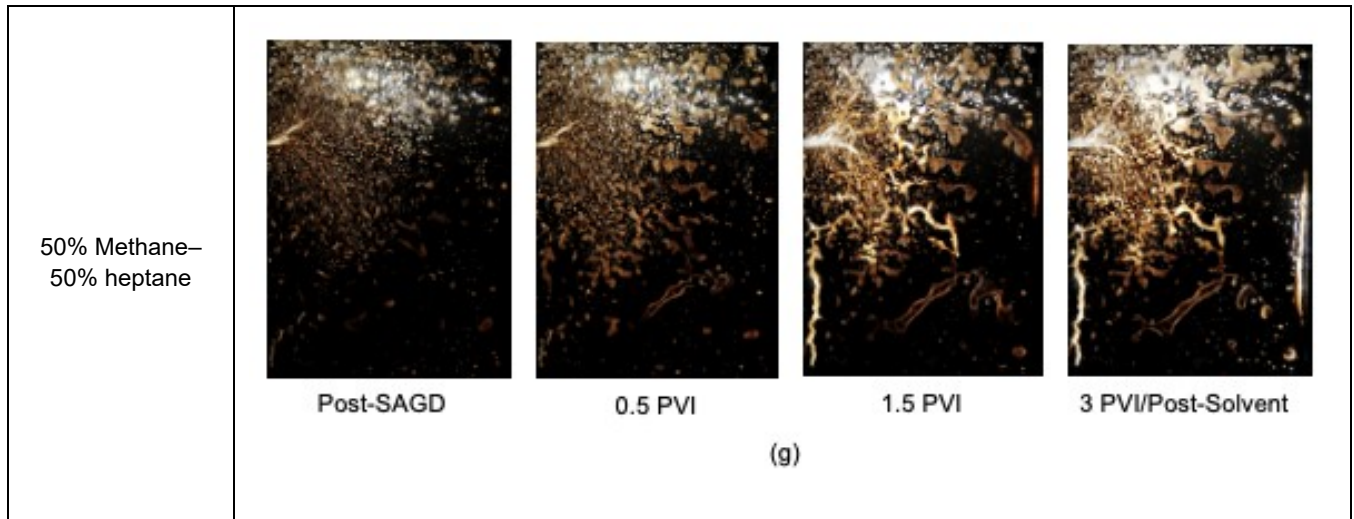


**Figure 75—Summary of Hele-Shaw experimental results with solvent(s). Color representation: black = heavy-oil, orange = condensed steam displacement result, and bright yellow = solvent-oil mixture.**

**Figure 75a** displays the further steam propagation as a result of the continuous steam injection at 1.5 PVI. It is clearly perceived that the steam phase follows the flow path established by the steam condensate displacement at the early stage of SAGD. More essentially, the existence of the steam phase (steam propagation) is also validated by the temperature profile of the Hele-Shaw cell captured by temperature sensors mounted at the different locations of the Hele-Shaw cell (**Figure 76**). The temperature reached over 90°C on average near the injection port at 1.5 PVI (45–50 minutes after the steam injection was initiated). It was also observed that the bright white spots started to appear in the Hele-Shaw cell, indicating that the steam phase has propagated, and the steam chamber has been established in the cell. As the steam phase traveled toward the upper part of the Hele-Shaw cell, the heat transfer into the oleic phase continued to occur. However, the rounded fingers with a light orange color were evidenced during the SAGD process as the indication of rapid heat losses and steam condensate dominant displacement. At this stage, the unstable displacement pathway toward the production port was clearly observed, and the oleic phase was mobilized as a result of the heat transfer and affecting the gravity force.

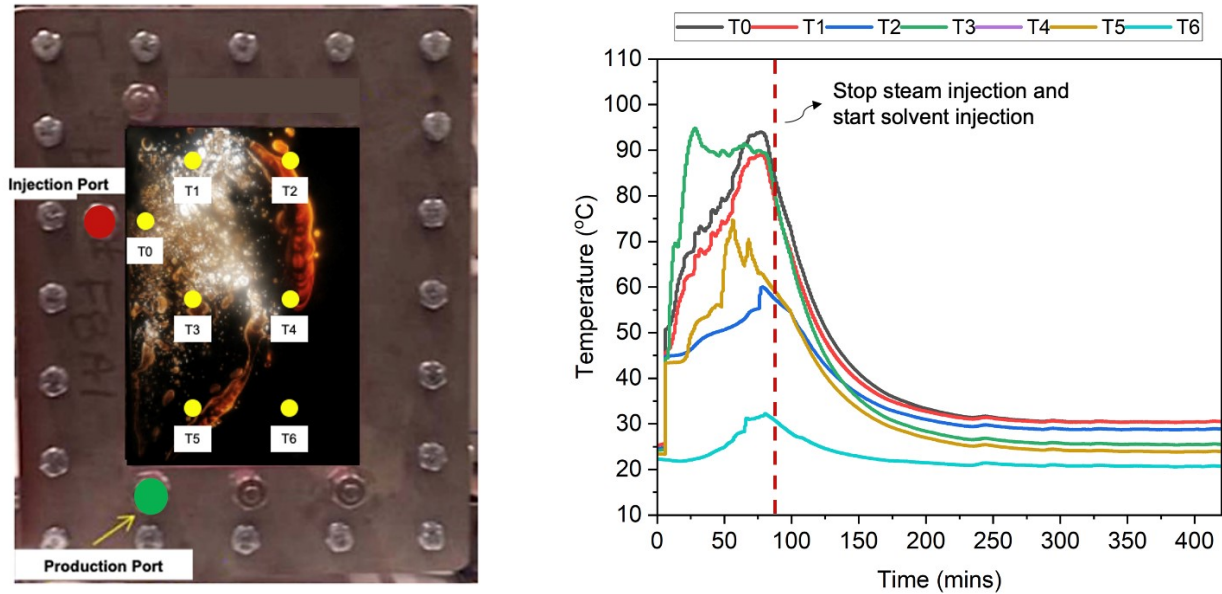


**Figure 76—Average temperature profile observed on Hele-Shaw experiments during SAGD and solvent injection. The dashed line indicates the period when the steam injection was 100% cut-off, and solvent injection was started.**

As the steam was constantly injected into the cell until 3 PVI, the steam phase was perceived to continuously propagate toward the top and the lower part of the Hele-Shaw cell, developing and expanding the steam chamber as an essential part of the SAGD process—creating a more stable steam-heavy-oil interface—indicated by the extensive bright white spots in the cell. This steam chamber expansion was also corroborated by the temperature profile at the upper part (T1) and the lower part (T3) of the Hele-Shaw cell. At this point, the temperature of T1 and T3 rose to over 90°C and 85°C within 90 minutes, respectively, after the early stage of SAGD. Despite the steam propagation and steam chamber expansion, a more continuous rounded and unstable finger was still evidenced. At this particular location (T2), the temperature was much lower than the locations close to the injection port. The temperature profile only showed 58°C on average, even after injecting the pure steam (up to 240°C) for 3 PVI (90 minutes). At the end of the SAGD process, the ROS was less than 60% on average near the injection point but still 80–100% of ROS at the unswept areas. This typical ROS is observed in each experiment when establishing the base/reference case. In the case of solvent(s) injection, the qualitative visual analysis should be

established based on the changes/phenomena (e.g., mixing/dissolution mechanism, changes in color intensity, phase distribution) observed inside the model (e.g., Hele-Shaw cell, porous media) relative to the base/reference case.

This experimental study is able to corroborate the importance of the injected phase (steam) influenced by the temperature and the heat losses on the stability and efficiency of the heavy-oil displacement. When the pure steam arrives inside the model (e.g., Hele-Shaw, porous media), the steam quality can be potentially reduced to 80% (or even lower) due to the heat losses and first contact with cold oil—triggering the steam condensation and viscous fingering.

#### **5.4.1.2 100% Propane Injection**

When the SAGD process reached 3 PVI of injection, the steam was 100% cut-off (no injection), and propane injection (100% composition) was started. The main objective of light hydrocarbon injection (propane) is to achieve further viscosity reduction on such extremely highly viscous crude oil by the solvency effect to achieve a better sweep as well as the removal of residual oil in the steam-swept areas.

**Figure 75b** presents the experimental results when the Hele-Shaw cell was injected with 100% propane post-SAGD. In the early stage of the solvent injection, the improvement of the previously established and developed steam chamber is noticeable. More bright white spots appeared in the Hele-Shaw cell, indicating that more residual oil is diminished due to the mixing/dissolution process of heavy-oil by solvent. Another noticeable phenomenon that occurred during the early stage of the solvent injection was the mixing of the lighter hydrocarbon (propane) and the heavy-oil. The rounded finger became longer, wider, and lighter in terms of its color intensity. At this stage, more heavy-oil was mobilized and produced.

As the solvent was continuously injected into the Hele-Shaw cell, the expansion of the bright white spots was clearly observed. On top of this phenomenon, the rounded finger was perceived to become much longer and wider, and even the color intensity was much lighter than in the early stage of the solvent injection. More critically, at the end of the solvent injection (3 PVI), the bright white spots became much more extensive, and the improvement of the areal displacement efficiency (as well as the microscopic displacement efficiency) was clearly evidenced. All these

phenomena confirmed that the dissolution and mixing of the injected solvent into the heavy-oil favorably occurred at the given post-SAGD temperature, thus, further leading to the heavy-oil viscosity reduction and eventually improving the oil recovery. At steam chamber zones, the ROS could be diminished to less than 40% on average by the end of the solvent injection period.

#### **5.4.1.3 30% Methane–70% Propane Injection**

While non-condensable gas (methane) injection has been considered as a post-SAGD recovery method, solvent addition can potentially play an important role in the improvement of heavy-oil/solvent miscibility—further diminishing the interface between the solvent and the heavy-oil (Novosad 1989). In addition to the proven propane injection on the heavy-oil recovery to improve miscibility, the injection of methane into the heavy-oil reservoir would promote the effect of the insulation at the upper part of the reservoir that potentially reduces the heat losses to the surrounding reservoir rocks (Canbolat et al., 2014). Moreover, Butler (1999) and Jiang et al. (2000) showed that the addition of methane could potentially improve the overall SAGD performance by enhancing heavy oil recovery at relatively low SOR. From an economic point of view, mixing two light hydrocarbons as enriched gaseous solvents could potentially improve cost-effectiveness. Considering all this favorable evidence, we investigated the potency of enriched gaseous solvents for post-SAGD application by adding a methane composition of up to 30% and lowering the propane composition to 70%.

**Figure 75c** shows the experimental results of a solvent mixture injected right after the SAGD process. At the beginning of the solvent(s) injection, it was clearly observed that the bright white spots started to expand, and the bright orange rounded fingers appeared as the mixing/dissolution process was initiated. As the solvent injection was continuously injected into the Hele-Shaw cell, the mixing of solvent into the heavy-oil was evidenced—indicated by an even larger and brighter yellowish rounded finger, moving from the top to the bottom part of the model, resulting from the propagation of a solvent mixture to the upper part of the Hele-Shaw model at the given pressure and temperature. At this stage, the heavy-oil viscosity reduction was attained, a larger swept area was evidenced, and the oleic phase could be mobilized toward the production point by also involving the gravity force. By the end of the solvent(s) injection period, the ROS—particularly in the steam chamber—could be reduced from an average of 75% to less than 50% on average.

#### 5.4.1.4 50% Methane–50% Propane Injection

In another trial, the composition of the solvent mixture (enriched gas) was changed. The composition of methane was increased to 50%. On the other hand, to further investigate the influence of propane on the whole system, the propane composition was reduced to 50%.

**Figure 75d** presents the results obtained from the solvent mixture of 50% methane and 50% propane compositions that was injected into the Hele-Shaw cell right after the SAGD process without any steam injection. At the early stage of the solvent injection (0.5 PVI), it was observed that the formation of the rounded finger with a much lighter orange color at the upper part of the model was present. This phenomenon has indicated that the propagation/expansion of the solvent(s) occurred—leading to the mixing/dissolution process of the solvent(s) into the heavy-oil—and then moved along with the heavy-oil toward the production point due to the effect of gravity force.

Furthermore, as the solvent was continuously injected into the model until 1.5 PVI and 3 PVI, noticeable changes in the Hele-Shaw cell were observed (**Figure 75d**). A continuous mixing/dissolution process of solvent and heavy-oil was clearly evidenced on the top right corner of the model, indicated by a much larger bright yellowish swept area—moving down to the production point. Despite the successful mixing process of the solvent and the heavy-oil, no substantial expansion of the bright white spots was observed. The ROS was diminished from initially 80% to less than 60% on average.

#### 5.4.1.5 100% Heptane Injection

To further investigate the effect of solvent type on the post-SAGD efficiency improvement, we expanded the solvent selection to a heavier one, and heptane was selected for this purpose. Heptane is a non-polar solvent and encompasses a boiling point of 98.4°C, which can vaporize at the given steam pressure and temperature; therefore, this type of solvent is suitable for SAGD application.

The experimental result involving heptane injection post-SAGD at 100% composition is presented in **Figure 75e**. In the beginning, when the solvent was injected at 0.5 PVI, bright yellowish spots were formed near the injection point and at the top part of the model. At this stage, the

mixing/dissolution process between the solvent and heavy-oil was initiated. The solvent-oil mixture then moved downward as the gravity force was in effect. This evidence confirms that the heptane propagated as a vapor phase toward the upper part of the model, which is also substantiated by the temperature sensor at the injection point (**Figure 76**).

As the solvent injection was continued until 3 PVI, extensive bright white spots were observed and expanded at the upper part of the model; therefore, indicating that there was an accumulation of heptane at the top part of the Hele-Shaw model. The amount of accumulated heptane promotes an even easier dissolution process of heavy-oil. By the end of solvent injection, the ROS at the steam chamber/zone reduced from initially 85% to nearly 0%.

#### **5.4.1.6 30% Methane–70% Heptane Injection**

A solvent mixture of methane and heptane was investigated to further study its performance for the post-SAGD application. In this experimental study, we added 30% methane composition and reduced the heptane composition to 70%. **Figure 75f** exhibits the experimental results of 30% methane and 70% heptane injection.

The propagation and expansion of the bright white spots toward the upper part of the model—as a result of solvent propagation and solvent-oleic phase interaction—were observed at the early stage of solvent mixture injection (0.5 PVI). Furthermore, at this period, a mixing/dissolution process of solvent into heavy-oil occurred, and heavy-oil viscosity was able to be significantly reduced as the ROS at the upper part of the model was mobilized toward the production point. The ROS could be diminished from 75% to less than 40% on average.

Continuing the solvent injection until 3 PVI, brighter white and yellowish spots were perceived as a manifestation of solvent accumulation at the upper part of the model. At this stage, the areal sweep efficiency was much improved, and the ROS was able to be diminished to less than 30% on average by the end of solvent injection.

#### **5.4.1.7 50% Methane–50% Heptane Injection**

In gaining a more thorough investigation of the solvent mixture, each solvent composition was further modified. The heptane composition was reduced to 50%, whereas the methane composition was increased to 50%. The results of this experiment are summarized in **Figure 75g**.

There was no substantial improvement observed in the Hele-Shaw model at the early stage of the solvent mixture injection (0.5 PVI) once the heptane composition was reduced, compared to the case of 30% methane–70% heptane solvent mixture injection—having a more favorable ROS reduction due to the impact of solvent propagation. This phenomenon validates that the contribution of heptane (as a solvent) plays a significant role in further diminishing ROS.

A noticeable improvement occurred in the Hele-Shaw model was perceived after increasing the solvent mixture injection volume to 1.5 PVI. At this stage, the dissolution effect presented by the injected solvent improved—represented by the expansion of the bright white spots at the upper part of the Hele-Shaw model. These bright white spots continued to expand until the late stage of solvent injection (3 PVI). However, this experimental case presented a least favorable post-SAGD improvement compared to other experimental cases encompassing higher heptane concentration.

This evidence could validate that a more injection volume of the heavier solvent is needed to initiate the dissolution mechanism in a lower solvent concentration to further diminish the ROS.

#### **5.4.2 Porous Media Visualization**

Using a model representing porous media rather than Hele-Shaw-type models is needed to qualitatively investigate the mechanics of the recovery processes at the pore scale. More specifically, the phase distribution mechanism is a very critical factor comprehended in the application of hydrocarbon solvents as four phases (oil, water, steam, and solvent) exist in the reservoir system.

Similar to the Hele-Shaw experiments, the porous media model comprises the dimension of 10 cm width x 15 cm length with the clearance adjusted to the diameter of the glass bead (3 mm). This porous media model was also mounted in between the two steel frames and placed inside the vacuum chamber to minimize the heat losses during the experiments. The band heater and

temperature sensor (connected to the temperature controller—maintained at 240°C) were also utilized as the effort to lessen further heat losses in the metal tubes when injecting the generated steam to the porous media model (**Figure 73**). The porous media was initially saturated with highly viscous oil, but a -transparent- mineral oil was used rather than crude oil. To mimic the SAGD process, 0.2–0.3 cc/min of superheated steam (up to 240°C) was constantly injected into the porous media until it reached 3 PVI. The injection was then followed by the solvent without any steam injection (100% solvent injection) until 3 PVI.

#### 5.4.2.1 Base Case

For the porous media experimental study, the base case was established by pure steam injection into the porous media model. The SAGD chamber growth and the formation of ROS are visualized in **Figure 77a**. Through the images provided in this figure, five distinctive zones can be identified: (1) the steam chamber (dominant steam zone), (2) the steam condensate zone, (3) the residual oil zone, (4) the mobilized zone—containing steam, steam condensate, oleic phase—and (5) heavy-oil filled zone containing immobilized and low-temperature heavy-oil. As the steam was injected through the injection port, the heating process of the oleic phase was initiated. During this process, the heavy-oil viscosity was reduced, and then the heated oil was produced from the upper part of the porous media under the influence of the gravity force.

Case	Results			
Base/reference case				
	Initial Condition	0.5 PVI	1.5 PVI	3 PVI/Post-SAGD

(a)

<p>100% Propane</p>	 <p>Post-SAGD</p>	 <p>0.5 PVI</p>	 <p>1.5 PVI</p>	 <p>3 PVI/Post-Solvent</p>
(b)				
<p>30% Methane– 70% propane</p>	 <p>Post-SAGD</p>	 <p>0.5 PVI</p>	 <p>1.5 PVI</p>	 <p>3 PVI/Post-Solvent</p>
(c)				
<p>50% Methane– 50% propane</p>	 <p>Post-SAGD</p>	 <p>0.5 PVI</p>	 <p>1.5 PVI</p>	 <p>3 PVI/Post-Solvent</p>
(d)				

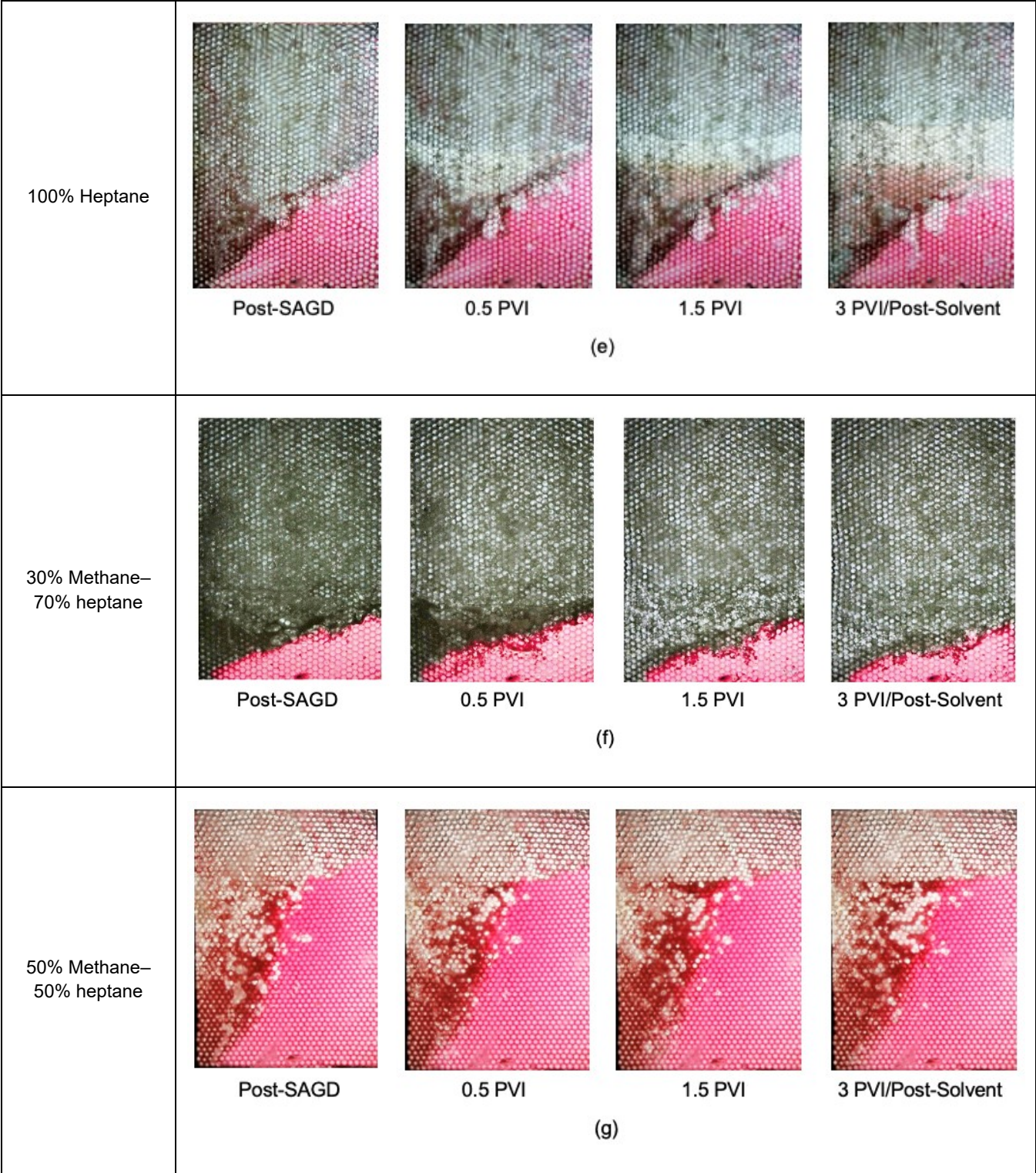


**Figure 77—Summary of porous media experimental results with solvent(s). White-dashed circle = oleic phase, and yellow-dashed circle = water-in-oil emulsion/solvent-oil mixture.**

At this early stage of SAGD (0.5 PVI), displacement instability was clearly perceived in the porous media. This phenomenon confirms the rapid heat losses instigating the rapid steam condensation; therefore, the displacement of the oleic phase was dominated by the steam condensate. In such conditions, the steam-condensate and the oleic phase mobility contrast is highly unstable—potentially causing viscous fingering and tip-splitting to occur. In addition, it is also noticeable that the unstable fingers move downward toward the production port as the gravity force is in effect.

As the steam was continuously injected, the steam propagated and penetrated toward the upper part of the porous media model. At this stage, the process of gravity drainage took place. Additionally, the steam invaded in vertical and horizontal directions, further contributing to the thinning of the oil zone in addition to the gravity force. This steam propagation and steam chamber expansion are also corroborated by the temperature profile of each thermocouple placed on the porous media model (**Figure 78**). At 1.5 PVI, the temperature profiles close to the injection port (T0) and the upper part of the porous media (T1) raised to over 100°C on average, validating that the steam propagated from the region close to the injection port to the upper part of the porous media. At this stage, the viscosity of the oleic phase could be reduced, and the oleic phase could be mobilized toward the lower part of the porous media as the oleic phase started to accumulate and be produced throughout the production point. Nevertheless, the upper right region of the porous media was still filled up with the steam condensate (**Figure. 79**), which is confirmed by the temperature profile (T2), showing a temperature value of 60–70°C on average. Furthermore, **Figure 77a** shows the continuous process of the steam injection until the end of SAGD (3 PVI). Despite the successful steam propagation and the steam chamber expansion, residual oil (snap-off of oil blobs and islands of oil) was still observed (**Figure 79**).

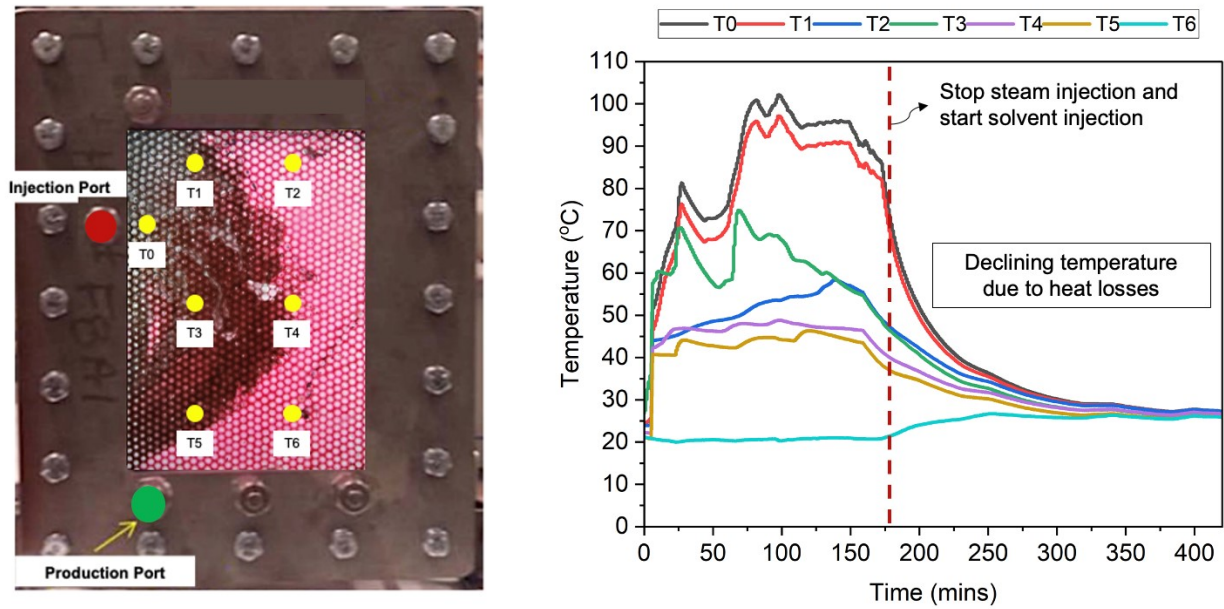


**Figure 78—Average temperature profile observed on porous media experiments during SAGD and solvent injection. The dashed line indicates the period when the steam injection was 100% cut-off, and solvent injection was started.**

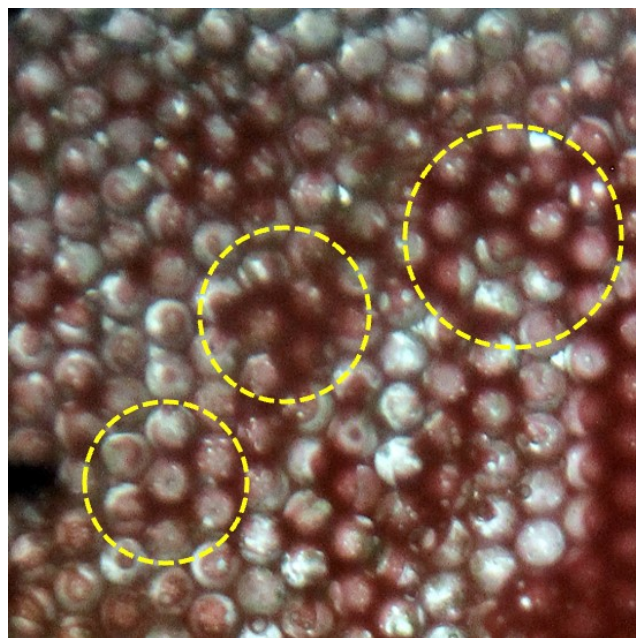


**Figure 79—Observation of residual oil formation in pore spaces (oil blobs and island of oil) post-SAGD process.**

#### 5.4.2.2 100% Propane Injection

In this case, we tested the propane gas with 100% composition as a solvent applied post-SAGD without any steam injection involved. The solvent was continuously injected into the porous media model after the SAGD process reached 3 PVI. **Figure 77b** visualizes the phase distribution behavior with 100% propane injection. We evidenced that the extensive residual oil at the upper part of the model—resulting from the post-SAGD—could be diminished and mobilized toward the production point at the early stage of the solvent injection. This evidence indicates that propane propagated toward the top part of the model. Some of the propane mixed with the oleic phase and some of it would stay at the upper part of the model. It is also noticeable that the mobilized residual oil accumulated at the lower part of the model (darker color) indicates the influence of the gravity force.

As the solvent was continuously injected until 3 PVI, more residual oil was mobilized toward the production point of the porous media model; thus, promoting the recovery improvement. This can be attributed to the miscibility and reduced interfacial tension, and wettability alteration (physicochemical effect) caused by propane.

#### 5.4.2.3 30% Methane–70% Propane Injection

To further investigate the influence of the solvent composition on the displacement efficiency, we modified the composition of each solvent gas to 30% composition for methane and 70% composition for propane. **Figure 77c** exhibits the results gained from the continuously enriched gas injection post-SAGD. Reducing methane composition and increasing propane composition could lead to a more favorable displacement efficiency improvement as well as residual oil mobilization compared to the enriched gas injection containing 50% methane and 50% propane.

At the early stage of the enriched gas injection (0.5 PVI), the initiation of the oleic phase mobilization was visible as the residual oil at the top of the porous media started to diminish and move toward the lower part of the model due to the influence of the gravity force. As the enriched gas injection was continued throughout the end of the injection (3 PVI), even more, residual oil mobilization from the upper part of the porous media model was clearly observed—indicating that

the dissolution process of the solvent in the oleic phase and the viscosity reduction of the oleic phase was successful; thus, further leading to the improvement of the displacement efficiency.

#### **5.4.2.4 50% Methane–50% Propane Injection**

We also included the enriched gas injection—containing 50% methane composition and 50% propane composition in the porous media experimental study to further investigate the potency of this enriched gas (applied post-SAGD) on the phase distribution behavior in the pore spaces. It is, however, observed that no substantial improvement in oleic phase mobilization was perceived, despite the solvent mixture propagation at the upper part of the model. Only a small portion of the residual oil region (at the top of the porous media) could only be mobilized (**Figure 77d**).

When the solvent mixture injection was continued until 3 PVI, no further changes in terms of phase distribution were perceived. The ROS was still evidenced at the steam chamber and most of the swept areas by the end of the solvent(s) injection period. This indicates that the solvent(s) injection at this composition is less effective in the influence of capillary force.

#### **5.4.2.5 100% Heptane Injection**

Comparable to the Hele-Shaw experiment, we also utilized another liquid type of solvent (heptane) with 100% composition for this porous media experiment. At the beginning of the solvent injection period, due to a high-temperature maintained post-SAGD (**Figure 78**), some portions of heptane changed its phase to a vapor phase and moved toward the upper part of the model—diminishing some portions of unswept oil at the steam chamber and dissolved/mixing with the oleic phase—then recovered downward to the production point along with the oil (**Figure 77e**).

As this solvent was continuously injected into the porous media model, the dissolution/mixing process between the solvent and the oleic phase was observed to continue. At this period, the viscosity of the oleic phase has been reduced; thus, allowing more recovery of the oil toward the production point under the influence of the gravity force—represented by the clear and brighter white regions and the discernible fluid flow path pointed by the yellow arrow in **Figure 77e**.

However, due to the rapid decline of the temperature, the solvent (heptane) has altered its phase from the vapor phase to its original phase (liquid phase), accumulated in the middle region of the porous media model, mixed and produced along with the oil. When the solvent injection reached the maximum designated injection volume (3 PVI), more recovery and improvement of displacement efficiency were acquired—indicated by the reduction of ROS at the lower region of the model and a larger fluid flow path (**Figure 77e**).

#### **5.4.2.6 30% Methane–70% Heptane Injection**

In this case, the composition of the liquid solvent (heptane) was reduced to 70% of the total amount and introduced a gaseous solvent (methane) into the system as high as 30% of its composition. **Figure 77f** displays the entire process of solvent(s) injection for each injection volume. At the early stage of injection, due to the high-temperature region (soon after the steam injection was cut off), it can be substantiated that the solvent(s) propagated to the upper region of the porous media model and diminished the residual oil at the unswept regions by mixing with/dissolving into the oleic phase. Then, by the effect of the gravity force, it moved downward and accumulated at the lower region of the porous media model. This phenomenon could be validated by the observation of the dynamics inside the porous media model. It is noticeable (from the visualization) that the upper region of the model has transformed to a brighter shade, signifying that the residual oil at the unswept region has been mobilized.

By the time the solvent(s) injection reached higher injection volumes (1.5–3 PVI), the accumulated solvent–oil mixture at the lower region of the porous media was able to be mobilized and recovered throughout the production point. Nevertheless, the displacement/areal sweep efficiency presented by these solvent compositions was less favorable compared to what we perceived from a pure heptane injection. Much brighter white regions were observed. In other words, the "cleaning effect" was way more effective in the case of pure heptane (100% composition) injection.

#### **5.4.2.7 50% Methane–50% Heptane Injection**

In evaluating the significance of the heavier solvent (heptane) to the entire displacement/areal

sweep efficiency as well as the recovery performance, we further reduced the heptane composition to 50%, whereas the composition of the methane was escalated to 50%. At the early stage of solvent(s) injection, we did not perceive any significant changes in terms of areal sweep efficiency and recovery (**Figure 77g**) compared to the previous case.

Even though after increasing the solvent(s) injection by up to 3 PVI, only a few portions of the residual oil at the upper region were noticeable to be mobilized. This phenomenon is explained by the yellow arrow in **Figure 77g**, pointing out the slight changes in the porous media model. The darker red color (by the change of the solvent(s) injection volume) at the upper region of the model indicates the accumulation of the mobilized ROS/unswept oil.

In general, this solvent(s) injection composition did not present favorable sweep or recovery performance.

### 5.4.3 Oil and Solvent Recoveries

The ultimate goal of this portion of the research was to investigate the dynamics of fluid-to-fluid interactions and phase distribution visually under the influence of capillary force. In supporting this experimental study, a semi-quantitative analysis was also performed to further evaluate the oil recovery performance and solvent recovery presented by the studied solvent types and compositions. Even though this methodology is not ultimately comparable with core flooding, this would be valuable information to obtain a better understanding of post-SAGD efficiency improvements.

The produced samples from each experiment were collected for further gas chromatography (GC) analysis. Both gas and liquid samples were collected using the vacuumed vessel connected to the Erlenmeyer flask. **Table 14** presents the results gained from the GC analysis after solvent injections for each injection case. According to the GC analysis, it was perceived that methane, propane, and heptane could be qualitatively detected by the gas and liquid GC instruments, indicating that the solvent(s) is potentially retrievable, as methane, propane, and heptane have their own solubility in both the water phase and oleic phase. More importantly, the recovery potential of these hydrocarbon solvents is also proportional to their solubility in both the water phase and the oleic phase.

**Table 14—Gas and liquid GC analysis result of solvent(s) injection post-SAGD.**

Case	Unit (%)		
	Methane	Propane	Heptane
100% Propane	-	0.433	-
30% Methane–70% Propane	0.041	0.385	-
50% Methane–50% Propane	0.088	0.243	-
100% Heptane	-	-	45.60
30% Methane–70% Heptane	1.180	-	39.18
50% Methane–50% Heptane	1.745	-	37.90

**Figures 80 and 81** present the oil recovery and solvent recovery profiles during solvent(s) injection applied post-SAGD at designated injection volumes and given pressure and temperature. The base/reference case generated from each experiment present consistent recovery profile (up to 40%)—further validating the ROS established post-SAGD. The GC analysis was utilized to calculate the solvent recovery factor. It is noticeable that pure propane and heptane injections were able to present 30–40% additional recovery post-SAGD. On the other hand, involving methane gas as a solvent mixture did not present a favorable recovery improvement. These types of solvent mixtures could only recuperate 10–20% of the incremental recovery. In a more extreme case, a mixture of 50% methane and 50% propane showed almost no improvements in oil recovery.

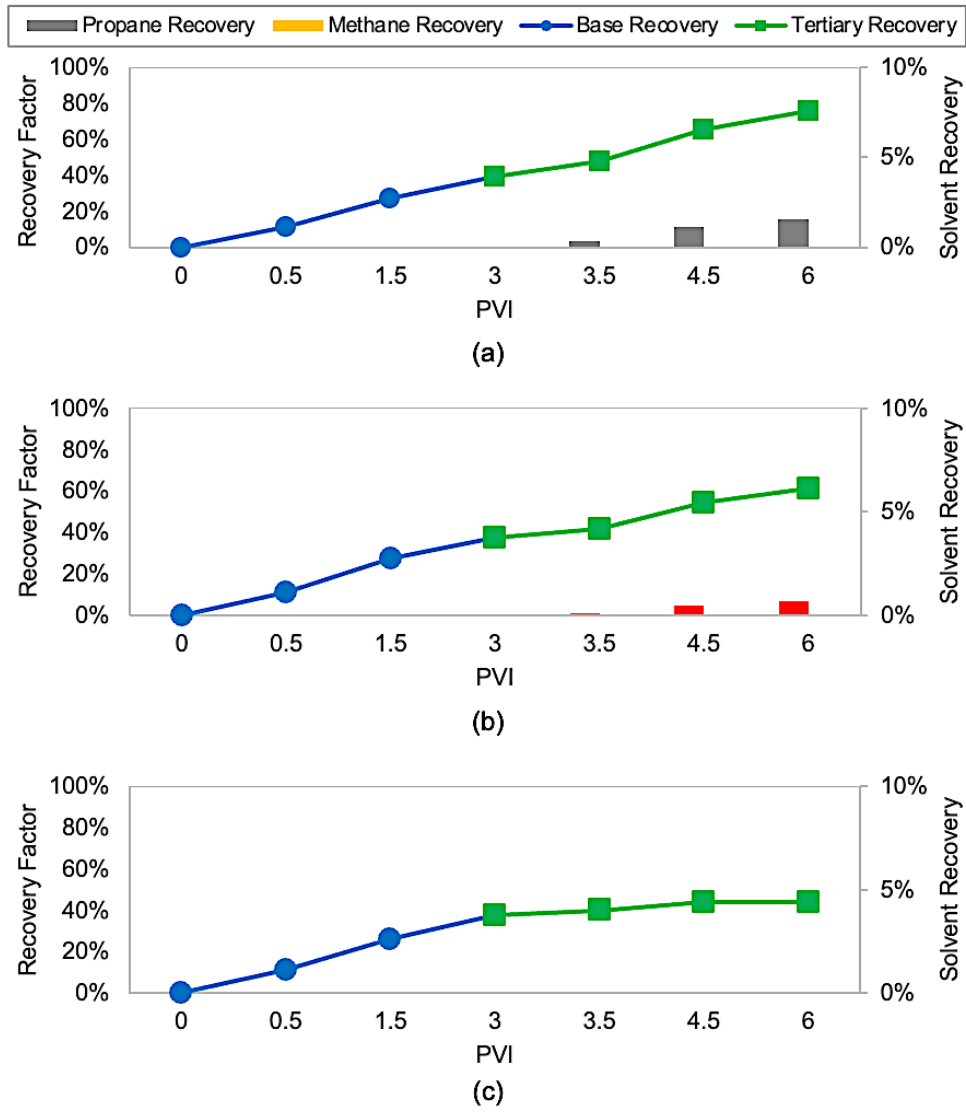


**Figure 80—Oil recovery and solvent recovery profiles during propane and methane–propane mixture injections at designated injection volumes. (a) 100% propane, (b) 30% methane–70% propane, and (c) 50% methane–50% propane.**

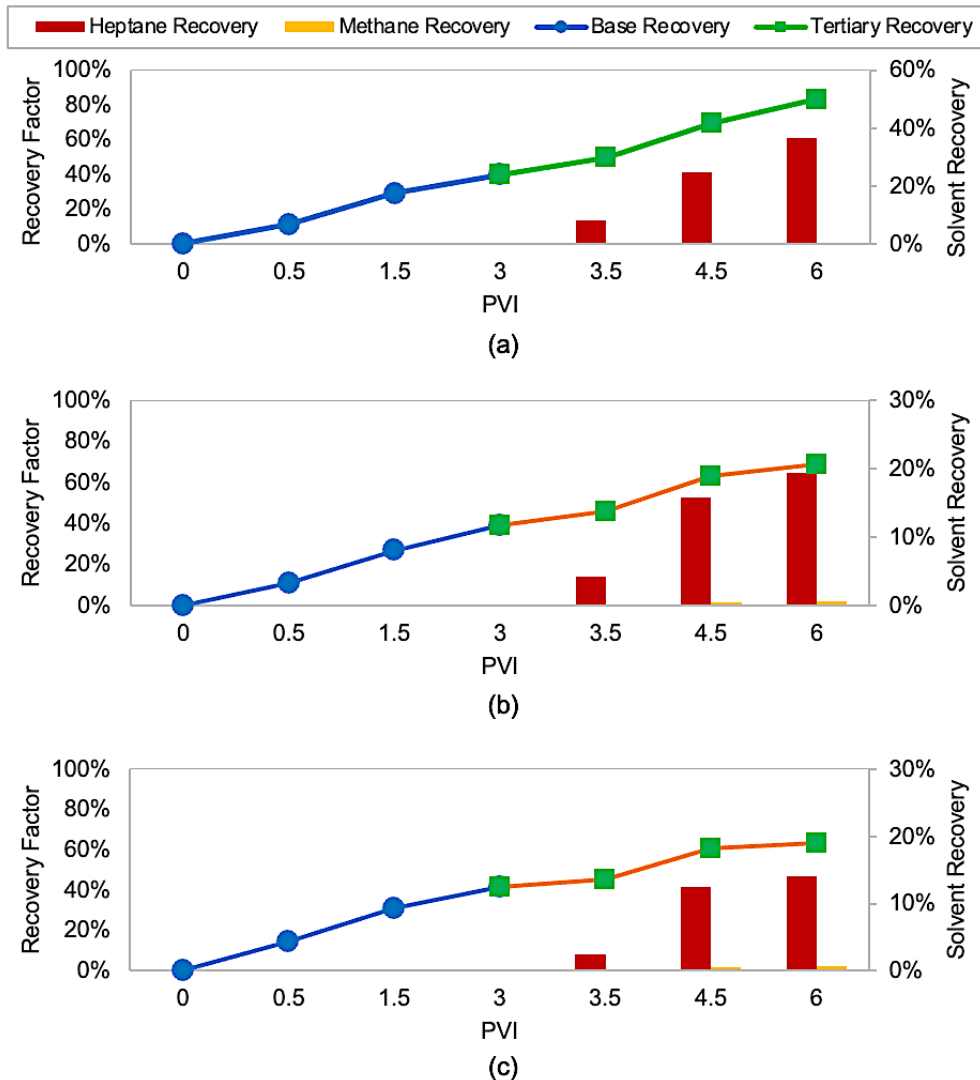


**Figure 81—Oil recovery and solvent recovery profiles during heptane and methane–heptane mixture injections at designated injection volumes. (a) 100% heptane, (b) 30% methane–70% heptane, and (c) 50% methane–50% heptane.**

In terms of solvent recovery, even though the propane injection case could still present a small amount of solvent recovery, the experimental case with heptane injection provided the most favorable performance of solvent recovery at the given pressure and temperature. By referring to these oil recovery and solvent recovery profile plots, we are able to conclude that most of the solvent gas (particularly methane gas) could not be retrieved. It remains and stays at the top of the studied model. Liquifying the injected solvent is a positive effect on the recovery of it by gravity

as well as improving the dissolution of the solvent in the oil. In this case, the proper solvent type and composition should be determined to maximize the oil recovery and solvent recovery based on given pressure and temperature conditions, which are not to be changed during the post-SAGD applications. Hence, phase behavior studies are needed for given oil conditions in the reservoir to select the suitable solvent type and composition.

#### **5.4.4 Viscosity Measurement and SARA Analysis**

In addition to phase behavior, further physical and chemical analyses are needed to achieve more solid conclusions and recommendations. Therefore, we performed viscosity measurements and SARA tests to evaluate and validate the effect of injecting the studied solvent(s) to the heavy-oil/bitumen properties.

##### **5.4.4.1 Heavy-Oil Viscosity Measurement**

Each oil sample from these experiments was collected after the solvent injection to evaluate the viscosity reduction performance for each solvent injection case. The viscosity profiles are presented in **Figure 82**. According to these viscosity profiles, it is clearly evidenced that the solvent injection could exhibit auspicious heavy-oil/bitumen viscosity reduction. The heavy-oil viscosity could be diminished to below 1 cP by involving solvent injection (particularly pure heptane injection).

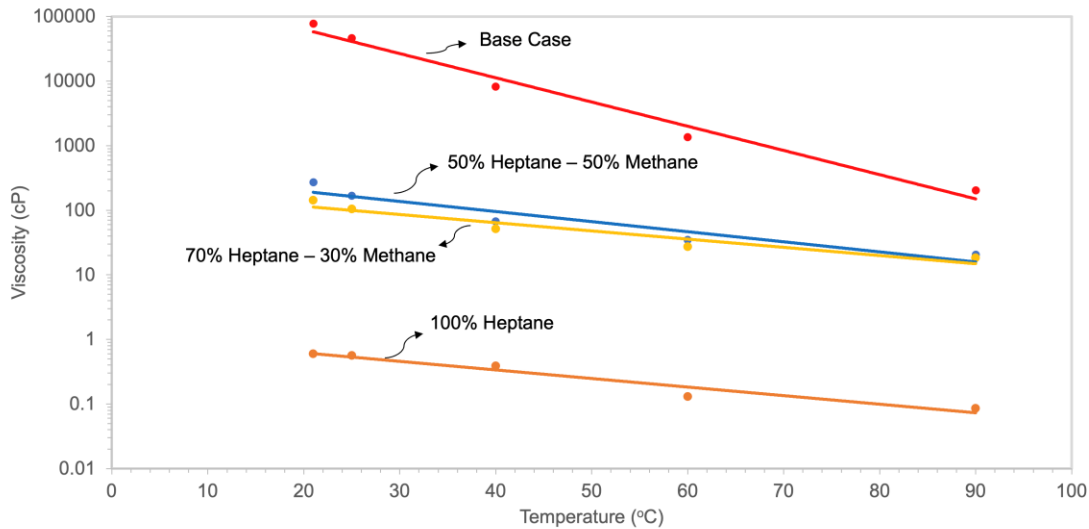


**Figure 82**—Example of viscosity measurements for heptane and methane-heptane injection cases.

#### 5.4.4.2 SARA Tests

To further evaluate the changes in oil properties/compositions, we also performed the SARA analysis for each solvent injection case. **Figure 83** summarizes the SARA test results relative to the base/reference case. It is noticeable that there were significant changes in oil components after solvent(s) injections. The presence of lighter components has validated that the studied solvent(s) presented the desirable performance for post-SAGD applications.

Furthermore, it is clearly evidenced that the asphaltene components significantly reduced after injecting the studied solvent(s) into the model. It can be speculated that the asphaltene precipitation occurred during the solvent(s) injection period. In validating this speculation, the dark greyish solid samples were collected from the Hele-Shaw cell after solvent(s) injection—indicating the asphaltene precipitation. Asphaltene is a polar component contained in heavy-oil/bitumen. Dissolution tests with non-polar and polar types of solvent could corroborate this asphaltene precipitation. It is perceived that the solid sample (generated from the experiments) did not dissolve in the non-polar solvent but then dissolved in the polar solvent. According to this test, we are able to validate and confirm that the asphaltene precipitation occurred during the solvent(s) injection process.

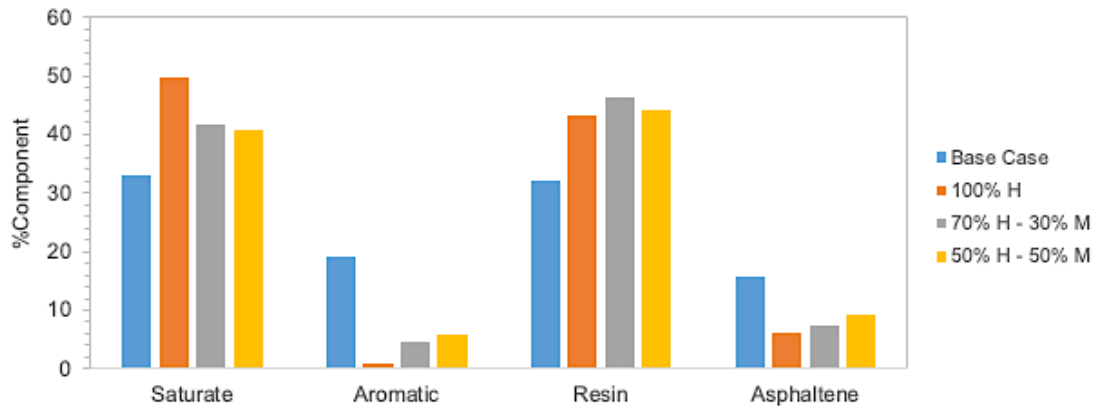


Figure 83—Example of SARA analysis for heptane and methane-heptane injection cases. H = heptane, and M = methane.

## 5.5 Discussions

### 5.5.1 Hele-Shaw Visualization

It is undeniable that SAGD is a unique and complex process that requires further investigation to understand its dynamics. In our experimental study, the SAGD process is represented by the establishment of a base/reference case. After injecting pure steam for the desired injection volume, viscous fingering—due to displacement instability—was observed. This phenomenon is predominantly due to condensed steam displacement. Rapid heat losses and the contact with initially cold oil caused the rapid condensation of the generated steam; therefore, the early stage heavy-oil displacement is by condensed steam only. More importantly, due to the unfavorable mobility contrast between the steam condensate and heavy-oil, the displacement is highly unstable, resulting in viscous fingering as well as the tip-splitting of the viscous fingering. These unstable displacement phenomena were also observed through the previous experimental studies in steam injection/SAGD performed by Kong et al. (1992) and Bruns and Babadagli (2020). The unstable fingering phenomenon also applies at more distant locations due to more progressive heat losses and condensed steam dominant displacement.

Furthermore, in addition to the viscous fingering, we also evidenced that the steam phase propagation would travel along the flow path created by the condensed steam displacement. This phenomenon was also confirmed by Kong et al. (1992). Throughout their experimental visual

studies, they observed and concluded that the steam would follow the steam condensate pathway, which resulted during the initial stage of steam injection, and the steam vapor rapid burst occurred immediately after—further occupying the location where the steam condensation occurred beforehand.

In the case of gaseous solvent(s) injection, the viscosity of the mixture of light hydrocarbon and heavy-oil could potentially reduce the original viscosity of the heavy-oil; therefore, more incremental heavy-oil recovery is achievable by improved sweep. More essentially, the solubility (K-value) of the propane in the heavy-oil (at a comparable pressure) is considerably low at post-SAGD temperature (Deng 2005). K-value represents the solubility of solvent(s) in the hydrocarbon (e.g., heavy-oil, bitumen)—depending on the type of solvent(s) and given pressure and temperature. A lower K-value means higher solubility of the solvent(s) in heavy-oil/bitumen, whereas a higher K-value indicates lower solubility of the solvent(s). At this given pressure (relatively low pressure) and temperature (close to steam temperature), gaseous solvents (e.g., methane, heptane) comprise higher K-value and more liquid solvent(s), like heptane, encompasses much lower K-value. Hence, the experimental results gained from this study have satisfied this K-value. In other words, the experimental results are valid.

In addition to the K-value, propane is miscible with crude oil at given conditions; thus, the mixing process of the propane in the heavy-oil could be expected. Furthermore, a gaseous solvent, by its density, could move toward the upper part of the reservoir to potentially improve the steam chamber and diminish the ROS by initiating the mixing/dissolution process, thus, generating more oil production.

Another interesting finding that was evidenced in the 30% methane–70% propane injection compared to the 50% methane–50% propane was the injection of a higher propane composition resulted in way more improvement in terms of the bright white spots. This phenomenon indicates that the solvent injection composition presented better solvent propagation and mixing or "cleaning" effect. A reasonable and possible scientific explanation regarding this phenomenon is the K-value (solubility in the heavy-oil/bitumen) of this gas. Propane gas has a much lower K-value compared to the K-value encompassed by methane gas in the heavy-oil/bitumen (at comparable pressure) at the given temperature post-SAGD (Deng 2005; Azinfar et al., 2018). In other words, when the heavier solvent is present, the total solubility of the injected solvent(s) will

increase. This behavior will potentially present a better improvement in viscosity reduction, heavy-oil mobilization, and areal displacement efficiency. Nevertheless, in a lower propane composition, almost no substantial improvement in areal sweep efficiency was perceived. A possible indication of this phenomenon is most of the gaseous solvent(s) moved toward and accumulated at the upper part of the model. Only a portion of the heavier solvent (e.g., propane) was mixed with heavy-oil.

At the same solvent composition (**Figure 75d**), both solvents (methane and propane) traveled toward the upper region of the model. Due to the particular characteristics of each solvent type (K-value) -much less soluble for methane and more soluble for propane in heavy-oil- there was a possibility of no interaction between methane gas and the oleic phase. This presumption is strengthened by the analytical and numerical study of non-condensable gas (e.g., methane) performed by Sharma et al. (2012), concluding that the methane gas prefers to accumulate at the steam chamber zone; thus, inhibiting the heat transfer to the oleic phase and leading to low oil recovery. Even though methane gas (as a non-condensable solvent) has been mentioned to present advantageous results on SAGD application (Butler et al. 1999; Jiang et al. 2000), the result was predominantly due to the impact of the gas-insulation and gas "push" mechanisms. The methane gas only presents a "pushing" effect rather than mixing with the oleic phase and stays at the top of the reservoir. Oppositely, a few portions of the heavier solvent, like propane, tend to deliver a dissolution/mixing effect; therefore, the bright orange spots were observed and produced along with the oleic phase as a result of the mixing/dissolution process. The formation of the bright orange spots at the top right corner of the Hele-Shaw model also confirms the gas "push" mechanism presented by the methane gas and the dissolution/mixing mechanism presented by the propane gas. These mechanisms are also corroborated by our GC test, resulting in a lower percentage unit of methane, and a higher percentage unit of propane was detected. In other words, more propane and only a small amount of methane could be retrieved/recovered.

For a heavier solvent injection like heptane, according to the experimental results, it is very clear that the performance of heptane injection exceeds the other gaseous solvent like propane, even though it is combined with much lighter gaseous solvent (methane) for enriched solvents. Thermodynamically, heptane encompasses much higher solubility (much lower K-value) compared to propane gas. Therefore, heptane would easily mix/dissolve with heavy-oil—

promoting greater viscosity reduction and areal sweep efficiency. The significant contribution of heptane lessens as the composition changes, as validated by this experimental study.

In conclusion, by diversifying the solvent types and compositions, a pure propane or heptane injection is much preferable. They are able to provide a more optimal process (maximum recovery and maximum solvent recovery) for post-SAGD application at the given pressure and temperature, as heat transfer is still needed in the presence of methane gas.

### 5.5.2 Porous Media Visualization

A porous media experimental study could favorably represent the dynamics of phase distribution in reservoirs. Throughout this study, we perceived consistent results presenting the displacement instability which occurred in the pore spaces, particularly at the beginning of SAGD (**Figure 77a**). This evidence explains that the heat transfer between the steam phase and the oleic phase still occurred as well as the rapid heat losses. At the end of the SAGD process, extensive ROS was still observed in pore spaces (**Figure 78**). The possible explanation of this phenomenon is the significant contribution of the unfavorable wettability alteration toward a more oil-wet state due to the phase change, as validated by our previous research (Pratama and Babadagli 2020a, b, c). This unfavorable wettability alteration leads to higher capillary pressure. Due to the condition of a higher capillary force, the viscous force was not able to mobilize the entirety of the oleic phase from the pore spaces; therefore, further triggering the ROS formation in the porous media.

In the case of gaseous solvent(s) injection, the same principle of solubility (K-values) is applied. At the same solvent compositions, the solvent(s) injection performance was perceived to be less effective. One possible explanation for this phenomenon is the displacement contribution of each solvent gas in the enriched gas injection. Due to the higher K-value, methane gas has low solubility in the oleic phase; thus, lowering the total solubility of the solvent mixture and causing this solvent gas not to mix/dissolve in the oleic phase in all proportions. Therefore, methane gas accumulated at the upper part of the porous media model and presented a more immiscible displacement of the oleic phase. On the other hand, the mobilization of a small portion of the ROS was possible due to the contribution of propane. As a consequence of encompassing much higher solubility in the oleic phase, propane could dissolve in the oleic phase and deliver a more miscible displacement.

More essentially, **Figure 84** could provide an explanation honoring ROS reduction, displacement/sweep improvement, oil recovery, and solvent recovery. We discovered that there was a column (indicated by the arrow)—containing solvent(s) gas and residual oil—present in the porous media model after applying solvent(s) injection. It is very clear that the column height in the porous media model changes as the solvent(s) composition changes. As exhibited by the experimental results, a pure propane injection undoubtedly presents the most extensive column height compared to all studied cases. This phenomenon occurred due to the favorable dissolution/mixing process presented by the pure propane (lower K-value and higher solubility). As the propane was injected and propagated, the extensive amount of residual/unswept oil was able to be diminished. Furthermore, due to the gravity force, it moved down, accumulated at the lower region of the porous media model, and then recovered throughout the production point. At this stage, the production rate was perceived to be high, leading to maximum oil recovery. In the case of lower propane composition and with the presence of methane gas, due to the lower total solubility of the solvent mixture, the displacement/sweep efficiency became less effective; thus, yielding to less auspicious recovery and affecting the porous media model to comprise shorter column height.

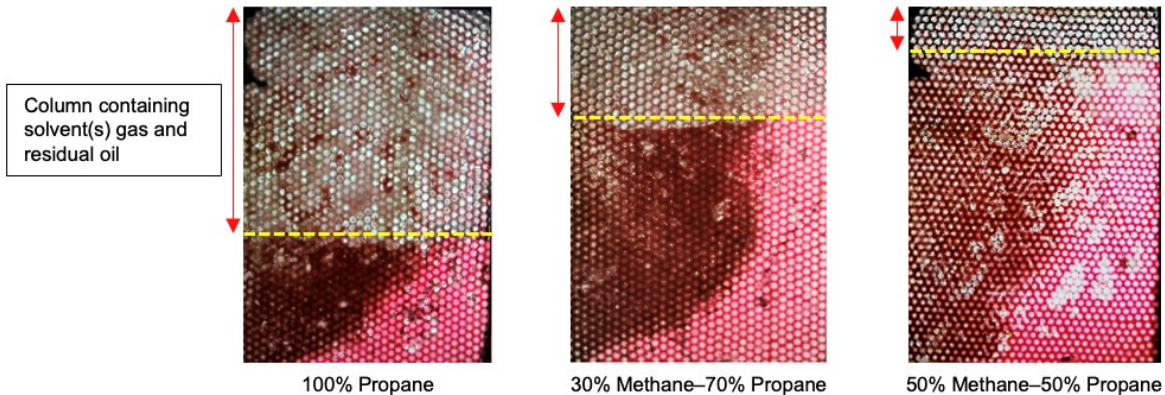


**Figure 84—Columns containing solvent(s) gas and residual oil (relative to post-SAGD condition) observed in porous media model at the end of solvent(s) injection.**

The presence of solvent(s) gas in the column could be scientifically explained by **Table 14** and **Figure 80**. The GC test results (**Table 14**) and recovery plots (**Figure 80**) show that only a small

amount of solvent(s) gas (e.g., methane, propane) could be retrieved along with the oleic phase. This evidence validates that most of the injected solvent(s)—by gravity—moved and accumulated at the top region of the porous media. Moreover, **Table 14** and **Figure 80** highlight the changes in oil recovery and solvent recovery performances in various solvent(s) compositions. Pure propane (100% composition) injection delivered the most favorable oil recovery and solvent recovery, resulting in a more extensive column height. As the solvent(s) composition changes by adding methane, the amount of oil recovery and solvent recovery becomes less, yielding a shorter column height.

Similar to the lighter solvents' case (methane and propane), the total solvent solubility plays an essential role when it comes to heptane injection. As heptane comprises high solvent solubility, a mixing/dissolution process would be much easier and favorable—even in the presence of capillary force—compared to the other tested solvents. This explanation aligns with the results obtained from our experimental study, presenting that the ROS could be much more favorably mobilized due to the contribution of the solvent (heptane). The same principle is applied to the case of heptane and/or methane–heptane injections when it comes to the column height observed in the porous media model. **Figures 77e–g** also depicts the observation of column height—containing heptane in the vapor phase (and methane in methane–heptane mixture), condensed heptane, and residual oil—relative to the post-SAGD condition for different types of solvent(s) injection, as well as the solvent(s) composition. **Table 14** and **Figure 81** corroborate the existence of heptane and/or methane (in the column) inside the porous media after solvent(s) injection. Most of the solvent(s) portion accumulated in the model. These data and plots also explain that more auspicious oil recovery and solvent(s) recovery were observed in the case of pure heptane injection—resulting in a larger column height—whereas the solvent(s) injection case with less heptane composition resulted in much lower oil recovery and solvent(s) recovery; thus, yielding to a shorter column height. In other words, in the case of heptane and/or methane–heptane injection, the column height is also proportional to the oil recovery and solvent(s) recovery.

Consistent with the experimental results, implementing a propane or heptane injection with 100% composition would be beneficial for post-SAGD applications in improving displacement/sweep efficiency, oil recovery, and solvent recovery at the given pressure and temperature.

### 5.5.3 Future Potential Improvement for Post/Mature SAGD

The coverage of this research is the injection of pure solvents (without any steam) instead of as an additive to steam. From this perspective, the study can be considered as original (or even novel) since no study has been published in the area of pure solvent(s) injection to replace steam in SAGD operations as a mid- or late-stage and environmentally friendly application.

This methodology can be applied in the mid or even long-run (e.g., mature stage, wind-down stage) SAGD operations, meaning that, according to this study, these solvents are able to potentially replace the steam injection (not like steam additives) in SAGD operations to auspiciously improve SAGD operational efficiency, substantially reduce SOR, diminish residual oil saturation post-SAGD, improve bitumen recovery, attain sustainable SAGD operation, and eventually achieve zero GHG emissions. This was shown qualitatively (visually) and quantitatively that makes this research original (and even novel).

Unlike the steam additives or other methods like expanding solvent-SAGD (ES-SAGD), solvent aided process (SAP), solvent assisted SAGD (SA-SAGD), and hybrid solvent process, from this point of view, the potential of these hydrocarbon solvent(s) in alternating the steam injection for SAGD applications (covered in this study) has never been previously researched or published. In comparison to the vapor extraction (VAPEX), both methods apply vaporized solvent(s) to recover the heavy-oil/bitumen under the influence of the gravity force. However, the substantial difference between VAPEX and this study is at the time of applying the solvent(s) injection. VAPEX applies the solvent(s) injection at the early/beginning of the production stage—reflected by the development of the solvent chamber—whereas this study applied the solvent(s) injection at the late-production stage (post-SAGD) or even mid-production stage. The vapor phase of the injected solvent(s) will move toward the upper part of the reservoir and replace the steam chamber—eventually developing solvent chamber. Moreover, the methodology applied in this study is more advantageous than VAPEX. It allows the practitioners to employ broader range of solvent types (from gas to liquid) since the heat energy (from the steam injection) is preserved in the reservoir and as long as the vaporization temperature of the solvent(s) is close to the steam temperature. In comparison with this study, the selection of the solvent(s) for VAPEX application is limited to the gaseous type of solvents (e.g., propane, butane) since this recovery method only relies on the original reservoir temperature. Additionally, it has also been reported that VAPEX has the most

common drawback which is low production (James et al. (2007); Esmaeili and Ayoub (2015); Zhang et al. (2018); Moussa (2019))—presenting 20–60% of the total heavy-oil/bitumen recovery (Das (2018); Pourabdollah et al. (2018); Moussa (2019)). Meanwhile, this study was able to prove that up to 85% of the total recovery could be attained after implementing the proposed methodology.

A comparison between these two methods reflects that the proposed methodology in this study is still novel and presents more advantages for recovery improvement. In other words, this proposed methodology could present a great potential for the future of heavy-oil/bitumen recovery—particularly post-SAGD applications. The valuable findings of this study will deliver advantageous recommendations for high-efficiency and low-emission SAGD operations, particularly at the late stage as post- or mature SAGD applications.

## **5.6 Research Limitations**

The ultimate intention of this study is to evaluate the potency of a wide range of hydrocarbon solvents (e.g., methane, propane, heptane) specifically for post-SAGD applications. The investigation was performed, and the recommendations were gained based on—and limited to—the solvent–to–heavy-oil interactions (thermodynamics, physicochemical) and phase distribution phenomena in porous media at the given conditions (pressure and temperature) through Hele-Shaw and porous media visualizations. However, some field application realizations, such as solvent recovery, complex solvent–fluid phase behavior, ROS at the steam chamber, steam channeling, and temperature post-steam injection—that occurred in the reservoir—might not be covered due to the 2-D nature and model volume/size (a very small solvent injection volume), relatively lower pressure and temperature conditions, much smaller steam and solvent(s) injections volume, and rapid heat losses even if the phase representations (propane in the gas form, heptane in the liquid form at reservoir conditions) have been captured. In addition, the detailed discussion of mass transfer and the utilization of additional instruments (e.g., mass flow controller, additional sensor) were not covered since the gaseous solvent(s) injection volume was very small; therefore, gas compressibility effect and injected solvent(s) volume deviation could be negligible.

Hence, for larger scale experiments, such as core flood experiments (assisted with mass flow controller and additional sensor) and numerical reservoir simulation, are still needed to accommodate the reservoir performance analysis for post-SAGD applications and more reliable solvent injection control—particularly for gaseous solvent(s). This study will play a leading role in designing this kind of succeeding research studies and even practical field-scale applications.

## **5.7 Conclusions**

The 2D visual experiments have been performed and presented in this paper. Both visual experiments presented consistent trends. By way of explanation, both experimental methodology and results could be validated. Furthermore, by performing a series of experiments on solvents (pure and enriched solvents) as low GHG and high-efficiency tertiary recovery options, the potency of solvents in post-SAGD applications was investigated. The conclusions can be listed as follow:

### **5.7.1 Hele-Shaw Experiments:**

1. Propane and heptane injection in 100% composition presented the most favorable steam areal displacement efficiency improvement even though the temperature post-SAGD declined substantially due to severe heat losses. However, heptane performance in 100% composition exceeded the performance of other tested solvents.
2. The enriched gaseous solvent (30% methane–70% propane or 30% methane–70% heptane) could potentially be another alternative for post-SAGD application as the solvent injection presented promising displacement efficiency. Nevertheless, the economic analysis should also be considered in determining the most suitable solvent type and composition for post-SAGD application.
3. Despite the declining temperature of the system post-SAGD, a mixing/dissolution process of the solvent in the heavy-oil could still be observed and was successful, which could

potentially reduce the heavy-oil viscosity—promoting favorable mobilization of the oleic phase post-SAGD.

4. Injecting the solvent(s)—particularly with heavier solvent—for post-SAGD application could potentially trigger the asphaltene precipitation in the reservoirs.

### **5.7.2 Porous Media Experiments:**

1. Heptane with 100% injection composition presented the most promising results in terms of phase distribution improvement, residual oil mobilization, and oil displacement efficiency post-SAGD. However, methane addition could be an alternative from a cost-effectiveness point of view.
2. Throughout the gas and liquid GC analyses for each collected sample, this research is able to prove that the solvents recovery at the given post-SAGD temperature is possible, particularly for propane and heptane, as the recovery of these solvents is proportional to their K-value/solubility in the heavy-oil/bitumen.
3. Both propane and heptane in pure composition exhibited favorable performance among the studied cases. They both presented the utmost recovery performance. However, in terms of solvent recovery, pure propane injection was not able to deliver favorable solvent recovery at given pressure and temperature. The most desirable solvent recovery was obtained from a pure heptane injection case.
4. At first sight, the addition of methane might present a more economical case for post-SAGD applications. However, the presence of methane could not deliver favorable additional recovery and solvent recovery improvement. The recovery of the injected methane in both heavier and lighter solvent cases was not feasibly possible.
5. In the case of propane injection, instead of the solvent(s) composition, phase behavior (K-value/solubility) plays an essential role as a liquid type of solvent presents much more favorable solvent(s) recovery. Therefore, for propane injection application, it is recommended to employ pressurized solvent injection as the temperature of the system will not be changed during the process.

6. In practice, heavier/liquid-type solvents (heptane in our particular case) present more favorable results (displacement/areal sweep efficiency, oil recovery, solvent recovery) compared to lighter solvent cases (propane in our particular case).
7. Even though valuable and beneficial information honoring the post-SAGD improvement efficiency was gained through this research, the experimental studies utilizing core flood are still needed to accommodate the reservoir performance analysis post-SAGD.

## **Chapter 6: An Experimental and Visual Investigation on Energy-Efficient Post-SAGD Recovery Improvement Alternatives**

This chapter of thesis is a modified version of a research paper. The journal version of this research paper has been submitted to the scientific journal for peer-review and publication.

## 6.1 Preface

Our recent core scale visualization studies proved that the utilization of hydrocarbon solvents alternating steam injection deployment is very auspicious for post-SAGD optimization. This practice can also promote more sustainable hydrocarbon production and higher economic viability while reducing greenhouse gas emissions. Despite the promising results, follow-up studies (e.g., non-hydrocarbon solvents, core flooding tests) are still required to attain more robust comparisons and recommendations. This paper discusses the results of core flooding experiments, supported by visual laboratory tests, using selected hydrocarbon and non-hydrocarbon solvents for post-SAGD applications.

A 295,000 cP (at 25°C and atmospheric pressure) Canadian heavy crude sample was used in the core flooding experiments. In alternating steam injection for post-SAGD applications, a hydrocarbon (heptane) and a non-hydrocarbon (CO<sub>2</sub> gas) solvent were applied to steam-displaced models. The core flood model was employed to represent the reservoir condition and its dynamics. All experiments were conducted at pressure and temperature conditions similar to existing matured SAGD reservoirs to further assess the performance of the studied solvent to displacement efficiency and their compatibility with existing condensed steam.

It was observed that non-hydrocarbon, non-condensable solvents, and liquid hydrocarbon solvents could substantially improve incremental heavy-oil/bitumen recovery by up to 50%. More essentially, aggressive steam utilization could be terminated entirely, and energy efficiency could be significantly improved by nearly 100% by applying this technique. For a more efficient process, solvent recovery potential was also evaluated.

**Keywords:** Steam injection, mature SAGD, non-condensable gas, low GHG emission, high efficiency.

## 6.2 Introduction

The concept of steam-assisted gravity drainage (SAGD) was first introduced by Butler (1985) with the principal purpose of recovering immobile heavy-oil/bitumen. Two years after its conception, this proposed recovery technique was funded by the Alberta Oil Sands Technology and Research Authority (AOSTRA) and further tested at the designated testing facility entitled Underground Testing Facility (UTF) located in Fort McMurray. The effort ended with the realization of the bitumen recovery beyond 60%, surpassing the original forecasted recovery of up to 45% (Edmunds and Gittins 1993; Collins 1994). Since the successful establishment of the first pilot SAGD, more than 20 SAGD projects have rapidly emerged in Canada for the past three decades. At present, the majority (over 85%) of operating SAGD projects are in Athabasca, and the remaining is in Cold Lake areas, contributing to nearly 1.4 million bbl/day or 25% of Canada's total oil production (Pratama and Babadagli 2023a, b).

SAGD has been substantiated to be technically and commercially effective in heavy-oil/bitumen recovery—specifically in Canada. In a more technical fashion, SAGD is able to provide favorable heat energy and generate steam chamber growth in the heavy-oil/bitumen reservoirs, which could potentially recuperate up to 60% of total oil-in-place. However, the complexity of the SAGD process and the performance controlling factors (e.g., reservoir geology, condensate flow, bottom water, well spacing, pad density, steam injection pressure) could hinder the utmost performance of this technique (Ali 1997; Pratama and Babadagli 2023a, b). Some SAGD projects exhibit a limited capacity, attaining a recovery factor below 20% despite their prolonged operational span, functioning for decades. Presently, the steam-to-oil ratio (SOR) prevalent in the majority of SAGD projects fluctuates within the range of 2 to 4 bbl steam/bbl oil. However, certain projects persist in encountering SOR values exceeding 4 bbl/bbl due to the implementation of intensive steam injection (Pratama and Babadagli 2023a, b). The aggressive use of steam injection, in fact, presents a significant direct impact on the environment—further intensifying greenhouse gas (GHG) emission with a 1.9% annual emission growth rate contribution globally (Energy Institute 2023; Lee and Babadagli 2021) and projected to escalate by 100% in a decade with current process and base business. This necessitates the exploration of various techniques aimed at the ecologically sustainable depletion of the remaining oil reserves.

The forthcoming prospect of SAGD is contingent upon the advancement of novel methodologies geared towards the mitigation of GHG emissions arising from steam generation procedures. Concurrently, there is a need to augment ultimate recovery rates in the post-SAGD phase. The effort includes involving solvents in the SAGD process, which can potentially reduce GHG emissions by 90% (CERI 2017; Lee and Babadagli 2021). In a more classical study centered upon the utilization of a solvent, specifically naphtha, in conjunction with steam injection, the investigation conducted by Ali and Abad (1976) yielded the finding that incremental recovery of bitumen surpassed 20%. This outcome was attributed to the phenomenon of solvent evaporation and the subsequent dissolution mechanism that transpired between the solvent and oleic phase during the steam injection process. The efficacy of solvent-based approaches for the extraction of heavy oil/bitumen was further substantiated in the work of Das and Butler (1998). Their analysis unveiled that upon injecting vapor-phase solvents (e.g., propane, butane) into the systems, two primary mechanisms were observed: first, the diffusion of the solvent into the heavy oil, and second, the dissolution mechanism contributing to the reduction of oil viscosity and thus facilitating the mobilization of the oleic phase.

In more modern SAGD applications, approximately 80% of SAGD operations in Canada have integrated the practice of introducing non-condensable gases (NCGs), primarily methane injection. Nevertheless, these incorporations have failed to yield a substantial enhancement in overall performance, encompassing metrics like production rates and the cumulative steam-to-oil ratio (SOR). The success rate of this approach within SAGD operations is modest, typically ranging from 5% to 10% (Pratama and Babadagli 2023a, b). The discouraging results associated with NCG co-injection have been substantiated by prior research conducted by Butler et al. (1999) and Jiang et al. (2000), which concurred that although NCG co-injection may yield certain advantages, these benefits primarily stem from gas insulation and the "gas push" mechanisms. In essence, methane gas predominantly exerts a "pushing effect" rather than inducing mixing or dissolution, tending to migrate toward the upper stratum of the reservoir. Another potential method to enhance the efficiency of SAGD operations for recovery involves the injection of condensable gases (CGs), with propane being a commonly used option. Propane, at SAGD operating temperatures, exhibits a notably low K-value (Deng 2005), which implies greater propane solubility in heavy oil/bitumen. This enhances the process of mixing and dissolution between the solvent and heavy oil/bitumen, ultimately resulting in a favorable reduction in viscosity within the reservoir. This reduction in

viscosity aids in increasing incremental recovery, facilitated by the force of gravity. In the area of liquid solvent injection, Nasr et al. (2003) initially introduced and developed the concept of Expanding Solvent–SAGD (ES-SAGD), which integrates steam and low-concentration hydrocarbon at steam temperature. The success of this technique hinges on the choice of the hydrocarbon. Hexane was proposed as the most suitable solvent in this context, mainly because it has a vaporization temperature close to that of injected steam. This alignment allows both steam and solvent to move simultaneously towards the steam chamber, effectively mixing with heavy oil/bitumen and reducing viscosity. The first implementation of ES-SAGD took place during the Long Lake Pilot in 2005–2006, resulting in a 6% increase in oil production (Orr 2009). Although the utilization of these types of solvents in SAGD applications has been claimed to present promising results, these techniques have a limited impact on reducing greenhouse gas (GHG) emissions since steam remains the primary component of the injected material.

This paper is a continuation of our recent work concluding that the use of solvents could interchange steam in SAGD operations as an environmentally friendly approach in the mid- or late-stages of SAGD operations (Pratama and Babadagli 2023c, d). The focus of this study is on laboratory scale 2-D visual experiments (Hele-Shaw and glass bead models) to comprehend the solvent-oil interaction and phase behavior as well as core scale experimentation to evaluate the mid-stage and late-stage SAGD process using solvents to gain more vigorous conclusions and recommendations toward efficient and environmentally friendly post-SAGD operations. These smaller-scale-to-larger-scale experimental studies are essential to cross-validate the overall solvent injection performance for post-SAGD applications. The study involved hydrocarbon solvent (selected based on our previous work) and non-hydrocarbon solvent injected at the mid- and late-stage of the SAGD process without utilizing any steam injection. The insights from this research will provide valuable guidance for achieving high-efficiency and environmentally friendly SAGD operations, especially in the advanced stages, such as post-SAGD or when the process has matured.

## **6.3 Problem Statement and Proposed Solution**

### **6.3.1 Problem Statement**

In essence, the mature SAGD holds significant importance and demands heightened attention, especially since many SAGD fields have experienced declining production and low recovery during this phase (Pratama and Babadagli 2023a, b). Alongside other challenges faced by SAGD fields, such as reservoir geology, condensate flow, bottom water, well spacing, pad density, steam injection pressure, adverse alterations in wettability due to phase changes at high temperatures have been a major factor affecting heavy-oil recovery and SAGD process efficiency. This leads to an increase in the steam-to-oil ratio (SOR) and directly contributes to a rise in GHG emissions.

Technical hurdles and concerns regarding GHG emissions from the steam-based recovery process have generated negative perceptions, both among the public and within the technical community. These perceptions drive the quest for new applications that make the most of existing investments, such as field operations, production facilities, and capital expenditures.

A recent trend in SAGD operations is to partially or completely reduce steam usage, aiming to lower operational costs and minimize environmental impacts. Chemical additives and solvents are being considered as potential alternatives to achieve these objectives. However, the current effort still requires steam as a co-injection process. In addition to the physicochemical aspects of the process, the thermodynamic behavior of hydrocarbon solvents, influenced by pressure and temperature, must also be considered, and understood.

### **6.3.2 Proposed Solution**

The primary aim of this research is to conduct a thorough assessment of two solvents (heptane and CO<sub>2</sub>) as high-efficiency post-SAGD methods. This evaluation seeks to reduce residual oil and lower the steam-to-oil ratio (SOR). Furthermore, incorporating solvents into the SAGD process has the potential to significantly reduce GHG emissions, with the potential for up to an 80% reduction (CERI 2020). Hence, given the anticipated increase in energy-intensive in-situ heavy-oil/bitumen recovery methods and the growing global demand for reducing GHG emissions in

pursuit of more sustainable fossil fuel production and addressing environmental concerns, this research endeavors to identify a practical solution to address these issues.

To arrive at more robust conclusions and recommendations, laboratory-based experiments, such as core flooding and core scale visual tests, were conducted to **mimic SAGD reservoir conditions** and assess the performance of selected solvents when applied at the mid- and late-stage of the SAGD process. The focus was on accommodating the SAGD process and quantitatively examining how potential solvents interacted with the complex phase (oil, water, steam, solvent) in the system and their recovery performance. To further evaluate the suitability of solvents for post-SAGD applications, hydrocarbon, and non-hydrocarbon solvents were evaluated. This involved a liquid type of hydrocarbon solvent (e.g., heptane)—encompassing vaporization temperature close to steam temperature—and a non-condensable–non-hydrocarbon solvent (e.g., CO<sub>2</sub> gas), all tested at given post-SAGD pressure and temperature to provide more definitive recommendations for post-SAGD applications.

By introducing solvents in the post-SAGD stage, we have confidence in achieving several post-SAGD goals, including reducing residual oil saturation, improving recovery mechanisms, lowering the SOR, enhancing energy efficiency, and promoting a more sustainable approach to heavy-oil/bitumen production. This research focuses on introducing pure solvents as a replacement for steam injection in SAGD operations rather than using them as additives to steam. From this perspective, this study can be regarded as novel, as there have been no previous publications on the use of pure solvents in mid- or late-stage SAGD operations as an environmentally friendly alternative. The methodology presented here has the potential to be applied in the medium to long term, such as in the mature or wind-down stages of SAGD operations. These solvents could potentially replace steam injection (unlike steam additives) in SAGD operations, leading to significant enhancements in SAGD operational efficiency, a substantial reduction in SOR, decreased residual oil saturation post-SAGD, improved bitumen recovery, the achievement of sustainable SAGD operations, and ultimately the goal of zero GHG emissions. These findings were demonstrated both qualitatively and quantitatively, making this research innovative and original.

In contrast to methods like steam additives, expanding solvent-SAGD (ES-SAGD), solvent-aided process (SAP), solvent-assisted SAGD (SA-SAGD), and hybrid solvent process, the potential of

using hydrocarbon solvents to replace steam injection in SAGD applications, as explored in this study, has never been previously investigated or published. It can be realized that when compared to the vapor extraction (VAPEX) recovery method, both approaches utilize vaporized solvents for heavy-oil/bitumen recovery under gravity's influence. Nonetheless, a significant distinction between VAPEX and the approach discussed in this study lies in the timing of solvent injection. VAPEX introduces solvents at the early stages of production, characterized by the development of a solvent chamber. In contrast, this study introduced solvents at later production stages (post-SAGD) or even mid-production stages. The vapor phase of the injected solvents migrates towards the upper part of the reservoir, displacing the steam chamber and eventually creating a solvent chamber. Furthermore, the technique employed in this study offers distinct benefits over VAPEX. The utilization of a broader range of solvent types is possible with this technique, spanning from gaseous to liquid, as long as the solvent's vaporization temperature is close to that of steam. Conversely, VAPEX is limited to gaseous solvents, such as propane and butane, due to its reliance on the SAGD reservoir's initial temperature. In addition, VAPEX is associated with common downsides, namely low production, as reported in the previous studies (James et al. 2007; Esmaili and Ayoub 2015; Zhang et al. 2018; Moussa 2019), which typically results in 20–60% of the total recovery (Das 2018; Pourabdollah et al. 2018; Moussa 2019). Concurrently, this study has demonstrated that the proposed technique could achieve up to 85% of the total recovery.

A comparative analysis of these two approaches accentuates the innovative nature of the methodology introduced in this research and its superior attributes in terms of enhancing recovery. In essence, this novel methodology has the potential to significantly shape the future of heavy-oil/bitumen recovery, particularly in the context of post-SAGD applications.

## **6.4 Material and Experimental Setups**

### **6.4.1 Oleic Phase**

Heavy-oil sourced from Western Alberta, Canada, with a viscosity of 295,000 cP at 25°C, was employed for core flooding experiments. **Figure 85a** and **Table 15** provide additional fluid

properties pertinent to the oleic phase utilized in this study. Furthermore, a Saturates, Aromatics, Resins, and Asphaltenes (SARA) test was conducted on the heavy oil to determine its composition, revealing the following percentages: 25.4% saturates, 15.7% aromatics, 35.8% resins, and 23.1% asphaltenes (**Figure 85b**).

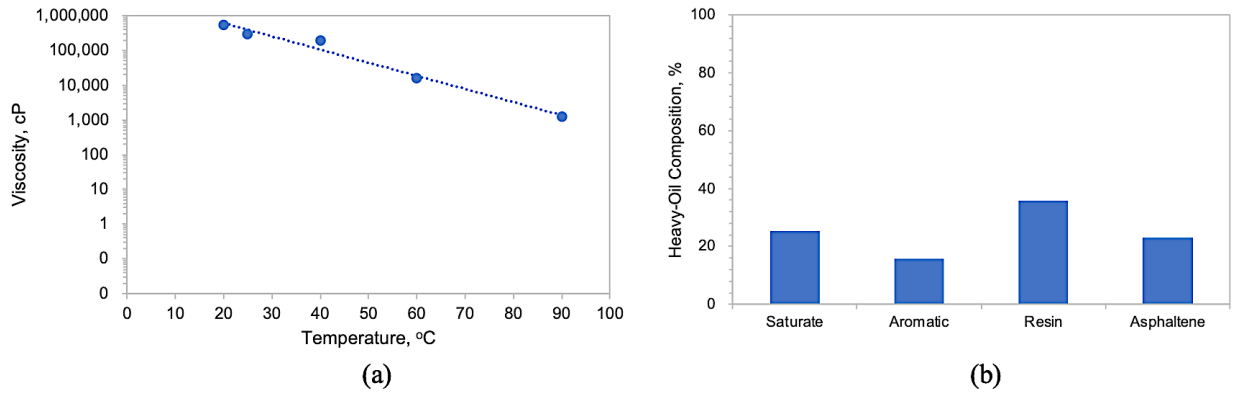


**Figure 85—Heavy-oil properties: (a) oil viscosity measurement, and (b) SARA analysis. SARA = saturate, aromatic, resin, asphaltene.**

**Table 15—Fluid properties of the utilized heavy-oil.**

Oil Type	Viscosity (cP)	Density (g/cm <sup>3</sup> )	API gravity	Temperature
Heavy-Oil 1	295,000	0.9985	9.79	25°C
Heavy-Oil 2	46,140	0.9916	11.20	25°C
Mineral Oil	111,600	0.9963	10.53	25°C

### 6.4.2 Studied Solvents

In this study, we conducted experiments using a liquid type of hydrocarbon solvent and non-hydrocarbon solvent, according to our recent study, to further assess their potential for enhancing post-SAGD reservoirs:

- pure heptane with 100% composition,
- pure CO<sub>2</sub> gas with 100% composition.

A denser hydrocarbon solvent, such as heptane, may offer improved "cleaning effects." Given its boiling temperature of 98.4°C (with vaporization pressure of 46 mmHg or 0.06 atm at 25°C), heptane boils at the same temperature as the injected steam (even thermodynamically vaporizes at room temperature), making it recoverable alongside heavy-oil/bitumen due to the influence of gravity. A favorable improvement in post-SAGD application has been proven through our recent visualization experiments, concluding that the ultimate recovery could be realized by up to 85% after heptane injection (Pratama and Babadagli 2023c, d). A gaseous non-hydrocarbon solvent, like CO<sub>2</sub>, offers potential advantages due to its ability to ascend naturally through the reservoir driven by gravity. As a consequence of this inherent behavior, upon injection into the reservoir, such a solvent will migrate towards the upper region of the reservoir, potentially further reducing residual oil saturation (ROS) in proximity to the steam chamber zone. Moreover, the potential use of non-hydrocarbon–non-condensable (e.g., CO<sub>2</sub> gas) injection in the area of SAGD applications has also been previously studied, presenting up to 10% of incremental recovery (Wang et al. 2018; Jaimes et al. 2019; Song et al. 2020; Gong et al. 2022). The combination of these two types of solvents with a selected solvent composition could potentially lead to a more optimized recovery process.

### **6.4.3 Solvents Injection Procedure**

The pre-selected solvent(s) were introduced into the pump for subsequent post-SAGD injection, with no concurrent steam injection. The injection rate of the solvent(s) was meticulously regulated using a Teledyne® ISCO piston-driven pump with a digital flow controller. This pump is capable of handling extremely low injection rates, a necessity for our research, which utilized a rate of 0.1 cc/min. Notably, this pump is widely employed in research and laboratory experiments, particularly for smaller-scale investigations, as evidenced by prior studies (Zhao et al. 2004; Mazumder et al. 2008; Sun et al. 2018; Min et al. 2020; Mohammed et al. 2020; Liang et al. 2023). Consequently, the methodology adopted in this research aligns well with the primary objectives and accurately represents the injection of solvent(s) for SAGD applications.

#### 6.4.4 Hele-Shaw and Porous Media Visualization

Hele-Shaw and porous media visualization experiments were performed as cross-validation with the SAGD core flooding experiments. Hele-Shaw serves as a practical approach for visualizing interactions between the steam or solvent(s) phase and oleic phase under SAGD conditions in a two-dimensional context and is a simpler model compared to the porous media model. The Hele-Shaw cell was constructed using two plexiglass plates separated by a rubber sleeve, creating a rectangular structure measuring 10 cm in width and 15 cm in length. The gap between the two plexiglass plates was precisely set at 0.5 mm, and the entire assembly was secured within two steel frames (**Figure 86**) saturated with heavy-oil from western Alberta with a viscosity of 46,000 cP (**Table 15**). The Hele-Shaw cell can be effectively employed to delve into the macroscopic dynamics of recovery and displacement mechanisms, as well as phase behavior, particularly phenomena like viscous fingering due to steam condensation while considering variations in pressure and temperature. Moreover, the Hele-Shaw cell is valuable for tracking steam propagation and delineating the interface between steam/condensate and heavy-oil.

Consecutively, phase distribution analysis to enhance post-SAGD efficiency was carried out using a porous media model, which proves to be a highly valuable and efficient approach for studying how phases distribute within pore spaces, particularly in the presence of capillary interactions. Our porous media model was assembled with a 3-mm packed silica glass bead and positioned between two 9-mm acrylic plates. This porous media assembly was then mounted and pressurized within a steel frame and placed inside a sealed, vacuumed chamber to minimize heat losses during experiments (**Figure 87**). A heavy-mineral oil (with a viscosity of 111,600 cP) was used in the experiments due to its transparent nature.

Both Hele-Shaw and porous media models were initially saturated with heavy oil to simulate the initial condition. The superheated steam, reaching temperatures of up to 240°C with nearly 100% steam quality, was produced by passing water through a high-temperature oven/steam generator. This process was regulated by a Teledyne® ISCO syringe-driven pump, ensuring a constant flow rate. The steam was introduced into the models through low-pressure injection to establish the initial base/reference scenario. To simulate both the tertiary recovery process and improvements in energy efficiency, we discontinued steam injection entirely and began continuous injection of pre-selected solvent(s). Throughout this transition, we closely monitored the areal sweep

efficiency. This allowed us to conduct a more in-depth analysis of steam propagation and condensation, investigate the phenomenon of viscous fingering, and evaluate the contribution of various types of solvents to the recovery process.

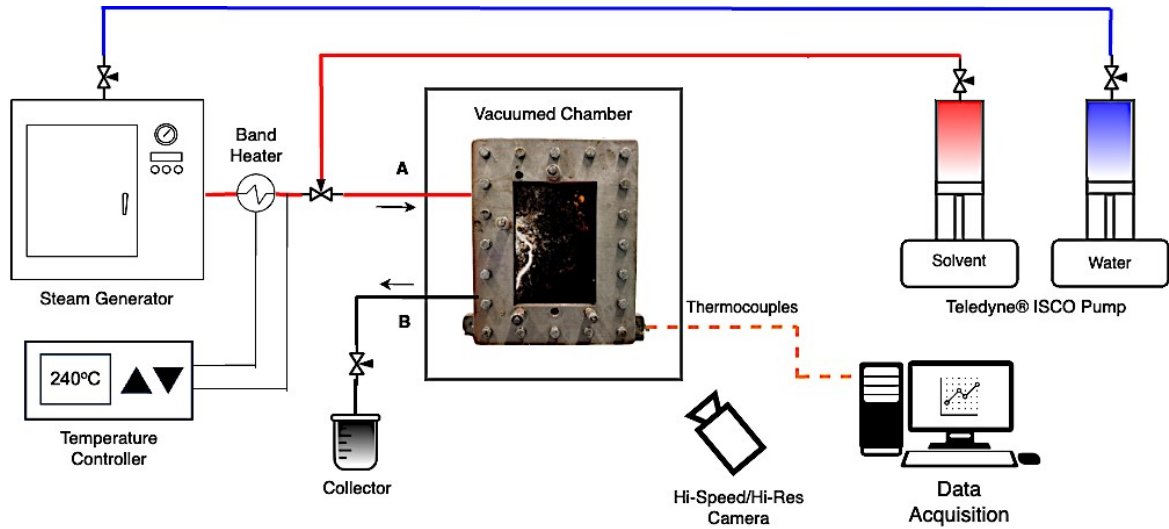


**Figure 86—Hele-Shaw cell experimental setup in investigating fluid-to-fluid interaction and displacement mechanism under post-SAGD conditions. A = injection, and B = production.**

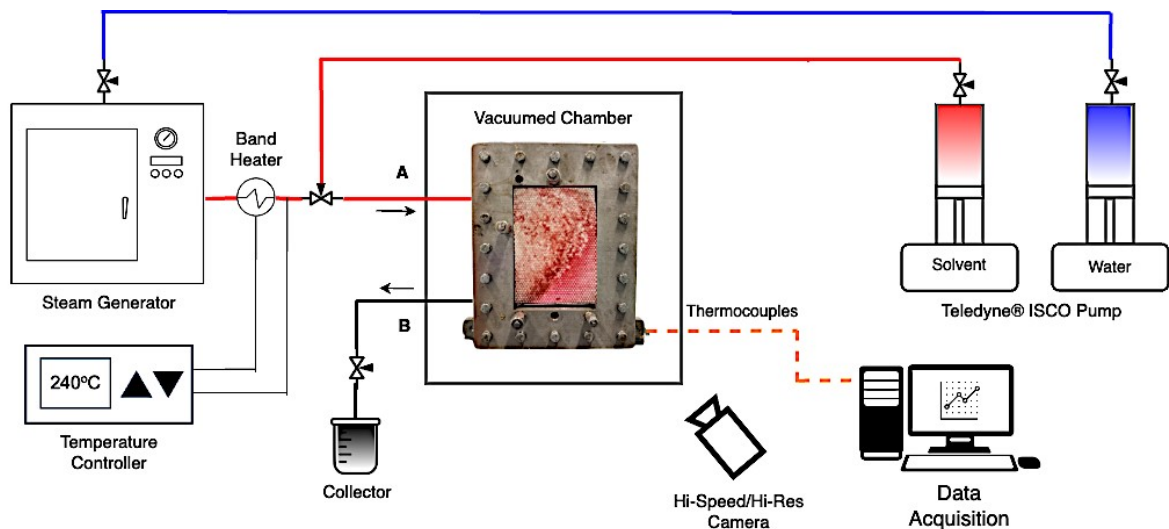


**Figure 87—Porous media experimental setup in investigating phase distribution behavior and displacement mechanism under post-SAGD conditions. A = injection, and B = production.**

### 6.4.5 Core Flooding Experiments

A dynamic core flooding experiment was performed to comprehensively assess and analyze the oil recovery performance and mechanisms associated with pre-selected solvent(s). In this investigation, we employed a sand pack to simulate SAGD reservoirs containing heavy-oil/bitumen. Initially, the sand pack was prepared by using sand that had been sieved with screens to achieve a particle size ranging from 250 to 500  $\mu\text{m}$ . In replicating the saturation history of sandstone reservoirs, the sand pack was saturated by mixing it with crude oil that had been prepared previously. Following this, the oil sands were loaded into the core holder, and manual compressions were applied to ensure uniformity among all core samples. **Table 16** provides specific details regarding the properties of the sand packs used in our core flooding experiment.

**Table 16—SAGD core flooding properties.**

Parameter	Value
Core diameter, in	1.5
Core length, in	5.0
Porosity, %	30.0
Permeability, D	10–14
Steam temperature, °C	240
Backpressure, psi	200
Differential pressure, psi	5
Overburden pressure, psi	500
Injection rate, cc/min	0.1

The initial SAGD process commenced by injecting steam into the core, reaching temperatures of up to 240°C, differential pressures of 5 psi, and overburden pressures of 500 psi, lasting for a maximum of 1,600 minutes or equivalent to 11 pore volume injected (PVI). Subsequently, the pre-selected solvent(s) was introduced into the process as a pure solvent(s) injection (100% composition) without involving any steam injection. The results obtained from this recovery process were then subjected to analysis to draw robust conclusions and recommendations

regarding the effectiveness of this solvent(s) for post-SAGD applications. Additionally, a detailed illustration of the complete steam flooding experimental setup is provided in **Figure 88**.

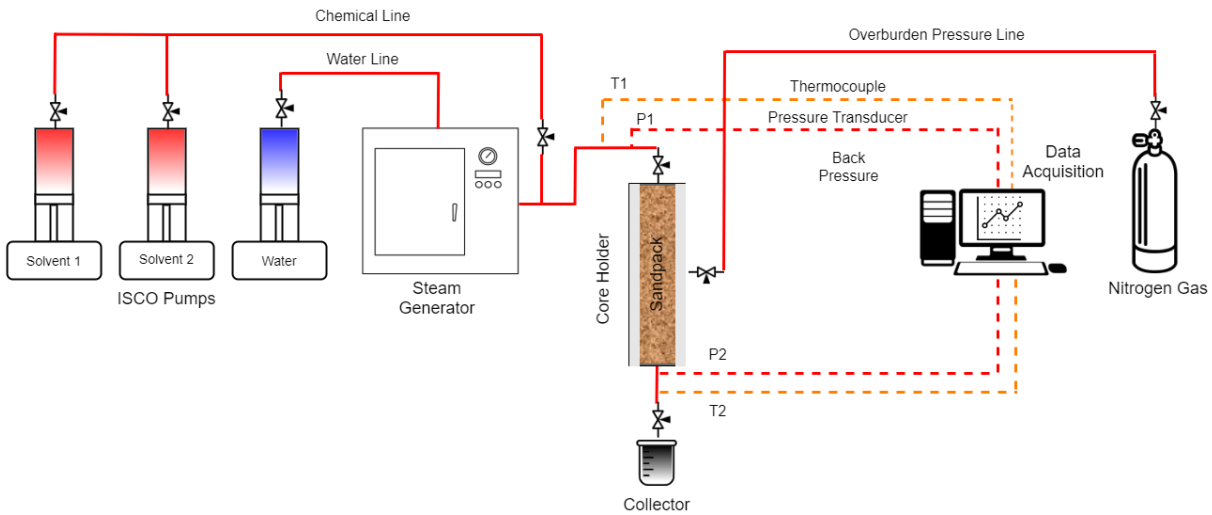


**Figure 88—SAGD core flooding experimental setup.**

## 6.5 Experimental Results and Discussions

### 6.5.1 CO<sub>2</sub> Injection

#### 6.5.1.1 Hele-Shaw and Porous Media Visualization Experiments

**Figure 89** summarizes the entire Hele-Shaw experiments for the CO<sub>2</sub> injection case. The base case refers to the SAGD experiment that serves as the reference, involving the injection of pure steam. In **Figure 89a**, we have presented data on the flow characteristics and the growth of the steam chamber at various stages of the heavy-oil displacement process by SAGD. These stages include the initial conditions, the early stage (0.5 PVI), the middle stage (1.5 PVI), and the late stage (3 PVI/post-SAGD). During the early stage of steam injection, we observed the initiation of heat transfer from the steam phase to the oleic phase. Despite this heat transfer, we observed the presence of displacement instability, commonly referred to as viscous fingering, within the Hele-Shaw cell, as shown by the yellow dotted circles. This phenomenon primarily arises from the

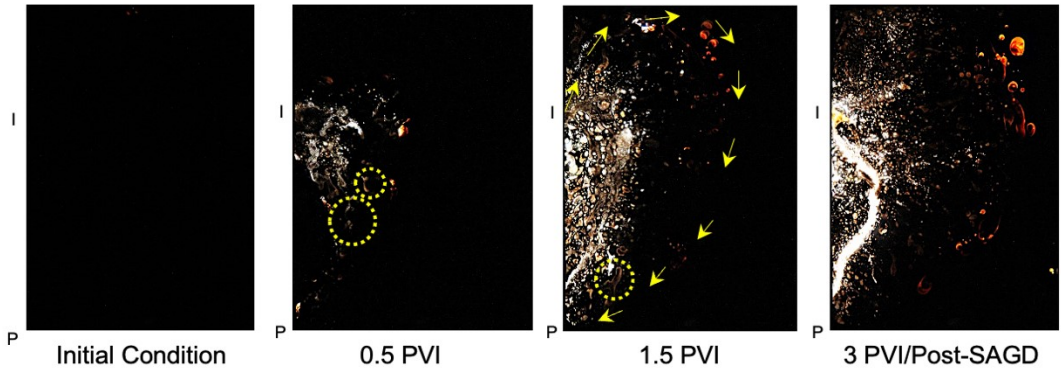
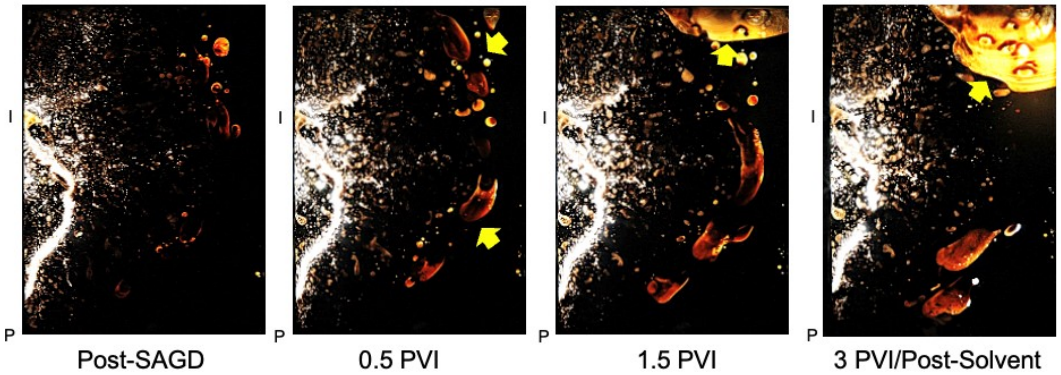
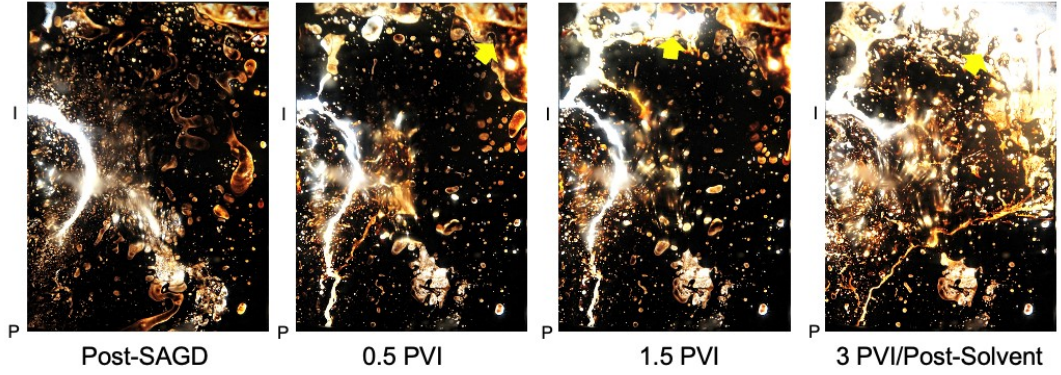
displacement of condensed steam. Rapid heat dissipation and contact with initially cold oil led to the swift condensation of the steam. Consequently, during the early stage of heavy-oil displacement, the process is driven solely by condensed steam. What is particularly significant is that because of the unfavorable contrast in mobility between the steam condensate and heavy-oil, this displacement becomes highly unstable, resulting in both viscous fingering and the splitting of the fingering tips. These unstable displacement phenomena have been observed in previous experimental studies involving steam injection and SAGD conducted by Kong et al. (1992), Huang and Babadagli (2019), and Bruns and Babadagli (2020). This unstable fingering behavior also extends to more distant locations due to greater heat losses and the dominance of condensed steam in the displacement process.

Furthermore, during the early stage of SAGD, we also noticed the influence of gravity as some of the fingers moved toward the production port of the Hele-Shaw cell (indicated by the yellow dotted circle). Ongoing propagation and steam chamber development process were observed as the steam was injected until 1.5 PVI (shown by the yellow arrows). It was evidenced that the steam phase follows the established flow path created by the displacement of steam condensate during the early stages of SAGD. The steam propagation that occurred during the SAGD process is confirmed by the temperature profile of the Hele-Shaw cell, using temperature sensors placed within the cell (**Figure 90**). At 1.5 PVI or approximately 50 minutes after starting steam injection, the bright white spots began to emerge within the Hele-Shaw cell, indicating that the steam phase had advanced, and a steam chamber had formed within the cell. As the steam phase continued its journey toward the upper part of the Hele-Shaw cell, heat transfer into the oleic phase persisted. Nonetheless, the presence of rounded fingers with a light orange hue (at the upper region of Hele-Shaw) during the SAGD process indicated rapid heat losses and a displacement process primarily dominated by steam condensate. As the steam injection was continued until 3 PVI, the unstable displacement pathway toward the production port turned out to be clearer, larger bright white spots could be observed, and the oleic phase became mobile due to heat transfer.

When the steam injection was entirely cut off, CO<sub>2</sub> (at pure composition) injection was started (**Figure 89b**). At the initial stage of solvent injection, the dissolution process between the oleic phase and solvent initiated, which was indicated by brighter yellow fingers moving toward the lower part of the Hele-Shaw cell controlled by the gravity force as pointed by the yellow arrows.

As the solvent was constantly injected, the bright yellow spots started to show up at the upper part of the model (1.5 PVI) and developed into a larger area as the injection persisted until 3 PVI—specified by the yellow arrows. This phenomenon evidently indicates that the dissolution process of crude oil and CO<sub>2</sub> gas, which moved and accumulated at the top part of the Hele-Shaw cell, was successful; therefore, the mobilization of the oleic phase was possible under the gravitational force. In a more scientific fashion, CO<sub>2</sub> is able to dissolve in the oleic phase due to its nature of encompassing solubility in heavy-oil/bitumen (Jaimes et al. 2019). This ability allows the dissolution process to initiate. Hence, the oil viscosity could be potentially reduced due to this mechanism. However, it has to be taken into consideration that the solubility of CO<sub>2</sub> is way lower in the oleic phase than in water due to higher K-value (Bahadori et al. 2008). Hence, the performance of CO<sub>2</sub> injection can be less effective with the presence of steam condensate/water in SAGD reservoirs.

In the case of pure heptane injection (**Figure 89c**), at a solvent injection of 0.5 PVI, noticeable yellowish regions emerged proximate to the injection site and the upper region of the model—indicated by the yellow arrows. This reflects the commencement of the mixing process between the solvent and the heavy-oil (shown by the yellow arrow). Subsequently, the solvent-oil mixture descended and was produced due to the influence of gravity. This observation substantiates the vapor phase propagation of heptane toward the upper section of the model, as also corroborated by the temperature reading at the injection point T0 (**Figure 90**). Continuing the solvent injection until 3 PVI, we observed the substantial development and expansion of prominent bright white areas in the upper region of the model. This phenomenon suggests the accumulation of heptane in the upper part of the Hele-Shaw model. The increased concentration of accumulated heptane facilitates a more efficient dissolution process between solvent and heavy-oil. Ultimately, by the end of the solvent injection phase, the ROS in the steam chamber/zone decreased significantly. In the context of heavier solvent injection, such as heptane, the experimental findings unequivocally demonstrate the superior performance of heptane injection in comparison to other gaseous solvents (e.g., CO<sub>2</sub>). From a thermodynamic perspective, it is evident that heptane exhibits substantially higher solubility, as indicated by its significantly lower K-value when contrasted with CO<sub>2</sub> gas. This means that heptane encompasses way higher solubility in heavy-oil than CO<sub>2</sub> gas, thereby facilitating a more pronounced reduction in viscosity, an enhanced areal sweep efficiency, and more recovery could be anticipated.

Case	Results			
Base/Reference Case	 <p style="text-align: center;">(a)</p>			
CO <sub>2</sub> Injection	 <p style="text-align: center;">(b)</p>			
Heptane Injection	 <p style="text-align: center;">(c)</p>			

**Figure 89—Hele-Shaw experimental results with solvent(s). Color representation: black = heavy-oil, orange = condensed steam displacement result, bright white = displaced oil by steam/solvent, and bright yellow = solvent-oil mixture. I = injection port and P = production port.**

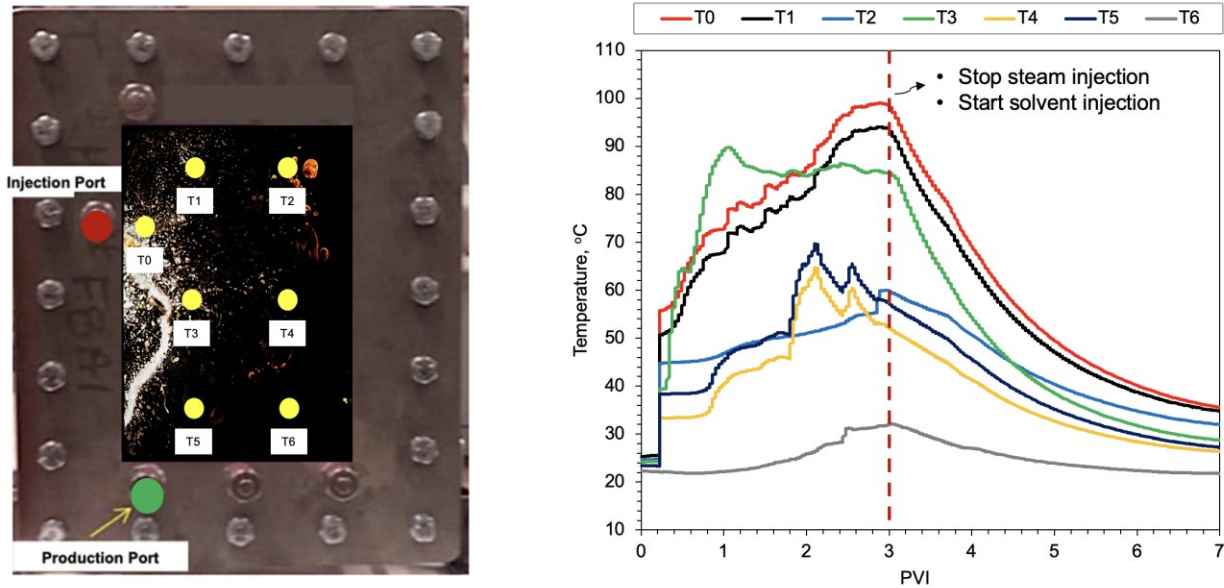


**Figure 90—Average temperature profile observed on Hele-Shaw experiments during SAGD and solvent injection. The dashed line indicates the period when the steam injection was entirely stopped, and solvent injection was started.**

In addition to Hele-Shaw experiments, conducting an experimental study in porous media models provides a valuable means to accurately model how phases distribute within reservoirs. For the porous media case, mineral oil (**Table 15**) was selected due to its transparent properties, enabling the investigation of phase distribution at the microscopic level. Similar to what has been observed in the Hele-Shaw cell, displacement instability was evidenced, taking place within the pore spaces, especially during the initial stage of SAGD. **Figure 91** summarizes the porous media experimental results with CO<sub>2</sub> injection. The base case scenario consisted of injecting pure steam into the porous media model (**Figure 91a**). By evaluating the images obtained from the experimental results, we can distinguish several zones:

- area predominantly filled with steam (steam chamber zone),
- condensed steam zone,
- unswept/residual oil zone,
- mobilized zone (comprising steam, condensed steam, oil, and emulsion),
- immobilized zone (cold oil).

A heat transfer process (between pure steam and oleic phase) occurred as the steam was continuously injected into the model. This process led to a reduction in the viscosity of the heavy oil, and subsequently, the heated oil was produced from the upper section of the porous media due to the influence of gravitational forces. At the beginning of steam injection (at 0.5 PVI), the displacement instability (e.g., viscous fingering) occurred in porous media caused by rapid heat losses, triggering steam condensation as denoted by the yellow dotted circles. At this stage, the oil displacement was principally driven by the condensed steam, which is greatly unstable in terms of mobility contrast. The initial production of the oleic phase—even under this displacement mechanism—was possible due to the influence of gravity force. As the steam was continuously injected until 1.5 PVI, further steam propagation toward the upper section of the porous media model was clearly observed (indicated by the yellow arrows), causing further steam chamber expansion—corroborated by the temperature profile gained from the temperature sensors mounted on some region of the porous media (**Figure 92**). From the temperature profiles, it can be observed that the temperature near the injection port (T0) and the temperature at the higher region of the model (T1) escalated beyond 100°C. The rise in the temperature profile confirms the occurrence of steam propagation and steam chamber expansion. At this stage, more oil production was realized with gravity drainage and more heated oil zones. However, the temperature at the location farther from the steam injection port (T2 and T4) persisted lower than 60°C, indicating the rapid heat losses at the farther region and confirming the presence of steam condensate.

During the base case experiment, the steam injection was continued and stopped at 3 PVI. Even though steam chamber expansion was efficaciously achieved, there was still residual oil (e.g., oil blobs, isolated oil islands) evidenced in the porous media—shown by the yellow dotted circles. The development of the residual oil saturation (ROS)—particularly at the steam chamber zone—is primarily due to the inauspicious wettability alteration toward a much less water-wet state triggered by the phase change during the SAGD process, leading to a substantial rise in capillary pressure. In this circumstance, high capillary force dominates in the pore spaces, and the viscous force (steam displacement) could not mobilize the oil, hence further promoting ROS development in the porous media.

In the case of CO<sub>2</sub> injection post-SAGD (**Figure 91b**), the improvement presented by this non-hydrocarbon–non-condensable solvent was not favorably evidenced at the beginning of the

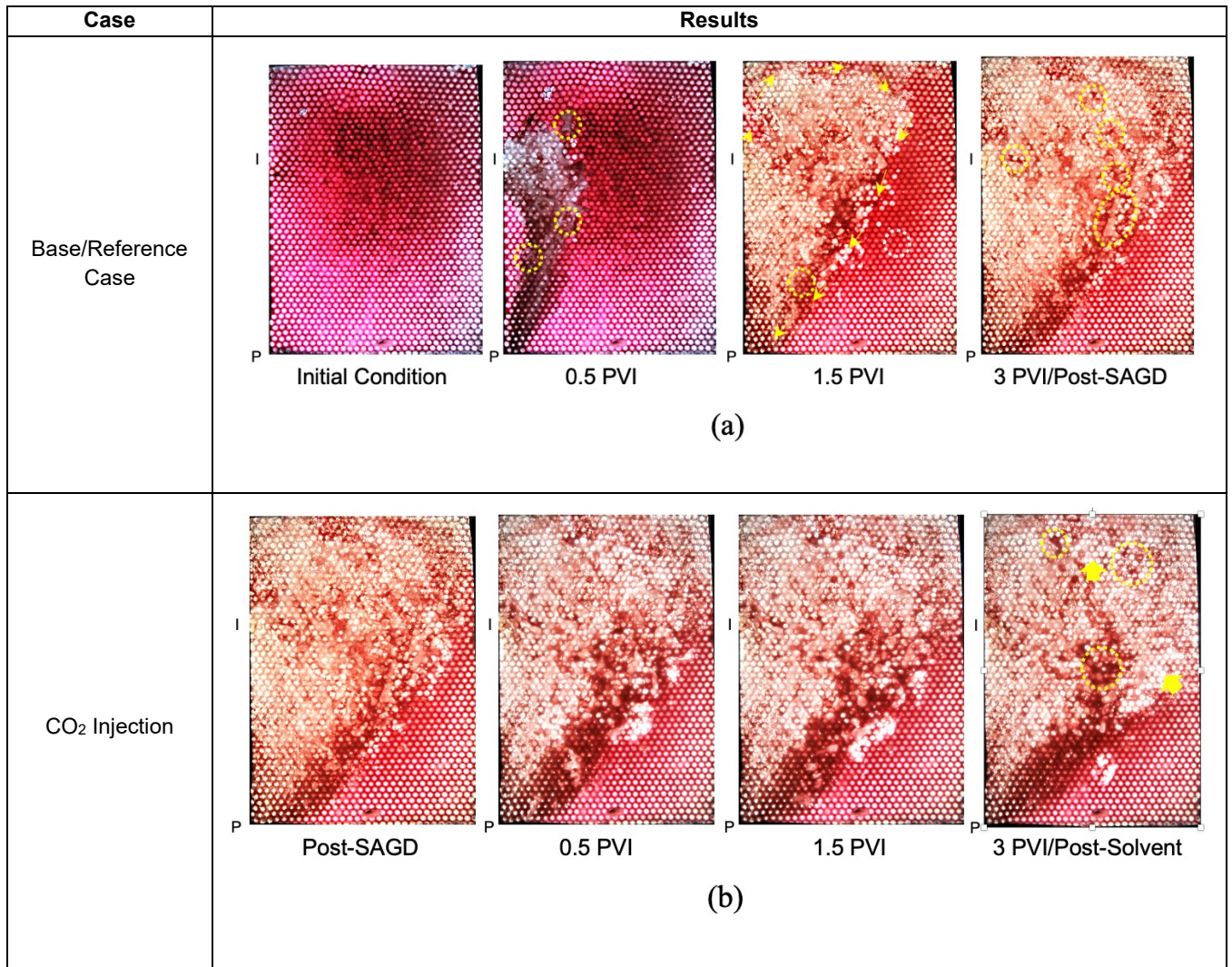
injection process. The effect of CO<sub>2</sub> injection could be noticed when the cumulative injection reached 3 PVI. The CO<sub>2</sub> gas moved toward the upper section of the porous media model, and the dissolution process between the solvent and the oleic phase occurred—further diminishing and mobilizing residual oil at the steam chamber zone (pointed by the yellow arrows). The successful reduction and mobilization of residual oil was reflected by:

- the progression of a brighter white region at the steam chamber zone,
- the reduction of the immobilized oil zone at the right side of the porous media model,
- more oil recovery.

However, more ROS could still be perceived in the porous media model—specified by the yellow dotted circles—denoting that this CO<sub>2</sub> injection was less effective. In other words, the presence of hot water (from steam condensation) could affect the effectiveness of CO<sub>2</sub> since this type of solvent comprises higher solubility in water rather than in the oleic phase (high K-value). This could potentially present drawbacks in overall SAGD performance.

For the heptane injection case, during the initial phase of solvent injection, certain portions of heptane underwent a phase transition into the vapor state due to the elevated SAGD temperature (as depicted in **Figure 92**). These vaporized segments then migrated toward the upper section of the model, resulting in the reduction of unswept oil volumes (indicated by the yellow arrow). Concurrently, the heptane mixed with the oleic phase and subsequently produced toward the production point (as detailed in **Figure 91c**). Continuing the solvent injection process within the porous media model, the mixing/dissolution dynamics between the solvent and the oleic phase persisted. During this phase, the viscosity of the oleic phase progressively decreased, facilitating enhanced oil recovery towards the production point under the influence of gravitational forces. This phenomenon is evidenced by the conspicuous and brighter white regions, as well as the discernible fluid flow pathway indicated by the yellow arrow in **Figure 91c**. Nevertheless, due to the rapid heat losses (**Figure 92**), heptane transitioned from its vapor phase back to its original liquid phase, accumulating in the central region of the porous media model (pointed by the yellow arrow). It subsequently mixed with the oil and was jointly produced. Upon reaching the maximum injection volume (3 PVI), greater recovery and an enhancement in displacement efficiency were attained. This is corroborated by the reduction in ROS in the lower region of the model and the

expansion of the fluid flow pathway, as depicted in **Figure 91c**. Due to its notably high solvent solubility, heptane facilitates a substantially more advantageous mixing/dissolution process, even in the presence of capillary forces and steam condensate, when contrasted with CO<sub>2</sub> solvents experimented in the present study. This rationale aligns seamlessly with the outcomes derived from our experimental investigation, wherein we observed that the ROS could be more significantly and effectively mobilized, owing to the contribution of heptane as the solvent.



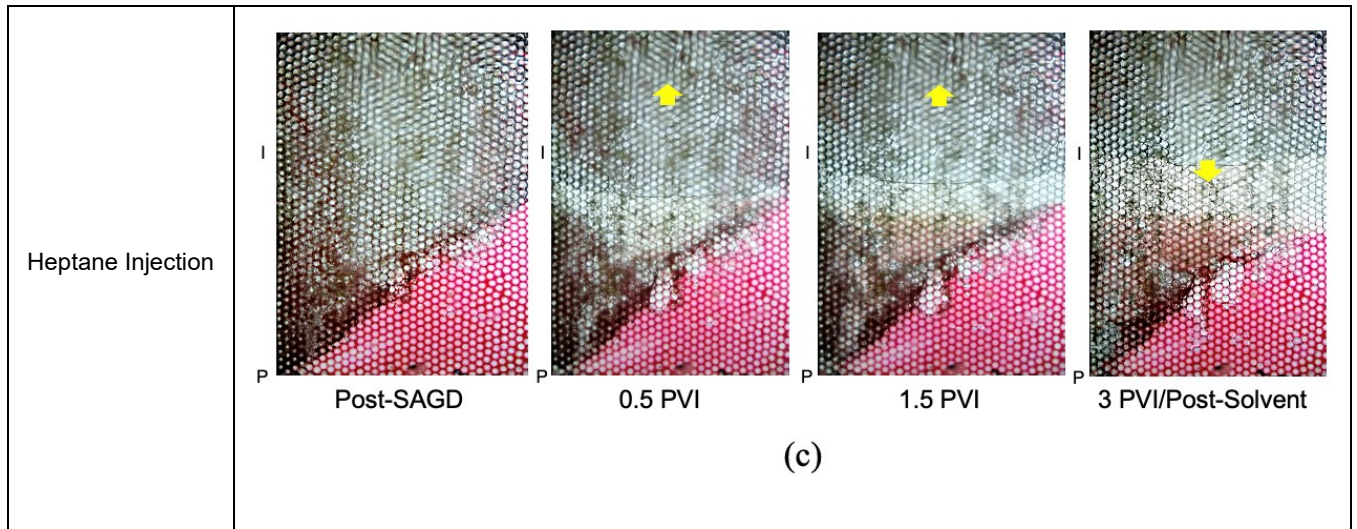


Figure 91—Porous media experimental results with solvent(s). White-dashed circle = oleic phase, and yellow-dashed circle = water-in-oil emulsion/solvent-oil mixture. I = injection port and P = production port.

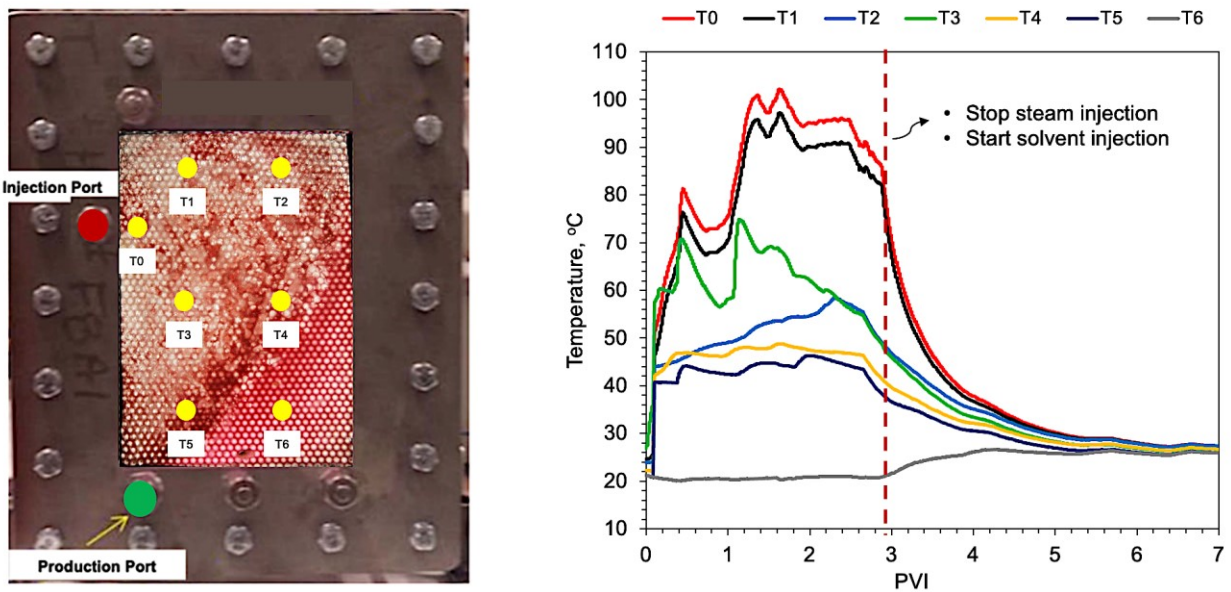


Figure 92—Average temperature profile observed on porous media experiments during SAGD and solvent injection. The dashed line indicates the period when the steam injection was entirely stopped, and solvent injection was started.

### 6.5.1.2 Core Flooding Recovery Performance

Core flooding experiments were conducted to accommodate the dynamics in SAGD reservoirs. In this study, two cases were established to further evaluate the optimal time to switch to solvent injection:

- *Late-stage case.* This case reflects the post-SAGD or mature SAGD case. In this case, the steam was continuously injected into the core until there was only a little or no more oil production—reflecting the declining stage or wind-down SAGD stage. At this stage, a complete steam chamber development was anticipated. Then, the solvent injection was initiated without any steam injection involved to further evaluate the recovery performance.
- *Mid-stage case.* In this case, the steam was constantly injected until the first oil production was perceived. At this stage, the heat energy was sufficient to mobilize the oil and be maintained at the designated conditions (pressure and temperature). Consecutively, the solvent injection process was started with no more steam injection.

The performance of CO<sub>2</sub> injection for the entire case is presented in **Figure 93**. From these performance profiles, it can be highlighted that SAGD performance could be improved in general. In comparison with performed experimental cases, only up to 20% incremental oil recovery could be recuperated after implementing CO<sub>2</sub> injection on average (**Figures 93a** and **b**). According to these studies, the mid-stage CO<sub>2</sub> injection case (**Figure 93b**) performed better than that obtained from the late-stage injection case (**Figure 93a**). However, there was no substantial discrepancy in incremental recovery between the two cases. Only about 9% of recovery difference was perceived after implementing CO<sub>2</sub> injection. This incremental recovery obtained from core flooding experiments is aligned with our visual experiments with CO<sub>2</sub> gas, presenting higher ROS, lower sweep efficiency, and lower oil recovery (**Figure 91b**) at the late-stage case in comparison to the mid-stage case. The performance of CO<sub>2</sub> at the late-stage injection case was hindered by the lower solubility of this solvent in the oleic phase and the presence of the condensed steam (hot-water phase).

By its physicochemical properties, CO<sub>2</sub> is still able to present a dissolution/mixing mechanism to further reduce the oil viscosity; thus, the mobilization of the oleic phase is still possible.

Nevertheless, its characteristic of encompassing way lower solubility in hydrocarbon (high K-value) could hinder the overall recovery performance. In summary, this type of solvent could potentially exhibit advantageous results to SAGD recovery performance. For the optimum time of switching to solvent injection, according to this study, technically, it is better to apply mid-stage solvent injection since this technique could present a more favorable ultimate recovery and remarkable reduction of GHG caused by steam generation. However, for practitioners, the analysis of economic viability is still required to determine the most optimum injection case.

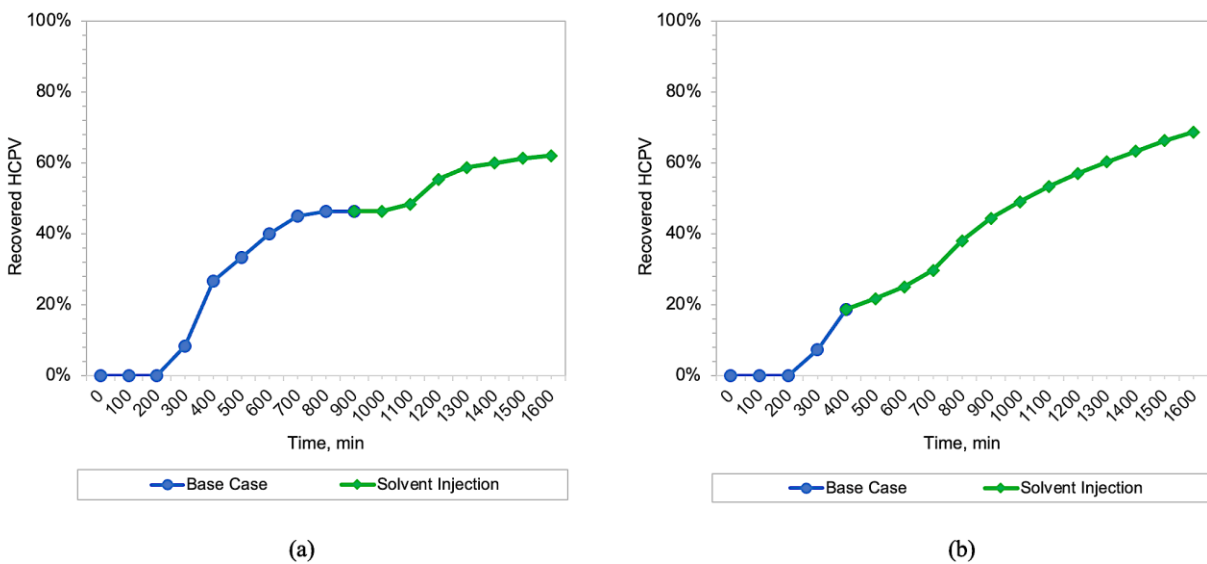


Figure 93—Overall performance of SAGD with CO<sub>2</sub> injection: (a) late-stage case and (b) mid-stage case.

## 6.5.2 Heptane Injection

### 6.5.2.1 Core Flooding Recovery Performance

Heptane injection (at 100% composition) was also employed to gain the recovery performance comparison between these types of solvent at the designated SAGD conditions. Similar to the CO<sub>2</sub> injection case, a reference (steam-only) case was established by continuous steam injection until no more oil recovery to mimic the late-stage or mature SAGD. At this stage, the steam was completely cut off, and the heptane injection was initiated. On the other hand, a mid-stage case

was conducted by continuously injecting steam until perceiving the initial phase of oil production, which indicates the adequacy of heat energy to reduce the heavy-oil viscosity, mobilize, and eventually produce the heavy-oil under the gravity force. **Figure 94** summarizes the overall SAGD performance before and after implementing heptane injection. According to the experimental results, for a reference case, steam-only injection was able to deliver about 40% oil recovery until there was no more oil production observed. This reference case is consistent with the result obtained from the CO<sub>2</sub> injection case, as well as from our previous visual experiments (Pratama and Babadagli 2023c, d), signifying that the reproducibility of these experiments is valid.

Furthermore, the heptane injection case could favorably deliver the ultimate oil recovery of up to 95% on average. In other words, more than 50% incremental oil recovery could be attained by implementing heptane injection post-SAGD. Based on these results gained from the heptane injection case, several key messages can be elaborated:

- The ultimate recovery achieved by the mid-stage heptane injection case was higher than that in the late-stage case. However, the difference between these two ultimate recoveries was only 2% (**Figure 94**).
- Despite the insignificant ultimate recovery discrepancies between the two injection cases (mid-stage and late-stage), a noticeable difference was observed in the mid-stage heptane injection case. This injection case was able to present substantial oil production acceleration (as exhibited in **Figure 95**), which is very auspicious in terms of technical, economic, and environmental points of view: (1) potential recovery improvement, (2) earlier steam injection cut-off, and (3) better GHG emissions mitigation. The mid-stage heptane injection case allows longer interaction time between the solvent and the heavy-oil; hence, a more favorable mixing/dissolution process could be expected.
- In comparison with the CO<sub>2</sub> injection case, overall, heptane presented very auspicious SAGD recovery performance as a solvent far better than CO<sub>2</sub> in alternating steam injection. This favorable recovery performance by heptane injection is parallel to the visual experiments (Hele-Shaw and porous media), showing a larger area of bright white spots and delivering a better “cleaning effect” (**Figures 89c and 91c**).

- The substantial difference in SAGD recovery performance is predominantly due to their physicochemical properties. Scientifically, heptane comprises a lower K-value and more carbon atoms, meaning that heptane is highly soluble in hydrocarbon (even in heavy-oil/bitumen) compared to other types of hydrocarbon solvents (Pratama and Babadagli 2023a, b). Therefore, the heavy-oil/bitumen viscosity could be greatly reduced. The presence of hot water (from steam condensation) did not hinder its performance since the hydrocarbon solubility in water lessens with increasing carbon chain length (Bahadori et al. 2008; Zirrahi et al. 2014; Jaimes et al. 2019).
- With such favorable incremental recovery presented by heptane for post-SAGD applications, this injection can potentially deliver significant SOR reduction, better economic viability, and prominent GHG emissions reduction.

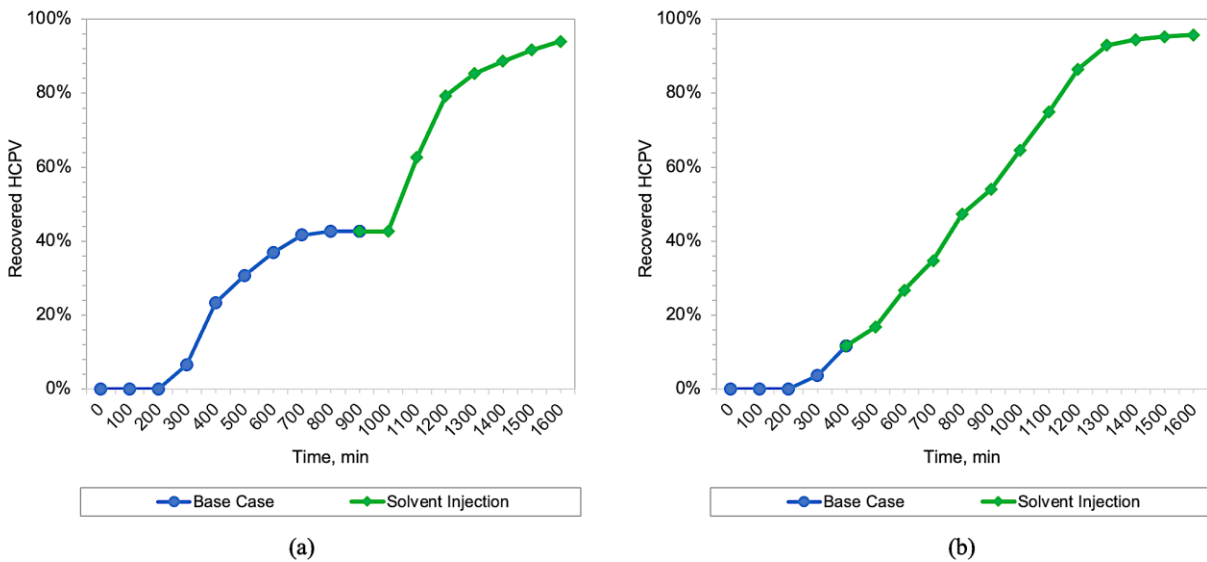


Figure 94—Overall performance of SAGD with late-stage heptane injection. (a) late-stage case, and (b) mid-stage case.

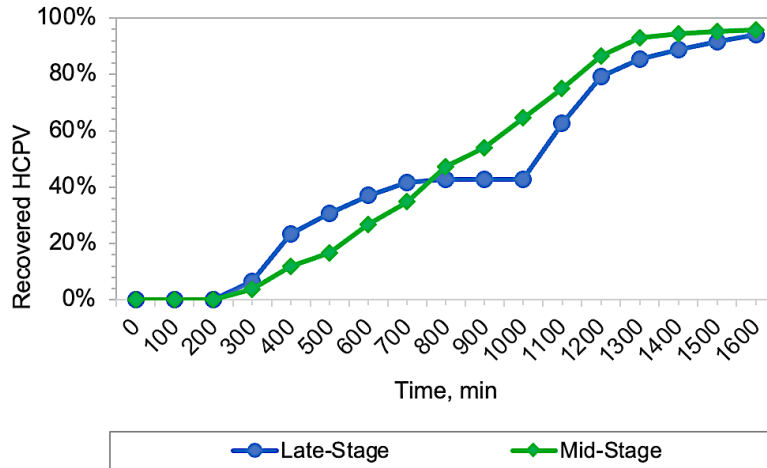


Figure 95—Performance comparison between late-stage and mid-stage heptane injection cases.

### 6.5.3 SAGD Pressure and Temperature

In the core flooding tests, the experimental conditions were maintained to represent the SAGD process. Pressure and temperature were monitored and recorded during entire experiments for further evaluation of overall SAGD performance (Figure 95). For each experiment, the designated differential pressure was 5 psi—establishing a slow injection/dripping rate to maintain purely gravity-dominated displacement—and the temperature condition was set close to 240°C, simulating the steam temperature.

According to the pressure and temperature profiles shown in Figure 96, the differential pressure was successfully maintained at 5 psi on average. However, it is noticeable that the differential pressure increases at the beginning of steam injection. This phenomenon might occur as more heat energy was required to heat up the cold oil—meaning that more steam injection was needed to initiate steam chamber expansion and heavy-oil/bitumen mobilization. In this circumstance, lower latent heat of vaporization, favorable viscosity reduction, and better production rate could be achieved (Pratama and Babadagli 2023a, b). As the heavy-oil/bitumen started to produce, the differential pressure value decreased and equalized at around 5 psi. Lower differential pressure could potentially deliver lower vaporization latent heat—leading to lower SOR and improved energy efficiency (Pratama and Babadagli 2023a, b). In terms of SAGD temperature, the temperature close to the injection point was able to be maintained close to the designated steam

temperature—indicating that the heat energy could be favorably reserved inside the core during the period of the experiment. However, the recorded temperature near the outlet/production point shows way lower magnitude (below 70°C) due to the rapid heat losses.

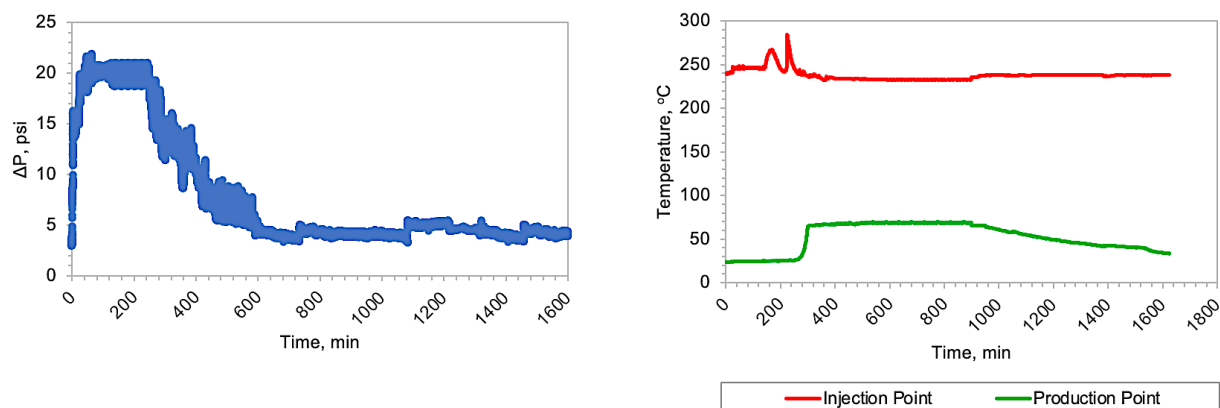


**Figure 96—Average pressure and temperature profiles during SAGD and solvent injection processes: (a) pressure profile and (b) temperature profile.**

## 6.5.4 Sample Analysis

In pursuit of enhancing the robustness and comprehensiveness of our research findings, we undertook supplementary physical and chemical analyses. These endeavors were aimed at bolstering our conclusions and delivering more substantiated recommendations regarding the viability of the proposed methodologies. As part of this effort, we meticulously executed viscosity measurements and SARA tests. These analytical procedures were undertaken to systematically evaluate and validate the repercussions of introducing the studied solvents into heavy-oil/bitumen, thereby elucidating their influence on the physical and chemical properties of these substances.

### 6.5.4.1 Viscosity Measurements

We collected oil samples following each solvent injection to assess how effectively each solvent injection scenario reduced viscosity. **Figure 97** presents the oil viscosity profiles applied to each solvent injection case. In comparison with solvent injection cases, it is clearly evidenced that

heptane injection could outstandingly deliver favorable viscosity reduction amidst all cases. Notably, in the case of mid-stage heptane injection, a favorable reduction in viscosity was observed. Specifically, this injection strategy facilitated a substantial decrease in oil viscosity, with the original high viscosity of 295,000 cP diminishing to a considerably lower value of 67.9 cP at a temperature of 25°C. This outcome underscores a significant improvement in the rheological properties of the heavy oil/bitumen, indicating a more effective solvent-solute interaction. In essence, the prolongation of the contact period between the solvent and the oleic phase, as achieved in the mid-stage injection case, is directly correlated with the enhanced viscosity reduction. This finding underscores the critical role of the duration of solvent-oil interaction in achieving desirable outcomes in the context of heavy oil/bitumen viscosity reduction. On the other hand, no substantial oil viscosity reduction was presented after implementing CO<sub>2</sub> injection compared to the base case.

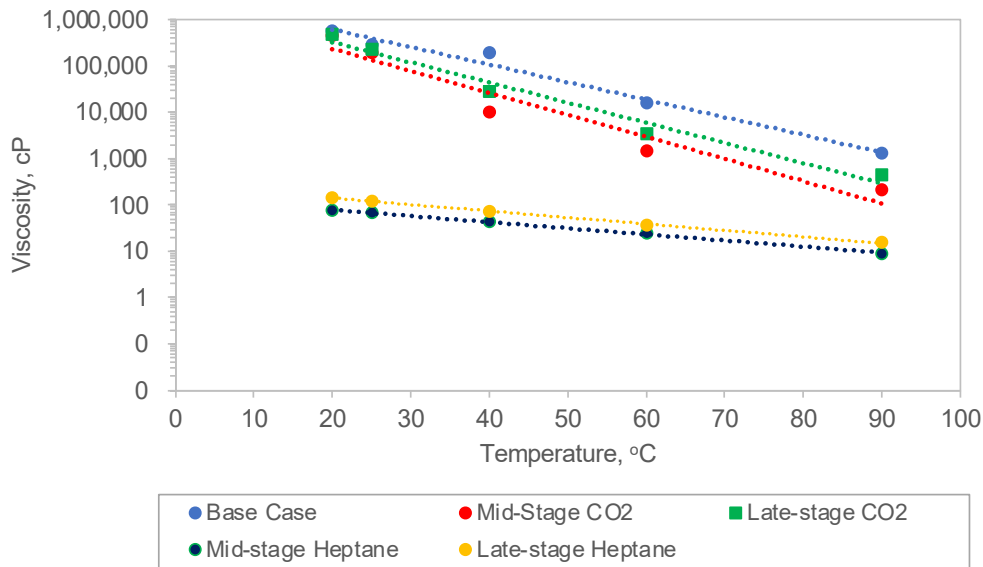


Figure 97—Viscosity measurements for each experimental case.

In elucidating this phenomenon, it is imperative to highlight the significance of using a hydrocarbon-based solvent (compared to other types of non-hydrocarbon-based solvents, e.g., CO<sub>2</sub>), particularly one characterized by an extended carbon chain, in the context of SAGD applications. The justification behind this preference is based on the fundamental principles of

solvent-oil interactions and thermodynamic considerations. A hydrocarbon solvent—particularly heavier and liquid-type ones—is characterized by a protracted carbon chain and its compatibility with the complex physicochemical properties of heavy-oil/bitumen. In the case of post-SAGD, the oleic phase typically contains a substantial fraction of long-chain hydrocarbons. The presence of this heptane (with extended carbon chains) facilitates a more cohesive interaction with heavy-oil/bitumen. The longer carbon chains in the hydrocarbon-based solvent grant the capacity to effectively penetrate and solubilize the components with higher molecular weight contained in the heavy-oil/bitumen; thus, inducing a more auspicious viscosity reduction. The capability of the hydrocarbon-based solvent (e.g., heptane) to engage in Van der Waals forces and dispersion interactions with the heavy-oil/bitumen—in post-SAGD scenarios—further contributes to the mixing/dissolution process of heavy-oil/bitumen components (with solvent), leading to a significant improvement in the rheological properties of the oleic phase.

By way of explanation, the utilization of a hydrocarbon-based solvent—in this case, heptane—featuring elongated carbon chains in post-SAGD applications is underpinned by:

- compatibility with the composition of the heavy-oil/bitumen,
- enhanced solubilization capacity in the oleic phase,
- thermodynamic advantages in attaining substantial viscosity reduction.

The strategic solvent selection is pivotal in optimizing the performance of the post-SAGD process in improving the recovery efficiency.

#### **6.5.4.2 SARA Tests**

We also performed a SARA analysis for each solvent injection case to further assess changes in oil properties. In relation to the base case and reference case, **Figure 98** summarizes the results of the SARA tests. Changes to the oil components were noticeable after solvent injection. In the case of CO<sub>2</sub> injection, it is perceived that this solvent was able to improve the lighter components in the oleic phase. The saturate component could be improved from 25% to 34.5% on average. It is possible for CO<sub>2</sub> to extract lighter hydrocarbons, which will certainly disrupt the colloidal balance

in the crude oil system (Gong et al., 2022). However, there is no noticeable difference in oil composition presented by both mid- and late-stage CO<sub>2</sub> injection.

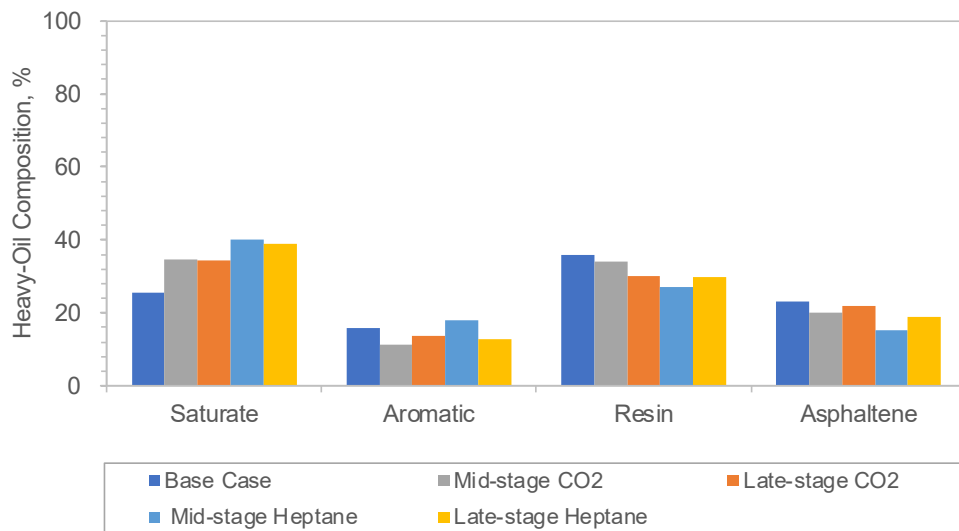


**Figure 98—SARA analysis for the entire solvent injection cases in comparison with the base (steam-only) case.**

Furthermore, in comparison with the CO<sub>2</sub> injection case, the heptane injection cases could favorably improve the oil properties, especially with the mid-stage heptane injection case. The substantial improvement in the oil composition is reflected by the increase in lighter components (saturate), which remarkably improved from 25% to up to 40%. Alongside this improvement, the asphaltene components were dramatically reduced from 23% to a minimum of 15% after injecting heptane into the core—indicating the occurrence of asphaltene precipitation (**Figure 100**) as verified by our recent work (Pratama and Babadagli 2023c, 2023d). Asphaltene precipitation occurs because of the non-dissolvable characteristic encompassed by this component in a polar solvent (e.g., heptane) since asphaltene is a non-polar component contained in heavy-oil/bitumen. The presence of lighter components confirmed that the studied solvents had shown a desirable performance for post-SAGD applications. In addition, a noticeable difference between the two heptane injection cases was primarily observed through the saturate and asphaltene components. For a mid-stage heptane injection case, the saturate component exhibits a higher value (about 2% higher), whereas the asphaltene component has shown a lower value (about 4% lower)

than that in the late-stage heptane injection case. This evidence implies that a higher number of lighter components are present in the produced oil sample due to the longer solvent-oil interaction that occurred during the mid-stage heptane injection process. Nonetheless, it is reasonable to anticipate a heightened occurrence of asphaltene precipitation, a phenomenon evidenced by a diminished asphaltene component. The SARA tests serve as a valuable tool in elucidating the rationale behind the superior incremental oil recovery achieved through heptane injection cases in comparison to CO<sub>2</sub> injection cases.

#### 6.5.4.3 Recovered Sands After Core Flooding

Visual evaluation and analysis of recovered sands—from core flooding experiments—were conducted to support overall post-SAGD recovery performance. The visual evaluation includes bulk sample visual evaluation and sand particle evaluation using a microscope. These sand samples embody the entire core utilized in each experiment. **Figure 99** shows the entire visualization of the sands recovered after each experimental case. It is clearly observed that each solvent injection case presented various visualizations of the recovered sands in terms of the oil content, change in color intensity, and the quality of sand particles.

For the base case, it is perceived that the recovered bulk sands appeared to be very dark—indicating high oil content (**Figure 99a**). A similar appearance was also perceived in the sand particles. These sand particles were observed to be very dark and intact each other, reflecting the high oil content. This evidence is consistent with the SAGD recovery performance delivered by the base case (**Figure 93**). Moreover, there is no significant difference in terms of the visual appearance of bulk sands and sand particles presented by the late-stage CO<sub>2</sub> injection case compared with that in the base case—validated by the post-SAGD recovery with late-stage CO<sub>2</sub> injection (**Figure 93a**). A better sand quality was exhibited by the mid-stage CO<sub>2</sub> injection case in comparison with the late-stage CO<sub>2</sub> injection case since this solvent injection case comprises better post-SAGD recovery performance (**Figure 93b**). This is confirmed by the sand quality encompassing less dark and less consolidated bulk sands, and less intact sand particles—signifying lower oil content. Among all performed cases, the heptane injection cases present the best sand quality (**Figures 99d and e**) due to the remarkable post-SAGD recovery performance (**Figure 94**). In terms of the bulk sand quality, the sands appear to be in bright color (like the original sand) and

very loose. From the microscopic perspective, the sand particles are not intact with each other. Moreover, these sand particles showed relatively high translucency with almost no oil trace on the surface of the sand particles. By way of explanation, the sand samples collected after the heptane injection encompass very low oil to almost no oil content.

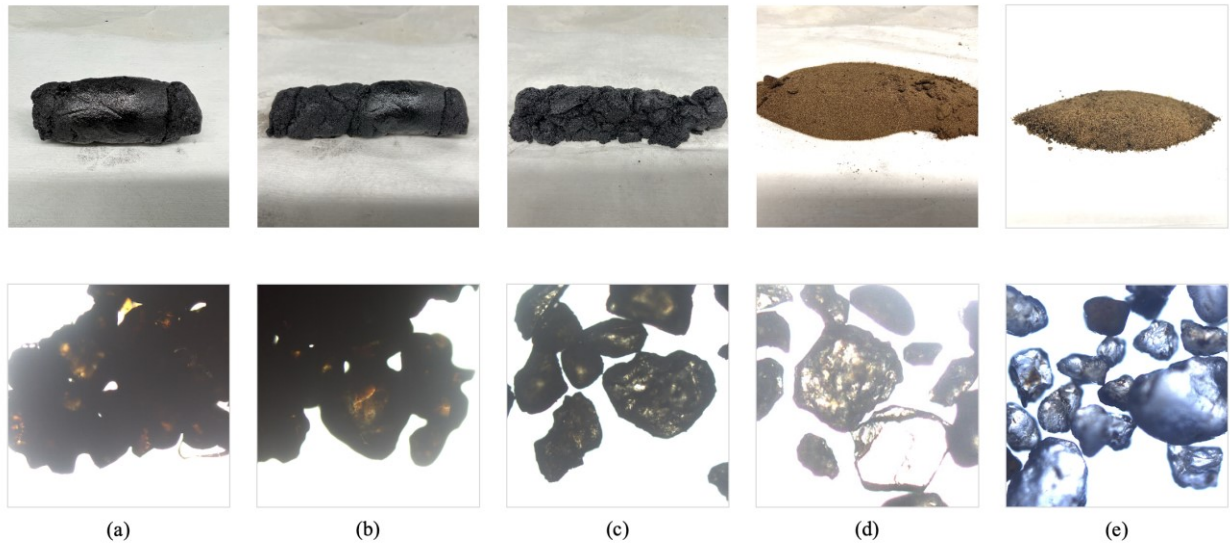


**Figure 99—Recovered sand and sand particles under the microscope with 100X magnification taken after each experiment: (a) base case, (b) late-stage CO<sub>2</sub> injection, (c) mid-stage CO<sub>2</sub> injection, (d) late-stage heptane injection, and (e) mid-stage heptane injection.**

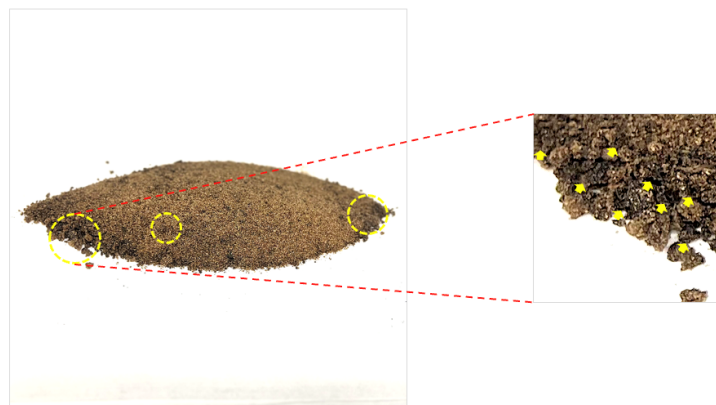


**Figure 100—Example of potential asphaltene precipitation in the recovered sands. Dark solid accumulations were perceived after solvent injection.**

### 6.5.5 Solvent Recovery Potential

Solvent recovery is one of the crucial components to be considered when selecting the solvents for post-SAGD improvement. Optimal solvent recovery determines the economic viability of the overall post-SAGD improvement process. Therefore, we evaluated the potential of solvent recovery presented by the solvents for each solvent injection case. Produced samples from each experiment were gathered for additional gas chromatography (GC) examination for both gas and liquid GCs. The vacuumed vessel coupled to the Erlenmeyer flask was used to collect both gas and liquid samples. The findings of the GC analysis following solvent injections for each injection case are shown in **Table 17**, which will then be used for solvent recovery estimation.

**Table 17—Results of the gas and liquid GC analysis after solvent injection.**

Case	Unit (%)	
	CO <sub>2</sub>	Heptane
Mid-Stage CO <sub>2</sub> Injection	25.78	-
Late-Stage CO <sub>2</sub> Injection	4.58	-
Mid-Stage Heptane Injection	-	61.25
Late-Stage Heptane Injection	-	40.36

Based on the results acquired from both GC tests (gas and liquid), both solvents were detectable and quantifiable through the GC instruments, thus signifying that these studied solvents are potentially recoverable. The solvent recovery process was possible due to the solvents' physicochemical properties comprising their solubility in hydrocarbon. Furthermore, it is clearly observed that the percentage of the retrieved CO<sub>2</sub> gas alongside the production stage was much lower than that in the heptane injection case since CO<sub>2</sub> gas prefers to dissolve in the water phase and mostly accumulates at the upper part of the core. This phenomenon is consistent with the solubility of each solvent type in hydrocarbon. It is also noticeable that between two CO<sub>2</sub> injection cases (mid- and late-stage), the mid-stage CO<sub>2</sub> injection case presents better retrievability than the late-stage CO<sub>2</sub> gas injection case might be due to the longer interaction and exposure experienced

by the CO<sub>2</sub> gas, and the oleic phase in the mid-stage CO<sub>2</sub> injection case. Besides, the presence of a higher amount of water phase (from steam condensation) in late-stage CO<sub>2</sub> injection case could hinder the effectiveness of CO<sub>2</sub> gas as a solvent.

In accordance with the assessment of solvent recovery presented in this investigation, it is apparent that solvents characterized by a high degree of solubility in the oleic phase, such as heptane, are the preferred selection in this context. Nevertheless, despite heptane's advantageous attributes in terms of solvent solubility, the findings of this study, as determined through liquid GC analysis, reveal that up to 62% of the total injected heptane could only be recovered. This signifies that a remaining portion of the heptane persists in the models as a liquid phase, primarily due to the cooling and condensation process (from a vapor phase) inside the core holder, while another fraction becomes co-produced alongside the oil in a liquid phase state. However, due to a higher temperature at the production point (**Figure 96**), this liquid heptane might evaporate and be released into the air as heptane comprises a vaporization pressure of 46 mmHg or 0.06 atm at 25°C. In addition, the visual experiments could support and validate this evidence (**Figures 89 and 91**). For the CO<sub>2</sub> injection case, larger portions of the gas remained in the upper region of the models, whereas a greater percentage of heptane mixed and could be produced with the oleic phase in the case of heptane injection.

In other words, the recovery potential is proportional to the solubility of each solvent in the oleic phase and the water phase. In addition, the quantification of the solvent recovery potential is summarized in **Figure 101**. According to this solvent recovery evaluation and analysis, the appropriate selection of solvent type is essential to achieve optimal recovery and economically viable solvent recovery under the given pressure and temperature conditions during post-SAGD applications.

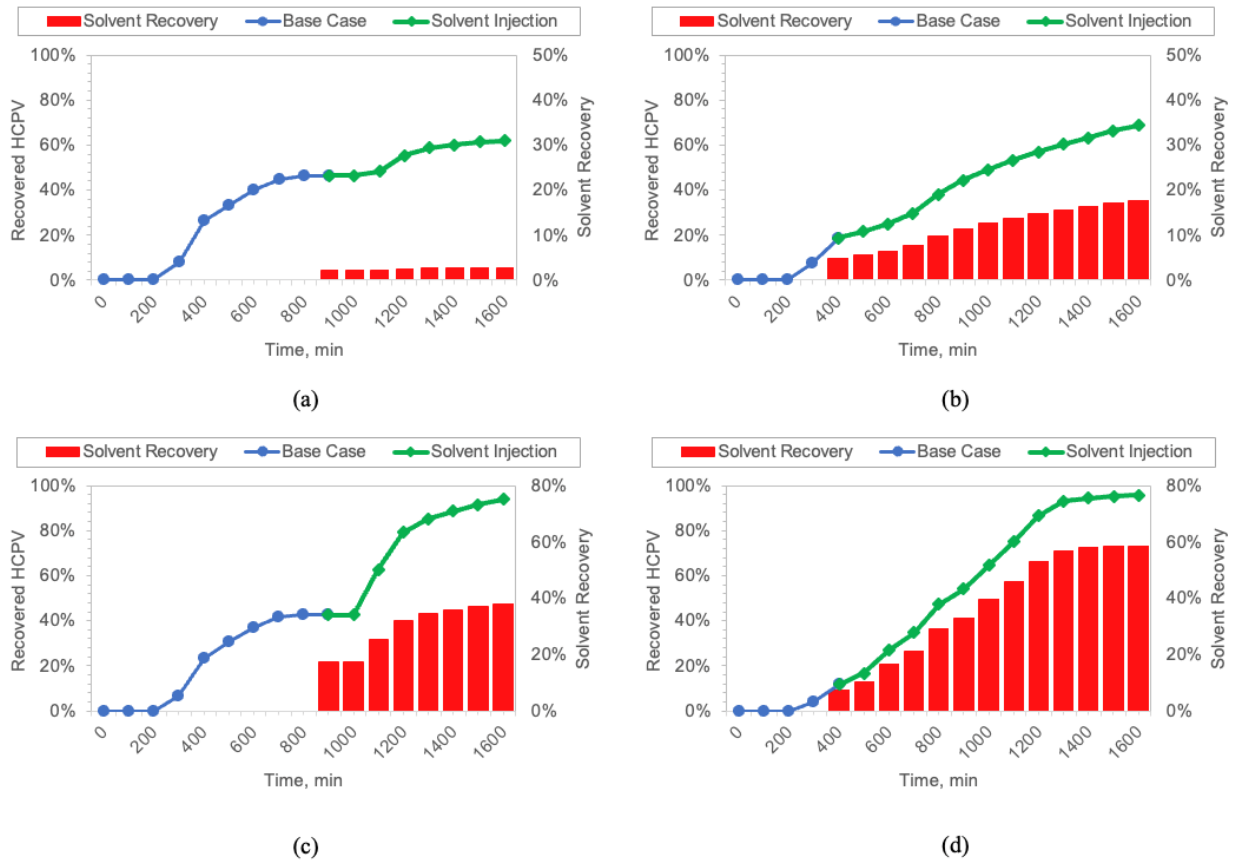


**Figure 101—Quantification of solvent recovery potential alongside heavy-oil/bitumen recovery post-SAGD: (a) mid-stage CO<sub>2</sub> injection, (b) late-stage CO<sub>2</sub> injection, and (c) late-stage heptane injection.**

## 6.6 Research Limitations

The principal objective of this research is to further investigate the efficacy and technical viability of a potential hydrocarbon solvent (e.g., heptane) and non-condensable solvent (e.g., CO<sub>2</sub>), specifically in post-SAGD applications. The research entails comprehensive evaluations grounded in the interactions between the solvents and the oleic phase, focusing on thermodynamics and physicochemical aspects (Hele-Shaw visualization), phase distribution phenomena within porous media (porous media visualization), as well as the overall SAGD performance (core flooding) under given post-SAGD conditions of pressure and temperature.

However, certain practical considerations encountered in the field applications, such as multi-component and complex phase behavior, ROS at the steam chamber, and steam channeling might not be comprehensively addressed due to inherent limitations. These limitations include the two-dimensional nature of the models (for 2-D visualization), the constrained volume of oil in place, smaller volumes of steam and solvent injection, and heat dissipation, even though representations of solvent phases have been captured. Consequently, for more extensive or larger-scale applications, numerical reservoir simulation and complex phase behavior analysis remain imperative. These endeavors are essential to:

- accommodate the reservoir performance analysis for post-SAGD applications and more reliable solvent injection control, particularly for gaseous solvents,
- determine the solvent behavior at a given post-SAGD temperature in the reservoir in terms of additional heavy-oil recovery and solvent recovery as we are dealing with complex or multi-component phases (e.g., oil, steam, condensed steam, solvents).

The outcomes of this research are anticipated to serve as a pivotal foundation for the formulation and execution of subsequent research initiatives, including practical field-scale applications in the relevant domain.

## **6.7 Conclusions**

The effectiveness of solvents in post-SAGD applications was examined through a series of core flooding and visual experiments using pre-selected solvents as low GHG and high-efficiency tertiary recovery solutions in alternating steam injection. The following conclusions can be withdrawn from the observations and analyses presented in this paper:

1. All studied solvents presented improvement in overall post-SAGD performance. However, pure heptane injection delivered the utmost outcomes in terms of oil recovery, viscosity reduction, and improvement in oil composition.

2. Non-condensable solvent (CO<sub>2</sub> gas) injection could still present some improvements in post-SAGD recovery performance. Between the two solvent injection cases, the mid-stage CO<sub>2</sub> injection case exhibited more favorable incremental oil recovery than the late-stage CO<sub>2</sub> injection case.
3. Technically, mid-stage solvent injection is recommended for a better post-SAGD recovery and efficiency improvement than that in late-stage solvent injection. In mid-stage solvent injection, the heat energy was sufficient to mobilize the oil and be maintained at the designated conditions (pressure and temperature). Moreover, a mid-stage solvent injection technique can provide a longer exposure and interaction between the solvent and the oleic phase. Hence, this will potentially improve the post-SAGD efficiency (steam cut-off) and solvent effectiveness. However, economic analysis is still required when applying this technique for field applications to determine the economic viability of the project.
4. The solvent effectiveness is governed by its physiochemistry (K-value/solubility). The presence and accumulation of the condensed steam may hinder the efficacy of the solvent, the solvent–oil interaction, and the development of the solvent chamber in SAGD reservoirs, particularly for the types of solvents that are highly soluble in water phase rather than the oleic phase (e.g., CO<sub>2</sub>).
5. Solvent injection could trigger the asphaltene precipitation in reservoirs, which may hinder reservoir performance and deliverability due to the potential pore blockage.
6. The heptane injection case presented the most promising solvent recovery potential due to its high solubility in the oleic phase. The effectiveness of this solvent type could still be maintained at the given post-SAGD conditions, even with the presence of the condensed steam in the reservoirs.
7. This study is able to prove and quantify that solvent recovery at the given post-SAGD conditions is possible. The solvent recovery potential is proportional to the solubility of each solvent in the oleic phase and the water phase. Hence, the solvents comprising high solubility (low K-value and longer carbon chain) in the oleic phase are preferable.
8. The appropriate selection of solvent type is essential to achieve optimal recovery and economically viable solvent recovery under the given post-SAGD conditions (pressure and

temperature). This requires further experimental (PVT studies and core flooding tests) and computational work (numerical simulation with phase behavior) to determine the solvent behavior at a given post-SAGD temperature in the reservoir in terms of additional heavy-oil recovery and solvent recovery.

## **Chapter 7: Conclusions, Contributions, and Future Work**

## 7.1 General Conclusions

While SAGD has been effectively deployed in Canada, significant apprehensions persist concerning its oil recovery efficiency and environmental consequences. One critical aspect that significantly influences the performance of SAGD, such as the characteristics of the reservoir geology, remains inadequately understood. Notably, even in cases where SAGD projects share similar reservoir properties, certain projects are encountering difficulties in achieving efficient oil recovery. The determinants affecting this recovery, including the complexities of thermodynamics, the intricacies of well design, and operational strategies, require more in-depth and meticulous analysis to provide a clearer understanding of their roles and interactions within the SAGD process. Simultaneously, there are notable technical obstacles and concerns regarding the impact of GHG emissions associated with steam-based operations. These concerns have the effect of generating unfavorable opinions both within the public and among technical experts. These perceptions have prompted a drive to explore fresh avenues for utilizing existing investments, which encompass various aspects of the industry such as field operations, production facilities, and capital expenditures. In essence, the industry is grappling with challenges that have not only led to negative public sentiment but have also raised technical concerns. This has catalyzed the search for innovative applications and strategies to make the most of prior investments to mitigate these challenges and move towards more sustainable and environmentally friendly practices.

The consideration of chemical additives and solvents represents a potential alternative and proposed solution for achieving the previously mentioned objectives. However, it is important to recognize that when these methods are put into practice, a range of intricate phenomena must be carefully managed. Two significant aspects include wettability alteration and the mechanisms involved in trapping oil within the reservoir. Even more fundamentally, it is crucial to gain a comprehensive understanding of the distribution of phases at the pore level. This becomes especially essential in the application of hydrocarbon solvents, given that the reservoir system comprises four distinct phases: oil, water, steam, and solvent. Grasping the intricate mechanisms that determine how these phases are distributed within the reservoir is vital for the success of this approach. Moreover, beyond the physicochemical characteristics of the process, the thermodynamic aspect of the phase behavior of hydrocarbon solvents must be considered. This is

influenced by variations in pressure and temperature and plays a significant role in how these solvents interact within the reservoir system. Therefore, both the physical and thermodynamic aspects of the process are critical considerations in the effective application of chemical additives and solvents to enhance post-SAGD efficiency.

The principal aim of this thesis was to conduct an extensive and in-depth evaluation of various types of solvents with the intention of determining their potential as highly efficient options for tertiary oil recovery. This involves reducing the amount of residual oil left behind in the reservoir, improving the mechanisms used for oil retrieval, and ultimately decreasing the SOR. Achieving these goals can significantly enhance the overall efficiency of the oil recovery process. Moreover, there is a prevailing trend towards more energy-intensive, in-situ heavy oil and bitumen recovery methods. At the same time, there is a growing demand for reducing GHG emissions to make fossil fuel production more sustainable and address pressing environmental concerns. Therefore, this research serves a dual purpose by striving to find a practical solution that can address the urgency of improving oil recovery while also aligning with the imperative need for reducing the environmental impact associated with the energy-intensive recovery processes in the oil industry.

According to this research, some conclusions can be generated as follows:

1. In the overall of Canadian SAGD projects, it's noteworthy that a substantial majority, approximately 65%, have not reached the maturity phase. This indicates that a significant portion of SAGD projects is still in the early or intermediate stages of development, and there is further room for optimization. Among the existing SAGD operations, only 45% are considered to be high-performing. These are the projects that have achieved their maximum potential in terms of oil recovery and operational efficiency. The remaining 55% are operating less efficiently, which highlights the need for improvement in various aspects of their processes. To enhance and sustain the performance of SAGD operations, there are several critical areas that require attention: production optimization, production-injection strategy, well-pair development, operational excellence, and tertiary recovery options. These measures collectively play a pivotal role in optimizing SAGD performance and ensuring that a higher percentage of projects can transition into the maturity phase while minimizing inefficiencies in the SAGD operations.

2. Reducing GHG emissions and increasing recovery by replacing steam with condensable (preferentially liquid hydrocarbon) gas injection is a strategic approach to enhance both environmental sustainability and oil recovery efficiency in well-established SAGD applications. The approach involves substituting traditional steam injection with condensable gases, particularly liquid hydrocarbons. The primary goals of this transition are to reduce GHG emissions and substantially improve the oil recovery from the SAGD reservoirs.
3. Certain chemical additives have undergone validation and have been confirmed to possess a mechanism characterized by the synergistic displacement of substances within a given reservoir. This signifies that these additives operate in a concerted and multifaceted manner when introduced into the reservoir environment, as opposed to employing a solitary, straightforward displacement process.
4. Based on a sensitivity analysis of each displacement mechanism, it is evident that wettability alteration emerges as the predominant factor influencing the performance of heavy-oil recovery under steam conditions. Consequently, it is advisable to consider the co-injection of steam along with chemical additives that incorporate the potential for wettability alteration as a displacement mechanism, in addition to other combined mechanisms, when applying these methods in steam injection field applications.
5. A newly developed switchable-solvent as a steam additive has demonstrated enhancements in interfacial characteristics, consequently resulting in an advantageous improvement in the efficiency of heavy oil recovery and a reduction in the residual oil saturation. These advancements were observed when employing a relatively low concentration of SHTA. Moreover, this additive could potentially present other recovery mechanisms, such as foamy oil and oil-in-water emulsification. By indicating that SHTA might offer these recovery mechanisms, it highlights the versatility and potential value of this surfactant in enhancing the efficiency of oil recovery, extending its significance in the field.
6. This research has uncovered that when a switchable-solvent is used at a low concentration, it leads to significant enhancements in heavy-oil displacement within high-pressure and high-temperature SAGD scenarios. These include the most pronounced alteration in

wettability, the minimal reduction in interfacial tension, the optimal recovery of heavy-oil/bitumen, the formation of a particularly stable foamy oil, and a highly favorable oil-in-water emulsion. In addition, this steam additive has the capacity to auspiciously alter the characteristics of heavy-oil/bitumen.

7. The most significant enhancement in steam-driven displacement efficiency occurred when pure propane and heptane were injected, despite a notable post-SAGD temperature drop caused by considerable heat losses. Notably, heptane in its pure form outperformed all other tested solvents in terms of efficiency.
8. The injection of heptane in its pure form, constituting 100% of the composition, yielded the most favorable outcomes regarding improvements in phase distribution, mobilization of residual oil, and the efficiency of oil displacement following SAGD. Nonetheless, the addition of methane may represent a cost-effective alternative worth considering.
9. Initially, it may appear that introducing methane could offer a cost-effective solution for post-SAGD applications. However, it is worth noting that the inclusion of methane did not result in substantial improvements in additional recovery or solvent recovery. In practical terms, the recovery of the injected methane in both cases involving heavier and lighter solvents proved to be unfeasible.
10. Regarding the injection of propane, it is crucial to consider the phase behavior, specifically the K-value (a measure of solubility), as it significantly influences the recovery of the solvent(s). A liquid-type solvent exhibits a more favorable solvent(s) recovery. Therefore, for the application of propane injection, it is advisable to utilize pressurized solvent injection. This approach ensures that the system's temperature remains constant throughout the process.
11. The injection of non-condensable solvent, specifically CO<sub>2</sub> gas, may offer certain enhancements in the post-SAGD recovery performance. Comparing the two scenarios of solvent injection, it was observed that the mid-stage injection of CO<sub>2</sub> exhibited more advantageous incremental oil recovery than the late-stage CO<sub>2</sub> injection.
12. Technically, mid-stage solvent injection is recommended for a better post-SAGD recovery and efficiency improvement than that in late-stage solvent injection. In mid-stage solvent

injection, the heat energy was sufficient to mobilize the oil and be maintained at the designated conditions (pressure and temperature). Moreover, a mid-stage solvent injection technique can provide a longer exposure and interaction between the solvent and the oleic phase. Hence, this will potentially improve the post-SAGD efficiency (steam cut-off) and solvent effectiveness. However, economic analysis is still required when applying this technique for field applications to determine the economic viability of the project.

13. The efficacy of a solvent is primarily determined by its physicochemical properties, specifically the K-value, which signifies its solubility. It is important to note that the accumulation of condensed steam could potentially impede the effectiveness of the solvent, the interactions between the solvent and oleic phase, as well as the establishment of the solvent chamber in SAGD reservoirs. This effect is particularly pronounced when dealing with solvents that exhibit high solubility in the water phase as opposed to the oleic phase, such as CO<sub>2</sub>.
14. The injection of solvent(s) has the potential to induce the precipitation of asphaltenes within reservoirs. This phenomenon, characterized by the formation of solid deposits, has the capacity to impede the overall performance of the reservoir and its deliverability, primarily due to the risk of pore blockage.
15. The heptane injection case presented the most promising solvent recovery potential due to its high solubility in the oleic phase. The effectiveness of this solvent type could still be maintained at the given post-SAGD conditions, even with the presence of the condensed steam in the reservoirs.
16. The solvent recovery at the given post-SAGD conditions is possible. The solvent recovery potential is proportional to the solubility of each solvent in the oleic phase and the water phase. Therefore, the solvents comprising high solubility (low K-value and longer carbon chain) in the oleic phase are preferable.
17. The appropriate choice of solvent types plays a pivotal role in attaining the most optimal recovery efficiency and ensuring the cost-effectiveness of solvent recovery. This selection is of utmost importance, particularly in the context of the prevailing post-SAGD conditions, characterized by specific pressure and temperature. Making the right decision

concerning the solvent type under these conditions is critical for the overall success and economic viability of the recovery process. It influences not only the recovery of valuable resources but also the efficiency of the entire operation, impacting factors like reservoir performance, production costs, and environmental considerations. Therefore, a thorough understanding of the interplay between the chosen solvent and the given post-SAGD conditions is fundamental to achieving optimal outcomes and ensuring the sustainable and economic use of this recovery method.

## 7.2 Contributions

This study possesses the capability to address the prevailing challenges and bridge the existing void within the area of SAGD applications. The prospective merits of this research can be enumerated as follows:

1. This research represents an up-to-date and comprehensive review of SAGD field data, surpassing prior SAGD analyses conducted by distinguished scholars, namely Ali (1997, 2016) and Jimenez (2008). It is pertinent to note that these earlier works primarily concentrated on relatively limited scales of field data, specifically those tied to individual pads or well-pair operations. As complementary to those works, this research offers a meticulous and far-reaching examination of active SAGD fields across Canada. This extensive approach is poised to provide substantial benefits to practitioners, who stand to gain invaluable insights for enhancing the prospects of future SAGD field development.
2. The scope of this research encompasses a comprehensive array of experimental investigations, specifically focusing on the evaluation of novel lab-formulated steam additives, as well as of solvent types for mature SAGD applications. These investigations span a range of scales, extending from the pore- to core-scale visual data, and core flooding tests. It is imperative to emphasize that, to the best of our knowledge, this such effort has not been previously undertaken—experimentally or computationally—in the extant body of research literature. Of particular importance is the changes in the wettability states caused by steam injection and following chemical additives (as presented in Chapters 3 and 4).
3. This research introduces innovative concepts of the application of a novel switchable-solvent, denoted as SHTA, and pure solvent injections. These techniques are strategically proposed for implementation during the mid-stage and late-stage of the SAGD process. The overarching goal of these novel ideas is to yield significant improvements in the post-SAGD operational efficiency while concurrently affecting substantial reductions in GHG emissions.

4. In contrast to the conventional methods (e.g., VAPEX, ES-SAGD), in terms of their methodologies and time of applications, this research has notably demonstrated the feasibility and efficacy of employing a thermally stable, lab-developed switchable-solvent (SHTA) as a steam additive and pure solvents (as replacement to steam) injections at the mature stage of the SAGD operations. Notably, these newly proposed techniques encompass scenarios wherein minimal or even no steam injection is required, rendering its suitability for mid-stage and late-stage SAGD applications.

It is believed that the above listed contributions are useful for scientific communities and practitioners.

### **7.3 Future Works**

The overarching goal of this research is to conduct a comprehensive assessment of the potential of various solvents, with a specific focus on their applicability in post-SAGD applications. To fulfill this objective, a rigorous and systematic investigation was undertaken, yielding valuable insights and recommendations. It is essential to note that the scope of this study was deliberately confined to the examination of interactions between solvents and heavy-oil/bitumen, primarily emphasizing their thermodynamic and physicochemical aspects. Additionally, the study delved into the intricate phenomena associated with phase distribution within porous media, all under the specific operational conditions, including pressure and temperature. By scrutinizing these aspects with a dedicated focus on the chosen conditions and the nature of interactions between solvents and the oleic phase, this research aims to provide a robust understanding of the viability and potential efficacy of various hydrocarbon solvents in post-SAGD applications. The knowledge derived from this study can contribute significantly to the advancement of practices in heavy oil recovery and the development of more efficient and environmentally sustainable techniques for the industry.

However, some field application realizations, such as solvent recovery, complex solvent–fluid phase behavior, ROS at the steam chamber, steam channeling, and temperature post-steam injection—that occurred in the reservoir—might not be covered. Based on the general conclusions,

suppositions, and several uncertainties, potential future works are generated with the intent to attain a more comprehensive study as follows:

- Numerical reservoir simulation to accommodate the reservoir performance analysis for post-SAGD applications and more reliable solvent injection control, particularly for gaseous solvents. This is recommended as a supporting analysis for larger scale applications.
- Phase behavior analysis and/or simulation to determine the solvent behavior at a given post-SAGD temperature in the reservoir in terms of additional heavy-oil recovery and solvent recovery as we are dealing with complex or multi-component phases (e.g., oil, steam, condensed steam, solvents).
- Steam additive/solvent retention is also essential to be further investigated when it comes to the field applications as this could potentially affect the solvent recovery process as well as the economic viability of SAGD projects.

## References

### Chapter 1

- Al-Bahlani, A.M. and Babadagli, T. 2009. Heavy-Oil Recovery in Naturally Fractured Reservoirs with Varying Wettability by Steam Solvent Co-Injection. Paper presented in the SPE International Thermal Operation and Heavy-Oil Symposium, Calgary, Alberta, Canada, 20–23 October. SPE-117626-MS. <https://doi.org/10.2118/117626-ms>.
- Ali, S. M. F. 1974. Current Status of Steam Injection as a Heavy Oil Recovery Method. *J. Can. Pet. Technol.* **13**(1): 54–68. PETSOC-74-01-06. <https://doi.org/10.2118/74-01-06>.
- Ali, S. M. F., Abad, B. 1976. Bitumen Recovery from Oil Sands, Using Solvents in Conjunction with Steam. *J. Can. Petrol. Technol.* **15**(03): 20–24. PETSOC-76-03-11. <https://doi.org/10.2118/76-03-11>.
- Ali, S. M. F. and Meldau, R. F. 1979. Current Steam flood Technology. *J. Pet. Technol.* **31**(10): 1332–1342. SPE-7183-PA. <https://doi.org/10.2118/7183-PA>.
- Ali, S. M. F. 1997. Is There Life After SAGD?. *J. Can. Pet. Technol.* **36**(06): 20–23. PETSOC-97-06-DAS. <https://doi.org/10.2118/97-06-DAS>.
- Alomair, O. and Alajmi, A. 2016. Experimental Study for Enhancing Heavy Oil Recovery by Nanofluid Followed by Steam Flooding NFSF. Paper presented at the SPE Heavy Oil Conference and Exhibition, Kuwait City, Kuwait, 6–8 December. SPE-184117-MS. <https://doi.org/10.2118/184117-MS>.
- Alshaikh, M., Lee, Y. S., and Hascakir, B. 2019. Anionic Surfactant and Heavy Oil Interaction during Surfactant-Steam Process. Paper presented at the SPE Western Regional Meeting, San Jose, CA, USA, 23–26 April. SPE-195254-MS. <https://doi.org/10.2118/195254-MS>.
- Blevins, T. R., Doerksen, J. H., and Ault, J. W. 1984. Light-Oil Steam flooding: An Emerging Technology. *J. Pet. Technol.* **36**(7): 1115–1122. SPE-10928-PA. <https://doi.org/10.2118/10928-PA>.

- Blevins, T. R. 1990. Steam flooding in the U.S.: A Status Report. *J. Pet. Technol.* **42**(5): 548–554. SPE-20401-PA. <http://doi.org/10.2118/20401-PA>.
- Boyd, A. R., Champagne, P., McGinn, P. J. et al. 2012. Switchable Hydrophilicity Solvents for Lipid Extraction from Microalgae for Biofuel Production. *J. Biortech.* **118**: 628–632. <https://doi.org/10.1016/j.biortech.2012.05.084>.
- Butler, R. M., McNab, G., and Lo, H. 1979. Steam-Assisted Gravity Drainage. Paper Presented at the Oil Sands Conference, Jasper, Alberta, Canada.
- Butler, R. M. 1985. A New Approach to The Modelling of Steam-Assisted Gravity Drainage. *J. Can. Petrol. Technol.* **24**(03): 42–51. <https://doi.org/10.2118/85-03-01>.
- Butler, R. M. 1994. *Horizontal Wells for the Recovery of Oil, Gas, and Bitumen*, Vol. 2, 169–199. Richardson, Texas, USA: Monograph Series, Society of Petroleum Engineers.
- Butler, R. 1999. The Steam and Gas Push (SAGP). *J. Can. Petrol. Technol.* **38**(03): 54–61. <https://doi.org/10.2118/99-03-05>.
- Bruns, F. and Babadagli, T. 2020a. Initial Screening of New Generation Chemicals Using Sandpack Flooding Tests for Recovery Improvement of Gravity Driven Steam Applications. *J. Pet. Sci. Eng.* **194**(April): 107462. <https://doi.org/10.1016/j.petrol.2020.107462>.
- Cao, N., Mohammed, M. A., and Babadagli, T. 2017. Wettability Alteration of Heavy-Oil-Bitumen-Containing Carbonates by Use of Solvents, High-pH Solutions, and Nano/Ionic Liquids. *SPE Res. Eval. and Eng.* **20**: 363-371. SPE-183646-PA. <http://doi.org/10.2118/183646-PA>.
- Canadian Energy Research Institute (CERI). 2017. *Study No. 164: Economic Potentials and Efficiencies of Oil Sands Operations: Processes and Technologies*. [https://ceri.ca/assets/files/Study\\_164\\_Full\\_Report.pdf](https://ceri.ca/assets/files/Study_164_Full_Report.pdf).
- Chiwetelu, C. L., Neale, G. H., Hornof, V. et al. 1994. Recovery of a Saskatchewan Heavy Oil Using Alkaline Solutions. *J. Can. Petrol. Technol.* **33**(04). <https://doi.org/10.2118/94-04-05>.

- Collins, P. M. 1994. Design of the Monitoring Program for AOSTRA's Underground Test Facility, Phase B Pilot. *J. Can. Petrol. Technol.* **33**(03): 46–53. <https://doi.org/10.2118/94-03-06>.
- Das, S. K. and Butler, R. M. 1998. Mechanism of the Vapour Extraction Process for Heavy Oil and Bitumen. *J. Pet. Sci. and Eng.* **21**(1998): 43-59. [https://doi.org/10.1016/S0920-4105\(98\)00002-3](https://doi.org/10.1016/S0920-4105(98)00002-3).
- De Haan, H. J. and Schenk, L. 1969. Performance Analysis of a Major Steam Drive Project in the Tia Juana Field, Western Venezuela. *J. Petrol. Technol.* **21**(01): 111–119. <https://doi.org/10.2118/1915-pa>.
- Deng, X. 2005. Recovery Performance and Economics of Steam/Propane Hybrid Process. Paper presented at SPE/PS-CIM/CHOA International Thermal Operations and Heavy Oil Symposium, Calgary, Alberta, Canada, 1–3 November. SPE/PS-CIM/CHOA 97760. <https://doi.org/10.2118/97760-MS>.
- Du, Y., Schuur, B., Kersten, S. R. A. et al. 2015. Opportunities For Switchable Solvents for Lipid Extraction from Wet Algal Biomass: An Energy Evaluation. *J. Algal.* **11**: 271–283. <https://doi.org/10.1016/j.algal.2015.07.004>.
- Durelle, J., Vanderveen, J. R., Quan, Y. et al. 2015. Extending the Range of Switchable-Hydrophilicity Solvents. *Phys. Chem. Chem. Phys.* **17**(7): 5308–5313. <https://doi.org/10.1039/C4CP05313C>.
- Edmunds, N., and Gittins, S. D. 1993. Effective Application of Steam-Assisted Gravity Drainage of Bitumen to Long Horizontal Well Pairs. *J. Can. Petrol. Technol.* **32**(06): 49–55. <https://doi.org/10.2118/93-06-05>.
- Edmunds, N. R., Kovalsky, J. A., Gittins, S. D., et al. 1994. Review of Phase A Steam-Assisted Gravity-Drainage Test. *SPE Res. Eng.* **9**(02): 119–124. SPE-21529-PA. <https://doi.org/10.2118/21529-PA>.
- Energy Institute Statistical Review of World Energy 2023, BP, accessed 9 August 2023, [https://www.energyinst.org/\\_\\_data/assets/pdf\\_file/0004/1055542/EI\\_Stat\\_Review\\_PDF\\_single\\_3.pdf](https://www.energyinst.org/__data/assets/pdf_file/0004/1055542/EI_Stat_Review_PDF_single_3.pdf).

- Fu, D., Farag, S., Chaouki, J. et al. 2014. Extraction of Phenols from Lignin Microwave-Pyrolysis Oil Using a Switchable Hydrophilicity Solvent. *J. Biortech.* **154**: 101–108. <https://doi.org/10.1016/j.biortech.2013.11.091>.
- Fuaadi, I. M., Pearce, J. C., and Gael, B. T. 1991. Evaluation of Steam-Injection Designs for the Duri Steamflood Project. Paper presented at the SPE Asia-Pacific Conference, Perth, Australia, 4–7 November. SPE-22995-MS. <https://doi.org/10.2118/22995-MS>.
- Gael, B. T., Putro, E. S., and Masykur, A. 1994. Reservoir Management in the Duri Steamflood. Paper presented at the SPE/DOE Improved Oil Recovery Symposium, Tulsa, OK, USA, 17–20 April. SPE-27764-MS. <https://doi.org/10.2118/27764-MS>.
- Gates, I. D. and Wang, J. 2011. Evolution of In Situ Oil Sands Recovery Technology: What Happened and What’s New? Paper presented at the SPE International Heavy Oil Conference and Exhibition, Kuwait City, Kuwait, 12–14 December. SPE-150686-MS. <https://doi.org/10.2118/150686-MS>.
- Gupta, S. C., and Zeidani, K. 2013. Surfactant-Steam Process: An Innovative Enhanced Heavy Oil Recovery Method for Thermal Applications. Paper presented at the SPE Heavy Oil Conference, Calgary, Alberta, Canada, 11–13 June. SPE-165545-MS. <https://doi.org/10.2118/165545-MS>.
- Haas, T. W., Fadaei, H., Guerrero, U., et al. 2013. Steam-on-a-Chip for Oil Recovery: The Role of Alkaline Additives in Steam Assisted Gravity Drainage. *Lab Chip.* **13**(19): 3832–3839. <https://doi.org/10.1039/c3lc50612f>.
- Haghighi, M. and Yortsos, Y. C. 1997. Visualization of Steam Injection in Fractured Systems Using Micromodels. Paper presented at the International Thermal Operations and Heavy Oil Symposium, Bakersfield, CA, USA, 10–12 February. SPE-37520-MS. <https://doi.org/10.2523/37520-MS>.
- Hall, A. L., and Bowman, R. W. 1970. Operation and Performance of Slocum Field Thermal Recovery Project. Paper presented at the SPE Practical Aspects of Improved Recovery Techniques Symposium, Fort Worth, TX, USA, 8–9 March. SPE-2843-MS. <https://doi.org/10.2118/2843-ms>.

- Hanamertani, A., Pilus, R., and Irawan, S. 2015. A Review on the Application of Ionic Liquids for Enhanced Oil Recovery. *Springer Singapore*. 133.147. ISBN: 978-981-287-367-5.
- Harmsen, G. J. 1979. Steam Flooding in a Water Drive Reservoir in The Schoonebeek Field in The Netherlands. Paper presented at the 10<sup>th</sup> World Petroleum Congress Proceedings, Bucharest, Romania, 9–14 September. WPC-18233.
- Hashim Noori, W., Cinar, M., Salehian, M. et al. 2018. Experimental Investigation of Steam-Alkali Flooding with Borax: A Case Study on Bati Raman Oil Field. Paper presented at the SPE International Heavy Oil Conference and Exhibition, Kuwait City, Kuwait, 10–12 December. SPE-193797-MS. <https://doi.org/10.2118/193797-MS>.
- Huang, J. and Babadagli, T. 2020a. Efficiency Improvement of Heavy-Oil Recovery by Steam-Assisted Gravity Drainage Injection Using New Generation Chemicals. *Energy Fuels*. **34**(4): 4433–4447. <https://doi.org/10.1021/acs.energyfuels.0c00208>.
- Huang, J. and Babadagli, T. 2020b. Mechanics of SAGD Efficiency Improvement Using Combination of Chemicals: An Experimental Analysis through 2D Visual Models. *SPE Res. Eval. Eng.* In Press. SPE-199940-PA. <https://doi.org/10.2118/199940-PA>.
- Holland, A., Wechsler, D., Patel, A. et al. 2012. Separation Of Bitumen from Oil Sands Using a Switchable Hydrophilicity Solvent. *J. Can. Chem.* **90**(10): 805–810. <https://doi.org/10.1139/v2012-061>.
- Jessop, P. G., Phan, L., Carrier, A. et al. 2010. A Solvent Having Switchable Hydrophilicity. *Green Chem.* **12**(5): 809. <https://doi.org/10.1039/b926885e>.
- Jessop, P. G., Kozycz, L., Rahami, Z. G. et al. 2011. Tertiary Amine Solvents Having Switchable Hydrophilicity. *Green Chem.* **13**(3): 619–623. <https://doi.org/10.1039/c0gc00806k>.
- Jimenez, J. 2008. The Field Performance of SAGD Projects in Canada. Paper presented at the International Petroleum Technology Conference, Kuala Lumpur, Malaysia, 3–5 December. IPTC-12860-MS. <https://doi.org/10.2523/iptc-12860-ms>.

- Jiang, Q., Butler, R., and Yee, C. T. 2000. The Steam and Gas Push (SAGP)-2: Mechanism Analysis and Physical Model Testing. *J. Can. Petrol. Technol.* **39**(04): 52–61. <https://doi.org/10.2118/00-04-04>.
- Jones, J., McWilliams, M., and Sturm, D. 1995. Kern River Revisited: Life After Steam Flood. Paper presented at the SPE Western Regional Meeting, Bakersfield, CA, USA, 8–10 March. SPE-29664-MS. <http://dx.doi.org/10.2118/29664-MS>.
- Lee, J. and Babadagli, T. 2021. Mitigating Greenhouse Gas Intensity Through New Generation Techniques During Heavy Oil Recovery. *J. Clean. Prod.* **286**(March 2021): 124980. <https://doi.org/10.1016/j.jclepro.2020.124980>.
- Li, X., Hou, J., Sui, H. et al. 2018. Switchable-Hydrophilicity Triethylamine: Formation and Synergistic Effects of Asphaltenes in Stabilizing Emulsions Droplets. *Materials*. **11**(12): 2431. <https://doi.org/10.3390/ma11122431>.
- Madhavan, R. M., and Mamora, D. D. 2010. Experimental Investigation of Caustic Steam Injection for Heavy Oils. Paper presented at the SPE Improved Oil Recovery Symposium, Tulsa, OK, USA, 24–28 April. SPE-129086-MS. <https://doi.org/10.2118/129086-MS>.
- Mohammed, M. A. and Babadagli, T. 2015. Wettability Alteration: A Comprehensive Review of Materials/Methods and Testing the Selected Ones on Heavy-Oil Containing Oil-Wet Systems. *Adv. Colloid Interface Sci.* **220**: 54–77. <https://doi.org/10.1016/j.cis.2015.02.006>.
- Mozhdehei, A., Hosseinpour, N., and Bahramian, A. 2019. Dimethylcyclohexylamine Switchable Solvent Interactions with Asphaltenes toward Viscosity Reduction and in Situ Upgrading of Heavy Oils. *Energy Fuels*. **33**(9): 8403–8412. <https://doi.org/10.1021/acs.energyfuels.9b01956>.
- Nasr, T., Beaulieu, G., Golbeck, H., et al. 2003. Novel Expanding Solvent-SAGD Process “ES-SAGD”. *J. Can. Petrol. Technol.* **42**(1): 13–16. PETSOC-03-01-TN. <https://doi.org/10.2118/03-01-TN>.

- Orr, B. 2009. ES-SAGD: Past, Present, and Future. Paper presented at SPE Annual Technical Conference and Exhibition, New Orleans, Louisiana, USA, 4–7 October. SPE-129518-STU. <https://doi.org/10.2118/129518-STU>.
- Phan, L., Brown, H., White, J. et al. 2009. Soybean Oil Extraction and Separation Using Switchable or Expanded Solvents. *Green Chem.* **11**(1): 53–59. <https://doi.org/10.1039/b810423a>.
- Pratama, R., and Babadagli, T. 2023a. What Did We Learn from SAGD Applications in Three Decades, and What is Next? *Geoen. Sci. Eng.* Under review.
- Pratama, R., and Babadagli, T. 2023b. What Did We Learn from SAGD Applications in Three Decades, and What is Next? Paper presented at the SPE Western Regional Meeting, Anchorage, Alaska, USA, 22–25 May. SPE-212970-MS. <https://doi.org/10.2118/212970-MS>.
- Samorì, C., López Barreiro, D., Vet, R. et al. 2013. Effective Lipid Extraction from Algae Cultures Using Switchable Solvents. *Green Chem.* **15**(2): 353–356. <https://doi.org/10.1039/c2gc36730k>.
- Sheng, J. J. 2013. *Enhanced Oil Recovery Field Case Studies*. Waltham, Massachusetts, USA: Gulf Professional Publishing.
- Speight, J. 2013. Thermal Methods of Recovery. In *Enhanced Recovery Methods for Heavy Oil and Tar Sands*, Chap. 7, 221–260. Gulf Professional Publishing.
- Sui, H., Xu, L., Li, X. et al. 2016. Understanding the Roles of Switchable-Hydrophilicity Tertiary Amines in Recovering Heavy Hydrocarbons from Oil Sands. *J. Chem. Eng.* **290**: 312–318. <https://doi.org/10.1016/j.cej.2016.01.056>.
- Taylor, S. 2018. Interfacial Chemistry in Steam-Based Thermal Recovery of Oil Sands Bitumen with Emphasis on Steam-Assisted Gravity Drainage and the Role of Chemical Additives. *Colloids Interfaces* **2**(02): 16. <https://doi.org/10.3390/colloids2020016>.
- Van Dijk, C. 1968. Steam-Drive Project in the Schoonebeek Field, The Netherlands. *J. Pet. Technol.* **20**(03): 295–302. <https://doi.org/10.2118/1917-PA>.

- Wagner, O. R. and Leach, R. O. 1959. Improving Oil Displacement Efficiency by Wettability Adjustment. *Transactions of the AIME* **216**: 65–72. SPE-1101-G. <http://doi.org/10.2118/1101-G>.
- Wang, J., Dong, M., and Arhuoma, M. 2010. Experimental and Numerical Study of Improving Heavy Oil Recovery by Alkaline Flooding in Sandpacks. *J. Can. Pet. Technol.* **49**(03): 51–57. <https://doi.org/10.2118/134248-PA>.
- Wei, Y. and Babadagli, T. 2017a. Selection of New Generation Chemicals as Steam Additive for Cost-Effective Heavy-Oil Recovery Applications. Paper presented at the SPE Canada Heavy Oil Technical Conference. SPE-184975-MS. <https://doi.org/10.2118/184975-MS>.
- Wei, Y. and Babadagli, T. 2017b. Alteration of Interfacial Properties by Chemicals and Nanomaterials to Improve Heavy Oil Recovery at Elevated Temperatures. *Energy Fuels*. **31**: 11866–11883. <http://doi.org/10.1021/acs.energyfuels.7b02173>.
- Wei, Y. and Babadagli, T. 2019. Changing Interfacial Tension and Wettability Using New Generation Chemicals and Nano Metal Particles at Elevated Temperatures and Pressures: An Analysis Through a New Experimental Design for Heavy-Oil Recovery Applications. *J. Disp. Sci. Technol.* **40**(12): 1785–1794. <https://doi.org/10.1080/01932691.2018.1542311>.
- Wilson, A. D. and Stewart, F. F. 2014. Structure–Function Study of Tertiary Amines as Switchable Polarity Solvents. *RSC Adv.* **4**(22): 11039–11049. <https://doi.org/10.1039/C3RA47724J>.

## Chapter 2

- Al-Bahlani, A. M., and Babadagli, T. 2008. A Critical Review of the Status of SAGD: Where Are We and What Is Next? Paper presented at the SPE Western Regional and Pacific Section AAPG Joint Meeting, Bakersfield, California, USA, 31 March – 2 April. <https://doi.org/10.2118/113283-MS>.
- Ali, S. M. F. 1997. Is There Life After SAGD? *J. Can. Petrol. Technol.* **36**(06): 20–24. <https://doi.org/10.2118/97-06-DAS>.
- Ali, S. M. F. 2016. Life After SAGD – 20 Years Later. Paper presented at the SPE Western Regional Meeting, Anchorage, Alaska, USA, 23–26 May. SPE-180394-MS. <https://doi.org/10.2118/180394-MS>.
- Alkindi, A., Al-Azri, N., Said, D. et al. 2016. Persistence in EOR - Design of a Field Trial in a Carbonate Reservoir using Solvent-based Water-Flood Process. SPE EOR Conference at Oil and Gas West Asia, Muscat, Oman, 21–23 March. SPE-179838-MS. <https://doi.org/10.2118/179838-MS>.
- Almubarak, T., Ng, J. H., and Nasr-El-Din, H. 2017. Chelating Agents in Productivity Enhancement: A Review. SPE Oklahoma City Oil and Gas Symposium, Oklahoma City, OK, USA, 27–31 March. SPE-185097-MS. <https://doi.org/10.2118/185097-MS>.
- Alomair, O. and Alajmi, A. 2016. Experimental Study for Enhancing Heavy Oil Recovery by Nanofluid Followed by Steam Flooding NFSF. Paper presented at the SPE Heavy Oil Conference and Exhibition, Kuwait City, Kuwait, 6–8 December. SPE-184117-MS. <https://doi.org/10.2118/184117-MS>.
- Alshaikh, M., Lee, Y. S., and Hascakir, B. 2019. Anionic Surfactant and Heavy Oil Interaction during Surfactant-Steam Process. Paper presented at the SPE Western Regional Meeting, San Jose, CA, USA, 23–26 April. SPE-195254-MS. <https://doi.org/10.2118/195254-MS>.
- Argüelles-Vivas, F., Babadagli, T., Little, L. et al. 2012. High Temperature Density, Viscosity, and Interfacial Tension Measurements of Bitumen–Pentane–Biodiesel and Process Water Mixtures. *J. Chem. Eng. Dat.* **57**(10): 2878–2889. <https://doi.org/10.1021/je3008217>.

- Babadagli, T. and Ozum, B. 2010. Biodiesel as Surfactant Additive in Steam Assisted Recovery of Heavy Oil and Bitumen. SPE Western Regional Meeting, Anaheim, California, USA, 27–29 May. SPE-133376-MS. <https://doi.org/10.2118/133376-MS>.
- Babadagli, T., Er, V., Naderi, K. et al. 2010. Use of Biodiesel as an Additive in Thermal Recovery of Heavy Oil and Bitumen. *J. Can. Pet. Technol.* **49**(11): 43-48. SPE-141302-PA. <https://doi.org/10.2118/141302-PA>.
- Baek, K. H., Sheng, K., Argüelles-Vivas, F. J. et al. 2019. Comparative Study of Oil-Dilution Capability of Dimethyl Ether and Hexane as Steam Additives for Steam-Assisted Gravity Drainage. *SPE Res. Eval. Eng.* **22**(3): 9–11. <https://doi.org/10.2118/187182-PA>.
- Bayestehparvin, B., Farouq Ali, S. M., and Abedi, J. 2019. Solvent-Based and Solvent-Assisted Recovery Processes: State of the Art. *SPE Res. Eval. Eng.* **22**(01): 29–49. SPE-179829-PA. <https://doi.org/10.2118/179829-PA>.
- Butler, R. M. 1985. A New Approach to The Modelling of Steam-Assisted Gravity Drainage. *J. Can. Petrol. Technol.* **24**(03): 42–51. <https://doi.org/10.2118/85-03-01>.
- Butler, R. 1999. The Steam and Gas Push (SAGP). *J. Can. Petrol. Technol.* **38**(03): 54–61. <https://doi.org/10.2118/99-03-05>.
- Bruns, F. and Babadagli, T. 2020a. Initial Screening of New Generation Chemicals Using Sandpack Flooding Tests for Recovery Improvement of Gravity Driven Steam Applications. *J. Pet. Sci. Eng.* **194**(April): 107462. <https://doi.org/10.1016/j.petrol.2020.107462>.
- Bruns, F. and Babadagli, T. 2020b. Heavy-Oil Recovery Improvement by Additives to Steam Injection: Identifying Underlying Mechanisms and Chemical Selection through Visual Experiments. *J. Pet. Sci. Eng.* **188**(May): 106897. <https://doi.org/10.1016/j.petrol.2019.106897>.
- Canadian Energy Research Institute (CERI). 2020. *Study No. 191: Canadian Oil Sands Production and Emissions Outlook (2020–2039)*. [https://ceri.ca/assets/files/Study\\_191\\_Full\\_Report.pdf](https://ceri.ca/assets/files/Study_191_Full_Report.pdf).
- Cao, N., Mohammed, M. A., and Babadagli, T. 2017. Wettability Alteration of Heavy-Oil-Bitumen-Containing Carbonates by Use of Solvents, High-pH Solutions, and Nano/Ionic Liquids. *SPE Res. Eval. and Eng.* **20**: 363-371. SPE-183646-PA. <http://doi.org/10.2118/183646-PA>.

- Chiwetelu, C. L., Neale, G. H., Hornof, V. et al. 1994. Recovery of a Saskatchewan Heavy Oil Using Alkaline Solutions. *J. Can. Petrol. Technol.* **33**(04). <https://doi.org/10.2118/94-04-05>.
- Collins, P. M. 1994. Design of the Monitoring Program for AOSTRA's Underground Test Facility, Phase B Pilot. *J. Can. Petrol. Technol.* **33**(03): 46–53. <https://doi.org/10.2118/94-03-06>.
- Collins, P. M. 2007. The False Lucre of Low-Pressure SAGD. *J. Can. Petrol. Technol.* **46**(01): 20–27. <https://doi.org/10.2118/07-01-02>.
- Deng, X. 2005. Recovery Performance and Economics of Steam/Propane Hybrid Process. Paper presented at SPE/PS-CIM/CHOA International Thermal Operations and Heavy Oil Symposium, Calgary, Alberta, Canada, 1–3 November. SPE/PS-CIM/CHOA 97760. <https://doi.org/10.2118/97760-MS>.
- Edmunds, N. and Chhina, H. 2001. Economic Optimum Operating Pressure for SAGD Projects in Alberta. *J. Can. Petrol. Technol.* **40**(12): 13–17. <https://doi.org/10.2118/01-12-DAS>
- Edmunds, N., and Gittins, S. D. 1993. Effective Application of Steam-Assisted Gravity Drainage of Bitumen to Long Horizontal Well Pairs. *J. Can. Petrol. Technol.* **32**(06): 49–55. <https://doi.org/10.2118/93-06-05>.
- Edmunds, N. R., Kovalsky, J. A., Gittins, S. D., et al. 1994. Review of Phase A Steam-Assisted Gravity-Drainage Test. *SPE Res. Eng.* **9**(02): 119–124. SPE-21529-PA. <https://doi.org/10.2118/21529-PA>.
- Fehr, A., Telmadarreie, A., Berton, P. et al. 2020. Synergy Between Commodity Molecules and Nanoparticles as Steam Mobility Control Additives for Thermal Oil Recovery. Paper presented at the SPE Annual Technical Conference and Exhibition, Virtual Event, 26–29 October. SPE-201442-MS. <https://doi.org/10.2118/201442-MS>.
- Ito, Y. 2014. Oil Drainage Characteristics during the SAGD Process to Explain Observed Field Performance. Paper Presented at the SPE Heavy Oil Conference, Calgary, Alberta, Canada, 10–12 June. SPE-170071-MS. <https://doi.org/10.2118/170071-MS>.
- Gupta, S. C., and Zeidani, K. 2013. Surfactant-Steam Process: An Innovative Enhanced Heavy Oil Recovery Method for Thermal Applications. Paper presented at the SPE Heavy Oil Conference, Calgary, Alberta, Canada, 11–13 June. SPE-165545-MS. <https://doi.org/10.2118/165545-MS>.

- Haas, T. W., Fadaei, H., Guerrero, U., et al. 2013. Steam-on-a-Chip for Oil Recovery: The Role of Alkaline Additives in Steam Assisted Gravity Drainage. *Lab Chip*. **13**(19): 3832–3839. <https://doi.org/10.1039/c3lc50612f>.
- Haddadnia, A., Zirrahi, M., Hassanzadeh, H. et al. 2018a. Dimethyl ether-A Promising Solvent for ES-SAGD. SPE Canada Heavy Oil Technical Conference, Calgary, Alberta, Canada, 13–14 March. <https://doi.org/10.2118/189741-MS>.
- Haddadnia, A., Azinfar, B., Zirrahi, M., et al. 2018b. Thermophysical Properties of Dimethyl Ether/Athabasca Bitumen System. *Can. J. Chem. Eng.* **96**(02): 597–604. <https://doi.org/10.1002/cjce.23009>.
- Hanamertani, A., Pilus, R., and Irawan, S. 2015. A Review on the Application of Ionic Liquids for Enhanced Oil Recovery. *Springer Singapore*. 133.147. ISBN: 978-981-287-367-5.
- Hashim Noori, W., Cinar, M., Salehian, M. et al. 2018. Experimental Investigation of Steam-Alkali Flooding with Borax: A Case Study on Bati Raman Oil Field. Paper presented at the SPE International Heavy Oil Conference and Exhibition, Kuwait City, Kuwait, 10–12 December. SPE-193797-MS. <https://doi.org/10.2118/193797-MS>.
- Huang, J. and Babadagli, T. 2020a. Efficiency Improvement of Heavy-Oil Recovery by Steam-Assisted Gravity Drainage Injection Using New Generation Chemicals. *Energy Fuels*. **34**(4): 4433–4447. <https://doi.org/10.1021/acs.energyfuels.0c00208>.
- Huang, J. and Babadagli, T. 2020b. Mechanics of SAGD Efficiency Improvement Using Combination of Chemicals: An Experimental Analysis through 2D Visual Models. *SPE Res. Eval. Eng.* In Press. SPE-199940-PA. <https://doi.org/10.2118/199940-PA>.
- Jiang, Q., Butler, R., and Yee, C. T. 2000. The Steam and Gas Push (SAGP)-2: Mechanism Analysis and Physical Model Testing. *J. Can. Petrol. Technol.* **39**(04): 52–61. <https://doi.org/10.2118/00-04-04>.
- Jimenez, J. 2008. The Field Performance of SAGD Projects in Canada. Paper presented in the International Petroleum Technology Conference (IPTC), Kuala Lumpur, Malaysia, 3–5 December. IPTC-12860. <https://doi.org/10.2523/IPTC-12860-MS>.

- Lee, J., Babadagli, T., and Ozum, B. 2018. Microemulsion Flooding of Heavy Oil Using Biodiesel Under Cold Conditions. SPE International Heavy Oil Conference and Exhibition, Kuwait City, Kuwait, 10–12 December. SPE-193642-MS. <http://doi.org/10.2118/193642-MS>.
- Lee, J., and Babadagli, T. 2021. Mitigating Greenhouse Gas Intensity Through New Generation Techniques During Heavy Oil Recovery. *J. Clean. Prod.* **286**(March): 124980. <https://doi.org/10.1016/j.jclepro.2020.124980>.
- Madhavan, R. M., and Mamora, D. D. 2010. Experimental Investigation of Caustic Steam Injection for Heavy Oils. Paper presented at the SPE Improved Oil Recovery Symposium, Tulsa, OK, USA, 24–28 April. SPE-129086-MS. <https://doi.org/10.2118/129086-MS>.
- Maghzi, A., Mohammadi, S., Ghazanfari, M. H. et al. 2012. Monitoring Wettability Alteration by Silica Nanoparticles during Water Flooding to Heavy Oils in Five-Spot Systems: A Pore-Level Investigation. *J. Exp. Therm. Flu. Sci.* **40**: 168–176. <http://doi.org/10.1016/j.expthermflusci.2012.03.004>.
- Mahmoud, M. A. and Abdelgawad, K. Z. 2015. Chelating-Agent Enhanced Oil Recovery for Sandstone and Carbonate Reservoirs. *SPE J.* **20**(03): 483–495. SPE-172183-PA. <http://dx.doi.org/10.2118/172183-PA>.
- Medina, O. E., Olmos, C., Lopera, S. H. et al. 2019. Nanotechnology Applied to Thermal Enhanced Oil Recovery Processes: A Review. *Energies* **12**(24): 4671. <https://doi.org/10.3390/en12244671>.
- Mohammed, M. A. and Babadagli, T. 2015. Wettability Alteration: A Comprehensive Review of Materials/Methods and Testing the Selected Ones on Heavy-Oil Containing Oil-Wet Systems. *Adv. Colloid Interface Sci.* **220**: 54–77. <https://doi.org/10.1016/j.cis.2015.02.006>.
- Mohammed, M. A. and Babadagli, T. 2016. Experimental Investigation of Wettability Alteration in Oil-Wet Reservoirs Containing Heavy Oil. *SPE Res. Eval. Eng.* **19**(04): 633–644. SPE-170034-PA. <https://doi.org/10.2118/170034-PA>.
- Mozhdehei, A., Hosseinpour, N., and Bahramian, A. 2019. Dimethylcyclohexylamine Switchable Solvent Interactions with Asphaltenes toward Viscosity Reduction and in Situ Upgrading of Heavy Oils. *Energy Fuels.* **33**(09): 8403–8412. <https://doi.org/10.1021/acs.energyfuels.9b01956>.

- Nasr, T. N., Beaulieu, G., Golbeck, et al. 2003. Novel Expanding Solvent-SAGD Process “ES-SAGD.” *J. Can. Petrol. Technol.* **42**(01): 13–16. <https://doi.org/10.2118/03-01-TN>.
- Orr, B. 2009. ES-SAGD: Past, Present, and Future. Paper presented at SPE Annual Technical Conference and Exhibition, New Orleans, Louisiana, USA, 4–7 October. SPE-129518-STU. <https://doi.org/10.2118/129518-STU>.
- Pratama, R. A., and Babadagli, T. 2020. Reconsideration of Steam Additives to Improve Heavy-Oil Recovery Efficiency: Can New Generation Chemicals be Solution for Steam Induced Unfavorable Wettability Alteration?. *Energy & Fuels* **34**(07): 8283–8300. <https://doi.org/10.1021/acs.energyfuels.0c01406>.
- Pratama, R. A. and Babadagli, T. 2021. New Formulation of Tertiary Amines for Thermally Stable and Cost-Effective Chemical Additive: Synthesis Procedure and Displacement Tests for High-Temperature Tertiary Recovery in Steam Applications. *SPE J.* In-Press. SPE-201769-PA. <https://doi.org/10.2118/201769-PA>.
- Pratama, R. A. and Babadagli, T. 2022. A Review of The Mechanics of Heavy-Oil Recovery by Steam Injection with Chemical Additives. *J. Petrol. Sci. Eng.* **208**(Part D): 109717. <https://doi.org/10.1016/j.petrol.2021.109717>.
- Pratama, R. A. and Babadagli, T. 2023. What is Next for SAGD?: Evaluation of Low GHG and High-Efficiency Tertiary Recovery Options. Submitted to *J. Petrol. Sci. Eng.* (Under Review).
- Rezk, M. Y., and Allam, N. K. 2019. Impact of Nanotechnology on Enhanced Oil Recovery: A Mini-Review. *Ind. Eng. Chem. Res.* **58**(36): 16287–16295. <https://doi.org/10.1021/acs.iecr.9b03693>.
- Shahbaz, M., Kevin, M., Sanchez, et al. 2012. The Effect of Bottom Water Coning and Its Monitoring for Optimization in SAGD. Paper presented in SPE Heavy Oil Conference, Calgary, Alberta, Canada, 12–14 June. SPE-157797-MS. <https://doi.org/10.2118/157797-MS>.
- Sugianto, S. and Butler, R. M. 1990. The Production of Conventional Heavy Oil Reservoirs with Bottom Water Using Steam-Assisted Gravity Drainage. *J. Can. Petrol. Technol.* **29**(02): 78–86. <https://doi.org/10.2118/90-02-03>.

- Sheng, K., Okuno, R. and Wang, M. 2018. Dimethyl Ether as an Additive to Steam for Improved Steam-Assisted Gravity Drainage. *SPE J.* **23**(04): 1201–1222. <https://doi.org/10.2118/184983-PA>.
- Taylor, S. 2018. Interfacial Chemistry in Steam-Based Thermal Recovery of Oil Sands Bitumen with Emphasis on Steam-Assisted Gravity Drainage and the Role of Chemical Additives. *Colloids Interfaces* **2**(02): 16. <https://doi.org/10.3390/colloids2020016>.
- Wagner, O. R. and Leach, R. O. 1959. Improving Oil Displacement Efficiency by Wettability Adjustment. *Transactions of the AIME* **216**: 65–72. SPE-1101-G. <http://doi.org/10.2118/1101-G>.
- Wang, J., Dong, M., and Arhuoma, M. 2010. Experimental and Numerical Study of Improving Heavy Oil Recovery by Alkaline Flooding in Sandpacks. *J. Can. Pet. Technol.* **49**(03): 51–57. <https://doi.org/10.2118/134248-PA>.
- Wei, Y. and Babadagli, T. 2017a. Selection of New Generation Chemicals as Steam Additive for Cost-Effective Heavy-Oil Recovery Applications. Paper presented at the SPE Canada Heavy Oil Technical Conference. SPE-184975-MS. <https://doi.org/10.2118/184975-MS>.
- Wei, Y. and Babadagli, T. 2017b. Alteration of Interfacial Properties by Chemicals and Nanomaterials to Improve Heavy Oil Recovery at Elevated Temperatures. *Energy Fuels*. **31**: 11866–11883. <http://doi.org/10.1021/acs.energyfuels.7b02173>.
- Wei, Y. and Babadagli, T. 2019. Changing Interfacial Tension and Wettability Using New Generation Chemicals and Nano Metal Particles at Elevated Temperatures and Pressures: An Analysis Through a New Experimental Design for Heavy-Oil Recovery Applications. *J. Disp. Sci. Technol.* **40**(12): 1785–1794. <https://doi.org/10.1080/01932691.2018.1542311>.

### Chapter 3

- Ahmadi, Y., Kharrat, R., Hashemi, A., et al. 2014. The Effect of Temperature and Pressure on The Reversibility of Asphaltene Precipitation. *J. Petrol. Sci. Technol.* **32** (18): 2263–2273. <https://doi.org/10.1080/10916466.2013.799180>.
- Al-Bahlani, A. M. and Babadagli, T. 2009. SAGD Laboratory Experimental and Numerical Simulation Studies: A Review of Current Status and Future Issues. *J. Pet. Sci. Eng.* **68**(3–4): 135–150. <https://doi.org/10.1016/j.petrol.2009.06.011>.
- Ali, S. M. F. 1974. Current Status of Steam Injection as a Heavy Oil Recovery Method. *J. Can. Pet. Technol.* **13**(1): 54–68. PETSOC-74-01-06. <https://doi.org/10.2118/74-01-06>.
- Ali, S. M. F. and Meldau, R. F. 1979. Current Steamflood Technology. *J. Pet. Technol.* **31**(10): 1332–1342. SPE-7183-PA. <https://doi.org/10.2118/7183-PA>.
- Alkindi, A., Al-Azri, N., Said, D. et al. 2016. Persistence in EOR - Design of a Field Trial in a Carbonate Reservoir using Solvent-based Water-Flood Process. SPE EOR Conference at Oil and Gas West Asia, Muscat, Oman, 21–23 March. SPE-179838-MS. <https://doi.org/10.2118/179838-MS>.
- Almubarak, T., Ng, J. H., and Nasr-El-Din, H. 2017. Chelating Agents in Productivity Enhancement: A Review. SPE Oklahoma City Oil and Gas Symposium, Oklahoma City, OK, USA, 27–31 March. SPE-185097-MS. <https://doi.org/10.2118/185097-MS>.
- Alomair, O. and Alajmi, A. 2016. Experimental Study for Enhancing Heavy Oil Recovery by Nanofluid Followed by Steam Flooding NFSF. Paper presented at the SPE Heavy Oil Conference and Exhibition, Kuwait City, Kuwait, 6–8 December. SPE-184117-MS. <https://doi.org/10.2118/184117-MS>.
- Alshaikh, M., Lee, Y. S., and Hascakir, B. 2019. Anionic Surfactant and Heavy Oil Interaction during Surfactant-Steam Process. Paper presented at the SPE Western Regional Meeting, San Jose, CA, USA, 23–26 April. SPE-195254-MS. <https://doi.org/10.2118/195254-MS>.
- Argüelles-Vivas, F., Babadagli, T., Little, L. et al. 2012. High Temperature Density, Viscosity, and Interfacial Tension Measurements of Bitumen–Pentane–Biodiesel and Process Water Mixtures. *J. Chem. Eng. Dat.* **57**(10): 2878–2889. <https://doi.org/10.1021/jc3008217>.

- Babadagli, T., Sahin, S., Kalfa, U., et al. 2009. Evaluation of Steam Injection Potential and Improving Ongoing CO<sub>2</sub> Injection of The Bati Raman Field, Turkey. *J. Pet. Sci. Eng.* **68**(1–2): 107–117. <https://doi.org/10.1016/j.petrol.2009.06.015>.
- Babadagli, T. and Ozum, B. 2010. Biodiesel as Surfactant Additive in Steam Assisted Recovery of Heavy Oil and Bitumen. SPE Western Regional Meeting, Anaheim, California, USA, 27–29 May. SPE-133376-MS. <https://doi.org/10.2118/133376-MS>.
- Babadagli, T., Er, V., Naderi, K. et al. 2010. Use of Biodiesel as an Additive in Thermal Recovery of Heavy Oil and Bitumen. *J. Can. Pet. Technol.* **49**(11): 43-48. SPE-141302-PA. <https://doi.org/10.2118/141302-PA>.
- Babadagli, T. 2020. Philosophy of EOR. *J. Pet. Sci. Eng.* **188**(November). <https://doi.org/10.1016/j.petrol.2020.106930>.
- Baek, K. H., Sheng, K., Argüelles-Vivas, F. J. et al. 2019. Comparative Study of Oil-Dilution Capability of Dimethyl Ether and Hexane as Steam Additives for Steam-Assisted Gravity Drainage. *SPE Res. Eval. Eng.* **22**(3): 9–11. <https://doi.org/10.2118/187182-PA>.
- Bata, T., Schamel, S., Fustic, M. et al. 2019. *Bitumen and Heavy Oil Committee Annual Commodity Report*. AAPG Energy Mineral Division. <https://www.aapg.org/Portals/0/docs/emd/reports/annual-meeting/2019-05-18/2019-05-19-AnnualMeetingCommitteeBitumen.pdf?ver=2019-05-15-132219-463>.
- Blevins, T. R., Duerksen, J. H., and Ault, J. W. 1984. Light-Oil Steamflooding: An Emerging Technology. *J. Pet. Technol.* **36**(7): 1115–1122. SPE-10928-PA. <https://doi.org/10.2118/10928-PA>.
- Blevins, T. R. 1990. Steamflooding in the U.S.: A Status Report. *J. Pet. Technol.* **42**(5): 548–554. SPE-20401-PA. <http://doi.org/10.2118/20401-PA>.
- Bruns, F. and Babadagli, T. 2020a. Initial Screening of New Generation Chemicals Using Sandpack Flooding Tests for Recovery Improvement of Gravity Driven Steam Applications. *J. Pet. Sci. Eng.* **194**(April): 107462. <https://doi.org/10.1016/j.petrol.2020.107462>.
- Bruns, F. and Babadagli, T. 2020b. Heavy-Oil Recovery Improvement by Additives to Steam Injection: Identifying Underlying Mechanisms and Chemical Selection through Visual

- Experiments. *J. Pet. Sci. Eng.* **188**(May): 106897.  
<https://doi.org/10.1016/j.petrol.2019.106897>.
- Canadian Energy Research Institute (CERI). 2017. *Study No. 164: Economic Potentials and Efficiencies of Oil Sands Operations: Processes and Technologies*.  
[https://ceri.ca/assets/files/Study\\_164\\_Full\\_Report.pdf](https://ceri.ca/assets/files/Study_164_Full_Report.pdf).
- Cao, N., Mohammed, M. A., and Babadagli, T. 2017. Wettability Alteration of Heavy-Oil-Bitumen-Containing Carbonates by Use of Solvents, High-pH Solutions, and Nano/Ionic Liquids. *SPE Res. Eval. and Eng.* **20**: 363-371. SPE-183646-PA.  
<http://doi.org/10.2118/183646-PA>.
- Castanier, L. M., Brigham, W. E. 1991. An Evaluation of Field Projects of Steam with Additives. *SPE Res. Eval. Eng.* **6**(01): 62–68. SPE-17633-PA. <https://doi.org/10.2118/17633-PA>.
- Chiwetelu, C. L., Neale, G. H., Hornof, V. et al. 1994. Recovery of a Saskatchewan Heavy Oil Using Alkaline Solutions. *J. Can. Petrol. Technol.* **33**(04). <https://doi.org/10.2118/94-04-05>.
- Cuenca, A., Lacombe, E., Morvan, M. et al. 2014. Design of Thermally Stable Surfactants Formulations for Steam Foam Injection. Presented at the SPE Heavy Oil Conference, Canada, Calgary, Alberta, 10–12 June. SPE-170129- MS. <http://doi.org/10.2118/170129-MS>.
- Bin Dahbag, M., AlQuraishi, A., and Benzagouta, M. 2015. Efficiency of Ionic Liquids for Chemical Enhanced Oil Recovery. *J. Pet. Expl. Prod. Technol.* **5**(04): 353–361.  
<https://doi.org/10.1007/s13202-014-0147-5>.
- De Haan, H. J. and Schenk, L. 1969. Performance Analysis of a Major Steam Drive Project in the Tia Juana Field, Western Venezuela. *J. Petrol. Technol.* **21**(01): 111–119.  
<https://doi.org/10.2118/1915-pa>.
- Du, X., Xi, C., Shi, L., et al. 2021. A Review on The Use of Chemicals as Steam Additives for Thermal Oil Recovery Applications. Paper presented at the ASME 2021 40<sup>th</sup> International Conference on Ocean, Offshore, and Arctic Engineering, Virtual Meeting, 21–30 June.
- El-Abbas, A., Shedid, S. 2001. Experimental Investigation of The Feasibility of Steam/Chemical Steam Flooding Processes Through Horizontal Wells. Presented at the SPE Asia Pacific Oil

- and Gas Conference and Exhibition, Jakarta, Indonesia, 17–19 April. SPE-68767-MS. <https://doi.org/10.2118/68767-MS>.
- Evdokimov, S. I., Gerasimenko, T. E., and Evdokimov, V. S. 2018. Temperature Impact on the Stability of Wetting Water Films on Quartz Surfaces. *Glass and Ceramics* **75**(3–4): 102–107. <https://doi.org/10.1007/s10717-018-0037-2>.
- Fehr, A., Telmadarreie, A., Berton, P. et al. 2020. Synergy Between Commodity Molecules and Nanoparticles as Steam Mobility Control Additives for Thermal Oil Recovery. Paper presented at the SPE Annual Technical Conference and Exhibition, Virtual Event, 26–29 October. SPE-201442-MS. <https://doi.org/10.2118/201442-MS>.
- Fair, D. R., Trudell, C. L., Boone, T. J. et al. 2008. Cold Lake Heavy Oil Development - A Success Story in Technology Application. Paper presented at the International Petroleum Technology Conference, Kuala Lumpur, Malaysia, 3–5 December. IPTC-12361. <https://doi.org/10.3997/2214-4609-pdb.148.iptc12361>.
- Flury, C., Afacan, A., Tamiz Bakhtiari et al. 2014. Effect of Caustic Type on Bitumen Extraction from Canadian Oil Sands. *Energy Fuels* **28**(01): 431–438. <https://doi.org/10.1021/ef4017784>.
- Friedmann, F., Smith, M., Guice, W. et al. 1994. Steam-Foam Mechanistic Field Trial in The Midway-Sunset Field. *SPE Res. Eval. Eng.* **9**(4): 297–304. SPE-21780-PA. <https://doi.org/10.2118/21780-PA>.
- Fuaadi, I. M., Pearce, J. C., and Gael, B. T. 1991. Evaluation of Steam-Injection Designs for the Duri Steamflood Project. Paper presented at the SPE Asia-Pacific Conference, Perth, Australia, 4–7 November. SPE-22995-MS. <https://doi.org/10.2118/22995-MS>.
- Gael, B. T., Putro, E. S., and Masykur, A. 1994. Reservoir Management in the Duri Steamflood. Paper presented at the SPE/DOE Improved Oil Recovery Symposium, Tulsa, OK, USA, 17–20 April. SPE-27764-MS. <https://doi.org/10.2118/27764-MS>.
- Gates, I. D. and Wang, J. 2011. Evolution of In Situ Oil Sands Recovery Technology: What Happened and What’s New? Paper presented at the SPE International Heavy Oil Conference and Exhibition, Kuwait City, Kuwait, 12–14 December. SPE-150686-MS. <https://doi.org/10.2118/150686-MS>.

- Glandt, C. A., and Chapman, W. G. 1995. The Effect of Water Dissolution on Oil Viscosity. *SPE Res. Eval. Eng.* **10**(01): 59–64. SPE-24631-PA. <https://doi.org/10.2118/24631-PA>.
- Gupta, S. C., and Zeidani, K. 2013. Surfactant-Steam Process: An Innovative Enhanced Heavy Oil Recovery Method for Thermal Applications. Paper presented at the SPE Heavy Oil Conference, Calgary, Alberta, Canada, 11–13 June. SPE-165545-MS. <https://doi.org/10.2118/165545-MS>.
- Haas, T. W., Fadaei, H., Guerrero, U., et al. 2013. Steam-on-a-Chip for Oil Recovery: The Role of Alkaline Additives in Steam Assisted Gravity Drainage. *Lab Chip.* **13**(19): 3832–3839. <https://doi.org/10.1039/c3lc50612f>.
- Haddadnia, A., Zirrahi, M., Hassanzadeh, H. et al. 2018a. Dimethyl ether-A Promising Solvent for ES-SAGD. SPE Canada Heavy Oil Technical Conference, Calgary, Alberta, Canada, 13–14 March. <https://doi.org/10.2118/189741-MS>.
- Haddadnia, A., Azinfar, B., Zirrahi, M., et al. 2018b. Thermophysical Properties of Dimethyl Ether/Athabasca Bitumen System. *Can. J. Chem. Eng.* **96**(02): 597–604. <https://doi.org/10.1002/cjce.23009>.
- Haghighi, M. and Yortsos, Y. C. 1997. Visualization of Steam Injection in Fractured Systems Using Micromodels. Paper presented at the International Thermal Operations and Heavy Oil Symposium, Bakersfield, CA, USA, 10–12 February. SPE-37520-MS. <https://doi.org/10.2523/37520-MS>.
- Hall, A. L., and Bowman, R. W. 1970. Operation and Performance of Slocum Field Thermal Recovery Project. Paper presented at the SPE Practical Aspects of Improved Recovery Techniques Symposium, Fort Worth, TX, USA, 8–9 March. SPE-2843-MS. <https://doi.org/10.2118/2843-ms>.
- Hammami, A., Phelps, C.H., Monger-McClure, T., et al. 2000. Asphaltene Precipitation from Live Oils: An Experimental Investigation of Onset Conditions and Reversibility. *Energy Fuels.* **14**(1): 14–18. <https://doi.org/10.1021/ef990104z>.

- Handy, L. L., Amaefule, J. O., Ziegler, V. M., et al. 1982. Thermal Stability of Surfactants for Reservoir Application. *SPE J.* **22**(05): 722–730. SOE-7867-PA. <https://doi.org/10.2118/7867-PA>.
- Hanamertani, A., Pilus, R., and Irawan, S. 2015. A Review on the Application of Ionic Liquids for Enhanced Oil Recovery. *Springer Singapore*. 133.147. ISBN: 978-981-287-367-5.
- Hanzlik, E. J. and Mims, D. S. 2003. Forty Years of Steam Injection in California - The Evolution of Heat Management. Paper presented at the SPE International Improved Oil Recovery Conference, Kuala Lumpur, Malaysia, 20–21 October. SPE-84848-MS. <https://doi.org/10.2523/84848-ms>.
- Harmsen, G. J. 1979. Steam Flooding in a Water Drive Reservoir in The Schoonebeek Field in The Netherlands. Paper presented at the 10<sup>th</sup> World Petroleum Congress Proceedings, Bucharest, Romania, 9–14 September. WPC-18233.
- Hashim Noori, W., Cinar, M., Salehian, M. et al. 2018. Experimental Investigation of Steam-Alkali Flooding with Borax: A Case Study on Bati Raman Oil Field. Paper presented at the SPE International Heavy Oil Conference and Exhibition, Kuwait City, Kuwait, 10–12 December. SPE-193797-MS. <https://doi.org/10.2118/193797-MS>.
- Hirasaki, G. J. 1991. Wettability: Fundamentals and Surface Forces. *SPE Form. Eval.* **6**(02): 217–226. SPE-17367-PA. <https://doi.org/10.2118/17367-PA>.
- Huang, W.S., Gassmann, Z.Z, Hawkins, J. et al. 1985. Method of Improving Conformance in Steam Floods with Carboxylate Steam Foaming Agents. United States Patent Number: US4540050A.
- Huang, H., Babadagli, T., Chen, X. et al. 2020. Performance Comparison of Novel Chemical Agents in Improving Oil Recovery from Tight Sands through Spontaneous Imbibition. *Pet. Sci.* **17**(2): 409–418. <https://doi.org/10.1007/s12182-019-00369-1>.
- Huang, J. and Babadagli, T. 2020a. Efficiency Improvement of Heavy-Oil Recovery by Steam-Assisted Gravity Drainage Injection Using New Generation Chemicals. *Energy Fuels.* **34**(4): 4433–4447. <https://doi.org/10.1021/acs.energyfuels.0c00208>.

- Huang, J. and Babadagli, T. 2020b. Mechanics of SAGD Efficiency Improvement Using Combination of Chemicals: An Experimental Analysis through 2D Visual Models. *SPE Res. Eval. Eng.* In Press. SPE-199940-PA. <https://doi.org/10.2118/199940-PA>.
- Hoffman, B. T. and Kovsky, A. R. 2004. Efficiency and Oil Recovery Mechanisms of Steam Injection into Low Permeability, Hydraulically Fractured Reservoirs. *Pet. Sci. Technol.* **22**(5–6): 537–564. <https://doi.org/10.1081/LFT-120034187>.
- Hogshead, C. G., Manias, E., Williams, P. et al. 2011. Studies of Bitumen–Silica and Oil–Silica Interactions in Ionic Liquids. *Energy Fuels.* **25**(01): 293–299. <https://doi.org/10.1021/ef101404k>.
- Holland, A., Wechsler, D., Patel, A. et al. 2012. Separation of Bitumen from Oil Sands Using a Switchable Hydrophilicity Solvent. *Can. J. Chem.* **90**(10): 805–810. <https://doi.org/10.1139/v2012-061>.
- Ito, Y. 2014. Oil Drainage Characteristics during the SAGD Process to Explain Observed Field Performance. Paper presented at the SPE Heavy Oil Conference-Canada, Alberta, Canada, 10–12 June. SPE-170071-MS. <https://doi.org/10.2118/170071-MS>.
- Issever, K., Pamir, A. N., Tirek, A. 1993. Performance of a Heavy-Oil Field Under CO<sub>2</sub> Injection, Bati Raman, Turkey. *SPE. Res. Eval. Eng.* **8**(04): 256–260. SPE-20883-PA. <https://doi.org/10.2118/20883-PA>.
- Jessup, R. S. 1930. Compressibility and Thermal Expansion of Petroleum Oils in the Range 0 Degrees to 300 Degrees C. *Bur. Stand. J. Res.* **5**(05): 985. <https://doi.org/10.6028/jres.005.062>.
- Jimenez, J. 2008. The Field Performance of SAGD Projects in Canada. Paper presented at the International Petroleum Technology Conference, Kuala Lumpur, Malaysia, 3–5 December. IPTC-12860-MS. <https://doi.org/10.2523/iptc-12860-ms>.
- Jones, J., McWilliams, M., and Sturm, D. 1995. Kern River Revisited: Life After Steam Flood. Paper presented at the SPE Western Regional Meeting, Bakersfield, CA, USA, 8–10 March. SPE-29664-MS. <http://dx.doi.org/10.2118/29664-MS>.

- Keshavarz, M., Okuno, R., and Babadagli, T. 2015. Optimal Application Conditions for Steam/Solvent Coinjection. *SPE Res. Eval. & Eng.* **18**(01): 20–38. SPE-165471-PA. <https://doi.org/10.2118/165471-PA>.
- Khatib, Ala K., Earlougher, R.C., and Kutluyil Kantar. 1981. CO<sub>2</sub> Injection as an Immiscible Application for Enhanced Recovery in Heavy Oil Reservoirs. Paper presented at the SPE California Regional Meeting, Bakersfield, California, USA, 25–26 March, SPE-9928. <https://doi.org/10.2118/9928-MS>.
- Lau, H. C., Borchardt, J. K. 1991. Improved Steam-Foam Formulations: Concepts and Laboratory Results. *SPE Res. Eval. Eng.* **6**(04): 470–476.
- Lee, J., Babadagli, T., and Ozum, B. 2018. Microemulsion Flooding of Heavy Oil Using Biodiesel Under Cold Conditions. SPE International Heavy Oil Conference and Exhibition, Kuwait City, Kuwait, 10–12 December. SPE-193642-MS. <http://doi.org/10.2118/193642-MS>.
- Lee, J., and Babadagli, T. 2021. Mitigating Greenhouse Gas Intensity Through New Generation Techniques During Heavy Oil Recovery. *J. Clean. Prod.* **286**(March): 124980. <https://doi.org/10.1016/j.jclepro.2020.124980>.
- Leyva-Gomez, H., Babadagli, T. 2017. High-Temperature Solvent Injection for Heavy-Oil Recovery from Oil Sands: Determination of Optimal Application Conditions Through Genetic Algorithm. *SPE Res. Eval. & Eng.* **20**(02): 372–382. SPE-183638-PA. <https://doi.org/10.2118/183638-PA>.
- Li, S., Qiao, C., Ji, G. et al. 2019. Experimental Study of Profile Control with Foam Stabilized by Clay Particle and Surfactant. *Energies.* **12**(5): 781. <https://doi.org/10.3390/en12050781>.
- Madhavan, R. M., and Mamora, D. D. 2010. Experimental Investigation of Caustic Steam Injection for Heavy Oils. Paper presented at the SPE Improved Oil Recovery Symposium, Tulsa, OK, USA, 24–28 April. SPE-129086-MS. <https://doi.org/10.2118/129086-MS>.
- Maghzi, A., Mohammadi, S., Ghazanfari, M. H. et al. 2012. Monitoring Wettability Alteration by Silica Nanoparticles during Water Flooding to Heavy Oils in Five-Spot Systems: A Pore-Level Investigation. *J. Exp. Therm. Flu. Sci.* **40**: 168–176. <http://doi.org/10.1016/j.expthermflusci.2012.03.004>.

- Mahmoud, M. A. and Abdelgawad, K. Z. 2015. Chelating-Agent Enhanced Oil Recovery for Sandstone and Carbonate Reservoirs. *SPE J.* **20**(03): 483–495. SPE-172183-PA. <http://dx.doi.org/10.2118/172183-PA>.
- Masliyah, J. H., Czarnecki, J., and Xu, Z. 2011. *Handbook on Theory and Practice of Bitumen Recovery from Athabasca Oil Sands Volume I: Theoretical Basis*, 323–343. Cochrane, Alberta, Canada: Kingsley Knowledge Publishing.
- Medina, O. E., Olmos, C., Lopera, S. H. et al. 2019. Nanotechnology Applied to Thermal Enhanced Oil Recovery Processes: A Review. *Energies* **12**(24): 4671. <https://doi.org/10.3390/en12244671>.
- Mohammed, M. A. and Babadagli, T. 2015. Wettability Alteration: A Comprehensive Review of Materials/Methods and Testing the Selected Ones on Heavy-Oil Containing Oil-Wet Systems. *Adv. Colloid Interface Sci.* **220**: 54–77. <https://doi.org/10.1016/j.cis.2015.02.006>.
- Mohammed, M. A. and Babadagli, T. 2016. Experimental Investigation of Wettability Alteration in Oil-Wet Reservoirs Containing Heavy Oil. *SPE Res. Eval. Eng.* **19**(04): 633–644. SPE-170034-PA. <https://doi.org/10.2118/170034-PA>.
- Mohammedalmojtaba, M., Lin, L., Istratescu, G., et al. 2020. Underlying Physics of Heavy Oil Recovery by Gas Injection: An Experimental Parametric Analysis when Oil Exists in The Form of Oil Based Emulsion. *Chem. Eng. Res. Des.* **163**: 192–203. <https://doi.org/10.1016/j.cherd.2020.09.003>
- Mohsenzadeh, A., Al-Wahaibi, Y., Jibril, A. et al. 2015. The Novel Use of Deep Eutectic Solvents for Enhancing Heavy Oil Recovery. *J. Pet. Sci. Eng.* **130**: 6–15. <https://doi.org/10.1016/j.petrol.2015.03.018>.
- Mohsenzadeh, A., Al-Wahaibi, Y., Al-Hajri, R. et al. 2015. Sequential Deep Eutectic Solvent and Steam Injection for Enhanced Heavy Oil Recovery and In-Situ Upgrading. *Fuel* **187**(2017): 417–428. <http://dx.doi.org/10.1016/j.fuel.2016.09.077>.

- Moore, T. F. and Slobod, R. L. 1955. Displacement of Oil by Water-Effect of Wettability, Rate, and Viscosity on Recovery. Proceedings of Fall Meeting of the Petroleum Branch of AIME, New Orleans, LA, USA, 2–5 October. <https://doi.org/10.2523/502-G>.
- Mozhdehei, A., Hosseinpour, N., and Bahramian, A. 2019. Dimethylcyclohexylamine Switchable Solvent Interactions with Asphaltenes toward Viscosity Reduction and in Situ Upgrading of Heavy Oils. *Energy Fuels*. **33**(09): 8403–8412. <https://doi.org/10.1021/acs.energyfuels.9b01956>.
- Mujis, H., Keijzer, P., Wiersma, R. 1988. Surfactants For Mobility Control in High-Temperature Steam-Foam Applications. Presented at the SPE Enhanced Oil Recovery Symposium, Tulsa, Oklahoma, USA, 16–21 April. SPE-17361-MS. <https://doi.org/10.2118/17361-MS>.
- Mukherjee, B., Patil, P., Gao, M. et al. 2018. Laboratory Evaluation of Novel Surfactant for Foam Assisted Steam EOR Method to Improve Conformance Control for Field Applications. Presented at the SPE Improved Oil Recovery Conference, Tulsa, Oklahoma, 14–18 April. SPE-190263-MS. <https://doi.org/10.2118/190263-MS>.
- Naderi, K. and Babadagli, T. 2012. Use of CO<sub>2</sub> as Solvent During Steam-Over-Solvent Injection in Fractured Reservoirs (SOS-FR) Method for Heavy Oil Recovery from Sandstones and Carbonates. Paper presented in the International Petroleum Technology Conference (IPTC), Bangkok, Thailand, 15-17 November. IPTC-14918-MS. <https://doi.org/10.2523/IPTC-14918-MS>.
- Naderi, K., Babadagli, T., and Coskuner, G. 2013. Bitumen Recovery by the SOS-FR (Steam-Over-Solvent Injection in Fractured Reservoirs) Method: An Experimental Study on Grosmont Carbonates. Paper presented in the SPE Heavy Oil Conference, Calgary, Alberta, Canada, 11-13 June. SPE-165530-MS. <https://doi.org/10.2118/165530-MS>.
- Naderi, K. and Babadagli, T. 2015. Solvent Selection Criteria and Optimal Application Conditions for Heavy-Oil/Bitumen Recovery at Elevated Temperatures: A Review and Comparative Analysis. *J. Energy Resour. Technol.* **138**(1): 012904. <https://doi.org/10.1115/1.4031453>.
- Nasr, T., Beaulieu, G., Golbeck, H., et al. 2003. Novel Expanding Solvent-SAGD Process “ES-SAGD”. *J. Can. Petrol. Technol.* **42**(1): 13–16. PETSOC-03-01-TN. <https://doi.org/10.2118/03-01-TN>.

- Nguyen, T., Rommerskirchen, R., Fernandez, J. et al. 2018. Surfactants as Steam Foam Additives for Thermal EOR Processes. Presented at the SPE EOR Conference at Oil and Gas West Asia, Muscat, Oman, 26–28 March. SPE-190473- MS. <https://doi.org/10.2118/190473-MS>.
- Nguyen, T., Raj, A., Rommerskirchen, R. et al. 2019. Development of Structure-Property Relationships for Steam Foam Additives for Heavy Oil Recovery. Presented at the SPE International Conference on Oilfield Chemistry, Galveston, Texas, USA, 8–9 April. SPE-193634-MS. <https://doi.org/10.2118/193634-MS>.
- Osterloh, W., Jante, M. 1994. Evaluation of Tall Oil Fatty Acid Salt as a Steam/Foam Surfactant. Presented at the SPE/DOE Improved Oil Recovery Symposium, Tulsa, Oklahoma, USA, 17–20 April. SPE-27776-MS. <https://doi.org/10.2118/27776-MS>.
- Pathak, V., Babadagli, T., and Edmunds, N. 2012. Mechanics Of Heavy Oil and Bitumen Recovery by Hot Solvent Injection. *SPE Res. Eval. Eng.* **15**(2): 182–194. SPE-144546-PA. <https://doi.org/10.2118/144546-PA>.
- Pratama, R. A., and Babadagli, T. 2020a. Effect of Temperature, Phase Change, and Chemical Additive on Wettability Alteration during Steam Applications in Sands and Carbonates. *SPE Res. Eval. and Eng.* **23**(01): 292–310. <http://doi.org/10.2118/191188-PA>.
- Pratama, R. A., and Babadagli, T. 2020b. Reconsideration of Steam Additives to Improve Heavy-Oil Recovery Efficiency: Can New Generation Chemicals be Solution for Steam Induced Unfavorable Wettability Alteration? *Energy & Fuels* **34**(07): 8283–8300. <https://doi.org/10.1021/acs.energyfuels.0c01406>.
- Pratama, R. A., and Babadagli, T. 2020c. Wettability State and Phase Distributions during Steam Injection with and without Chemical Additives: An Experimental Analysis Using Visual Micromodels. *SPE Res. Eval. Eng.* **23**(03): 1133–1149. <https://doi.org/10.2118/196253-PA>.
- Pratama, R. A. and Babadagli, T. 2020d. Tertiary-Recovery Improvement of Steam Injection Using Chemical Additives: Pore-Scale Understanding of Challenges and Solutions Through Visual Experiments. *SPE J.* In-Press. SPE-200841-PA. <https://doi.org/10.2118/200841-PA>.
- Pratama, R. A. and Babadagli, T. 2021. New Formulation of Tertiary Amines for Thermally Stable and Cost-Effective Chemical Additive: Synthesis Procedure and Displacement Tests for

- High-Temperature Tertiary Recovery in Steam Applications. *SPE J.* In-Press. SPE-201769-PA. <https://doi.org/10.2118/201769-PA>.
- Prats, Michael. 1982. *Thermal Recovery*, Vol. 7: 16–19. Richardson, Texas: Monograph Series, SPE.
- Punase, A., Zou, A., and Elputranto, R. 2014. How Do Thermal Recovery Methods Affect Wettability Alteration? *J. Pet. Eng.* 2014: 1–9. <https://doi.org/10.1155/2014/538021>.
- Ratnakar, R. R., Dindoruk, B., and Wilson, L. 2016. Experimental Investigation of DME–Water–Crude Oil Phase Behavior and PVT Modeling for the Application of DME-Enhanced Waterflooding. *Fuel* **182**: 188–197. <https://doi.org/10.1016/j.fuel.2016.05.096>.
- Rezk, M. Y., and Allam, N. K. 2019. Impact of Nanotechnology on Enhanced Oil Recovery: A Mini-Review. *Ind. Eng. Chem. Res.* **58**(36): 16287–16295. <https://doi.org/10.1021/acs.iecr.9b03693>.
- Sahin, S., Kalfa, U., Celebioglu, D. 2008. Bati Raman Field Immiscible CO<sub>2</sub> Application—Status Quo and Future Plans. *SPE Res. Eval. Eng.* **11**(04): 778–791. SPE-106575-PA. <https://doi.org/10.2118/106575-PA>.
- Seng, L. Y., and Hascakir, B. 2021. Role of Intermolecular Forces on Surfactant-Steam Performance into Heavy Oil Reservoirs. *SPE J.* In-Press. SPE-201513-PA. <https://doi.org/10.2118/201513-PA>.
- Silalahi, H., Aji, M., Elisa, A. et al. 2019. Advancing Steamflood Performance Through a New Integrated Optimization Process: Transform the Concept into Practical. Paper presented at the SPE/IATMI Asia Pacific Oil and Gas Conference and Exhibition, Bali, Indonesia, 29–31 October. SPE-196249-MS. <https://doi.org/10.2118/196249-ms>.
- Shallcross, D., Castanier, L., Brigham, W. 1990. Characterization Of Steam Foam Surfactants Through One-Dimensional Sandpack Experiments. *Technical Report*. U.S. Department of Energy Office of Scientific and Technical Information
- Sheng, J. J. 2013. *Enhanced Oil Recovery Field Case Studies*. Waltham, Massachusetts, USA: Gulf Professional Publishing.

- Sheng, K., Okuno, R. and Wang, M. 2018. Dimethyl Ether as an Additive to Steam for Improved Steam-Assisted Gravity Drainage. *SPE J.* **23**(04): 1201–1222. <https://doi.org/10.2118/184983-PA>.
- Shepherd, A. G., Mcgregor, S., Trompert, R. et al. 2012. Integrated Production Chemistry Management of the Schoonebeek Heavy Oil Redevelopment in the Netherlands: From Project to Start-Up and Steady State Production. Paper presented at the SPE Heavy Oil Conference Canada, Calgary, Alberta, Canada, 12–14 June. <https://doi.org/10.2118/150635-MS>.
- Shilov, E., Cheremisin, A., Maksakov, K., et al. 2019. Huff-n-Puff Experimental Studies of CO<sub>2</sub> with Heavy Oil. *Energies*. **12**: 4308. <https://doi.org/10.3390/en12224308>.
- Speight, J. G. 2009. *Enhanced Recovery Methods for Heavy Oil and Tar Sands*. Gulf Professional Publishing.
- Taylor, S. 2018. Interfacial Chemistry in Steam-Based Thermal Recovery of Oil Sands Bitumen with Emphasis on Steam-Assisted Gravity Drainage and the Role of Chemical Additives. *Colloids Interfaces* **2**(02): 16. <https://doi.org/10.3390/colloids2020016>.
- Van Dijk, C. 1968. Steam-Drive Project in the Schoonebeek Field, The Netherlands. *J. Pet. Technol.* **20**(03): 295–302. <https://doi.org/10.2118/1917-PA>.
- Wagner, O. R. and Leach, R. O. 1959. Improving Oil Displacement Efficiency by Wettability Adjustment. *Transactions of the AIME* **216**: 65–72. SPE-1101-G. <http://doi.org/10.2118/1101-G>.
- Wang, J., Dong, M., and Arhuoma, M. 2010. Experimental and Numerical Study of Improving Heavy Oil Recovery by Alkaline Flooding in Sandpacks. *J. Can. Pet. Technol.* **49**(03): 51–57. <https://doi.org/10.2118/134248-PA>.
- Wei, Y. and Babadagli, T. 2017a. Selection of New Generation Chemicals as Steam Additive for Cost-Effective Heavy-Oil Recovery Applications. Paper presented at the SPE Canada Heavy Oil Technical Conference. SPE-184975-MS. <https://doi.org/10.2118/184975-MS>.
- Wei, Y. and Babadagli, T. 2017b. Alteration of Interfacial Properties by Chemicals and Nanomaterials to Improve Heavy Oil Recovery at Elevated Temperatures. *Energy Fuels*. **31**: 11866–11883. <http://doi.org/10.1021/acs.energyfuels.7b02173>.

- Wei, Y. and Babadagli, T. 2019. Changing Interfacial Tension and Wettability Using New Generation Chemicals and Nano Metal Particles at Elevated Temperatures and Pressures: An Analysis Through a New Experimental Design for Heavy-Oil Recovery Applications. *J. Disp. Sci. Technol.* **40**(12): 1785–1794. <https://doi.org/10.1080/01932691.2018.1542311>.
- Winderasta, W., Lestari, E. S., Budiman, A. et al. 2018. Managing Reservoir Surveillance in the Duri Steam Flood Field. Paper presented at Indonesian Petroleum Association Forty-Second Annual Convention & Exhibition, Jakarta, Indonesia, 2–4 May. [http://archives.datapages.com/data/ipa\\_pdf/2018/IPA18-577-E](http://archives.datapages.com/data/ipa_pdf/2018/IPA18-577-E).
- Xu, Z., Li, Z., Li, B., et al. 2020. Investigation of the Heat Transfer Mechanism of CO<sub>2</sub>-Assisted Steam Injection via Experimental and Simulation Evaluation. *Front. Energy. Res.* **8**: 592142. <https://doi.org/10.3389/fenrg.2020.592142>.
- Yuan, J.Y., Law, D. H. S., and Nasr, T. N. 2006. Impacts of Gas on SAGD: History Matching of Lab Scale Tests. *J. Can. Pet. Technol.* **45**(01). <https://doi.org/10.2118/06-01-01>.
- Zhao, L., Law, D. H.-S., Nasr, T. N. et al. 2003. SAGD Wind-Down: Lab Test and Simulation. *J. Can. Pet. Technol.* **44**(01). <https://doi.org/10.2118/05-01-04>.
- Zhao, Y. 2020. Laboratory Experiment and Field Application of High Pressure and High-Quality Steam Flooding. *J. Pet. Sci. Eng.* **189**(February): 107016. <https://doi.org/10.1016/j.petrol.2020.107016>.

## Chapter 4

- Amyx, J. W., Bass, D. M., and Whiting, R. L. 1960. Petroleum Reservoir Engineering: Physical Properties. *McGraw-Hill Book Company, Inc.* 36-38. ISBN 10: 0070016003/ISBN 13: 9780070016002.
- Baker, R. O., Jensen, J. L., and Yarranton, H. W. 2015. *Practical Reservoir Engineering and Characterization*. Gulf Professional Publishing. 239–295. ISBN: 978-0-12-801811-8.
- Blevins, T. R., Duerksen, J. H., and Ault, J. W. 1984. Light-Oil Steamflooding an Emerging Technology. *J. Petrol. Technol.* **36**(7): 1115–1122. <https://doi.org/10.2118/10928-PA>.
- Boyd, A. R., Champagne, P., McGinn, P. J. et al. 2012. Switchable Hydrophilicity Solvents for Lipid Extraction from Microalgae for Biofuel Production. *J. Biortech.* **118**: 628–632. <https://doi.org/10.1016/j.biortech.2012.05.084>.
- Bruns, F., and Babadagli, T. 2020a. Initial Screening of New Generation Chemicals Using Sandpack Flooding Tests for Recovery Improvement of Gravity Driven Steam Applications. *J. Pet. Sci. Eng.* **194**(April 2019): 107462. <https://doi.org/10.1016/j.petrol.2020.107462>.
- Bruns, F., and Babadagli, T. 2020b. Heavy-Oil Recovery Improvement by Additives to Steam Injection: Identifying Underlying Mechanisms and Chemical Selection through Visual Experiments. *J. Pet. Sci. Eng.* **188**(December 2019): 106897. <https://doi.org/10.1016/j.petrol.2019.106897>.
- Butler, R. M. 1994. Horizontal Wells for the Recovery of Oil, Gas, and Bitumen. In SPE Monograph Series, Vol. 2, pp. 169-199, Richardson, Texas: Society of Petroleum Engineers.
- Du, Y., Schuur, B., Kersten, S. R. A. et al. 2015. Opportunities For Switchable Solvents for Lipid Extraction from Wet Algal Biomass: An Energy Evaluation. *J. Algal.* **11**: 271–283. <https://doi.org/10.1016/j.algal.2015.07.004>.
- Durelle, J., Vanderveen, J. R., Quan, Y. et al. 2015. Extending the Range of Switchable-Hydrophilicity Solvents. *Phys. Chem. Chem. Phys.* **17**(7): 5308–5313. <https://doi.org/10.1039/C4CP05313C>.

- Fu, D., Farag, S., Chaouki, J. et al. 2014. Extraction Of Phenols from Lignin Microwave-Pyrolysis Oil Using a Switchable Hydrophilicity Solvent. *J. Biortech.* **154**: 101–108. <https://doi.org/10.1016/j.biortech.2013.11.091>.
- Huang, J. and Babadagli, T. 2020. Efficiency Improvement of Heavy-Oil Recovery by Steam-Assisted Gravity Drainage Injection Using New Generation Chemicals. *Energy & Fuels.* **34**(4): 4433–4447. <https://doi.org/10.1021/acs.energyfuels.0c00208>.
- Huygens, R. J. M., Boersma, D. M., Ronde, H. et al. 1995. Interfacial Tension Measurement of Oil/Water/Steam Systems Using Image Processing Techniques. *SPE. Adv. Tech.* **3**(1): 129–138. SPE-24169-PA. <http://dx.doi.org/10.2118/24169-PA>.
- Holland, A., Wechsler, D., Patel, A. et al. 2012. Separation Of Bitumen from Oil Sands Using a Switchable Hydrophilicity Solvent. *J. Can. Chem.* **90**(10): 805–810. <https://doi.org/10.1139/v2012-061>.
- Jessop, P. G., Phan, L., Carrier, A. et al. 2010. A Solvent Having Switchable Hydrophilicity. *Green Chem.* **12**(5): 809. <https://doi.org/10.1039/b926885e>.
- Jessop, P. G., Kozycz, L., Rahami, Z. G. et al. 2011. Tertiary Amine Solvents Having Switchable Hydrophilicity. *Green Chem.* **13**(3): 619–623. <https://doi.org/10.1039/c0gc00806k>.
- Li, X., Hou, J., Sui, H. et al. 2018. Switchable-Hydrophilicity Triethylamine: Formation and Synergistic Effects of Asphaltenes in Stabilizing Emulsions Droplets. *Materials.* **11**(12): 2431. <https://doi.org/10.3390/ma11122431>.
- Masliyah, J. H., Czarnecki, J., and Xu, Z. 2011. *Handbook on Theory and Practice of Bitumen Recovery from Athabasca Oil Sands Volume I: Theoretical Basis*. Kingsley Knowledge Publishing. 323-343. ISBN: 978-1-926832-03-6.
- Meyer, R. F., Attanasi, E. D., and Freeman, P. A. 2007. *Heavy Oil and Natural Bitumen Resources in Geological Basins of the World*. U.S. Geological Survey Open-File Report 2007–1084. <http://pubs.usgs.gov/of/2007/1084>.

- Moore, T. F. and Slobod, R. L. 1955. Displacement of Oil by Water-Effect of Wettability, Rate, and Viscosity on Recovery. Proceedings of Fall Meeting of the Petroleum Branch of AIME, New Orleans, Louisiana, 2–5 October. <https://doi.org/10.2523/502-G>.
- Mozhdehei, A., Hosseinpour, N., and Bahramian, A. 2019. Dimethylcyclohexylamine Switchable Solvent Interactions with Asphaltenes toward Viscosity Reduction and in Situ Upgrading of Heavy Oils. *Energy Fuels*. **33**(9): 8403–8412. <https://doi.org/10.1021/acs.energyfuels.9b01956>.
- Naser, M. A., Permadi, A. K., Bae, W. et al. 2015. A Laboratory Investigation of the Effects of Saturated Steam Properties on the Interfacial Tension of Heavy-Oil/Steam System Using Pendant Drop Method. *J. Energy. Env. Resch.* **5**(1): 94–109. <http://www.ccsenet.org/journal/index.php/eer/article/view/47447>.
- Phan, L., Brown, H., White, J. et al. 2009. Soybean Oil Extraction and Separation Using Switchable or Expanded Solvents. *Green Chem.* **11**(1): 53–59. <https://doi.org/10.1039/b810423a>.
- Pratama, R. A., and Babadagli, T. 2020a. Effect of Temperature, Phase Change, and Chemical Additive on Wettability Alteration during Steam Applications in Sands and Carbonates. *SPE Res. Eval. Eng.* **23**(01): 292–310. <http://doi.org/10.2118/191188-PA>.
- Pratama, R. A., and Babadagli, T. 2020b. Reconsideration of Steam Additives to Improve Heavy-Oil Recovery Efficiency: Can New Generation Chemicals be Solution for Steam Induced Unfavorable Wettability Alteration? *Energy & Fuels*. <https://doi.org/10.1021/acs.energyfuels.0c01406>.
- Pratama, R. A., and Babadagli, T. 2020c. Wettability State and Phase Distributions during Steam Injection with and without Chemical Additives: An Experimental Analysis Using Visual Micromodels. *SPE Res. Eval. Eng.* In Press. <https://doi.org/10.2118/196253-PA>.
- Pratama, R. A., and Babadagli, T. 2020d. Tertiary Recovery Improvement of Steam Injection Using Chemical Additives: Pore Scale Understanding of Challenges and Solutions through Visual Experiments. SPE Western Regional Meeting, Bakersfield, California, USA, 27–30 April. SPE-200841-MS. <https://doi.org/10.2118/200841-MS>.

- Rameh Hart. DROPimage Advanced. 2019. <http://www.ramehart.com/diadv.htm>.
- Samorì, C., López Barreiro, D., Vet, R. et al. 2013. Effective Lipid Extraction from Algae Cultures Using Switchable Solvents. *Green Chem.* **15**(2): 353–356. <https://doi.org/10.1039/c2gc36730k>.
- Shen, C. 2013. SAGD for Heavy Oil Recovery. In *Enhanced Oil Recovery Field Case Studies*, Chap. 17. 413–445. Kidlington, Oxford, United Kingdom: Gulf Professional Publishing. <https://doi.org/10.1016/B978-0-12-386545-8.00017-8>.
- Sheng, J. J. 2013. Estimation of Oil Recovery Performance. In *Enhanced Oil Recovery Field Case Studies*, Chap. 15.5, 370–371. Kidlington, Oxford, United Kingdom: Gulf Professional Publishing. <https://doi.org/10.1016/B978-0-12-386545-8.00015-4>.
- Sui, H., Xu, L., Li, X. et al. 2016. Understanding the Roles of Switchable-Hydrophilicity Tertiary Amines in Recovering Heavy Hydrocarbons from Oil Sands. *J. Chem. Eng.* **290**: 312–318. <https://doi.org/10.1016/j.cej.2016.01.056>.
- Wei, Y. and Babadagli, T. 2018. Changing Interfacial Tension and Wettability using New Generation Chemicals and Nano Metal Particles at Elevated Temperatures and Pressures: An Analysis through a New Experimental Design for Heavy-Oil Recovery Applications. *J. Disp. Sci. and Technol.* **40**(12): 1785–1794. <https://doi.org/10.1080/01932691.2018.1542311>.
- Wilson, A. D. and Stewart, F. F. 2014. Structure–Function Study of Tertiary Amines as Switchable Polarity Solvents. *RSC Adv.* **4**(22): 11039–11049. <https://doi.org/10.1039/C3RA47724J>.

## Chapter 5

- Al-Bahlani, A.M. and Babadagli, T. 2008. Heavy-Oil Recovery in Naturally Fractured Reservoirs with Varying Wettability by Steam Solvent Co-Injection. Paper presented in the SPE International Thermal Operation and Heavy-Oil Symposium, Calgary, Alberta, Canada, 20–23 October. SPE-117626-MS. <https://doi.org/10.2118/117626-ms>.
- Al-Bahlani, A.-M., and Babadagli, T. 2012. Laboratory scale experimental analysis of Steam-Over-Solvent injection in Fractured Reservoirs (SOS-FR) for heavy-oil recovery. *J. Petrol. Sci. Eng.* 84–85: 42–56. <https://doi.org/10.1016/j.petrol.2012.01.021>.
- Ali, S. M. F. 1974. Current Status of Steam Injection as a Heavy Oil Recovery Method. *J. Can. Pet. Technol.* **13**(1): 54–68. PETSOC-74-01-06. <https://doi.org/10.2118/74-01-06>.
- Ali, S. M. F., Abad, B. 1976. Bitumen Recovery from Oil Sands, Using Solvents in Conjunction with Steam. *J. Can. Petrol. Technol.* **15**(03): 20–24. PETSOC-76-03-11. <https://doi.org/10.2118/76-03-11>.
- Ali, S. M. F. and Meldau, R. F. 1979. Current Steam flood Technology. *J. Pet. Technol.* **31**(10): 1332–1342. SPE-7183-PA. <https://doi.org/10.2118/7183-PA>.
- Ali, S. M. F. 1997. Is There Life After SAGD?. *J. Can. Pet. Technol.* **36**(06): 20–23. PETSOC-97-06-DAS. <https://doi.org/10.2118/97-06-DAS>.
- Ali, S. M. F. 2016. Life After SAGD – 20 Years Later. Paper presented at the SPE Western Regional Meeting, Anchorage, Alaska, USA, 23–26 May. SPE-180394-MS. <https://doi.org/10.2118/180394-MS>.
- Aznar, B., Haddadi, A., Sarahi, M., et al. 2018. Generalized Approach to Predict k-Values of Hydrocarbon Solvent/Bitumen Mixtures. Paper presented at SPE Canada Heavy Oil Technical Conference, Calgary, Alberta, Canada, 13–14 March. SPE-189744-MS. <https://doi.org/10.2118/189744-MS>.

- Blevins, T. R., Doerksen, J. H., and Ault, J. W. 1984. Light-Oil Steam flooding: An Emerging Technology. *J. Pet. Technol.* **36**(7): 1115–1122. SPE-10928-PA. <https://doi.org/10.2118/10928-PA>.
- Blevins, T. R. 1990. Steam flooding in the U.S.: A Status Report. *J. Pet. Technol.* **42**(5): 548–554. SPE-20401-PA. <http://doi.org/10.2118/20401-PA>.
- BP Statistical Review of World Energy 2021, BP, accessed 10 September 2021, <https://www.bp.com/content/dam/bp/business-sites/en/global/corporate/xlsx/energy-economics/statistical-review/bp-stats-review-2021-all-data.xlsx>.
- Butler, R. M., McNab, G., and Lo, H. 1979. Steam-Assisted Gravity Drainage. Paper Presented at the Oil Sands Conference, Jasper, Alberta, Canada.
- Butler, R. M. 1994. *Horizontal Wells for the Recovery of Oil, Gas, and Bitumen*, Vol. 2, 169–199. Richardson, Texas, USA: Monograph Series, Society of Petroleum Engineers.
- Butler, R. 1999. The Steam and Gas Push (SAGP). *J. Can. Petrol. Technol.* **38**(03): 54–61. <https://doi.org/10.2118/99-03-05>
- Canadian Energy Research Institute (CERI). 2017. *Study No. 164: Economic Potentials and Efficiencies of Oil Sands Operations: Processes and Technologies*. [https://ceri.ca/assets/files/Study\\_164\\_Full\\_Report.pdf](https://ceri.ca/assets/files/Study_164_Full_Report.pdf).
- Canadian Energy Research Institute (CERI). 2020. *Study No. 191: Canadian Oil Sands Production and Emissions Outlook (2020–2039)*. [https://ceri.ca/assets/files/Study\\_191\\_Full\\_Report.pdf](https://ceri.ca/assets/files/Study_191_Full_Report.pdf).
- Camas, C and Kantzas, A. 2012. A Mechanism of Gas Production in SAGD. Paper presented at SPE Heavy Oil Conference, Calgary, Alberta, Canada, 12–14 June. SPE-157773. <https://doi.org/10.2118/157773-MS>
- Canola, S., Akin, S., and Policar, M. 2004. Evaluation of SAGD Performance in the Presence of Non-Condensable Gases. Paper Presented at Canadian International Petroleum Conference, Calgary, Alberta, Canada, 8–10 June. <https://doi.org/10.2118/2004-222>.
- Das, S. K. 1998. Vapex: An Efficient Process for the Recovery of Heavy Oil and Bitumen. *SPE J.* **3**(03): 232–237. SPE-50941-PA. <https://doi.org/10.2118/50941-PA>.

- Das, S. K. and Butler, R. M. 1998. Mechanism of the Vapour Extraction Process for Heavy Oil and Bitumen. *J. Pet. Sci. and Eng.* **21**(1998): 43-59. [https://doi.org/10.1016/S0920-4105\(98\)00002-3](https://doi.org/10.1016/S0920-4105(98)00002-3).
- De Haan, H. J. and Schenk, L. 1969. Performance Analysis of a Major Steam Drive Project in the Tia Juana Field, Western Venezuela. *J. Petrol. Technol.* **21**(01): 111–119. <https://doi.org/10.2118/1915-pa>.
- Deng, X. 2005. Recovery Performance and Economics of Steam/Propane Hybrid Process. Paper presented at SPE/PS-CIM/CHOA International Thermal Operations and Heavy Oil Symposium, Calgary, Alberta, Canada, 1–3 November. SPE/PS-CIM/CHOA 97760. <https://doi.org/10.2118/97760-MS>.
- Esmaili, A. and Ayoub, M. 2015. Local Thermal Effect on Vapor Extraction (VAPEX) for Heavy Oil Enhanced Recovery. Paper presented at the International Field Exploration and Development Conference, Xi'an, China, 20–21 September. <https://doi.org/10.1049/cp.2015.0591>.
- Evocator, S. I., Gerasene, T. E., and Evdokimov, V. S. 2018. Temperature Impact on the Stability of Wetting Water Films on Quartz Surfaces. *Glass and Ceramics* **75**(3–4): 102–107. <https://doi.org/10.1007/s10717-018-0037-2>.
- Fuaadi, I. M., Pearce, J. C., and Gael, B. T. 1991. Evaluation of Steam-Injection Designs for the Duri Steamflood Project. Paper presented at the SPE Asia-Pacific Conference, Perth, Australia, 4–7 November. SPE-22995-MS. <https://doi.org/10.2118/22995-MS>.
- Gael, B. T., Putro, E. S., and Masykur, A. 1994. Reservoir Management in the Duri Steamflood. Paper presented at the SPE/DOE Improved Oil Recovery Symposium, Tulsa, OK, USA, 17–20 April. SPE-27764-MS. <https://doi.org/10.2118/27764-MS>.
- Gates, I. D. and Wang, J. 2011. Evolution of In Situ Oil Sands Recovery Technology: What Happened and What's New? Paper presented at the SPE International Heavy Oil Conference and Exhibition, Kuwait City, Kuwait, 12–14 December. SPE-150686-MS. <https://doi.org/10.2118/150686-MS>.

- Haghighi, M. and Yortsos, Y. C. 1997. Visualization of Steam Injection in Fractured Systems Using Micromodels. Paper presented at the International Thermal Operations and Heavy Oil Symposium, Bakersfield, CA, USA, 10–12 February. SPE-37520-MS. <https://doi.org/10.2523/37520-MS>.
- Hall, A. L., and Bowman, R. W. 1970. Operation and Performance of Slocum Field Thermal Recovery Project. Paper presented at the SPE Practical Aspects of Improved Recovery Techniques Symposium, Fort Worth, TX, USA, 8–9 March. SPE-2843-MS. <https://doi.org/10.2118/2843-ms>.
- Harmsen, G. J. 1979. Steam Flooding in a Water Drive Reservoir in The Schoonebeek Field in The Netherlands. Paper presented at the 10<sup>th</sup> World Petroleum Congress Proceedings, Bucharest, Romania, 9–14 September. WPC-18233.
- Hirasaki, G. J. 1991. Wettability: Fundamentals and Surface Forces. SPE Form. Eval. **6**(02): 217–226. SPE-17367-PA. <https://doi.org/10.2118/17367-PA>.
- Ito, Y. 2014. Oil Drainage Characteristics during the SAGD Process to Explain Observed Field Performance. Paper presented at the SPE Heavy Oil Conference, Alberta, Canada, 10–12 June. SPE-170071-MS. <https://doi.org/10.2118/170071-MS>.
- James, L., Rezaei, N., Chatzis, I. 2007. VAPEX, Warm VAPEX, and Hybrid VAPEX-The State of Enhanced Oil Recovery for In Situ Heavy Oils in Canada. Paper presented at the Canadian International Petroleum Conference, Calgary, Alberta, Canada, 12 June. 10.2118/2007-200.
- Jessup, R. S. 1930. Compressibility and Thermal Expansion of Petroleum Oils in the Range 0 Degrees to 300 Degrees C. *Bur. Stand. J. Res.* **5**(05): 985. <https://doi.org/10.6028/jres.005.062>.
- Jiang, Q., Butler, R., and Yee, C. T. 2000. The Steam and Gas Push (SAGP)-2: Mechanism Analysis and Physical Model Testing. *J. Can. Petrol. Technol.* **39**(04): 52–61. <https://doi.org/10.2118/00-04-04>.
- Jimenez, J. 2008. The Field Performance of SAGD Projects in Canada. Paper presented at the International Petroleum Technology Conference, Kuala Lumpur, Malaysia, 3–5 December. IPTC-12860-MS. <https://doi.org/10.2523/iptc-12860-ms>.

- Jones, J., McWilliams, M., and Sturm, D. 1995. Kern River Revisited: Life After Steam Flood. Paper presented at the SPE Western Regional Meeting, Bakersfield, CA, USA, 8–10 March. SPE-29664-MS. <http://dx.doi.org/10.2118/29664-MS>.
- Kong, X., Haghghi, M., and Yortsos, Y. C. 1992. Visualization Of Steam Displacement of Heavy Oils in a Hele-Shaw Cell. *Fuel*, **71**(12): 1465–1471. [https://doi.org/10.1016/0016-2361\(92\)90220-I](https://doi.org/10.1016/0016-2361(92)90220-I).
- Lee, J. and Babadagli, T. 2021. Mitigating Greenhouse Gas Intensity Through New Generation Techniques During Heavy Oil Recovery. *J. Clean. Prod.* **286**(March 2021): 124980. <https://doi.org/10.1016/j.jclepro.2020.124980>.
- Liang, G., Xie, Q., Liu, Y., et al. 2023. Feasibility Evaluation of Warm Solvent Assisted Gravity Drainage Process in Low-Carbon Developing Super-Heavy Oil or Oil Sands Project. Paper Presented at the SPE Europe Energy Conference, Vienna, Austria, 5–8 June. SPE-214347-MS. <https://doi.org/10.2118/214347-MS>.
- Mazumder, S., Wolf, K. H. A. A., van Hemert, P., et al. 2008. Laboratory Experiments on Environmentally Friendly Means to Improve Coalbed Methane Production by Carbon Dioxide/Flue Gas Injection. *Transp. Porous. Med.* **75**(1): 63–92. <https://doi.org/10.1007/s11242-008-9222-z>.
- Min, B., Mamoudou, S., Dang, S., et al. 2020. Comprehensive Experimental Study of Huff-n-Puff Enhanced Oil Recovery in Eagle Ford: Key Parameters and Recovery Mechanism. Paper Presented at the SPE Improved Oil Recovery Conference, Tulsa, Oklahoma, USA, 31 August–4 September. SPE-200436-MS. <https://doi.org/10.2118/200436-MS>.
- Mohammed, N., Abbas, A. J., Enyi, G. C., et al. 2020. Alternating N<sub>2</sub> Gas Injection as a Potential Technique for Enhanced Gas Recovery and CO<sub>2</sub> Storage in Consolidated Rocks: An Experimental Study. *J. Petrol. Expl. Prod. Tech.* **10**(8): 3883–3903. <https://doi.org/10.1007/s13202-020-00935-z>.
- Moussa, T. 2019. Performance and Economic Analysis of SAGD and VAPEX Recovery Processes. *Arab J. Sci. Eng.* **44**: 6139–6153. <https://doi.org/10.1007/s13369-018-3665-5>.

- Naderi, K., Babadagli, T., and Coskuner, G. 2013. Bitumen Recovery by the Steam-Over-Solvent Injection in Fractured Reservoirs (SOS-FR) Method: An Experimental Study on Grosmont Carbonates. *Energy Fuels*. **27**(11): 6501–6517. <https://doi.org/10.1021/ef401333u>.
- Naderi, K. and Babadagli, T. 2016. Solvent Selection Criteria and Optimal Application Conditions for Heavy-Oil/Bitumen Recovery at Elevated Temperatures: A Review and Comparative Analysis. *J. Energy Resour. Technol.* **138**(1): 012904. <https://doi.org/10.1115/1.4031453>.
- Nasr, T., Beaulieu, G., Golbeck, H., et al. 2003. Novel Expanding Solvent-SAGD Process “ES-SAGD”. *J. Can. Petrol. Technol.* **42**(1): 13–16. PETSOC-03-01-TN. <https://doi.org/10.2118/03-01-TN>.
- Novosad, Z. 1989. EOR by Rich Gas Injection - The Role of Multiple Liquid Phases in Crude Oil-Solvent Miscibility Development. *Fluid Phase Equilibria*. **52**: 263–274. [https://doi.org/10.1016/0378-3812\(89\)80332-2](https://doi.org/10.1016/0378-3812(89)80332-2).
- O'Rourke, J.C., Begley, A.G., Boyle, H.A., et al. 1999. UTF Project Status Update, May 1997. *J. Can. Petrol. Technol.* **38**(09): 44–54. PETSOC-97-06-DAS. <https://doi.org/10.2118/97-06-DAS>.
- Pathak, V., Babadagli, T., and Edmunds, N. 2012. Mechanics of Heavy Oil and Bitumen Recovery by Hot Solvent Injection. *SPE Res. Eval. Eng.* **15**(2): 182–194. SPE-144546-PA. <https://doi.org/10.2118/144546-PA>.
- Pratama, R. A., and Babadagli, T. 2020a. Effect of Temperature, Phase Change, and Chemical Additive on Wettability Alteration during Steam Applications in Sands and Carbonates. *SPE Res. Eval. and Eng.* **23**(01): 292–310. <http://doi.org/10.2118/191188-PA>.
- Pratama, R. A., and Babadagli, T. 2020b. Wettability State and Phase Distributions during Steam Injection with and without Chemical Additives: An Experimental Analysis Using Visual Micromodels. *SPE Res. Eval. Eng.* **23**(03): 1133–1149. <https://doi.org/10.2118/196253-PA>.
- Pratama, R. A. and Babadagli, T. 2020c. Tertiary-Recovery Improvement of Steam Injection Using Chemical Additives: Pore-Scale Understanding of Challenges and Solutions Through Visual Experiments. *SPE J.* In-Press. SPE-200841-PA. <https://doi.org/10.2118/200841-PA>.

- Pourabdollah, K., Moghaddam, A., and Kharrat, R. Improvement of Heavy Oil Recovery in the VAPEX Process using Montmorillonite Nanoclays. *Oil. Gas. Sci. Technol.* **66**(6): 1005-1016. <https://doi.org/10.2516/ogst/2011109>.
- Sharma, J., Moore, R. G., and Mehta, S. A. 2012. Effect of Methane Co-Injection in SAGD-- Analytical and Simulation Study. *SPE J.* **17**(03): 687–704. SPE-148917-PA. <https://doi.org/10.2118/148917-PA>.
- Shen, C. 2013. SAGD for Heavy Oil Recovery. In *Enhanced Oil Recovery Field Case Studies*, Chap. 17, 413–445. Kidlington, Oxford, UK: Gulf Professional Publishing.
- Sheng, J. J. 2013. *Enhanced Oil Recovery Field Case Studies*. Waltham, Massachusetts, USA: Gulf Professional Publishing.
- Speight, J. 2013. Thermal Methods of Recovery. In *Enhanced Recovery Methods for Heavy Oil and Tar Sands*, Chap. 7, 221–260. Gulf Professional Publishing.
- Sun, R., Fan, Z., Yang, M., et al. 2019. In-Situ Observation of MH Formation/Decomposition in Unconsolidated Sands Recovered from the South China Sea. *Energy Procedia.* **158**: 5433–5438. <https://doi.org/10.1016/j.egypro.2019.01.605>.
- Taylor, S. 2018. Interfacial Chemistry in Steam-Based Thermal Recovery of Oil Sands Bitumen with Emphasis on Steam-Assisted Gravity Drainage and the Role of Chemical Additives. *Colloids Interfaces* **2**(02): 16. <https://doi.org/10.3390/colloids2020016>.
- Van Dijk, C. 1968. Steam-Drive Project in the Schoonebeek Field, The Netherlands. *J. Pet. Technol.* **20**(03): 295–302. <https://doi.org/10.2118/1917-PA>.
- Winderasta, W., Lestari, E. S., Budiman, A. et al. 2018. Managing Reservoir Surveillance in Duri Steam Flood Field. Paper presented at the Indonesian Petroleum Association Forty-Second Annual Convention & Exhibition, Jakarta, Indonesia, 2–4 May. IPA18-577-E.
- Zhang, K., Zhou, X., Peng, X., et al. 2019. A Comparison Study Between N-Solv Method and Cyclic Hot Solvent Injection (CHSI) Method. *J. Pet. Sci. Eng.* **173**: 258–268. <https://doi.org/10.1016/j.petrol.2018.09.061>.

Zhao, L., Nasr, T. N., Huang, H., et al. 2004. Steam Alternating Solvent Process: Lab Test and Simulation. Paper Presented at the Canadian International Petroleum Conference, Calgary, Alberta, Canada, 8–10 June. <https://doi.org/10.2118/2004-044>.

## Chapter 6

- Ali, S. M. F., Abad, B. 1976. Bitumen Recovery from Oil Sands, Using Solvents in Conjunction with Steam. *J. Can. Petrol. Technol.* **15**(03): 20–24. PETSOC-76-03-11. <https://doi.org/10.2118/76-03-11>.
- Butler, R. 1999. The Steam and Gas Push (SAGP). *J. Can. Petrol. Technol.* **38**(03): 54–61. <https://doi.org/10.2118/99-03-05>.
- Canadian Energy Research Institute (CERI). 2020. *Study No. 191: Canadian Oil Sands Production and Emissions Outlook (2020–2039)*. [https://ceri.ca/assets/files/Study\\_191\\_Full\\_Report.pdf](https://ceri.ca/assets/files/Study_191_Full_Report.pdf).
- Energy Institute Statistical Review of World Energy 2023, BP, accessed 9 August 2023, [https://www.energyinst.org/\\_data/assets/pdf\\_file/0004/1055542/EI\\_Stat\\_Review\\_PDF\\_single\\_3.pdf](https://www.energyinst.org/_data/assets/pdf_file/0004/1055542/EI_Stat_Review_PDF_single_3.pdf).
- Bahadori, A., Vuthaluru, H.B., Tadé, M.O., et al. 2008. Predicting Water-Hydrocarbon Systems Mutual Solubility. *Chem. Eng. Technol.* **31**: 1743-1747. <https://doi.org/10.1002/ceat.200800226>
- Butler, R. M. 1985. A New Approach to The Modelling of Steam-Assisted Gravity Drainage. *J. Can. Petrol. Technol.* **24**(03): 42–51. <https://doi.org/10.2118/85-03-01>.
- Bruns, F., and Babadagli, T. 2020b. Heavy-Oil Recovery Improvement by Additives to Steam Injection: Identifying Underlying Mechanisms and Chemical Selection through Visual Experiments. *J. Pet. Sci. Eng.* **188**(December 2019): 106897. <https://doi.org/10.1016/j.petrol.2019.106897>.
- Collins, P. M. 1994. Design of the Monitoring Program for AOSTRA's Underground Test Facility, Phase B Pilot. *J. Can. Petrol. Technol.* **33**(03): 46–53. <https://doi.org/10.2118/94-03-06>.
- Das, S. K. 1998. Vapex: An Efficient Process for the Recovery of Heavy Oil and Bitumen. *SPE J.* **3**(03): 232–237. SPE-50941-PA. <https://doi.org/10.2118/50941-PA>.

- Das, S. K. and Butler, R. M. 1998. Mechanism of the Vapour Extraction Process for Heavy Oil and Bitumen. *J. Pet. Sci. and Eng.* **21**(1998): 43-59. [https://doi.org/10.1016/S0920-4105\(98\)00002-3](https://doi.org/10.1016/S0920-4105(98)00002-3).
- Edmunds, N., and Gittins, S. D. 1993. Effective Application of Steam-Assisted Gravity Drainage of Bitumen to Long Horizontal Well Pairs. *J. Can. Petrol. Technol.* **32**(06): 49–55. <https://doi.org/10.2118/93-06-05>.
- Esmaili, A. and Ayoub, M. 2015. Local Thermal Effect on Vapor Extraction (VAPEX) for Heavy Oil Enhanced Recovery. Paper presented at the International Field Exploration and Development Conference, Xi'an, China, 20–21 September. <https://doi.org/10.1049/cp.2015.0591>.
- Gong, H., Yu, C., Jiang, Q., et al. 2022. Improving Recovery Efficiency by CO<sub>2</sub> Injection at Late Stage of Steam Assisted Gravity Drainage. *Adv. Geoen. Res.* **6**(4): 276–285. <https://doi.org/10.46690/ager.2022.04.02>.
- Huang, J., and Babadagli, T. 2019. Visual Analysis of SAGD with Chemical Additives. Paper presented at the SPE Kuwait Oil & Gas Show and Conference, Mishref, Kuwait, 13–16 October. SPE-198041-MS. <https://doi.org/10.2118/198041-MS>.
- Jaimes, D. M., Gates, I. D., and Clarke, M. 2019. Reducing the Energy and Steam Consumption of SAGD Through Cyclic Solvent Co-Injection. *Energies.* **12**(20): 3860. <https://doi.org/10.3390/en12203860>.
- James, L., Rezaei, N., Chatzis, I. 2007. VAPEX, Warm VAPEX, and Hybrid VAPEX-The State of Enhanced Oil Recovery for In Situ Heavy Oils in Canada. Paper presented at the Canadian International Petroleum Conference, Calgary, Alberta, Canada, 12 June. <https://doi.org/10.2118/2007-200>.
- Jiang, Q., Butler, R., and Yee, C. T. 2000. The Steam and Gas Push (SAGP)-2: Mechanism Analysis and Physical Model Testing. *J. Can. Petrol. Technol.* **39**(04): 52–61. <https://doi.org/10.2118/00-04-04>.

- Kong, X., Haghghi, M., and Yortsos, Y. C. 1992. Visualization Of Steam Displacement of Heavy Oils in a Hele-Shaw Cell. *Fuel*, **71**(12): 1465–1471. [https://doi.org/10.1016/0016-2361\(92\)90220-I](https://doi.org/10.1016/0016-2361(92)90220-I).
- Lee, J. and Babadagli, T. 2021. Mitigating Greenhouse Gas Intensity Through New Generation Techniques During Heavy Oil Recovery. *J. Clean. Prod.* **286**(March 2021): 124980. <https://doi.org/10.1016/j.jclepro.2020.124980>.
- Liang, G., Xie, Q., Liu, Y., et al. 2023. Feasibility Evaluation of Warm Solvent Assisted Gravity Drainage Process in Low-Carbon Developing Super-Heavy Oil or Oil Sands Project. Paper Presented at the SPE Europe Energy Conference, Vienna, Austria, 5–8 June. SPE-214347-MS. <https://doi.org/10.2118/214347-MS>.
- Mazumder, S., Wolf, K. H. A. A., van Hemert, P., et al. 2008. Laboratory Experiments on Environmentally Friendly Means to Improve Coalbed Methane Production by Carbon Dioxide/Flue Gas Injection. *Transp. Porous. Med.* **75**(1): 63–92. <https://doi.org/10.1007/s11242-008-9222-z>.
- Min, B., Mamoudou, S., Dang, S., et al. 2020. Comprehensive Experimental Study of Huff-n-Puff Enhanced Oil Recovery in Eagle Ford: Key Parameters and Recovery Mechanism. Paper Presented at the SPE Improved Oil Recovery Conference, Tulsa, Oklahoma, USA, 31 August–4 September. SPE-200436-MS. <https://doi.org/10.2118/200436-MS>.
- Mohammed, N., Abbas, A. J., Enyi, G. C., et al. 2020. Alternating N<sub>2</sub> Gas Injection as a Potential Technique for Enhanced Gas Recovery and CO<sub>2</sub> Storage in Consolidated Rocks: An Experimental Study. *J. Petrol. Expl. Prod. Tech.* **10**(8): 3883–3903. <https://doi.org/10.1007/s13202-020-00935-z>.
- Moussa, T. 2019. Performance and Economic Analysis of SAGD and VAPEX Recovery Processes. *Arab J. Sci. Eng.* **44**: 6139–6153. <https://doi.org/10.1007/s13369-018-3665-5>.
- Nasr, T. N., Beaulieu, G., Golbeck, et al. 2003. Novel Expanding Solvent-SAGD Process “ES-SAGD.” *J. Can. Petrol. Technol.* **42**(01): 13–16. <https://doi.org/10.2118/03-01-TN>.

- Orr, B. 2009. ES-SAGD: Past, Present, and Future. Paper presented at SPE Annual Technical Conference and Exhibition, New Orleans, Louisiana, USA, 4–7 October. SPE-129518-STU. <https://doi.org/10.2118/129518-STU>.
- Pratama, R., and Babadagli, T. 2023a. What Did We Learn from SAGD Applications in Three Decades, and What is Next? *Geoen. Sci. Eng.* Under review.
- Pratama, R., and Babadagli, T. 2023b. What Did We Learn from SAGD Applications in Three Decades, and What is Next? Paper presented at the SPE Western Regional Meeting, Anchorage, Alaska, USA, 22–25 May. SPE-212970-MS. <https://doi.org/10.2118/212970-MS>.
- Pratama, R., and Babadagli, T. 2023c. What is Next for SAGD?: Evaluation of Low GHG and High-Efficiency Tertiary Recovery Options. *Geoen. Sci. Eng.* Under review.
- Pratama, R., and Babadagli, T. 2023d. What is Next for SAGD?: Evaluation of Low GHG and High-Efficiency Tertiary Recovery Options. Paper presented at the SPE Canadian Energy Technology Conference, Calgary, Alberta, Canada, 16–17 March. SPE-208876-MS. <https://doi.org/10.2118/208876-MS>.
- Pourabdollah, K., Moghaddam, A., and Kharrat, R. Improvement of Heavy Oil Recovery in the VAPEX Process using Montmorillonite Nanoclays. *Oil. Gas. Sci. Technol.* **66**(6): 1005-1016. <https://doi.org/10.2516/ogst/2011109>.
- Song, B. J., You, N., Lee, J. H., et al. 2014. Effect of CO<sub>2</sub> Injection in SAGD Process for Oil Sand Bitumen Recovery. *Appl. Chem. Eng.* **25**(3): 262–267. <http://doi.org/10.14478/ace.2014.1014>.
- Sun, R., Fan, Z., Yang, M., et al. 2019. In-situ Observation of MH Formation/Decomposition in Unconsolidated Sands Recovered from the South China Sea. *Energy Procedia.* 158: 5433–5438. <https://doi.org/10.1016/j.egypro.2019.01.605>.
- Wang, C., Liu, P., Wang, F., et al. 2018. Experimental Study on Effects of CO<sub>2</sub> and Improving Oil Recovery for CO<sub>2</sub> Assisted SAGD in Super-Heavy-Oil Reservoirs. *J. Pet. Sci. Eng.* **165**: 1073–1080. <https://doi.org/10.1016/j.petrol.2018.02.058>.

- Zirrahi, M., Hassanzadeh, H., Abedi, J., et al. 2014, Prediction of solubility of CH<sub>4</sub>, C<sub>2</sub>H<sub>6</sub>, CO<sub>2</sub>, N<sub>2</sub> and CO in bitumen. *Can. J. Chem. Eng.* **92**: 563-572. <https://doi.org/10.1002/cjce.21877>.
- Zhang, K., Zhou, X., Peng, X., et al. 2019. A Comparison Study Between N-Solv Method and Cyclic Hot Solvent Injection (CHSI) Method. *J. Pet. Sci. Eng.* **173**: 258–268. <https://doi.org/10.1016/j.petrol.2018.09.061>.
- Zhao, L., Nasr, T. N., Huang, H., et al. 2004. Steam Alternating Solvent Process: Lab Test and Simulation. Paper Presented at the Canadian International Petroleum Conference, Calgary, Alberta, Canada, 8–10 June. <https://doi.org/10.2118/2004-04>.